# New sphingolipid probes for metabolism and trafficking studies

María Garrido Martínez

**ADVERTIMENT**. La consulta d'aquesta tesi queda condicionada a l'acceptació de les següents condicions d'ús: La difusió d'aquesta tesi per mitjà del servei TDX (**www.tdx.cat**) ha estat autoritzada pels titulars dels drets de propietat intel·lectual únicament per a usos privats emmarcats en activitats d'investigació i docència. No s'autoritza la seva reproducció amb finalitats de lucre ni la seva difusió i posada a disposició des d'un lloc aliè al servei TDX. No s'autoritza la presentació del seu contingut en una finestra o marc aliè a TDX (framing). Aquesta reserva de drets afecta tant al resum de presentació de la tesi com als seus continguts. En la utilització o cita de parts de la tesi és obligat indicar el nom de la persona autora.

**ADVERTENCIA**. La consulta de esta tesis queda condicionada a la aceptación de las siguientes condiciones de uso: La difusión de esta tesis por medio del servicio TDR (**www.tdx.cat**) ha sido autorizada por los titulares de los derechos de propiedad intelectual únicamente para usos privados enmarcados en actividades de investigación y docencia. No se autoriza su reproducción con finalidades de lucro ni su difusión y puesta a disposición desde un sitio ajeno al servicio TDR. No se autoriza la presentación de su contenido en una ventana o marco ajeno a TDR (framing). Esta reserva de derechos afecta tanto al resumen de presentación de la tesis como a sus contenidos. En la utilización o cita de partes de la tesis es obligado indicar el nombre de la persona autora.

**WARNING**. On having consulted this thesis you're accepting the following use conditions: Spreading this thesis by the TDX (**www.tdx.cat**) service has been authorized by the titular of the intellectual property rights only for private uses placed in investigation and teaching activities. Reproduction with lucrative aims is not authorized neither its spreading and availability from a site foreign to the TDX service. Introducing its content in a window or frame foreign to the TDX service is not authorized (framing). This rights affect to the presentation summary of the thesis as well as to its contents. In the using or citation of parts of the thesis it's obliged to indicate the name of the author.

# “NEW SPHINGOLIPID PROBES FOR METABOLISM AND TRAFFICKING STUDIES”

Departamento de Química Biomédica; Institut de Química Avançada de Catalunya
(IQAC-CSIC)

Departamento de Farmacología y Química Terapéutica. Facultat de Farmàcia.
Universitat de Barcelona.

**MARIA GARRIDO MARTÍNEZ, 2012**

CONSEJO SUPERIOR DE INVESTIGACIONES CIENTÍFICAS (CSIC)
INSTITUT DE QUÍMICA AVANÇADA DE CATALUNYA (IQAC)

UNIVERSITAT DE BARCELONA
FACULTAT DE FARMÀCIA

DEPARTAMENTO DE FARMACOLOGÍA Y QUÍMICA TERAPÈUTICA
BIENIO 2008/2010

# “NEW SPHINGOLIPID PROBES FOR METABOLISM AND TRAFFICKING STUDIES”

Memoria presentada por Maria Garrido Martínez para optar al título de Doctor por la Universitat de Barcelona

Dirigida por

Prof. Dr. Antonio Delgado Cirilo
Dr. José Luís Abad

Doctoranda

Maria Garrido Martínez

Tutor

Antonio Delgado Cirilo

**MARIA GARRIDO, 2012**

This work has been completed thanks to the financial support of our group from the "Ministerio de Ciencia e Innovación" of Spain (Projects SAF2011-22444 and SAF2009-05589) and Generalitat de Catalunya, grant SGR 2009-1072.

I am also grateful to the CSIC predoctoral research training support within the JAE-Predoc program.

The work reported in this Doctoral Thesis has given rise to the following articles and patents:

- Garrido, M.; Abad, J. L.; Alonso, A.; Goñi, F. M.; Delgado, A.; Montes, R. **In situ synthesis of fluorescent membrane lipids (ceramides) using click chemistry.** *J. Chem. Biol.* **2012**, *5*, 119-123.
- Camacho, L.; Simbari, F.; Garrido, M.; Abad, J. L.; Casas, J.; Delgado, A.; Fabriàs**. 3-Deoxy-3,4-dehydro analogs of XM462. Preparation and activity on sphingolipid metabolism and cell fate.** *Bioorg. Med. Chem.* **2012**, *20*, 3173-3179.
- Nieves, I.; Garrido, M.; Abad, J. L.; Delgado, A**. An unexpected acces to a new sphingoid base containing a vinyl sulfide unit**. *Synlett* **2010**, *19*, 2950-2952.
- Garrido, M.; Navarro, F.; Mittler, F.; Garanto, A.; Jacquart, A.; Texier, I.; Delgado, A. **Live cell labeling of clickable sphingolipids with a new azadibenzocyclooctyne (ADIBO) fluorescent dye** (S*ubmitted*).
- Garrido, M.; Abad, J.L.; Fabrias, G.; Delgado, A.; Casas, J. **Tagging the sphingolipidome using click chemistry** (*In preparation*).
- Abad Saiz, J. L.; Camacho Castillo, L. C.; Casas Brugulat, J.; Fabrias Domingo, G.; Garrido Martínez, M.; Thomson Okatsu, T.; Meca Cortés, Ó.; Delgado Cirilo, A. *Amidas de 2-Amino-1,3-Propanodioles y su uso como inhibidores de ceramidasas*. España, P2011-31119, 2011, Consejo Superior de Investigaciones Científicas (CSIC) y Universidad de Barcelona (UB).
- Abad Saiz, J. L.; Fabriàs Domingo, G.; Casas Brugulat, J.; Garrido Martínez, M.; Camacho Castillo, L. C.; Simbari, F. M.; Delgado Cirilo, A. *Derivados de aminoetanol sustituidos en C2 y su uso como antitumorales.* España, P201031642, 8 de noviembre 2010, Consejo Superior de Investigaciones Científicas (CSIC) y Universidad de Barcelona (UB).

*A los que me quieren*

*El afán de perfección hace a algunas*
*personas totalmente insoportables*

Pearl S. Buck

## Agradecimientos

A todas las personas que han contribuido profesionalmente en esta tesis.

A Fina, a Gemma y, especialmente, a José Luís y a Antonio por ayudarme a aprender. Antonio, gracias por darme la oportunidad de participar en este proyecto y confiar en mí.

A todos mis compañeros del RUBAM, a los que están y a los que se han ido, por formar parte de mi día a día durante estos cuatro años.

A toda mi familia y amigos, por su apoyo incondicional. Y a Albert, por aguantarme a pesar de ser una perfecta insoportable.

## Abbreviations

| | |
|---|---|
| ABC | ATP-Binding cassette |
| ACER | Alkaline ceramidase |
| ACN | Acetonitrile |
| $BF_3\cdot OEt_2$ | Boron trifluoride diethyl etherate |
| Boc | *tert*-Butoxycarbonyl |
| $Boc_2O$ | Di-*tert*-butyl dicarbonate |
| BSA | *N,O*-Bis(trimethylsilyl)acetamide |
| BTTAA | 2-[4-{(bis[(1-*tert*-butyl-1*H*-1,2,3,-tri-azol-4-yl)methyl}amino]methyl}-1*H*-1,2-3-triazol-1-yl)]acetic acid |
| BTTES | 2-[4-{(bis[(1-*tert*-butyl-1*H*-1,2,3,-tri-azol-4-yl)methyl}amino]methyl}-1*H*-1,2-3-triazol-1-yl)]ethyl hydrogen sulfate |
| BuLi | *n*-Butyllithium |
| *t*BuOOH | *tert*-Butyl hydroperoxide |
| *t*BuOOK | Potassium-*tert*-butoxide |
| CAPP | Ceramide-activated Ser/Thr phosphatase |
| CDase | Ceramidase |
| Cer | Ceramide |
| CerS | Ceramide synthase |
| CERT | Ceramide Transport Protein |
| CK | Ceramide kinase |
| CM | Olefin cross metathesis |
| C1P | Ceramide-1-phosphate |
| CuAAC | Copper-catalyzed [3+2] azide-alkyne cycloaddition |
| DA | Diels-Alder |
| DBCO | Dibenzocyclooctyne |
| Des1 | Dihydroceramide desaturase |
| DhCer | Dihydroceramide |
| DhSM | Dihydrosphingomyelin |
| DhS1P | Sphinganine-1-phosphate |
| DhSph | Sphinganine (dihydrosphingosine) |
| DIFO | Difluorinated cyclooctyne systems |
| DIPEA | *N,N*-Diisopropylethylamine |
| DMAP | 4-Dimethylaminopyridine |
| DMF | Dimethylformamide |
| *N,O*-DMHA | *N,O*-Dimethylhydroxylamine hydrochloride |

| | |
|---|---|
| DMP | 2,2-Dimetoxypropane |
| DNA | Deoxyribonucleic acid |
| EDC | 1-Ethyl-3-(3-dimethylaminopropyl) carbodiimide |
| Equiv | Equivalent |
| ER | Endoplasmic Reticulum |
| ERK | Extracellular-signal-regulated kinase |
| $Et_3N$ | Triethylamine |
| EtOAc | Ethyl acetate |
| EtOH | Ethanol |
| FIAsh | Fluorescein derivative |
| GC | Gas chromatography |
| GCase | Glucosylceramidase |
| GCS | Glucosylceramide synthase |
| GL | Glycosphingolipid |
| GlcCer | Glucosylceramide |
| GPCR | G-protein coupled receptor |
| GUV | Giant unilamellar vesicle |
| HMPA | Hexamethylphosphoramide |
| HOBt | 1-Hydroxybenzotriazole |
| HPLC | High-performance liquid chromatography |
| HSQC | Heteronuclear single quantum coherence |
| HTS | High-throughput screening |
| IGF | Insulin-like growth factor |
| IL-1 | Interleukin-1 |
| LG | Leaving group |
| MeOH | Methanol |
| MLV | Multilamellar vesicle |
| MOM | Methoxymethyl |
| Ms | Mesylate |
| MS | Mass spectrometry |
| MsCl | Mesyl chloride |
| NMI | *N*-Methylimidazole |
| NMM | *N*-Methylmorpholine |
| NMR | Nuclear Magnetic Resonance |
| oxLDL | Oxidized low-density lipoprotein |
| PCC | Pyridinium chlorochromate |

| | |
|---|---|
| PDGF | Platelet-derived growth factor |
| PDT | Photodynamic therapy |
| PKC | Protein kinase C |
| PKH | PKB homologue |
| $PLA_2$ | Phospholipase A2 |
| ReAsH | Resorufin derivative |
| RT | Retention time |
| rt | Room temperature |
| RuAAC | Ruthenium-catalyzed [3+2] azide-alkyne cyloaddition |
| SK | Sphingosine kinase |
| SL | Sphingolipid |
| SM | Sphingomyelin |
| SMase | Sphingomyelinase |
| SMS | Sphingomyelin synthase |
| S1P | Sphingosine-1-phosphate |
| SPAAC | Strain-promoted alkyne-azide cycloaddition |
| Sph | Sphingosine |
| S1PL | Sphingosine-1-phosphate lyase |
| SPPase | Sphingosine phosphate phosphatase |
| SPT | Serine palmitoyltransferase |
| TAD | Triazacyclopentadione |
| TBTA | Tris[(1-benzyl-1*H*-1,2,3-triazol-4-yl)methyl]amine |
| THF | Tetrahydrofuran |
| THPTA | Tris(3-hydroxypropyltriazolylmethyl)amine |
| TLC | Thin layer chromatography |
| TMS | Trimethylsilyl |
| TMSBr | Bromotrimethylsilane |
| TNF | Tumor necrosis factor |
| TOF | Time of flight |
| TsCl | *para*-Toluenesulfonyl chloride |
| TsOH | *para*-Toluenesulphonic acid |
| Tz | Triazole |
| UPLC | Ultra performance liquid chromatography |
| VEGF | Vascular endothelial growth factor |
| YPK | Yeast protein kinase |

## Index

**1 Introduction** **25**

1.1 The chemical bioorthogonal approach to study biological systems 25

1.2 Azides as bioorthogonal chemical reporters 28

- 1.2.1 Bioorthogonal reactions with azides 29
  - 1.2.1.1 Staudinger Ligation 29
  - 1.2.1.2 [3+2] Azide-alkyne cycloaddition 31
    - *Ruthenium-catalyzed [3+2] azide-alkyne cycloaddition (RuAAC)* 32
    - *Copper-catalyzed [3+2] azide-alkyne cyloaddition (CuAAC)* 33
    - *CuAAC based Fluorogenic reactions* 35
  - 1.2.1.3 Strain-promoted azide-alkyne cycloaddition (SPAAC) 37

1.3 Sphingolipids 40

- 1.3.1 Structure 40
- 1.3.2 Sphingolipid metabolism 41
  - 1.3.2.1 *De novo* biosynthesis 41
  - 1.3.2.2 The sphingomyelin cycle 43
  - 1.3.2.3 The salvage pathway 43
- 1.3.3 Compartmentalization and regulation of bioactive sphingolipids 43
- 1.3.4 Bioactive sphingolipids 45
  - 1.3.4.1 Ceramide 45
  - 1.3.4.2 Sphingosine 46
  - 1.3.4.3 Phosphorylated metabolites: sphingosine-1-phosphate and ceramide-1-phosphate 46
  - 1.3.4.4 Sphingomyelin 47
  - 1.3.4.5 Dihydroceramide 48

1.4 References 48

**2 Objectives** **61**

**3 Results & Discussion** **67**

3.1 Synthesis of SL analogues with an azide group at ω position 67

- 3.1.1 Sphingosine and ceramide analogues 67
  - 3.1.1.1 Introduction 67
  - 3.1.1.2 Synthetic approaches to sphingoid bases 67

3.1.1.3 The olefin cross metathesis approach 68
3.1.1.4 Synthesis of Garner's aldehyde (**4**) 70
3.1.1.5 Synthesis of allylic alcohol (**7**) 71
3.1.1.6 Synthesis of ω-azidosphingosine (**RBM2-31**) and *N*-acylated analogues (**RBM2-32**, **RBM2-37**, **RBM2-46** and **RBM2-77**) 73
3.1.2 Dihydrosphingosine and dihydroceramide analogues 75
3.1.2.1 Introduction 75
3.1.2.2 Synthetic approaches to sphinganine 75
3.1.2.3 Synthesis of ω-azidodihydrosphingosine (**RBM2-40**) and *N*-acylated analogues (**RBM2-44**, **RBM2-45** and **RBM2-87**) 75
3.1.3 ω-Azidosphingosine-1-phosphate and ω-azidodihydrosphingosine-1-phosphate 76
3.1.3.1 Introduction 76
3.1.3.2 Synthetic approaches to phosphorylated derivatives 77
3.1.3.3 Synthesis of ω-azidosphingosine-1-phosphate (**RBM2-35**) and ω-azidodihydrosphingosine-1-phosphate (**RBM2-43**) 79
3.1.4 ω-Azidoceramide-1-phospate analogues 82
3.1.4.1 Introduction 82
3.1.4.2 Synthesis of ω-azidoceramide-1-phosphate (**RBM2-47**) 82
3.1.5 Synthesis of ω-azido-3-ketodihydrosphingosine (**RBM2-63**) 85
3.1.5.1 Introduction 85
3.1.5.2 Selected approach for the synthesis of **RBM2-63** 85
3.1.5.3 Synthesis of ω-Azido-3-ketodihydrosphingosine (**RBM2-63**) 86

3.2 Synthesis of C1-azidoceramides 87
3.2.1 Introduction 87
3.2.2 Synthetic approach to 1-azidoceramide (**RBM2-79**) 88
3.2.3 Synthesis of 1-azidoceramide (**RBM2-79**) 89

3.3 Applications of AzidoSLs as chemical probes 92
3.3.1 A new analytical method for the quantification of SL based on SPAAC 92
3.3.1.1 Effects of ω-azidoSLs on the sphingolipidome and metabolization 93
3.3.1.2 Tags based on the azacyclooctyne moiety 99
3.3.1.3 Model click reactions between azide **RBM2-37** and tags **1-5** in solution 100

3.3.1.4 Click reaction between $\omega$-azidoSL metabolites and tag **1** in cell pellets 101
3.3.1.5 Labeling of $\omega$-azidoSL metabolites with tags **1-5** 103
3.3.2 Live cell labeling of $\omega$-azidoSLs through click chemistry 106
3.3.2.1 Introduction 106
3.3.2.2 Design and synthesis of a fluorescent azadibenzocyclooctyne (**D1**) 107
3.3.2.3 Evaluation of click reactions between **D1** and the azido probe **RBM2-87** 109
3.3.2.4 Studies of fluorescence sensitivity for dye **D1** 111
3.3.2.5 Internalization of dye **D1** in cell membranes 112
3.3.2.6 Intracellular click reaction between dye **D1** and $\omega$-azidoSL metabolites 113
3.3.3 Visualization of ceramides in artificial membranes using fluorogenic CuAAC 115
3.3.3.1 Introduction 115
3.3.3.2 *In situ* fluorogenic CuAAC of membrane azido ceramides 117

3.4 New sphingolipid analogues as probes to determine Des1 activity 120
3.4.1 Introduction 120
3.4.2 Assays to evaluate Des1 activity 121
3.4.3 Design of a high-throughput screening assay for Des1 activity 122
3.4.4 Synthesis of (*E*)-$\Delta^{6}$-ceramide (**RBM2-85**) and (*E*,*E*)-$\Delta^{4-6}$-ceramide (**RBM2-76**) 123
3.4.4.1 (*E*)-$\Delta^{6}$-Ceramide **RBM2-85** 123
*Synthetic approach* 123
*Synthesis of $\Delta^{6}$-ceramide* ***RBM2-85*** 125
3.4.4.2 (*E*,*E*)-$\Delta^{4-6}$-ceramide **RBM2-76** 127
*Synthetic approach* 127
*Synthesis of $\Delta^{4,6}$-ceramide* ***RBM2-76*** 129
3.4.5 Reactivity of **RBM2-76** as dienophile against triazacyclopentadiones 131

3.5 References 132

**4 Summary & Conclusions** 143

5 **Experimental Section** 149

5.1 Synthesis and product characterization 149
5.1.1 Chemistry: general methods 149
5.1.2 Synthesis of chiral aldehyde **4** 150
5.1.3 Synthesis of synthon **7** 153
5.1.4 Synthesis of sphingosine **RBM2-31** and ceramides **RBM2-32**, **RBM2-37**, **RBM2-46** and **RBM2-77** 155
5.1.5 Synthesis of dihydrosphingosine **RBM2-40** and dihydroceramides **RBM2-44**, **RBM2-45** and **RBM2-87** 161
5.1.6 Synthesis of phosphorylated derivatives **RBM2-35**, **RBM2-43** and **RBM2-47** 165
5.1.7 Synthesis of ketone **RBM2-63** 172
5.1.8 Synthesis of 1-azidoceramide **RBM-79** 175
5.1.9 Synthesis of $\Delta^6$ and $\Delta^{4-6}$-ceramides **RBM2-85**, **RBM2-76** and **RBM2-82** 180
5.1.10 Synthesis of tags **1-5** and **St1** 187
5.1.11 Synthesis of fluorescent dye **D1** 190

5.2 Evaluation of click reactions in solution 192
5.2.1 SPAAC between azido probe **RBM2-37** and tags **1-5** 192
5.2.2 SPAAC between dye **D1** and azido probe **RBM2-87** 192
5.2.3 Diels-Alder reaction between **RBM2-76** and PTAD 193
5.2.4 Mass spectrometry 193
5.2.5 High-performance liquid chromatography 194

5.3 Biological assays 194
5.3.1 Materials and methods for cell culture 194
5.3.2 Cell viability 195
5.3.3 Labelling of cell extracts containing ω-azidoSLs through SPAAC 195
5.3.4 Live cells labeling through SPAAC 197

5.4 Extraction and detection of click adducts from GUVs 198

5.5 References 199

6 **Spanish Summary** **203**

7 **Supporting Information (CD)** **227**

# 1. Introduction

## 1.1 The chemical bioorthogonal approach to study biological systems

Compared to conventional biological methods, chemical probes offer a precise and powerful approach to study biological processes at the cellular and organism level with minimal perturbation to the intact native system.

A chemical probe offers the possibility to observe the object of interest in real time. What we are able to observe, however, depends in part on the probes introduced into the cells. While stains and fluorescent dyes for organelles and fluorescently labeled antibodies are very used, the staining of a protein of interest or other less accessible cellular molecules such as carbohydrates, nucleotides and lipids is not a trivial task. Therefore, specific labeling that attaches a fluorophore or any other label at a distinct location inside the living or fixed cell are highly desirable to study biological molecules.

In order to perform chemical reactions in living systems, it is fundamental that these processes occur under physiological conditions, including moderate temperatures, neutral pH, a large variety of competing functional groups, high ion concentrations and water as solvent. About a decade ago, Sharpless and coworkers established the so-called “click chemistry”, a type of processes that include a number of very reliable chemical reactions.[1] To consider a process as “click”, it must fulfill certain stringent criteria: (1) being high yielding and show fast reaction rates at low biomolecule concentrations; (2) to require simple reaction conditions and readily available starting materials and reagents; (3) simple product isolation and (4) benign solvents (as water); (5) to produce only inoffensive or no byproducts; (6) to be wide in scope and modular; (7) to be stereoespecific and (8) the reaction product must be stable under physiological conditions. Click reactions accomplish their required characteristics by having a high thermodynamic driving force, usually greater than 20 kcal $mol^{-1}$. The most common examples of “click chemistry” are carbon-heteroatom bond forming reactions, including the following types of chemical transformations:

- cycloadditions of unsaturated species, especially 1,3-dipolar cycloadditions and Diels-Alder (DA) reactions;

- nucleophilic substitution reactions, particularly ring-opening of strained heterocyclic electrophiles (epoxides, aziridines, aziridinium ions, and episulfonium ions);

- carbonyl chemistry of the "non-aldol" type, such as formation of ureas, thioureas, aromatic heterocycles, oxime ethers, hydrazones, and amides; and
- additions to carbon-carbon multiple bonds, especially oxidative cases such as epoxidation, dihydroxylation, aziridination, and sulfenyl halide addition, but also Michael additions of Nu-H reactants.

Even though many reactions satisfy all the above requirements, suitable reactions for chemical biology studies have to fulfill another important requirement: bioorthogonality. This property implies that the reactants must not cross-react with the abundant nucleophiles and electrophiles present inside the cells, but they should react selectively with the exogenous reaction partners.

Reaching bioorthogonality requires the incorporation of a unique chemical functionality (a bioorthogonal chemical reporter) into the required biomolecules by chemical modification or metabolic incorporation. These chemical reporters are non-native, non-perturbing chemical handles and, moreover, can be modified in living systems through selective reactions with exogenous probes (Fig. 1.1).

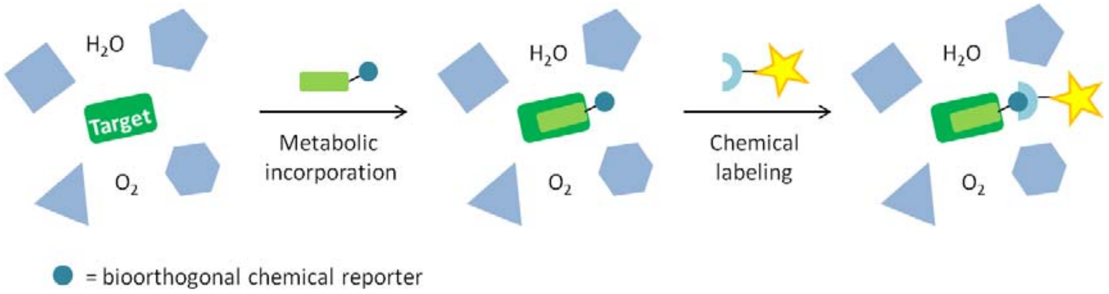

**Figure 1.1** The bioorthogonal chemical reporter strategy. A chemical reporter linked to a substrate is introduced into a target biomolecule through cellular metabolism. In a second step, the reporter is covalently tagged with an exogenously delivered probe.

Among the bioorthogonal processes, the Staudinger ligation, the 1,3-dipolar and Diels-Alder cycloadditions, the oxime ligation, and the hydrazone coupling are among the most representatives ones. All these reactions have been applied to the *in vitro* and *in vivo* labeling of biomolecules (Table 1.1).

**Table 1.1** Chemical reporters and bioorthogonal reactions used in living systems.

| Chemical reporter | Reactive partner (R' = probe) | Ligation product | Target (R) |
|---|---|---|---|
| 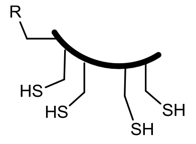<br>**Tetracysteine motif** | 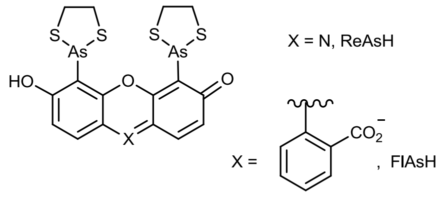 | 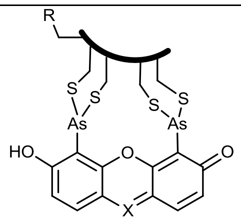 | Protein[2-3] |
| 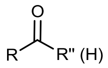<br>**Ketone/aldehyde** | 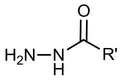 | 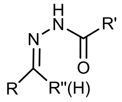 | Protein[4-5]<br>Glycan[6] |
|  | $H_2N—O—R'$ | 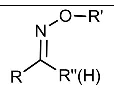 |  |
| $R—N_3$<br>**Azide** | Staudinger Ligation<br>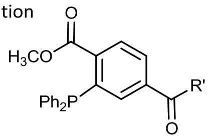 | 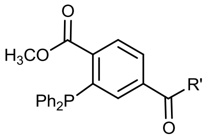 | Protein[7-8]<br>Glycan[9-10]<br>Lipid[11] |
|  | 'Click' chemistry<br>$\equiv$—R', Cu(I) | 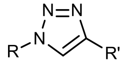 |  |
|  | Strain-promoted cycloaddition<br>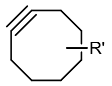 | 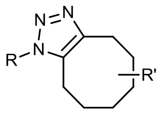 |  |
| R—$\equiv$<br>**Terminal alkyne** | 'Click' chemistry<br>$N_3—R'$, Cu(I) | 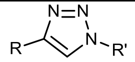 | Protein[12] |
| 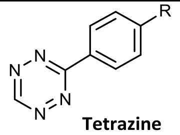<br>**Tetrazine** | 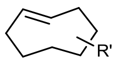 | 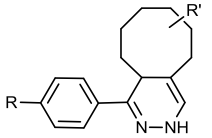 | Protein[13-14] |
| 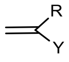<br>**Alkene** | 'Photoclick' chemistry<br>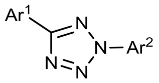 | 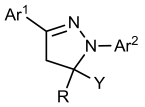 | Protein[15] |

As mentioned above, the Diels-Alder cycloaddition (DA) easily accomplishes most of the requirements of a click chemistry process. Thus, DA process involves a straightforward [4+2] cycloaddition reaction between an electron-rich diene and an electron-poor dienophile to form a stable cyclohexene adduct (Fig. 1.2).

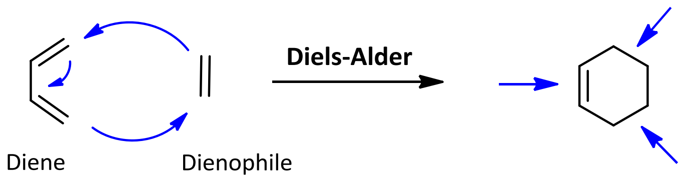

**Figure 1.2** General mechanism of Diels-Alder reactions of dienophile and diene.

The reaction occurs via a single transition state, which has a smaller volume than either the starting materials or the product. The required energy for this pericyclic reaction is very low and the driving force is the formation of new $\sigma$-bonds, which are energetically more stable than the $\pi$-bonds. The diene component in the DA reaction can be open-chain or cyclic and it can have many different substituents. Typically, the dienophile has an electron-withdrawing group conjugated to the alkene, though this feature is not exclusive of DA dienophiles.

DA reaction forms not only carbon-carbon bonds but also heteroatom-heteroatom bonds. Moreover, some DA reactions are thermally reversible and cyclic system decomposition can be controlled by temperature.[16]

Besides its numerous applications in organic synthesis, DA reaction is widely used in the synthesis of macromolecules with advanced architectures, such as homopolymers,[17-18] telechelic,[19] and dendronized polymers.[20] Moreover, the highly selective reaction between a diene and a dienophile is a reliable method for the bioconjugation and modification of biomolecules, since it proceeds within a short reaction times and in water, with a high efficiency and under mild conditions. In this field, DA reaction has been applied in the bioconjugation or immobilization of oligonucleotides,[21] proteins, peptides,[22-23] carbohydrates[24-25] and antibodies.[26]

## 1.2 Azides as bioorthogonal chemical reporters

In this section, we are focusing on the bioorthogonal ligations that involve the azide as chemical reporter, particularly on the azide-alkyne cycloadditions.

Azides are viable chemical reporters for labeling all kinds of biomolecules in any biological system. This versatile functional group is abiotic in animals and absent from nearly all naturally occurring species, since only one natural azido metabolite, isolated from unialgal cultures, has been reported to date.[27] Azides do not react appreciably with water and are resistant to oxidation. Moreover, azides are mild electrophiles and do not react with 'hard' nucleophiles, as amines, that are abundant in biological systems.

Despite its biorthogonality, the azide group has only recently been used as a chemical reporter in living systems. This may be due to perceptions of the azide as an unstable and/or toxic species. Azides are prone to decomposition at elevated temperatures, but they are quite stable at physiological temperatures.[27] Finally, although the azide anion is a widely used cytotoxin, organic azides are uncharged and nontoxic compounds.

Introduction of an azide group into a substrate can be easily achieved either by chemical or biological modifications. Chemically, the main strategies for the introduction of an azide group into an organic molecule involve nucleophilic substitution or diazo transfer reactions. Biologically, azides can be engineered into a protein, for example, by growing the autoxotrophic *E. coli* in methionine-deficient, azidohomoalanine-rich medium.[28]

## 1.2.1 Bioorthogonal reactions with azides

### 1.2.1.1 Staudinger Ligation

In 1919, Hermann Staudinger reported that azides react with triphenylphosphines (soft nucleophiles) under mild conditions to produce aza-ylide intermediates. In the presence of water, these intermediates hydrolyze spontaneously to provide a primary amine and the corresponding phosphine oxide (Fig. 1.3*A*). The bioorthogonal nature of this transformation suggested some potential applications of the azide as a chemical reporter. However, the aza-ylide instability in water was a serious drawback. Bertozzi and coworkers envisioned that an appropriately electrophilic trap, such as a methyl ester, within the phosphine structure would capture the nucleophilic aza-ylide by intramolecular cyclization (Fig. 1.3*B*).[29] This modification ultimately produces a stable amide bond rather than the products of aza-ylide hydrolysis.

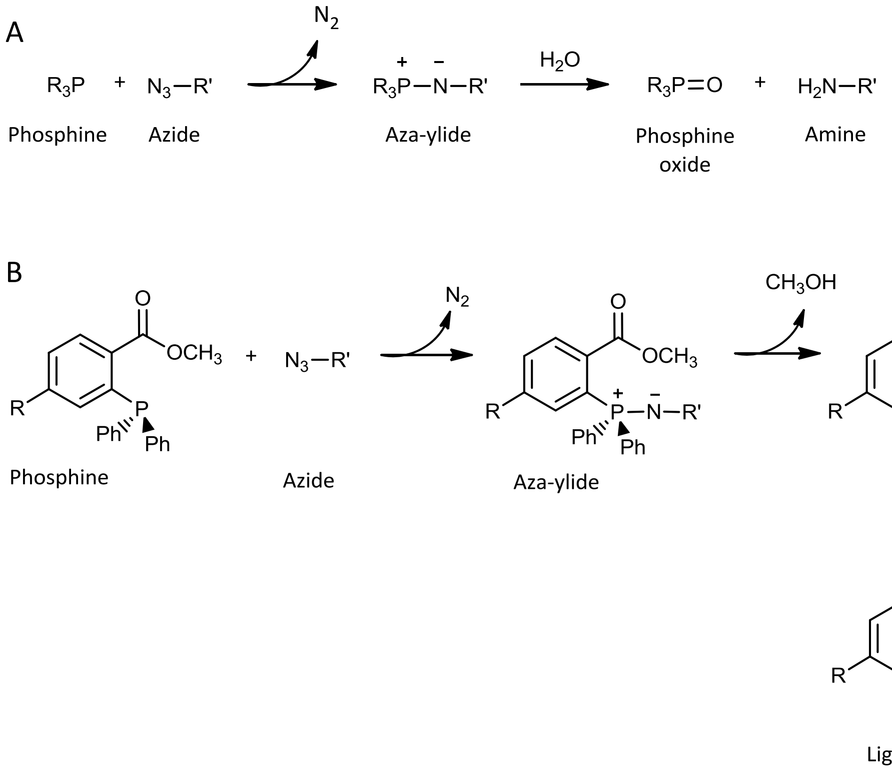
A
$N_2$
$R_3P$ + $N_3$—R'
Phosphine
Azide
+ –
$R_3P$—N—R'
Aza-ylide
$H_2O$
$R_3P$=O + $H_2N$—R'
Phosphine oxide
Amine
B
O
$OCH_3$
R
P
Ph
Ph
Phosphine
$N_3$—R'
Azide
$N_2$
Aza-ylide
$CH_3OH$
N—R'
$H_2O$
Ligation product

**Figure 1.3** (*A*) The classical Staudinger reaction of phosphines and azides. Hydrolysis of the aza-ylide produces an amine and a phosphine oxide. (*B*) A modified Staudinger reaction that produces a stable covalent adduct by amide bond formation even in the presence of water as solvent.

Afterwards, Raines and coworkers,[30] as well as the Bertozzi research group,[31] simultaneously reported the so-called traceless Staudinger ligation. Based on the inherent selectivity of the Staudinger reaction between azides and phosphines, in the traceless ligation the auxiliary phosphine reagent can be cleaved from the product after the ligation is completed, leaving a native amide bond. Among the suitable phosphines for this variant, diphenylphosphinemethanethiol, developed by Raines and co-workers, exhibits the best reactivity profile. In the reaction mechanism, this reagent is first acylated and after subsequent coupling with the target azide an intermediate reactive iminophosphorane is formed. The nucleophilic nitrogen atom then attacks intramolecularly the carbonyl group, cleaving the thioester moiety. Lastly, hydrolysis of the rearranged product produces a native amide and liberates the auxiliary reagent as its phosphine(V) oxide (Fig. 1.4).

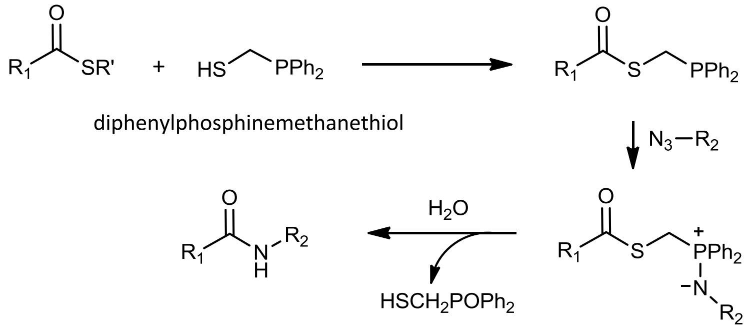

**Figure 1.4** Mechanism of the traceless Staudinger Ligation.

The traceless Staudinger ligation is a convenient approach for peptide ligation that suppresses the need for a cysteine residue and leaves no residual atoms in the peptide product.

*Applications*

The Staudinger ligation can be used to covalently attach artificial probes to azide-bearing biomolecules. Like azides, phosphines are not reactive with cellular systems and can therefore be considered as bioorthogonal. Moreover, the reaction proceeds at pH 7 with no toxic effects. Though highly specific for the azide group, the relatively slow kinetics of this reaction and the competing oxidation of the phosphine reagents by air or oxidizing enzymes have limited its use in biological systems. However, it has been used to modify glicans on living cells,[29] to enrich glycoprotein subtypes[32-33] and to impart new functionality to recombinant proteins.[34] Although this approach has not been used for bioconjugation in living systems, other applications as peptide ligation, synthesis of bioconjugates, metabolic engineering and preparation of arrays have been reported.[35]

#### 1.2.1.2 [3+2] Azide-alkyne cycloaddition

The azide group serves as an electrophile in the reaction with soft nucleophiles. In addition, it is a 1,3-dipole that shares four electrons in the π-system over three centers. It also presents a linear geometry and can undergo reaction with dipolarophiles, such as activated alkynes.[36] These π-systems are both extremely rare and inert in biological systems, further enhancing the bioorthogonality of the azide. The [3+2] cycloaddition between azides and terminal alkynes to provide stable triazole adducts was first described by Huisgen in 1963.[37] The reaction is thermodynamically favorable by a 30-35 kcal/mol. Without alkyne activation, however, the reaction requires elevated temperatures or pressures that are not compatible with living systems (Fig. 1.5*B*).

One possibility to achieve alkyne activation involves the use of a metal catalyst. In this context, ruthenium and copper have been used to accelerate these type of cycloadditions (see next sections).

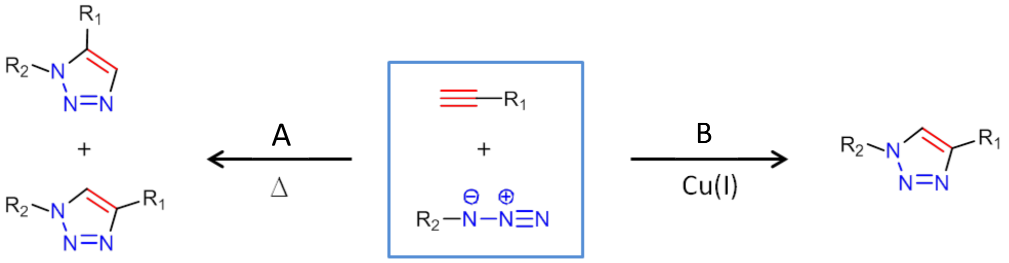

**Figure 1.5** (*A*) The copper-catalyzed reaction leads to the 1,4-disubstituted regioisomers at room temperature in high yields. (*B*) The thermal cycloaddition of alkynes with azides requires elevated temperatures and affords mixtures of the two possible regioisomers, being a non-regioselective reaction.

### *Ruthenium-catalyzed [3+2] azide-alkyne cycloaddition (RuAAC)*

The RuAAC, where $Cp^*RuCl(PPh_3)_2$ acts as catalyst, leads to regioselective formation of the 1,5-triazole system. Unlike CuAAC, in which only terminal alkynes are reactive (see next section), both therminal and internal alkynes can participate in RuAAC (Fig. 1.6).

Although the RuAAC was first described by the Fokin group in 2007,[38] the reaction has not yet been used in any biochemical application.

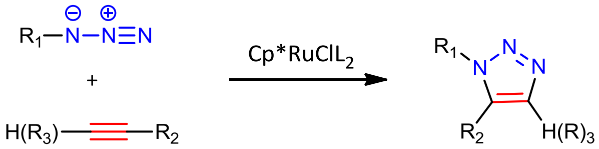

**Figure 1.6** RuAAC with terminal and internal alkynes to give 1,5-triazoles systems.

### *Copper-catalyzed [3+2] azide-alkyne cycloaddition (CuAAC)*

Almost simultaneously, Sharpless and coworkers and Meldal and coworkers demonstrated that the rate of cycloaddition between azides and alkynes can be accelerated $10^6$-fold using catalytic amounts of Cu(I).[39-40] This copper-catalyzed reaction, that nowadays has become the paradigm of 'click' chemistry, proceeds readily at physiological conditions to provide 1,4-disubstituted triazoles with nearly complete regioselectivity (Fig. 1.5*A*).[41]

The mechanistic proposal for CuAAC begins unexceptionally with the formation of the Cu(I) acetylide **I** (Fig. 1.7). Extensive density functional theory calculations[42] determined that in the next step (B in Fig. 1.7) the azide replaces one of the ligands and binds to the Cu atom via the nitrogen proximal to carbon, forming intermediate **II**. Subsequently, the distal nitrogen of the azide in **II** attacks the C2 of the acetylide, affording the unusual six membered Cu(III) metallacycle **III.** From **III**, the barrier of ring contraction, which forms the triazolyl-Cu derivative **IV** is very low. Proteolysis of **IV** releases the triazole product, thereby completing the catalytic cycle.

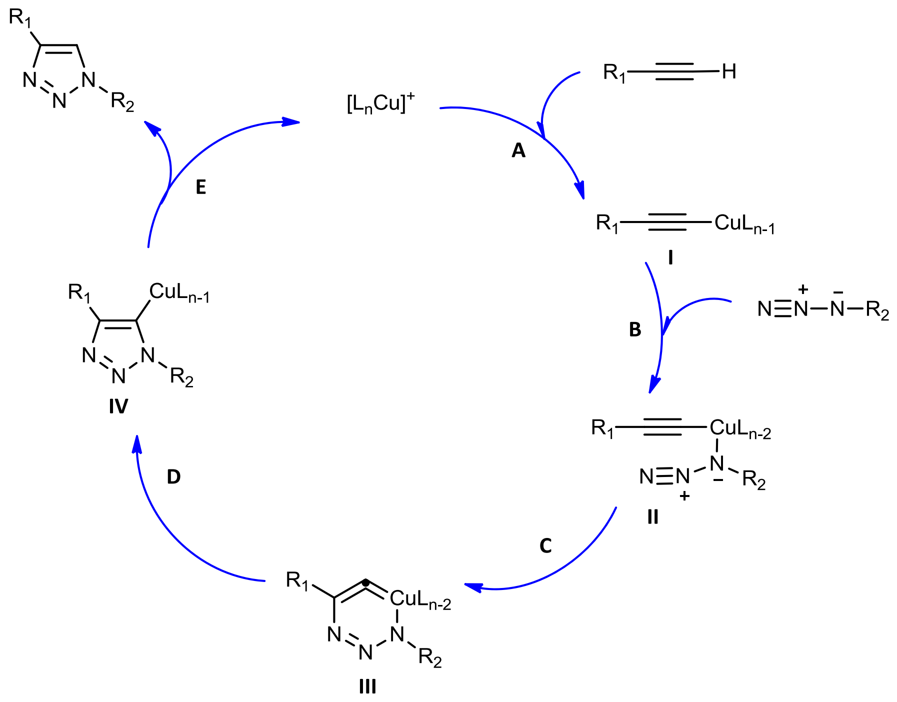

**Figure 1.7** Proposed catalytic cycle for the Cu(I)-catalyzed ligation.

*Applications*

Although the CuAAC is ideal for many applications, Cu(I) has the undesirable side effect of being cytotoxic at low concentrations and therefore, non suitable for bioconjugation in living systems. However, many ligands and catalytic systems have been developed to minimize the toxicity and accelerate the reaction rates, making CuAAC suitable for a bionconjugation process (Fig. 1.8).[43]

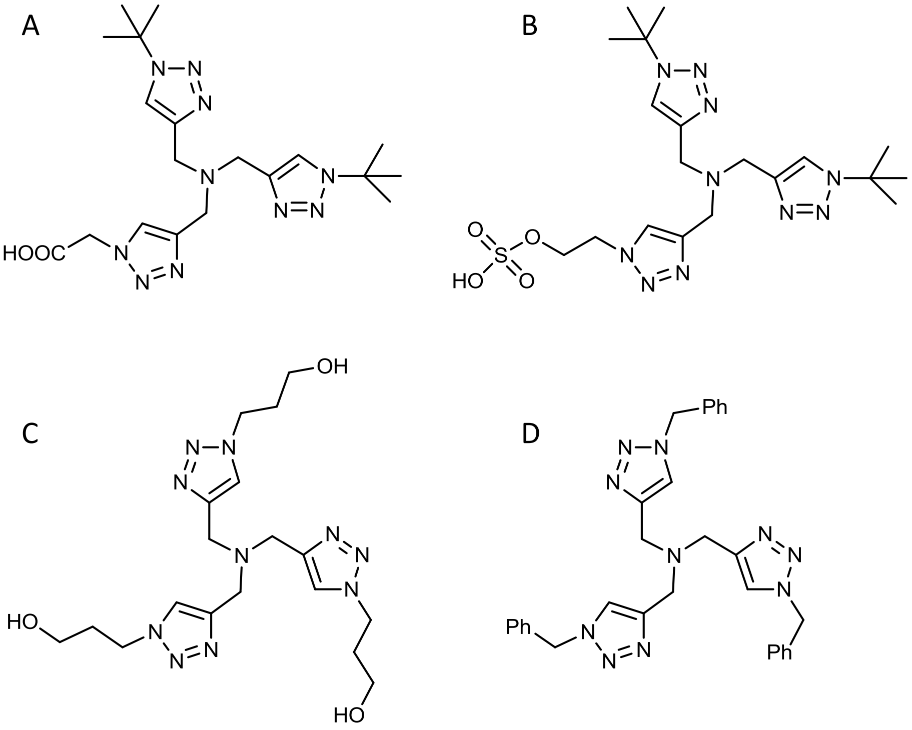

**Figure 1.8** Structures of tris(triazolylmethyl)amine-based ligands used for CuAAC bioconjugation reactions: (*A*) BTTAA; (*B*) BTTES; (*C*) THPTA, and (*D*) TBTA.

The copper-mediated reaction has been used for different bioconjugation applications. For example, activity-based protein profiling was developed in order to tag proteins with active site-directed probes and monitor their expression levels and function in complex proteomes.[8, 12] Tirret *et al.* incorporated nonnatural azido-amino acids into the *E. coli* cell membrane proteins, which were modified with biotin-alkyne via CuAAC.[7, 44] Schultz and coworkers introduced azido-amino acids into proteins, which were labeled with fluorescent dyes via click reactions.[45-46] Moreover, the use of click reactions to fluorescently label DNA has also been reported.[47-48]

*CuAAC based Fluorogenic Reactions*

One important application of bioconjugation is to selectively modify the cellular components with signaling probes for *in vivo* imaging, proteomics, cell biology and functional genomics. By means of an appropriate fluorescent tag, both the location and the abundance of the target biomolecules can be conveniently tracked. However, most dyes fluoresce continuously and show no difference in their fluorescence properties after labeling. Therefore, any unreacted free dye could interfere with the dye attached to the molecules of interest, lowering the signal to background contrast. An ideal alternative to avoid these drawbacks is to use fluorogenic fluorochromes able to show a shift on their emission wavelength after the labeling reaction. In this context, the CuAAC reaction is an ideal platform to develop new fluorogenic reactions, due to its biocompatibility, high reaction rates and quantitative transformation (Fig. 1.9).

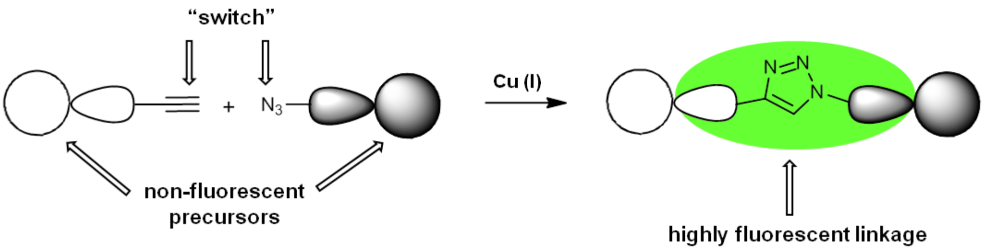

**Figure 1.9** Schematic representation of fluorogenic CuAAC reaction.

Different fluorogenic dyes suitable for CuAAC reactions have been designed to have low or no baseline fluoroscence by masking the core fluorophore with an electron-donating azide or electron-withdrawing alkyne, which quenches the fluorescence. After the click reaction, the resulting conjugated triazole structure allows the electron delocalization required for fluorescence. Many of the reported 'click-on' fluorogenic dyes derive from coumarin,[49-52] anthracene,[53] naphtalimide[54] and alkyne-containing benzothiazole systems (Fig. 1.10).[55]

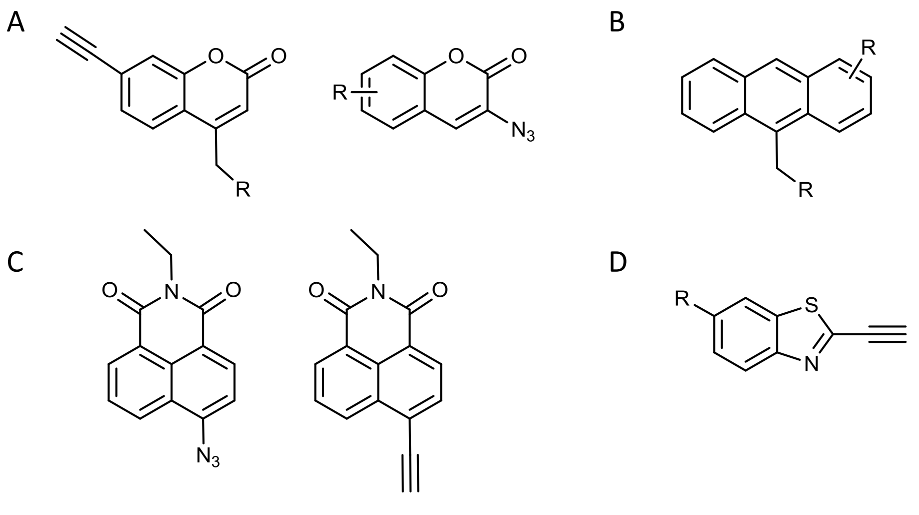

**Figure 1.10** Examples of existing fluorogenic dyes containing azido or alkyne functionalization. (*A*) coumarin derivatives; (*B*) anthracene derivatives; (*C*) naphtalimides, and (*D*) benzothiazole derivative.

*Applications*

Among the applications of fluorogenic CuAAC, *in situ* labeling of proteins is the most significant one. Tirrell and coworkers incorporated noncanonical amino acids with alkyne functionality into proteins in bacterial and mammalian cells. The newly synthesized proteins were labeled *in vivo* with an azido-profluorophore by CuAAC.[51, 56] It has also been described the use of fluorogenic CuAAC reactions to label fucosylated glycans tagged with an alkyne functionality *in vivo*.[54, 57]

Another remarkable application of this reaction is the labeling of DNA. Carell *et al.* developed a multiple postsynthetic labeling of alkyne modified DNA by fluorogenic click reactions with different azides.[58] On the other hand, Seela and coworkers designed a series of functionalized nucleosides with nonfluorescent azide-based coumarins. In this way, alkynyl chains were introduced into oligonucleotides and incorporated into oligodeoxyribonucelotides for further tagging.[59-61]

Furthermore, fluorogenic conjugation of viruses has also been reported. Finn *et al.* labeled the cowpea mosaic virus with fluorescein.[62] Other authors, as Wang and coworkers, modified the surface of tobacco mosaic virus by transforming tyrosine residues into alkynes and performing CuAAC reactions with different azides.[63]

### 1.2.1.3 Strain-promoted azide-alkyne cycloaddition (SPAAC)

As mentioned previously, exogenous metals can have mild to severe cytotoxic effects. Subsequently, they can disturb the delicate balance of the biological systems being studied.[64] In this context, the development of bioorthogonal reactions based on cycloadditions lacking an exogenous metal catalyst, called *Cu-free click reactions*, has been crucial in chemical biology.

In an effort to activate the alkyne component for the direct [3+2] cycloaddition with azides, the use of ring strain as a way to overcome the sluggish reactivity of alkynes has been explored. Thus, in 1961, Wittig and Krebs demonstrated for the first time that cyclooctyne, the smallest stable cycloalkyne, reacts with azides to form the corresponding 1,2,3-triazole.[65] The massive bond angle deformation of the alkyne to ~160° accounts for nearly 18 kcal/mol of ring strain (Fig. 1.11). This destabilization of the ground state versus the transition state of the reaction provides a dramatic rate acceleration compared to unstrained alkynes. In contrast to CuAAC, the cycloaddition with cyclooctynes forms a 1:1 mixture of regiosisomeric 1,2,3-triazoles. This process is known as "strain promoted alkyne-azide cycloaddition (SPAAC)" due to the requirement of the ring strain in the cyclooctyne system for the click reaction to take place.

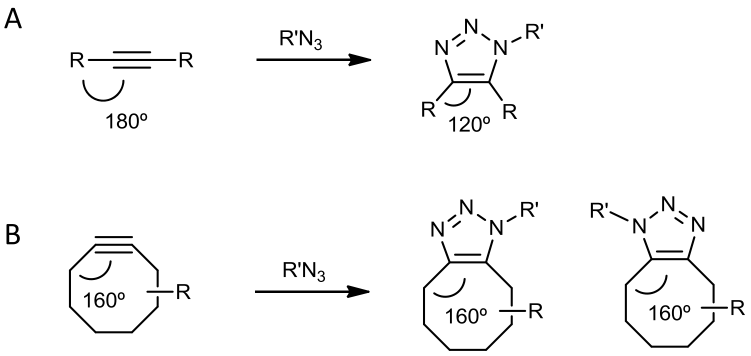

**Figure 1.11** 1,3-dipolar cycloadditions between azides and alkynes. (*A*) Cycloaddition involging azides and linear alkynes. (*B*) *Cu-free*, strain-promoted cycloaddition between azides and cyclooctynes.

The first cyclooctyne evaluated by the Bertozzi group (Fig. 1.12*A*) was shown to undergo cycloaddition with azides to give the corresponding triazoles. Although its reaction kinetics were faster, compared to the linear alkynes, they were still considerably slower than those of CuAAC reactions.[10]

In order to improve the kinetics of the SPAAC reaction, the installation of a LUMO-lowering electron withdrawing group, such as fluorine, was considered. Thus, α-monofluorinated[66] and α,α-difluorinated (DIFO)[67] cyclooctyne sytems were prepared (Fig. 1.12*B*-*C*). The reaction kinetics turned out to be 2-fold and 40-fold faster than those of the original reagent, respectively. However, while the rate of reaction for DIFO was exceptionally high, its solubility was less than ideal. Furthermore, the hydrophobicity of these cyclooctynes could also promote membrane sequestration or nonspecific binding. In order to enhance water solubility, a nitrogen atom within the strained ring system was introduced (Fig. 1.12*D*).[68] In addition, the presence of two metoxy groups in these azacyclooctyne derivatives also increased their polarity.

While Bertozzi and coworkers added fluorine atoms to their cyclooctynes to increase their reaction rates, the Boons' group increased the strain energy by means of a functionalized dibenzocyclooctyne derivative (Fig. 1.12*E*).[69] These systems are relatively easy to synthesize and can be derivatized at various aryl positions to enhance their reaction kinetics or water solubility. Moreover, dibenzocyclooctynes react with azides almost as fast as DIFO does.

On the other hand, Rutjes and co-workers developed an alkyne surrogate consisting of an oxanorbornadiene where the strained double bond is activated with trifluoromethyl groups (Fig. 1.12*F*).[70] This compound gives acceptable rate constants for the click reaction.

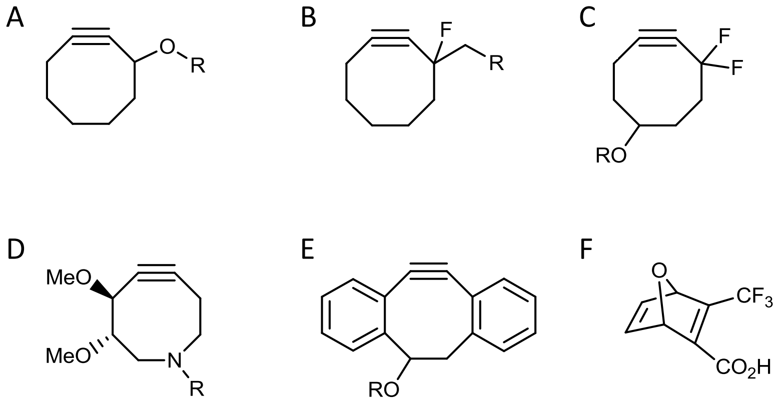

**Figure 1.12** Structures of strained alkynes or alkenes for *Cu-free* [3+2] cycloadditions with azides. (*A*) Simple cyclooctyne; (*B*) monofluorinated cyclooctyne; (*C*) difluorinated cyclooctyne (DIFO); (*D*) azacyclooctyne; (*E*) dibenzocyclooctyne probes, and (*F*) oxanorbornadiene.

*Applications*

Such activated cyclooctynes have allowed the selective labeling of cells bearing modified surface glycoproteins resulting from the metabolic incorporation of azidosugars. Following the same strategy, it has been possible to monitor glycan trafficking in zebrafish embryos (Fig. 1.13).[71]

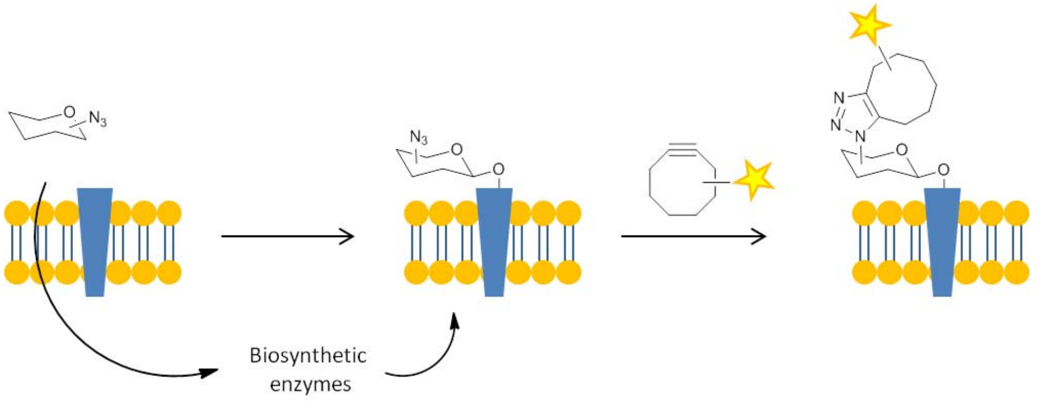

**Figure 1.13** Imaging cell-surface azidosugars with cyclooctyne probes. Azidosugars are metabolized by cells and incorporated into cell-surface glycans. The azide-labeled glycans are then reacted with a cyclooctyne-conjugated imaging probe.

Moreover, a tool for the screening of enzymes that are able to install azido amino acids in cell surface proteins of *Escherichia Coli* has been developed based on this type of *Cu-free* click chemistry methods.[72]

Other applications of the SPAAC reactions include the labeling of azido-tagged cellular proteins in living cells with a set of cell-permeable cyclooctynes[73] and the preparation of dybenzocyclooctyne modified oligonucleotides, suitable for *Cu-free* labeling of DNA.[74]

One of the main objectives of this Doctoral Thesis has been the development of suitable probes for their application to studies related to the biochemical and biophysical properties of sphingolipids by means of click-chemistry processes. In the next sections, we wish to provide the reader with a general overview of some of the most relevant roles played by sphingolipids in live cells, especially those concerning structural aspects and metabolic processes.

## 1.3 Sphingolipids

Sphingolipids (SLs), a class of lipids, are ubiquitous structural components of eukaryotic cell membranes. First discovered by J. L. W. Thudichum in 1876, for a long time were believed to play merely structural roles in membranes. However, intensive research over the last two decades have established that some SLs, including ceramide (Cer), sphingosine (Sph), sphingosine-1-phosphate (S1P), and ceramide-1-phosphate (C1P) are bioactive molecules which play important roles: from regulation of signal transduction pathways[75] to the mediation of cell-to-cell interactions and recognition. The concept of bioactivity implies that changes in SLs levels result in functional consequences.

Moreover, SLs have been reported to dynamically assemble with sterols to form lipid microdomains or rafts. One important property of these lipid rafts is the inclusion of proteins, which favor specific protein-protein interactions, activating specific signaling cascades.[76] In addition, these biochemical microstructures are intimately associated with cell signaling.[77-78]

On the other hand, disruption of SL metabolism leads to the establishment and progression of diseases, such as neurodegenerative diseases, cardiovascular diseases, chronic inflammation or cancer.[79-88]

All these discoveries have grown interest in the development of molecular and chemical tools[89] to study SL metabolism.

### 1.3.1 Structure

SLs contain a hydrophobic aminodiol backbone, known as sphingoid base, *N*-linked to a fatty acid and, some of them, also *O*-linked to a charged head group (Fig. 1.14).

The sphingoid bases are long-chain aliphatic compounds and comprehend a wide array of 2-amino-1,3-dihydroxyalkanes or 2-amino-1,3-dihydroxyalkenes with (2*S*,3*R*)-*erythro* configuration.[80] The most frequent in mammal tissues are sphingosine (Sph), sphinganine (dhSph), and phytosphingosine, also found abundantly in yeast and plants. These species can be found in its amino-free form or *N*-acylated with fatty acids of variable length and desaturation, generating a diversity of ceramide species.

The head groups define the diverse sphingolipid classes, with a hydroxyl group found in ceramides and a phosphate in the phosphorilated derivatives. Complex SLs hold a phosphorylcholine moiety in sphingomyelin (SM), and one or several carbohydrate units in the various known glycosphingolipids (GLs).

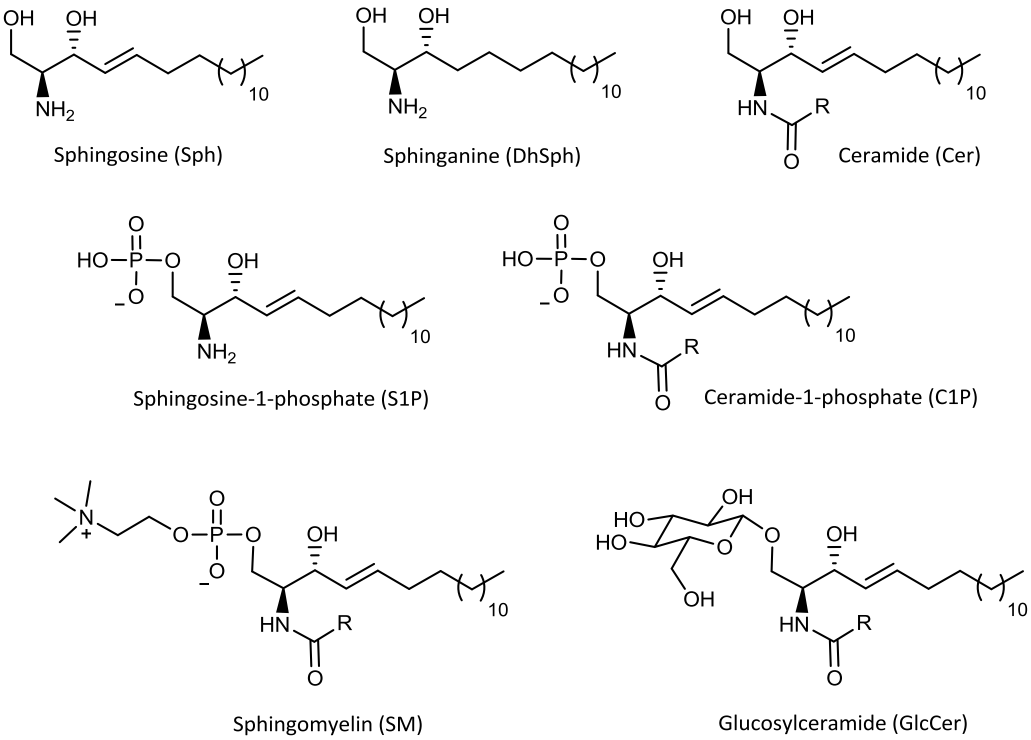
Sphingosine (Sph)
Sphinganine (DhSph)
Ceramide (Cer)
Sphingosine-1-phosphate (S1P)
Ceramide-1-phosphate (C1P)
Sphingomyelin (SM)
Glucosylceramide (GlcCer)

**Figure 1.14** Structure of diverse SL classes. R represents different acyl chains.

### 1.3.2 Sphingolipid metabolism

Ceramide is considered to be the central hub of sphingolipid metabolism. This molecule can be formed through four different pathways: (1) the *de novo* biosynthesis, (2) the sphingomyelin cycle, (3) the hydrolysis of glycosphingolipids, and (4) the salvage pathway (Fig. 1.15).

#### 1.3.2.1 *De novo* biosynthesis

*De novo* biosynthesis starts in the endoplasmic reticulum (ER) with the condensation of L-serine and palmitoyl-CoA to generate 3-ketosphinganine. This transformation is catalyzed by the enzyme serine palmitoyltransferase (SPT) and is the rate-limiting step of the pathway. This molecule is subsequently reduced to dihydrosphingosine and then acylated at the amide group by dihydroceramide synthase (CerS), forming dihydroceramide (dhCer).[90] CerS exhibits strict specificity of the fatty acid added to the sphingoid base and determine the fatty acid composition of SLs in the cell. Most dihydroceramides are immediately desaturated to ceramides by dihydroceramide desaturase (Des1).

Ceramide is transported to the Golgi apparatus, by vesicular or protein-facilitated transport, and further metabolized into more complex SLs, such as sphingomyelins or glycosphingolipids, respectively. Alternatively, ceramide can be phosphorylated into ceramide-1-phosphate by ceramide kinase (CK) or hydrolyzed into sphingosine by ceramidases (CDase).

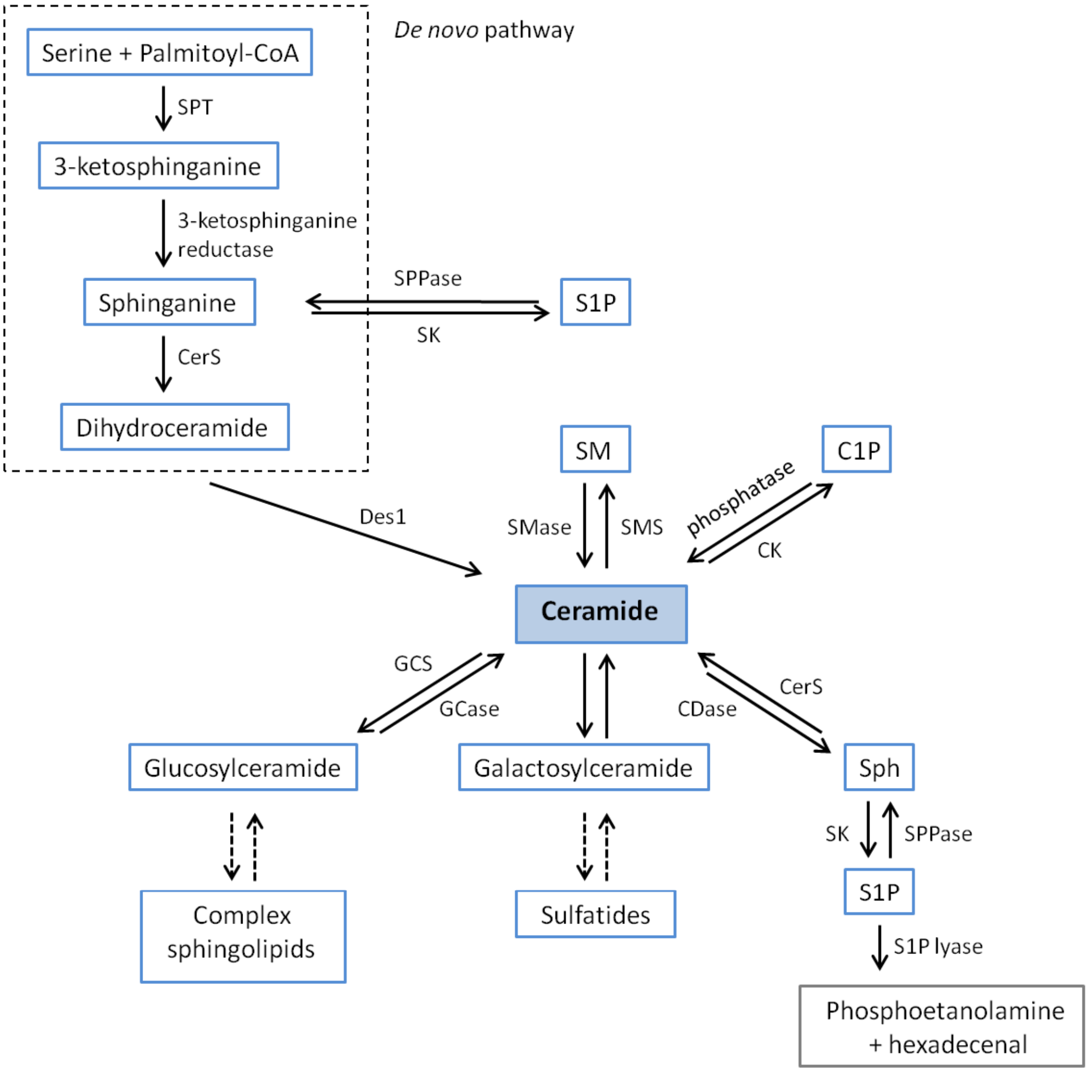
De novo pathway
Serine + Palmitoyl-CoA
SPT
3-ketosphinganine
3-ketosphinganine reductase
Sphinganine
SPPase
SK
S1P
CerS
Dihydroceramide
Des1
SM
SMase
SMS
C1P
phosphatase
CK
Ceramide
GCS
GCase
CDase
CerS
Glucosylceramide
Galactosylceramide
Sph
SK
SPPase
S1P
S1P lyase
Complex sphingolipids
Sulfatides
Phosphoethanolamine + hexadecenal

**Figure 1.15** The sphingolipid metabolic pathway.

#### 1.3.2.2 The sphingomyelin cycle

The sphingomyelin cycle is a metabolic pathway by which ceramide is generated from hydrolysis of sphingomyelin through the action of either acid or neutral sphingomyelinases (SMases).[91] These enzymes break down sphingomyelin to produce ceramide and phosphocoline. This pathway is stimulated in response to cell treatment with TNF-$\alpha$,[92] FAS ligand,[93] or oxidative stress.[94] According to their localization inside the cell (see section 1.3.3), the sphingomyelin cycle can be involved in different pathways with different implications in cell fate.

#### 1.3.2.3 The salvage pathway

Ceramide can also be accumulated from the catabolism of complex SLs that are broken down eventually into sphingosine, which is then reused through reacylation to produce ceramide. This latter pathway is known as either sphingolipid recycling or the salvage pathway. This complex mechanism involves a number of key enzymes that include SMases, possibly glucocerebrosidase (GCase), CDase and (dihydro)CerS.

There is evidence that ceramide generated through the salvage pathway plays roles in many biological responses, such as growth arrest, apoptosis, cellular signaling and trafficking.

### 1.3.3 Compartmentalization and regulation of bioactive sphingolipids

Enzymatic reactions in SL metabolism are distributed throughout different cellular compartments (Fig. 1.16). *De novo* synthesis of ceramide occurs on the cytosolic surface of the ER and possibly in ER-associated membranes, such as the perinuclear membrane and mitochondria-associated membranes.[95] Ceramide is transformed into more complex SLs, such as sphingomyelin and glucosylceramide (GlcCer), in the Golgi apparatus. The transport of ceramide to the Golgi occurs either through the action of a specific transfer protein (CERT), which specifically delivers ceramide for sphingomyelin synthesis, or through vesicular transport, which releases ceramide for the synthesis of glucosylceramide. In turn, transfer of glucosylceramide for glycosphingolipid synthesis requires the action of the transport protein FAPP2.[96] Finally, complex glycosphingolipids are formed in the luminal side of the Golgi. Therefore, glucosylceramide requires flipping from the cytosolic surface to the inside of the Golgi, possibly with the aid of the ABC transporter, P-glycoprotein.[97]

Subsequently, sphingomyelin and complex glycosphingolipids are transported to the plasma membrane via vesicular trafficking. There, sphingomyelin can be metabolized to ceramide, and subsequently to other bioactive SLs.

SLs may be recirculated from the plasma membrane through the endosomal pathway. In the lysosomal compartment, sphingomyelin and glucosylceramide are degraded to ceramide, which is subsequently hydrolyzed to sphingosine. Due to its ionizable positive charge, the salvaged sphingosine is able to leave the lysosome and shows adequate solubility in the cytosol to move between membranes, including ER, where it would be available for recycling.[98]

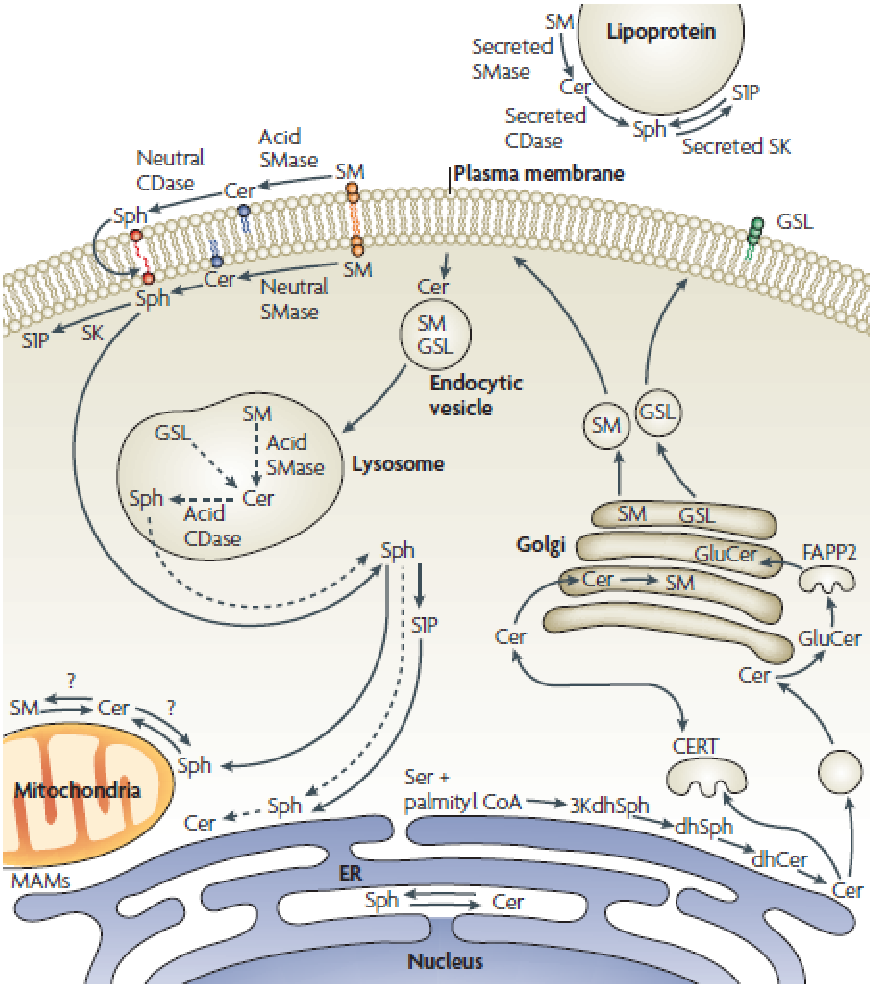
SM
Lipoprotein
Secreted SMase
Cer
S1P
Secreted CDase
Sph
Secreted SK
Acid SMase
Neutral CDase
SM
Cer
Plasma membrane
Sph
GSL
SM
Cer
Neutral SMase
Sph
Cer
S1P
SK
SM
GSL
Endocytic vesicle
SM
GSL
Acid SMase
Lysosome
Sph
Cer
Acid CDase
SM
GSL
Golgi
GluCer
FAPP2
Cer
SM
Sph
S1P
Cer
GluCer
Cer
?
SM
Cer
?
Sph
Mitochondria
CERT
Ser +
palmityl CoA
3KdhSph
dhSph
Cer
Sph
dhCer
Cer
MAMs
ER
Sph
Cer
Nucleus

**Figure 1.16** Compartmentalization of metabolites and enzymes of the SL pathway. Image taken from ref. [75].

## 1.3.4 Bioactive sphingolipids

### 1.3.4.1 Ceramide

All cells contain endogenous ceramides, which differ in their long chain sphingoid base, as well as in their fatty acid composition. These endogenous ceramides can be generated as previously described (see section 1.3.2), and serve as the precursor for all major SLs in eukaryotes.

Ceramide has been proposed as an important second messenger in various stress responses and growth mechanisms. Its formation by activation of either SMases or the *de novo* pathway, but also as a consequence of inhibition of ceramide clearance, occurs in response to many stress inducers (Fig. 1.17). Such inducers include cytokines (TNF, Fas, nerve growth factor),[99-100] environmental stresses (heat, UV radiation, hypoxia),[101] and chemotherapeutic agents (cytarabine or doxorubicin).[102-104]

Besides, ceramide is intimately involved in cellular processes such as differentiation,[105] senescence,[106] necrosis,[107] proliferation,[108] and apoptosis.[109] The identified key targets for ceramide action include the ceramide-activated protein phosphatases PP1 and PP2A, which exhibit specificity for the *D-erythro* stereoisomer *in vitro*.[110] Moreover, ceramide may regulate protein kinase C (PKC) ζ,[111] raf-1,[112] and the kinase-supressor of Ras,[113] significantly changing the level of phosphorylation of various key substrates. Another target is the cathepsin D, a ceramide-binding protein, which may mediate the actions of lysosomally generated ceramide.[114]

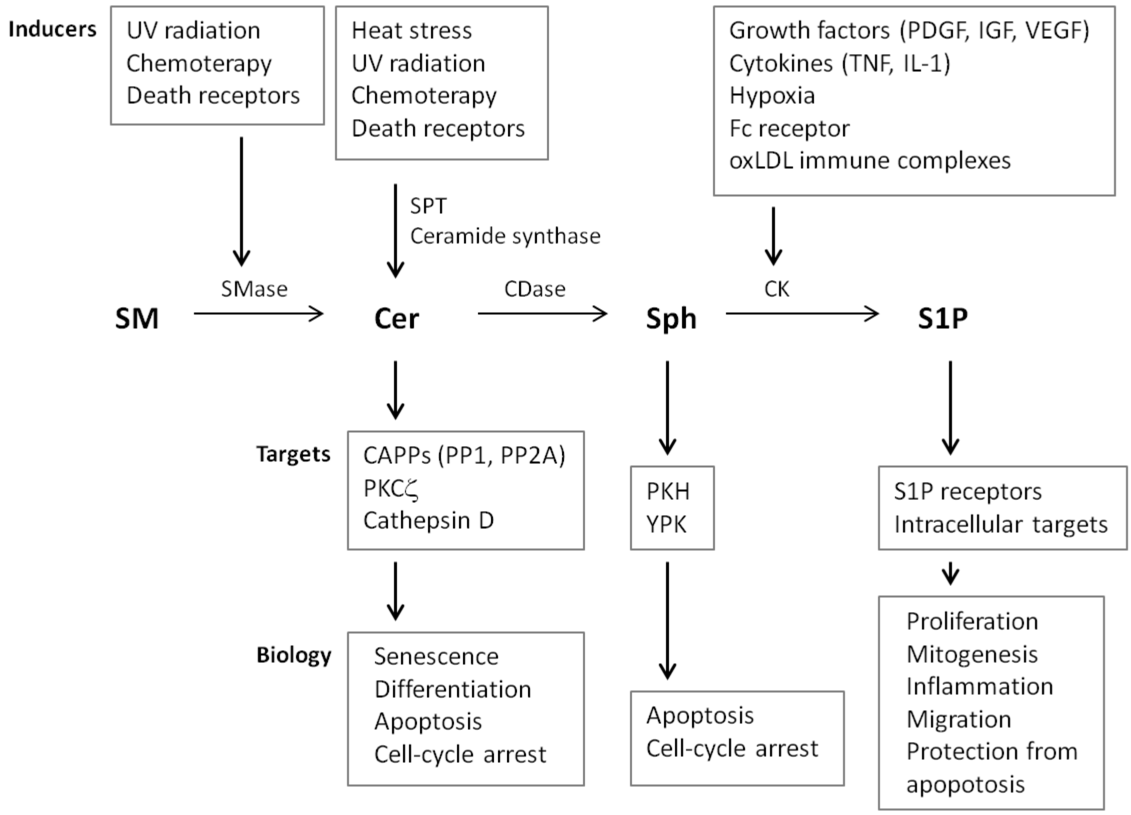
Inducers
UV radiation
Chemoterapy
Death receptors
Heat stress
UV radiation
Chemoterapy
Death receptors
Growth factors (PDGF, IGF, VEGF)
Cytokines (TNF, IL-1)
Hypoxia
Fc receptor
oxLDL immune complexes
SPT
Ceramide synthase
SMase
CDase
CK
SM
Cer
Sph
S1P
Targets
CAPPs (PP1, PP2A)
PKCζ
Cathepsin D
PKH
YPK
S1P receptors
Intracellular targets
Biology
Senescence
Differentiation
Apoptosis
Cell-cycle arrest
Apoptosis
Cell-cycle arrest
Proliferation
Mitogenesis
Inflammation
Migration
Protection from apopotosis

**Figure 1.17** An overview of the roles of sphingolipids in biology.

### 1.3.4.2 Sphingosine

Sphingosine has been described to induce double-stranded degradation of genomic DNA, and to limit the proliferative capacity and viability in a variety of cell types, involving the induction of apoptosis (Fig. 1.17).[115-118] Its apoptotic effect is based on the physiological inhibition of PKC, a protein whose activity is crucial for cell survival.[119] Moreover, sphingosine may involve the modulation of additional regulatory systems such as ERK and Akt/Protein kinase B.[117]

### 1.3.4.3 Phosphorylated metabolites: sphingosine-1-phosphate and ceramide-1-phosphate

Sphingosine-1-phosphate acts antagonistically to ceramide, by enhancing cell survival, as shown in Fig. 1.17. Angiogenesis, migration, adhesion and inflammation are other cellular processes in which sphingosine-1-phosphate is also involved.[120-121] Extracellular actions of sphingosine-1-phosphate are mediated by its interaction with a family of five

G-protein-coupled receptors (GPCRs). The signaling through these GPCRs has been shown to be atypical in a variety of cancers.[122] However, intracellular actions of this bioactive SL are independent of these receptors.

Ceramide-1-phosphate is also a potent stimulator of cell proliferation. In addition, ceramide-1-phosphate regulates apoptosis, and is involved in the inflammatory response.[123] Unlike sphingosine-1-phosphate, this phosphorylated SL is not believed to act through a cell surface receptor. It might function instead at the intracellular level. Ceramide-1-phosphate has been described to affect inflammation trough the direct activation of its target $cPLA_2$, stimulating arachidonic acid release.[124-125] As well as increasing DNA synthesis, ceramide-1-phosphate stimulates cell proliferation through activation of mitogenic pathways. In addition, ceramide-1-phosphate is a cell death potent inhibitor. This pro-survival effect is due to inhibition of apoptosis by inactivation of SMase, resulting in a reduction of endogenous ceramides.

#### 1.3.4.4 Sphingomyelin

Sphingomyelin is the most abundant sphingolipid found in animal cell membranes, especially in the membranous myelin sheath that surrounds some nerve cell axons. It is believed to be the only cell membrane phospholipid not derived from glycerol. In addition, sphingomyelin represents ~85% of all SLs in humans.

From studies on epithelial cell polarity, it has been established that SLs dynamically assemble with cholesterol to form lipid rafts, in the exoplasmic leaflet of the bilayer. The abundance of saturated hydrocarbon chains in SLs allows cholesterol to be tightly intercalated, mimicking the organization of the liquid-ordered state in model membranes. The inner leaflet is rich in phospholipids with saturated fatty acids and cholesterol, and it is not yet clear how the inner leaflet is coupled to the outer leaflet. One possibility is that SLs long fatty acids in the outer leaflet couple the exoplasmic and cytoplasmatic leaflets by interdigitation. Transmembrane proteins could also stabilize this coupling. Lipid rafts are considered liquid-ordered domains, which are dispersed in a liquid-disordered matrix of unsaturated glycerolipids.[126-127] One of the most important properties of lipid rafts is that they can include or exclude proteins to variable extents.[128-129] Proteins with raft affinity include glycosylphosphatidylinositol-anchored proteins, doubly acylated proteins, cholesterol-linked and palmitoylated proteins. The most important role of lipid rafts at the cell surface may be their function in signal transduction.[130]

Besides its structural function, sphingomyelin has been described to have potential effects as chemotherapeutic and chemopreventive agent.[131-132] This effect relies on the increase of the chemotherapy response of cancer cells.

#### 1.3.4.5 Dihydroceramide

Dihydroceramide is formed from dihydrosphingosine by action of CerS, and subsequently converted to ceramide by Des1.

Initially, dihydroceramide was thought not to play roles in apoptosis and cell cycle arrest.[133-134] However, intensive research revealed new roles of dihydroceramide in cells. Induction of autophagy upon treatment with exogenous dihydroceramide analogs is the first clue of dihydroceramide as a bioactive SL. This effect was demonstrated on both prostate and gastric cancer cells.[135-136] Moreover, levels of dihydroceramide were elevated after photodynamic therapy (PDT) in squamous cell carcinoma. This finding might support that the *de novo* SL pathway is a PDT target.[137] Besides its role in autophagy, dihydroceramide is also thought to be important in growth suppression and hypophosphorylation of Rb protein.[138-139] Exogenously applied dihydroceramide can be hydrolyzed by the enzymes ACER2/haCER2[140] and ACER3[141] to dihydrosphingosine, which might then be responsible for the cellular effects thought to be caused by the dihydroceramide itself. A recent study has supported this fact, showing that dihydroceramide and dihydrosphingosine levels are elevated in various tumor cells upon treatment with fenretinide, where dihydrosphingosine is likely to be the inducer of the observed cytotoxicity.[142]

## 1.4 References

1. Kolb, H. C.; Finn, M. G.; Sharpless, K. B., Click chemistry: diverse chemical function from a few good reactions. *Angew. Chem., Int. Ed.* **2001,** 40, 2004-2021.

2. Griffin, B. A.; Adams, S. R.; Tsein, R. Y., Specific covalent labeling of recombinant protein molecules inside live cells. *Science (Washington, DC, U.S.)* **1998,** 281, 269-272.

3. Adams, S. R.; Campbell, R. E.; Gross, L. A.; Martin, B. R.; Walkup, G. K.; Yao, Y.; Llopis, J.; Tsien, R. Y., New biarsenical ligands and tetracysteine motifs for protein labeling in vitro and in vivo: Synthesis and biological applications. *J. Am. Chem. Soc.* **2002,** 124, 6063-6076.

4. Chen, I.; Howarth, M.; Lin, W.; Ting, A. Y., Site-specific labeling of cell surface proteins with biophysical probes using biotin ligase. *Nat. Methods* **2005,** 2, 99-104.

5. Zhang, Z.; Smith, B. A. C.; Wang, L.; Brock, A.; Cho, C.; Schultz, P. G., A New Strategy for the Site-Specific Modification of Proteins in Vivo. *Biochemistry* **2003,** 42, 6735-6746.

6. Mahal, L. K.; Yarema, K. J.; Bertozzi, C. R., Engineering chemical reactivity on cell surfaces through oligosaccharide biosynthesis. *Science (Washington, DC, U.S.)* **1997,** 276, 1125-1128.

7. Link, A. J.; Vink, M. K. S.; Tirrell, D. A., Presentation and Detection of Azide Functionality in Bacterial Cell Surface Proteins. *J. Am. Chem. Soc.* **2004,** 126, (34), 10598-10602.

8. Speers, A. E.; Adam, G. C.; Cravatt, B. F., Activity-Based Protein Profiling in Vivo Using a Copper(I)-Catalyzed Azide-Alkyne [3 + 2] Cycloaddition. *J. Am. Chem. Soc.* **2003,** 125, (16), 4686-4687.

9. Prescher, J. A.; Dube, D. H.; Bertozzi, C. R., Chemical remodelling of cell surfaces in living animals. *Nature (London, U. K.)* **2004,** 430, 873-877.

10. Agard, N. J.; Prescher, J. A.; Bertozzi, C. R., A strain-promoted [3+2] azide-alkyne cycloaddition for covalent modification of biomolecules in living systems. *J. Am. Chem. Soc.* **2004,** 126, 15046-15047.

11. Kho, Y.; Kim, S. C.; Jiang, C.; Barma, D.; Kwon, S. W.; Cheng, J.; Jaunbergs, J.; Weinbaum, C.; Tamanoi, F.; Falck, J.; Zhao, Y., A tagging-via-substrate technology for detection and proteomics of farnesylated proteins. *Proc. Natl. Acad. Sci. U.S.A.* **2004,** 101, 12479-12484.

12. Speers, A. E.; Cravatt, B. F., Profiling Enzyme Activities In Vivo Using Click Chemistry Methods. *Chem. Biol.* **2004,** 11, (4), 535-546.

13. Devaraj, N. K.; Upadhyay, R.; Haun, J. B.; Hilderbrand, S. A.; Weissleder, R., Fast and Sensitive Pretargeted Labeling of Cancer Cells through a Tetrazine/trans-Cyclooctene Cycloaddition. *Angew. Chem., Int. Ed.* **2009,** 48, (38), 7013-7016.

14. Devaraj, N. K.; Hilderbrand, S.; Upadhyay, R.; Mazitschek, R.; Weissleder, R., Bioorthogonal Turn-On Probes for Imaging Small Molecules inside Living Cells. *Angew. Chem., Int. Ed.* **2010,** 49, (16), 2869-2872.

15. Song, W.; Wang, Y.; Qu, J.; Lin, Q., Selective Functionalization of a Genetically Encoded Alkene-Containing Protein via “Photoclick Chemistry” in Bacterial Cells. *J. Am. Chem. Soc.* **2008,** 130, (30), 9654-9655.

16. Ripoll, J. L.; Rouessac, A.; Rouessac, F., Recent applications of the retro-Diels-Alder reaction in organic synthesis. *Tetrahedron* **1978,** 34, 19-40.

17. Diakoumakos, C. D.; Mikroyannidis, J. A., Polyimides derived from Diels-Alder polymerization of furfuryl-substituted maleamic acids or from the reaction of bismaleamic with bisfurfurylpyromellitamic acids. *J. Polym. Sci., Part A: Polym. Chem.* **1992,** 30, 2559-67.

18. Gousse, C.; Gandini, A., Diels-Alder polymerization of difurans with bismaleimides. *Polym. Int.* **1999,** 48, 723-731.

19. Mantovani, G.; Lecolley, F.; Tao, L.; Haddleton, D. M.; Clerx, J.; Cornelissen, J. J. L. M.; Velonia, K., Design and Synthesis of N-Maleimido-Functionalized Hydrophilic Polymers via Copper-Mediated Living Radical Polymerization: A Suitable Alternative to PEGylation Chemistry. *J. Am. Chem. Soc.* **2005,** 127, 2966-2973.

20. Tonga, M.; Cengiz, N.; Kose, M. M.; Dede, T.; Sanyal, A., Dendronized polymers via Diels-Alder "click" reaction. *J. Polym. Sci., Part A: Polym. Chem.* **2010,** 48, 410-416.

21. Hill, K. W.; Taunton-Rigby, J.; Carter, J. D.; Kropp, E.; Vagle, K.; Pieken, W.; McGee, D. P. C.; Husar, G. M.; Leuck, M.; Anziano, D. J.; Sebesta, D. P., Diels–Alder Bioconjugation of Diene-Modified Oligonucleotides. *J. Org. Chem.* **2001,** 66, (16), 5352-5358.

22. Hackenberger, C. P.; Schwarzer, D., Chemoselective ligation and modification strategies for peptides and proteins. *Angew. Chem., Int. Ed.* **2008,** 47, (52), 10030-74.

23. Lin, P.-C.; Weinrich, D.; Waldmann, H., Protein Biochips: Oriented Surface Immobilization of Proteins. *Macromol. Chem. Phys.* **2010,** 211, (2), 136-144.

24. Monzo, A.; Guttman, A., Immobilization techniques for mono- and oligosaccharide microarrays. *QSAR Comb. Sci.* **2006,** 25, 1033-1038.

25. Love, K. R.; Seeberger, P. H., Carbohydrate arrays as tools for glycomics. *Angew. Chem., Int. Ed.* **2002,** 41, 3583-3586.

26. Shi, M.; Wosnick, J. H.; Ho, K.; Keating, A.; Shoichet, M. S., Immuno-polymeric nanoparticles by Diels-Alder Chemistry. *Angew. Chem., Int. Ed.* **2007,** 46, 6126-6131.

27. Griffin, R. J., 3 The Medicinal Chemistry of the Azido Group. In *Progress in Medicinal Chemistry*, Ellis, G. P.; Luscombe, D. K., Eds. Elsevier: 1994; Vol. 31, pp 121-232.

28. Kiick, K. L.; Saxon, E.; Tirrell, D. A.; Bertozzi, C. R., Incorporation of azides into recombinant proteins for chemoselective modification by the Staudinger ligation. *Proc. Natl. Acad. Sci. U.S.A.* **2002,** 99, 19-24.

29. Saxon, E.; Bertozzi, C. R., Cell surface engineering by a modified Staudinger reaction. *Science (Washington, DC, U.S.)* **2000,** 287, 2007-2010.

30. Nilsson, B. L.; Kiessling, L. L.; Raines, R. T., Staudinger Ligation: A Peptide from a Thioester and Azide. *Org. Lett.* **2000,** 2, (13), 1939-1941.

31. Saxon, E.; Armstrong, J. I.; Bertozzi, C. R., A “Traceless” Staudinger Ligation for the Chemoselective Synthesis of Amide Bonds. *Org. Lett.* **2000,** 2, (14), 2141-2143.

32. Vocadlo, D. J.; Hang, H. C.; Kim, E.-J.; Hanover, J. A.; Bertozzi, C. R., A chemical approach for identifying O-GlcNAc-modified proteins in cells. *Proc. Natl. Acad. Sci. U.S.A.* **2003,** 100, (16), 9116-9121.

33. Hang, H. C.; Yu, C.; Kato, D. L.; Bertozzi, C. R., A metabolic labeling approach toward proteomic analysis of mucin-type O-linked glycosylation. *Proc. Natl. Acad. Sci. U.S.A.* **2003,** 100, (25), 14846-14851.

34. Luchansky, S. J.; Argade, S.; Hayes, B. K.; Bertozzi, C. R., Metabolic Functionalization of Recombinant Glycoproteins. *Biochemistry* **2004,** 43, (38), 12358-12366.

35. Koehn, M.; Breinbauer, R., The Staudinger ligation - A gift to chemical biology. *Angew. Chem., Int. Ed.* **2004,** 43, 3106-3116.

36. Padwa, A., *1,3-dipolar cycloaddition chemistry*. Wiley: 1984.

37. Huisgen, R., 1,3-Dipolar Cycloadditions. Past and Future. *Angew. Chem., Int. Ed.* **1963,** 2, (10), 565-598.

38. Rasmussen, L. K.; Boren, B. C.; Fokin, V. V., Ruthenium-Catalyzed Cycloaddition of Aryl Azides and Alkynes. *Org. Lett.* **2007,** 9, 5337-5339.

39. Rostovtsev, V. V.; Green, L. G.; Fokin, V. V.; Sharpless, K. B., A Stepwise Huisgen Cycloaddition Process: Copper(I)-Catalyzed Regioselective "Ligation" of Azides and Terminal Alkynes. *Angew. Chem., Int. Ed.* **2002,** 41, (14), 2596-2599.

40. Tornoe, C. W.; Christensen, C.; Meldal, M., Peptidotriazoles on Solid Phase: [1,2,3]-Triazoles by Regiospecific Copper(I)-Catalyzed 1,3-Dipolar Cycloadditions of Terminal Alkynes to Azides. *J. Org. Chem.* **2002,** 67, 3057-3064.

41. Kolb, H. C.; Sharpless, K. B., The growing impact of click chemistry on drug discovery. *Drug Discovery Today* **2003,** 8, 1128-1137.

42. Himo, F.; Lovell, T.; Hilgraf, R.; Rostovtsev, V. V.; Noodleman, L.; Sharpless, K. B.; Fokin, V. V., Copper(I)-Catalyzed Synthesis of Azoles. DFT Study Predicts Unprecedented Reactivity and Intermediates. *J. Am. Chem. Soc.* **2005,** 127, 210-216.

43. Hong, V.; Presolski, S. I.; Ma, C.; Finn, M. G., Analysis and Optimization of Copper-Catalyzed Azide-Alkyne Cycloaddition for Bioconjugation. *Angew. Chem., Int. Ed.* **2009,** 48, 9879-9883.

44. Link, A. J.; Tirrell, D. A., Cell Surface Labeling of Escherichia coli via Copper(I)-Catalyzed [3+2] Cycloaddition. *J. Am. Chem. Soc.* **2003,** 125, (37), 11164-11165.

45. Deiters, A.; Cropp, T. A.; Mukherji, M.; Chin, J. W.; Anderson, J. C.; Schultz, P. G., Adding Amino Acids with Novel Reactivity to the Genetic Code of Saccharomyces Cerevisiae. *J. Am. Chem. Soc.* **2003,** 125, (39), 11782-11783.

46. Deiters, A.; Cropp, T. A.; Summerer, D.; Mukherji, M.; Schultz, P. G., Site-specific PEGylation of proteins containing unnatural amino acids. *Bioorg. Med. Chem. Lett.* **2004,** 14, (23), 5743-5745.

47. Seo, T. S.; Li, Z.; Ruparel, H.; Ju, J., Click Chemistry to Construct Fluorescent Oligonucleotides for DNA Sequencing. *J. Org. Chem.* **2002,** 68, (2), 609-612.

48. Seo, T. S.; Bai, X.; Ruparel, H.; Li, Z.; Turro, N. J.; Ju, J., Photocleavable fluorescent nucleotides for DNA sequencing on a chip constructed by site-specific coupling chemistry. *Proc. Natl. Acad. Sci. U.S.A.* **2004,** 101, (15), 5488-5493.

49. Sivakumar, K.; Xie, F.; Cash, B. M.; Long, S.; Barnhill, H. N.; Wang, Q., A Fluorogenic 1,3-Dipolar Cycloaddition Reaction of 3-Azidocoumarins and Acetylenes. *Org. Lett.* **2004,** 6, (24), 4603-4606.

50. Zhou, Z.; Fahrni, C. J., A Fluorogenic Probe for the Copper(I)-Catalyzed Azide–Alkyne Ligation Reaction: Modulation of the Fluorescence Emission via 3(n,π*)–1(π,π*) Inversion. *J. Am. Chem. Soc.* **2004,** 126, (29), 8862-8863.

51. Beatty, K. E.; Liu, J. C.; Xie, F.; Dieterich, D. C.; Schuman, E. M.; Wang, Q.; Tirrell, D. A., Fluorescence Visualization of Newly Synthesized Proteins in Mammalian Cells. *Angew. Chem., Int. Ed.* **2006,** 45, (44), 7364-7367.

52. Li, K.; Lee, A.; Lu, X.; Wang, Q., Fluorogenic "click" reaction for labeling and detection of DNA in proliferating cells. *BioTechniques* **2010,** 49, 525-527.

53. Xie, F.; Sivakumar, K.; Zeng, Q.; Bruckman, M. A.; Hodges, B.; Wang, Q., A fluorogenic 'click' reaction of azidoanthracene derivatives. *Tetrahedron* **2008,** 64, (13), 2906-2914.

54. Sawa, M.; Hsu, T.-L.; Itoh, T.; Sugiyama, M.; Hanson, S. R.; Vogt, P. K.; Wong, C.-H., Glycoproteomic probes for fluorescent imaging of fucosylated glycans in vivo. *Proc. Natl. Acad. Sci. U.S.A.* **2006,** 103, 12371-12376.

55. Qi, J.; Han, M.-S.; Chang, Y.-C.; Tung, C.-H., Developing Visible Fluorogenic 'Click-On' Dyes for Cellular Imaging. *Bioconjugate Chem.* **2011,** 22, 1758-1762.

56. Beatty, K. E.; Xie, F.; Wang, Q.; Tirrell, D. A., Selective Dye-Labeling of Newly Synthesized Proteins in Bacterial Cells. *J. Am. Chem. Soc.* **2005,** 127, (41), 14150-14151.

57. Hsu, T. L.; Hanson, S. R.; Kishikawa, K.; Wang, S. K.; Sawa, M.; Wong, C. H., Alkynyl sugar analogs for the labeling and visualization of glycoconjugates in cells. *Proc. Natl. Acad. Sci. U.S.A.* **2007,** 104, (8), 2614-9.

58. Gierlich, J.; Burley, G. A.; Gramlich, P. M. E.; Hammond, D. M.; Carell, T., Click Chemistry as a Reliable Method for the High-Density Postsynthetic Functionalization of Alkyne-Modified DNA. *Org. Lett.* **2006,** 8, (17), 3639-3642.

59. Seela, F.; Ming, X., Oligonucleotides containing 7-deaza-2'-deoxyinosine as universal nucleoside: synthesis of 7-halogenated and 7-alkynylated derivatives, ambiguous base pairing, and dye functionalization by the alkyne-azide 'click' reaction. *Helv. Chim. Acta* **2008,** 91, 1181-1200.

60. Seela, F.; Sirivolu, V. R., Pyrrolo-dC oligonucleotides bearing alkynyl side chains with terminal triple bonds: synthesis, base pairing and fluorescent dye conjugates prepared by the azide-alkyne "click" reaction. *Org. Biomol. Chem.* **2008,** 6, 1674-1687.

61. Seela, F.; Sirivolu, V. R.; Chittepu, P., Modification of DNA with Octadiynyl Side Chains: Synthesis, Base Pairing, and Formation of Fluorescent Coumarin Dye Conjugates of Four Nucleobases by the Alkyne-Azide "Click" Reaction. *Bioconjugate Chem.* **2008,** 19, 211-224.

62. Meunier, S.; Strable, E.; Finn, M. G., Crosslinking of and Coupling to Viral Capsid Proteins by Tyrosine Oxidation. *Chem. Biol.* **2004,** 11, (3), 319-326.

63. Bruckman, M. A.; Kaur, G.; Lee, L. A.; Xie, F.; Sepulveda, J.; Breitenkamp, R.; Zhang, X.; Joralemon, M.; Russell, T. P.; Emrick, T.; Wang, Q., Surface Modification of Tobacco Mosaic Virus with "Click" Chemistry. *ChemBioChem* **2008,** 9, (4), 519-523.

64. Gaetke, L. M.; Chow, C. K., Copper toxicity, oxidative stress, and antioxidant nutrients. *Toxicology* **2003,** 189, 147-163.

65. Wittig, G.; Krebs, A., On the existence of low-membered cycloalkynes. I. *Chem. Ber.* **1961,** 94, 3260-75.

66. Agard, N. J.; Baskin, J. M.; Prescher, J. A.; Lo, A.; Bertozzi, C. R., A comparative study of bioorthogonal reactions with azides. *ACS Chem. Biol.* **2006,** 1, 644-648.

67. Baskin, J. M.; Prescher, J. A.; Laughlin, S. T.; Agard, N. J.; Chang, P. V.; Miller, I. A.; Lo, A.; Codelli, J. A.; Bertozzi, C. R., Copper-free click chemistry for dynamic in vivo imaging. *Proc. Natl. Acad. Sci. U.S.A.* **2007,** 104, 16793-16797.

68. Sletten, E. M.; Bertozzi, C. R., A Hydrophilic Azacyclooctyne for Cu-Free Click Chemistry. *Org. Lett.* **2008,** 10, 3097-3099.

69. Ning, X.; Guo, J.; Wolfert, M. A.; Boons, G.-J., Visualizing metabolically labeled glycoconjugates of living cells by copper-free and fast huisgen cycloadditions. *Angew. Chem., Int. Ed.* **2008,** 47, 2253-2255.

70. van Berkel, S. S.; Dirks, A. J.; Debets, M. F.; van Delft, F. L.; Cornelissen, J. J. L. M.; Nolte, R. J. M.; Rutjes, F. P. J. T., Metal-Free Triazole Formation as a Tool for Bioconjugation. *ChemBioChem* **2007,** 8, (13), 1504-1508.

71. Laughlin, S. T.; Baskin, J. M.; Amacher, S. L.; Bertozzi, C. R., In Vivo Imaging of Membrane-Associated Glycans in Developing Zebrafish. *Science (Washington, DC, U.S.)* **2008,** 320, 664-667.

72. Link, A. J.; Vink, M. K. S.; Agard, N. J.; Prescher, J. A.; Bertozzi, C. R.; Tirrell, D. A., Discovery of aminoacyl-tRNA synthetase activity through cell-surface display of noncanonical amino acids. *Proc. Natl. Acad. Sci. U.S.A.* **2006,** 103, 10180-10185.

73. Beatty, K. E.; Fisk, J. D.; Smart, B. P.; Lu, Y. Y.; Szychowski, J.; Hangauer, M. J.; Baskin, J. M.; Bertozzi, C. R.; Tirrell, D. A., Live-cell imaging of cellular proteins by a strain-promoted azide-alkyne cycloaddition. *ChemBioChem* **2010,** 11, 2092-2095.

74. Marks, I. S.; Kang, J. S.; Jones, B. T.; Landmark, K. J.; Cleland, A. J.; Taton, T. A., Strain-Promoted "Click" Chemistry for Terminal Labeling of DNA. *Bioconjugate Chem.* **2011,** 22, 1259-1263.

75. Hannun, Y. A.; Obeid, L. M., Principles of bioactive lipid signalling: lessons from sphingolipids. *Nat. Rev. Mol. Cell Biol.* **2008,** 9, (2), 139-150.

76. Simons, K.; Toomre, D., Lipid rafts and signal transduction. *Nat. Rev. Mol. Cell Biol.* **2000,** 1, (1), 31-39.

77. Goñi, F. M.; Alonso, A., Biophysics of sphingolipids I. Membrane properties of sphingosine, ceramides and other simple sphingolipids. *Biochim. Biophys. Acta, Biomembr.* **2006,** 1758, (12), 1902-1921.

78. Goñi, F. M.; Alonso, A., Effects of ceramide and other simple sphingolipids on membrane lateral structure. *Biochim. Biophys. Acta, Biomembr.* **2009,** 1788, (1), 169-177.

79. Merrill, A. H., Jr., Cell regulation by sphingosine and more complex sphingolipids. *J. Bioenerg. Biomembr.* **1991,** 23, (1), 83-104.

80. Merrill, A. H., Jr., De novo sphingolipid biosynthesis: a necessary, but dangerous, pathway. *J. Biol. Chem.* **2002,** 277, 25843-25846.

81. Merrill, A. H., Jr.; Jones, D. D., An update of the enzymology and regulation of sphingomyelin metabolism. *Biochim. Biophys. Acta* **1990,** 1044, (1), 1-12.

82. Merrill, A. H., Jr.; Schmelz, E. M.; Dillehay, D. L.; Spiegel, S.; Shayman, J. A.; Schroeder, J. J.; Riley, R. T.; Voss, K. A.; Wang, E., Sphingolipids--the enigmatic lipid class: biochemistry, physiology, and pathophysiology. *Toxicol. Appl. Pharmacol.* **1997,** 142, (1), 208-25.

83. Kolesnick, R., The therapeutic potential of modulating the ceramide/sphingomyelin pathway. *J. Clin. Invest.* **2002,** 110, (1), 3-8.

84. Kolesnick, R.; Golde, D. W., The sphingomyelin pathway in tumor necrosis factor and interleukin-1 signaling. *Cell* **1994,** 77, (3), 325-8.

85. Kolesnick, R. N., 1,2-Diacylglycerols but not phorbol esters stimulate sphingomyelin hydrolysis in GH3 pituitary cells. *J. Biol. Chem.* **1987,** 262, (35), 16759-62.

86. Kolesnick, R. N.; Hemer, M. R., Characterization of a ceramide kinase activity from human leukemia (HL-60) cells. Separation from diacylglycerol kinase activity. *J. Biol. Chem.* **1990,** 265, (31), 18803-8.

87. Wennekes, T.; van, d. B. R. J. B. H. N.; Boot, R. G.; van, d. M. G. A.; Overkleeft, H. S.; Aerts, J. M. F. G., Glycosphingolipids - Nature, function, and pharmacological modulation. *Angew. Chem., Int. Ed.* **2009,** 48, 8848-8869.

88. Langeveld, M.; Aerts, J. M., Glycosphingolipids and insulin resistance. *Prog. Lipid Res.* **2009,** 48, (3-4), 196-205.

89. Delgado, A.; Casas, J.; Llebaria, A.; Abad, J. L.; Fabriás, G., Chemical Tools to Investigate Sphingolipid Metabolism and Functions. *ChemMedChem* **2007,** 2, (5), 580-606.

90. Merrill, A. H.; Wang, E., Biosynthesis of long-chain (sphingoid) bases from serine by LM cells. Evidence for introduction of the 4-trans-double bond after de novo biosynthesis of N-acylsphinganine(s). *J. Biol. Chem.* **1986,** 261, (8), 3764-9.

91. Marchesini, N.; Hannun, Y. A., Acid and neutral sphingomyelinases: roles and mechanisms of regulation. *Biochem. Cell Biol.* **2004,** 82, 27-44.

92. Kim, M. Y.; Linardic, C.; Obeid, L.; Hannun, Y., Identification of sphingomyelin turnover as an effector mechanism for the action of tumor necrosis factor α and γ-interferon. Specific role in cell differentiation. *J. Biol. Chem.* **1991,** 266, 484-9.

93. Brenner, B.; Ferlinz, K.; Grassme, H.; Weller, M.; Koppenhoefer, U.; Dichgans, J.; Sandhoff, K.; Lang, F.; Gulbins, E., Fas/CD95/Apo-I activates the acidic sphingomyelinase via caspases. *Cell Death Differ.* **1998,** 5, 29-37.

94. Goldkorn, T.; Balaban, N.; Shannon, M.; Chea, V.; Matsukuma, K.; Gilchrist, D.; Wang, H.; Chan, C., H2O2 acts on cellular membranes to generate ceramide signaling and initiate apoptosis in tracheobronchial epithelial cells. *J. Cell Sci.* **1998,** 111, 3209-3220.

95. Michel, C.; van, E.-D. G., Conversion of dihydroceramide to ceramide occurs at the cytosolic face of the endoplasmic reticulum. *FEBS Lett.* **1997,** 416, 153-155.

96. Yamaji, T.; Kumagai, K.; Tomishige, N.; Hanada, K., Two sphingolipid transfer proteins, CERT and FAPP2: Their roles in sphingolipid metabolism. *IUBMB Life* **2008,** 60, (8), 511-518.

97. Lannert, H.; Gorgas, K.; Meißner, I.; Wieland, F. T.; Jeckel, D., Functional Organization of the Golgi Apparatus in Glycosphingolipid Biosynthesis. *J. Biol. Chem.* **1998,** 273, (5), 2939-2946.

98. Riboni, L.; Bassi, R.; Caminiti, A.; Prinetti, A.; Viani, P.; Tettamanti, G., Metabolic Fate of Exogenous Sphingosine in Neuroblastoma Neuro2A Cells: Dose-dependence and Biological Effectsa. *Ann. N. Y. Acad. Sci.* **1998,** 845, (1), 46-56.

99. Hannun, Y. A.; Obeid, L. M., The Ceramide-centric Universe of Lipid-mediated Cell Regulation: Stress Encounters of the Lipid Kind. *J. Biol. Chem.* **2002,** 277, (29), 25847-25850.

100. Hannun, Y. A., Functions of ceramide in coordinating cellular responses to stress. *Science (Washington, DC, U.S.)* **1996,** 274, (5294), 1855-9.

101. Jenkins, G. M.; Richards, A.; Wahl, T.; Mao, C.; Obeid, L.; Hannun, Y., Involvement of yeast sphingolipids in the heat stress response of Saccharomyces cerevisiae. *J. Biol. Chem.* **1997,** 272, (51), 32566-72.

102. Dijkhuis, A. J.; Klappe, K.; Kamps, W.; Sietsma, H.; Kok, J. W., Gangliosides do not affect ABC transporter function in human neuroblastoma cells. *J. Lipid Res.* **2006,** 47, (6), 1187-95.

103. Klappe, K.; Hinrichs, J. W.; Kroesen, B. J.; Sietsma, H.; Kok, J. W., MRP1 and glucosylceramide are coordinately over expressed and enriched in rafts during multidrug resistance acquisition in colon cancer cells. *Int. J. Cancer* **2004,** 110, (4), 511-22.

104. Sietsma, H.; Veldman, R. J.; Kok, J. W., The involvement of sphingolipids in multidrug resistance. *J. Membr. Biol.* **2001,** 181, (3), 153-62.

105. Okazaki, T.; Bell, R. M.; Hannun, Y. A., Sphingomyelin turnover induced by vitamin D3 in HL-60 cells. Role in cell differentiation. *J. Biol. Chem.* **1989,** 264, (32), 19076-80.

106. Venable, M. E.; Lee, J. Y.; Smyth, M. J.; Bielawska, A.; Obeid, L. M., Role of ceramide in cellular senescence. *J. Biol. Chem.* **1995,** 270, (51), 30701-8.

107. Hetz, C. A.; Hunn, M.; Rojas, P.; Torres, V.; Leyton, L.; Quest, A. F., Caspase-dependent initiation of apoptosis and necrosis by the Fas receptor in lymphoid cells: onset of necrosis is associated with delayed ceramide increase. *J. Cell Sci.* **2002,** 115, (Pt 23), 4671-83.

108. Adam, D.; Heinrich, M.; Kabelitz, D.; Schutze, S., Ceramide: does it matter for T cells? *Trends Immunol.* **2002,** 23, (1), 1-4.

109. Obeid, L. M.; Linardic, C. M.; Karolak, L. A.; Hannun, Y. A., Programmed cell death induced by ceramide. *Science (Washington, DC, U.S.)* **1993,** 259, (5102), 1769-71.

110. Chalfant, C. E.; Kishikawa, K.; Mumby, M. C.; Kamibayashi, C.; Bielawska, A.; Hannun, Y. A., Long chain ceramides activate protein phosphatase-1 and protein phosphatase-2A. Activation is stereospecific and regulated by phosphatidic acid. *J. Biol. Chem.* **1999,** 274, (29), 20313-7.

111. Wang, G.; Silva, J.; Krishnamurthy, K.; Tran, E.; Condie, B. G.; Bieberich, E., Direct binding to ceramide activates protein kinase Czeta before the formation of a pro-apoptotic complex with PAR-4 in differentiating stem cells. *J. Biol. Chem.* **2005,** 280, (28), 26415-24.

112. Blazquez, C.; Galve-Roperh, I.; Guzman, M., De novo-synthesized ceramide signals apoptosis in astrocytes via extracellular signal-regulated kinase. *FASEB J.* **2000,** 14, (14), 2315-22.

113. Ruvolo, P. P., Intracellular signal transduction pathways activated by ceramide and its metabolites. *Pharmacol. Res.* **2003,** 47, (5), 383-92.

114. Heinrich, M.; Wickel, M.; Schneider-Brachert, W.; Sandberg, C.; Gahr, J.; Schwandner, R.; Weber, T.; Saftig, P.; Peters, C.; Brunner, J.; Kronke, M.; Schutze, S., Cathepsin D targeted by acid sphingomyelinase-derived ceramide. *EMBO J.* **1999,** 18, (19), 5252-63.

115. Sweeney, E. A.; Sakakura, C.; Shirahama, T.; Masamune, A.; Ohta, H.; Hakomori, S.; Igarashi, Y., Sphingosine and its methylated derivative N,N-dimethylsphingosine (DMS) induce apoptosis in a variety of human cancer cell lines. *Int. J. Cancer* **1996,** 66, (3), 358-66.

116. Jarvis, W. D.; Fornari, F. A.; Traylor, R. S.; Martin, H. A.; Kramer, L. B.; Erukulla, R. K.; Bittman, R.; Grant, S., Induction of apoptosis and potentiation of ceramide-mediated cytotoxicity by sphingoid bases in human myeloid leukemia cells. *J. Biol. Chem.* **1996,** 271, (14), 8275-84.

117. Jarvis, W. D.; Fornari, F. A., Jr.; Auer, K. L.; Freemerman, A. J.; Szabo, E.; Birrer, M. J.; Johnson, C. R.; Barbour, S. E.; Dent, P.; Grant, S., Coordinate regulation of stress- and mitogen-activated protein kinases in the apoptotic actions of ceramide and sphingosine. *Mol. Pharmacol.* **1997,** 52, (6), 935-47.

118. Ohta, H.; Sweeney, E. A.; Masamune, A.; Yatomi, Y.; Hakomori, S.; Igarashi, Y., Induction of apoptosis by sphingosine in human leukemic HL-60 cells: a possible endogenous modulator of apoptotic DNA fragmentation occurring during phorbol ester-induced differentiation. *Cancer Res.* **1995,** 55, (3), 691-7.

119. Hannun, Y. A.; Loomis, C. R.; Merrill, A. H., Jr.; Bell, R. M., Sphingosine inhibition of protein kinase C activity and of phorbol dibutyrate binding in vitro and in human platelets. *J. Biol. Chem.* **1986,** 261, (27), 12604-9.

120. Chalfant, C. E.; Spiegel, S., Sphingosine 1-phosphate and ceramide 1-phosphate: expanding roles in cell signaling. *J Cell Sci* **2005,** 118, (Pt 20), 4605-12.

121. Spiegel, S.; Milstien, S., Sphingosine-1-phosphate: an enigmatic signalling lipid. *Nat. Rev. Mol. Cell Biol.* **2003,** 4, 397-407.

122. Pyne, S.; Lee, S. C.; Long, J.; Pyne, N. J., Role of sphingosine kinases and lipid phosphate phosphatases in regulating spatial sphingosine 1-phosphate signalling in health and disease. *Cell. Signal.* **2009,** 21, (1), 14-21.

123. Levi, M.; Meijler, M. M.; Gomez-Munoz, A.; Zor, T., Distinct receptor-mediated activities in macrophages for natural ceramide-1-phosphate (C1P) and for phospho-ceramide analogue-1 (PCERA-1). *Mol. Cell. Endocrinol.* **2010,** 314, (2), 248-55.

124. Pettus, B. J.; Kitatani, K.; Chalfant, C. E.; Taha, T. A.; Kawamori, T.; Bielawski, J.; Obeid, L. M.; Hannun, Y. A., The coordination of prostaglandin E2 production by sphingosine-1-phosphate and ceramide-1-phosphate. *Mol. Pharmacol.* **2005,** 68, (2), 330-5.

125. Lamour, N. F.; Stahelin, R. V.; Wijesinghe, D. S.; Maceyka, M.; Wang, E.; Allegood, J. C.; Merrill, A. H., Jr.; Cho, W.; Chalfant, C. E., Ceramide kinase uses ceramide provided by ceramide transport protein: localization to organelles of eicosanoid synthesis. *J. Lipid Res.* **2007,** 48, (6), 1293-304.

126. Brown, D. A.; London, E., Functions of lipid rafts in biological membranes. *Annu Rev Cell Dev Biol* **1998,** 14, 111-36.

127. Schroeder, R.; London, E.; Brown, D., Interactions between saturated acyl chains confer detergent resistance on lipids and glycosylphosphatidylinositol (GPI)-anchored proteins: GPI-anchored proteins in liposomes and cells show similar behavior. *Proc Natl Acad Sci U S A* **1994,** 91, (25), 12130-4.

128. Levental, I.; Grzybek, M.; Simons, K., Greasing their way: lipid modifications determine protein association with membrane rafts. *Biochemistry* **2010,** 49, (30), 6305-16.

129. Brown, D. A.; Rose, J. K., Sorting of GPI-anchored proteins to glycolipid-enriched membrane subdomains during transport to the apical cell surface. *Cell* **1992,** 68, (3), 533-44.

130. Nicolau, D. V., Jr.; Burrage, K.; Parton, R. G.; Hancock, J. F., Identifying optimal lipid raft characteristics required to promote nanoscale protein-protein interactions on the plasma membrane. *Mol. Cell. Biol.* **2006,** 26, (1), 313-23.

131. Modrak, D. E.; Lew, W.; Goldenberg, D. M.; Blumenthal, R., Sphingomyelin potentiates chemotherapy of human cancer xenografts. *Biochem. Biophys. Res. Commun.* **2000,** 268, (2), 603-6.

132. Lemonnier, L. A.; Dillehay, D. L.; Vespremi, M. J.; Abrams, J.; Brody, E.; Schmelz, E. M., Sphingomyelin in the suppression of colon tumors: prevention versus intervention. *Arch. Biochem. Biophys.* **2003,** 419, (2), 129-38.

133. Bielawska, A.; Crane, H. M.; Liotta, D.; Obeid, L. M.; Hannun, Y. A., Selectivity of ceramide-mediated biology. Lack of activity of erythro-dihydroceramide. *J. Biol. Chem.* **1993,** 268, (35), 26226-26232.

134. Ahn, E. H.; Schroeder, J. J., Sphingoid Bases and Ceramide Induce Apoptosis in HT-29 and HCT-116 Human Colon Cancer Cells. *Exp. Biol. Med.* **2002,** 227, (5), 345-353.

135. Zheng, W.; Kollmeyer, J.; Symolon, H.; Momin, A.; Munter, E.; Wang, E.; Kelly, S.; Allegood, J. C.; Liu, Y.; Peng, Q.; Ramaraju, H.; Sullards, M. C.; Cabot, M.; Merrill Jr, A. H., Ceramides and other bioactive sphingolipid backbones in health and disease: Lipidomic analysis, metabolism and roles in membrane structure, dynamics, signaling and autophagy. *Biochim. Biophys. Acta, Biomembr.* **2006,** 1758, (12), 1864-1884.

136. Signorelli, P.; Munoz-Olaya, J. M.; Gagliostro, V.; Casas, J.; Ghidoni, R.; Fabriàs, G., Dihydroceramide intracellular increase in response to resveratrol treatment mediates autophagy in gastric cancer cells. *Cancer Lett.* **2009,** 282, (2), 238-243.

137. Separovic, D.; Bielawski, J.; Pierce, J. S.; Merchant, S.; Tarca, A. L.; Ogretmen, B.; Korbelik, M., Increased tumour dihydroceramide production after Photofrin-PDT alone and improved tumour response after the combination with the ceramide analogue LCL29. Evidence from mouse squamous cell carcinomas. *Br. J. Cancer* **2009,** 100, (4), 626-32.

138. Jiang, Q.; Wong, J.; Fyrst, H.; Saba, J. D.; Ames, B. N., γ-Tocopherol or combinations of vitamin E forms induce cell death in human prostate cancer cells by interrupting sphingolipid synthesis. *Proc. Natl. Acad. Sci. U.S.A.* **2004,** 101, (51), 17825-17830.

139. Kraveka, J. M.; Li, L.; Szulc, Z. M.; Bielawski, J.; Ogretmen, B.; Hannun, Y. A.; Obeid, L. M.; Bielawska, A., Involvement of Dihydroceramide Desaturase in Cell Cycle Progression in Human Neuroblastoma Cells. *J. Biol. Chem.* **2007,** 282, (23), 16718-16728.

140. Xu, R.; Jin, J.; Hu, W.; Sun, W.; Bielawski, J.; Szulc, Z.; Taha, T.; Obeid, L. M.; Mao, C., Golgi alkaline ceramidase regulates cell proliferation and survival by controlling levels of sphingosine and S1P. *FASEB J.* **2006,** 20, (11), 1813-1825.

141. Hu, W.; Xu, R.; Sun, W.; Szulc, Z. M.; Bielawski, J.; Obeid, L. M.; Mao, C., Alkaline Ceramidase 3 (ACER3) Hydrolyzes Unsaturated Long-chain Ceramides, and Its Down-regulation Inhibits Both Cell Proliferation and Apoptosis. *J. Biol. Chem.* **2010,** 285, (11), 7964-7976.

142. Wang, H.; Maurer, B. J.; Liu, Y. Y.; Wang, E.; Allegood, J. C.; Kelly, S.; Symolon, H.; Liu, Y.; Merrill, A. H., Jr.; Gouaze-Andersson, V.; Yu, J. Y.; Giuliano, A. E.; Cabot, M. C., N-(4-Hydroxyphenyl)retinamide increases dihydroceramide and synergizes with dimethylsphingosine to enhance cancer cell killing. *Mol. Cancer Ther.* **2008,** 7, (9), 2967-76.

# 2. Objectives

As described in Section 1.3, SLs are known to be essential bioactive signaling molecules involved in the regulation of cell growth, differentiation, senescence and apoptosis. Besides, SLs are found to dynamically cluster with sterols to form lipid rafts, whose function is crucial for the effective signal transduction and protein sorting. Understanding the many cell regulatory functions of SL metabolites requires an accurate knowledge of how and where they are generated, converted, or degraded in the cell. As a result of their biological importance, the synthesis of SL probes and the development of chemical tools to study SL metabolism and localization are object of current interest.

On the other hand, the recent advances in the development of bioorthogonal reactions have boosted their applications in chemical biology. These reactions, specifically those involving azide-alkyne cycloadditions, allow the selective labeling of a target biomolecule within the complex environments of live cells and cell extracts, helping the study of biological systems at the molecular level.

Taking into account the above considerations, the following goals were considered in the present thesis:

1. Design and synthesis of sphingolipid probes presenting an azide functionality either at ω (Fig. 2.1*A*) or at C1 positions (Fig. 2.1*B*) of the sphingoid base. Moreover, synthesis of ω-azidoSLs will comprise modifications at C1 position as well as different acyl chains in the amide linkage.

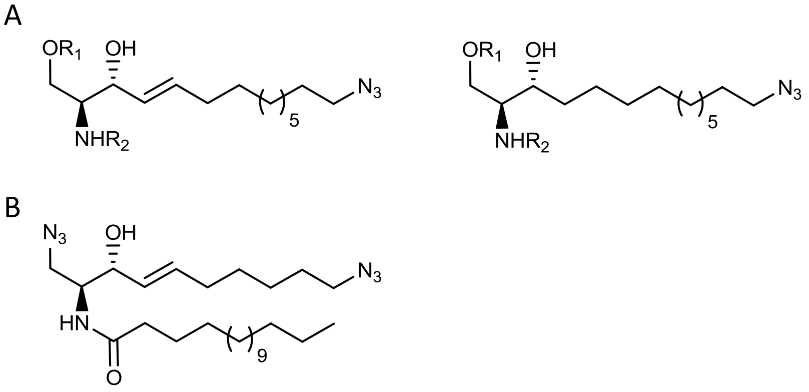

**Figure 2.1** Designed chemical probes bearing an azido group at: (*A*) ω position, and (*B*) C1 of the sphingoid base. $R_1$ represents H or phosphate, and $R_2$ represents H or different acyl chains.

2. Development of new methodologies to study SL metabolism and intracellular localization based on azide-alkyne cycloaddition reactions in live cells or cell extracts.

    2.1 New approach for the quantitative analysis of SLs based on SPAAC reactions. This goal includes:

    - Evaluation of the effect of some representative ω-azidoSLs on the sphingolipidome of the lung A549 and gastric HGC-27 cancer cell lines. In addition, the metabolization of these probes in the same cell line will be also studied.

    - Optimization of SPAAC reactions between selected ω-azidoSLs and different dibenzoazacyclooctyne-derived tags in cell extracts as a potential tool for the simultaneous analysis of sphingolipidomes arising from different cell populations.

    2.2 Method for the labeling of ω-azidoSL metabolites in live cells through a SPAAC reaction with a fluorescent dye. This objective involves:

    - Design and synthesis of a new fluorescent probe, **D1**, based on a dibenzoazocyclooctyne moiety linked to fluorescein.

    - Optimization of the SPAAC reaction between **D1** and an azido probe in both organic solvent and culture media.

    - Evaluation of **D1** internalization in cell membranes and study of its applicability for the labeling of ω-azidoSL metabolites in live cells by a SPAAC reaction.

    2.3 Method for the visualization of fluorescent ceramides in lipid membranes, involving the examination of the fluorescent properties of azidoceramides within an artificial lipidic environment after CuAAC reaction with a fluorogenic system.

3. New synthetic approaches for the preparation of non-natural C8 ceramides (Fig. 2.2), as chemical probes for a new assay for the determination of Des1 activity.

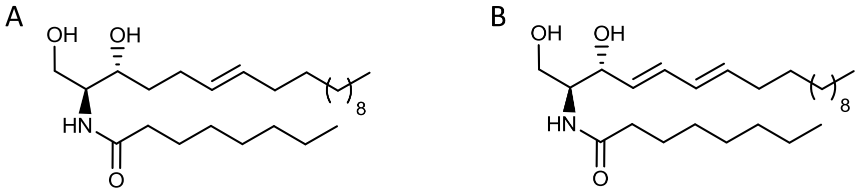

**Figure 2.2** Chemical structure of double-bond C8 ceramides: (*A*) $\Delta^{6}$, and (*B*) $\Delta^{4,6}$-ceramides.

# 3. Results & Discussion

## 3.1 Synthesis of SL analogues with an azide group at ω position

### 3.1.1 Sphingosine and ceramide analogues

#### 3.1.1.1 Introduction

Sphingosines are a class of long chain aliphatic compounds that present a 2-amino-1,3-diol moiety. The most common member of this group found in nature is (2*S*,3*R*,4*E*)-2-aminooctadec-4-en-1,3-diol, frequently referred to as sphingosine (Fig. 3.1). Sphingosines constitute the backbone of ceramide and more complex SLs, such as sphingomyelin, cerebrosides, and glycosphingolipids. Ubiquitous to all living organisms, SLs play many biologically important roles. As fundamental constituents of membranes, they contribute to the structural integrity of the cells. Furthermore, SLs facilitate cell-cell signaling, cell recognition, and adhesion processes.[1-2]

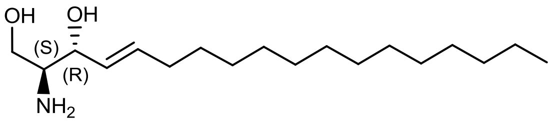

**Figure 3.1** Chemical structure of sphingosine.

Sphingoid bases possessing a 18-carbon backbone are the most abundant among mammalian SLs. This is due to the preference of mammalian SPT for saturated acyl-CoAS with 16 ± 2 carbon atoms, combined with the abundance of palmitoyl-CoA.[3] However, small amounts of sphingoid bases with other chain lengths of 12 to 26 carbon atoms have also been found in mammals.[4]

#### 3.1.1.2 Synthetic approaches to sphingoid bases

Since sphingosine was first synthesized by Shapiro,[5-6] many synthetic routes to enantiopure SLs have been reported. Some of them utilize inexpensive starting materials from the chiral pool, whereas other routes are based on asymmetric induction using chiral auxiliaries or catalysts. The synthetic methods that start from chiral precursors utilize L-serine[7-10] or carbohydrates.[11-13] Other synthetic approaches are based on asymmetric epoxidations,[14-16] aldol reactions,[17-20] and other miscellaneous methods. Some of the mentioned examples are illustrated in Fig. 3.2.

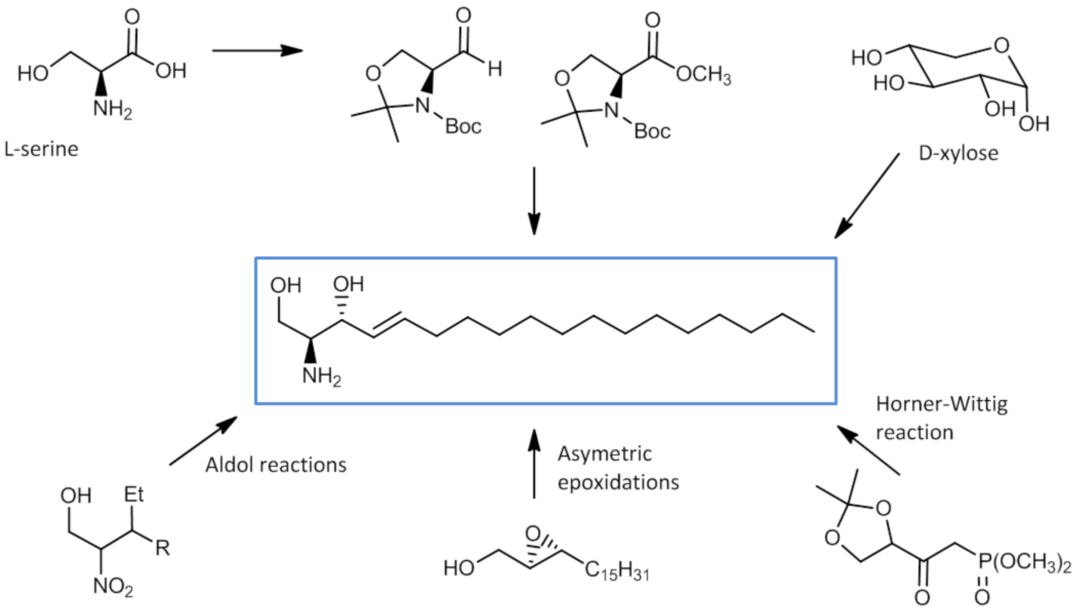

**Figure 3.2** Some representative examples of synthetic approaches to sphingosine.

### 3.1.1.3 The olefin cross metathesis approach

Among the wide range of synthetic strategies, we were interested in those based on L-serine as chiral pool precursor. This amino acid is commercially available and, moreover, allows the construction of the 2-amino-1,3-diol head of the sphingoid base. The stereocenter at the C2 carbon atom in L-serine is conserved in the sphingoid product, and the use of appropriate *N*-protection strategies can determine the stereochemistry at C3 position.

As mentioned above, most of the strategies rely on classical reactions to form the C-C double bond or the stereoselective reduction of a triple bond. However, in recent years, olefin cross metathesis (CM) has emerged as a convenient strategy to form the C4-C5 *trans* double bond of the sphingoid backbone.[21-23] The *E*-selectivity and the possibility of using a convergent synthetic approach prompted us to use this chemistry.

CM is a fundamental chemical reaction that allows the intermolecular formation of carbon-carbon double bonds. The reaction is catalyzed by metal complexes such as Mo(VI), W(VI), and Ru(II) carbenoid complexes. The reaction has recently gained prominence due to the availability of catalysts with varied activities, such as that shown in Fig. 3.3.

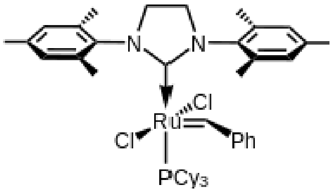

**Figure 3.3** Grubb's 2nd generation catalyst, based on Ru(II) and a saturated *N*-heterocyclic carbene.

The widely accepted mechanism of CM, first proposed by Hérisson and Chauvin,[24] involves the [2+2] cycloaddition of an alkene to a transition metal alkylidene to form a metallocyclobutane intermediate, which subsequently undergoes a [2+2] cycloreversion to generate ethylene and a substrate-loaded metal carbene (Fig. 3.4). This intermediate reacts with the second olefin in the same fashion to release the product and regenerate the catalyst. The catalytic cycle is a thermodynamically controlled process, and the reaction is driven forward by evolution of ethylene gas.

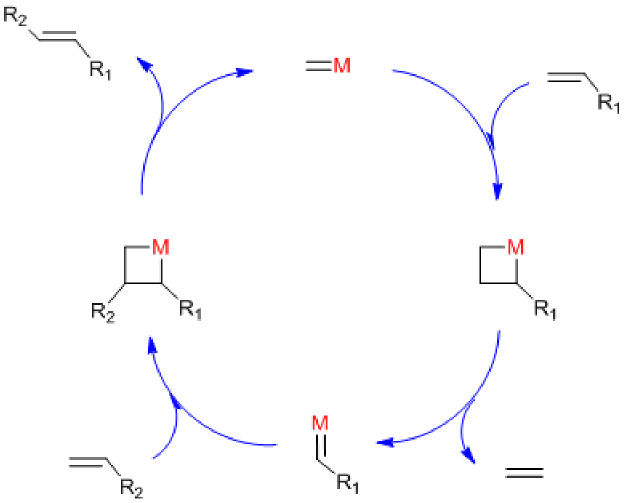

**Figure 3.4** Mechanism of olefin metathesis.

In our retrosynthetic strategy leading to ω-azidosphingoid bases, two terminal alkene compounds must undergo CM: one with a suitable ω-substituted aliphatic chain and another one bearing a masked 2-amino-1,3-diol moiety (**7**), as depicted in Fig. 3.5. Although several ω-substituted terminal alkenes are commercially available, the preparation of a suitable 2-amino-1,3-diol with a terminal double bond, such as **7**, is required. This chiral building block should be available from aldehyde **4** (Garner's aldehyde), which, in turn, is readily prepared from L-serine as chiral pool precursor.

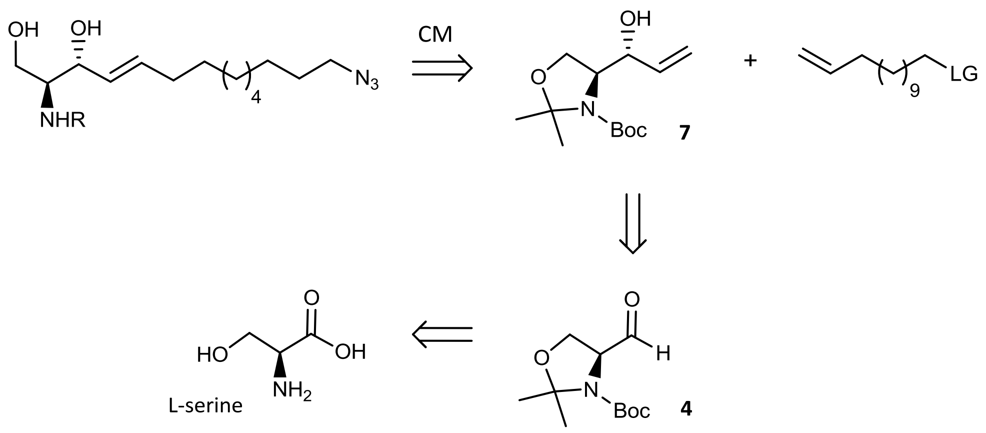

**Figure 3.5** Retrosynthetic analysis of sphingosine and ceramide bearing an azido group at ω position. LG represents a suitable leaving group or an azide group, and R represents an acyl chain or an H atom.

This synthetic route offers some attractive features, such as (1) the possibility of a convergent synthesis; (2) high *E*-selectivity in the product formation, and (3) functional group tolerance and reasonable stability of Grubb's catalyst in the presence of 2-amino-1,3-diol functionality.

### 3.1.1.4 Synthesis of Garner's aldehyde (4)

Garner's aldehyde is the common name of 1,1-dimethylethyl-4-formyl-2,2-dimethyl-oxazolidine-3-carboxylate (**4**). Since its preparation in 1984 by Garner,[25] this building block has been used extensively in asymmetric synthesis.

Several synthetic methods have been reported for the preparation of Garner's aldehyde,[25-30] all of them using L-serine as starting material from the chiral pool. Among the various synthetic approaches, we decided to follow a method based on the direct reduction of

Weinreb amide **3**, as represented in Fig. 3.6. This synthetic route was first reported by Bold *et al.*[31] and next improved by Campbell *et al.*[32]

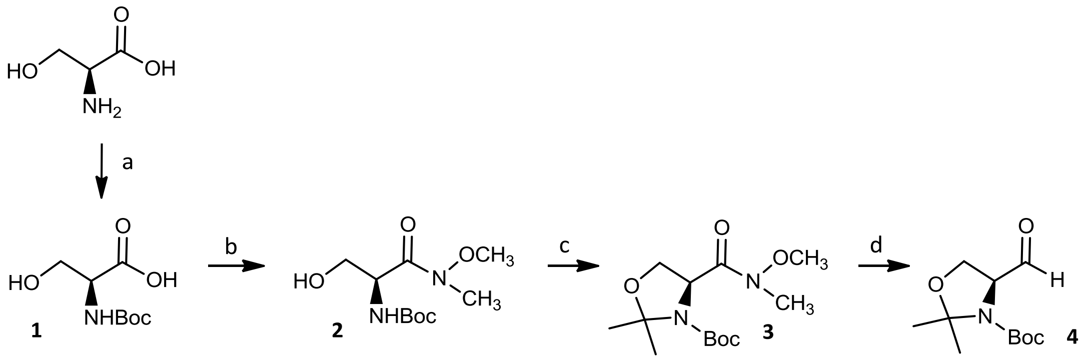

a) $Boc_2O$, 1 *N* NaOH, dioxane, 0 °C to rt, overnight, quantitative; b) NMM, *N*,*O*-DMHA, EDC, $CH_2Cl_2$, -15 °C, 2 h, 94%; c) $BF_3{\cdot}OEt_2$, 1:3 DMP/acetone, rt, 2 h, quantitative; d) $LiAlH_4$, THF, 0 °C, 2 h, 71%.

**Figure 3.6** Synthesis of aldehyde **4** *via* Weinreb amide **2**.

This synthesis started with Boc protection of L-serine using di-*tert*-butyl dicarbonate [$(Boc)_2O$] at pH ≥ 10 to form *N*-Boc-serine **1** in quantitative yield. Weinreb amide **2** was prepared by EDC promoted coupling of *N*,*O*-DMHA with acid **1** in 94% yield. Subsequently, treatment of **2** with 1:3 DMP/acetone, using $BF_3{\cdot}OEt_2$ as catalyst, gave oxazolidine **3** in quantitative yield. Finally, reduction of **3** with excess $LiAlH_4$ gave the desired aldehyde **4** in 71% yield.

### 3.1.1.5 Synthesis of allylic alcohol (7)

As shown previously (Fig. 3.5), the chiral building block **7** was required for the cross-metathesis approach.

In this context, addition of metal-activated carbon nucleophiles to aldehyde **4** represents a suitable approach. However, in most cases, such additions lead to mixtures of diastereomers. *anti*-Addition gives the *erythro* adducts, while *syn*-addition leads to the corresponding *threo* ones. Herold first reported that a high asymmetric induction could be achieved by using different reaction conditions.[9] Thus, products formation is explained either through the Felkin-Ahn model **A**, involving a non-chelating transition state leading to the *anti* adducts, or through a chelation-controlled transition state **B** (Cram model), which gives the corresponding *syn* adducts (Fig. 3.7). In the absence of a stabilizing $\alpha$-chelation effect, the formation of *syn* addcuts is disfavoured.

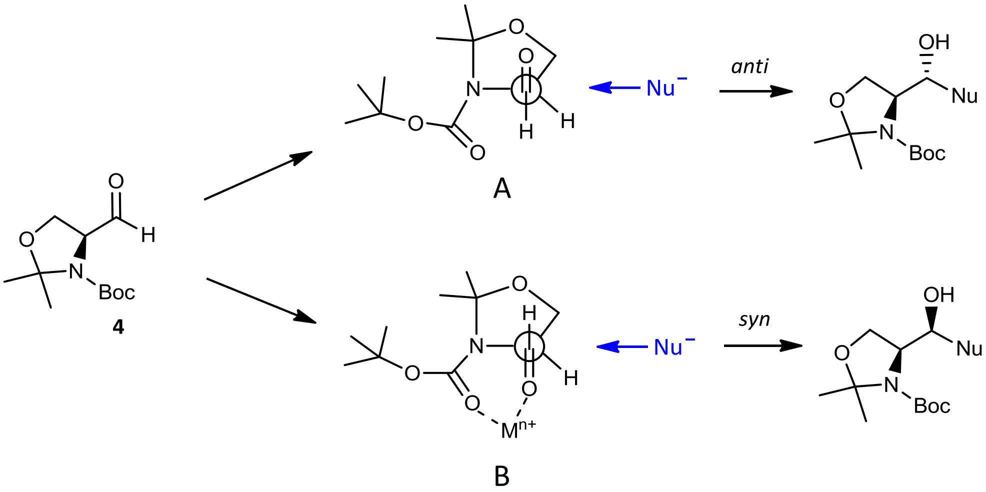

**Figure 3.7** L-*erythro* (*anti*) or L-*threo* (*syn*) product formation by nucleophilic additions to **4**; (*A*) *Felkin-Ahn* model, and (*B*) *Cram* model.

The addition of vinylmagnesium bromide to **4** has been reported to proceed at -78 °C in THF to give a *erythro*/*threo* 6:1 mixture of diastereomeric compounds.[25] However, Herold discovered that the reaction with lithiated ethynyltrimethylsilane under the same conditions was highly *erythro* selective.[9] Moreover, the addition of cation-complexing agents, such as HMPA, resulted in an increase of *erythro* selectivity. This high *erythro* selectivity prompted us to use this approach.

Thus, lithiated ethynyltrimethylsilane was added to aldehyde **4** at -78 °C in THF, using HMPA as additive (Fig. 3.8). The *erythro* alkynol **5** was obtained in 73% yield with high diastereoselectivity. Subsequent desilylation of **5** in methanolic $K_2CO_3$ gave the deprotected terminal alkyne **6** in 93% yield. The synthetic route ended with the selective triple to double bond reduction, using Lindlar's catalyst in EtOAc. This catalyst, based on palladium deposited on calcium carbonate, is "poisoned" with lead, which lowers the effectiveness of the metal surface and stops the reduction at the alkene stage. In our case, further deactivation of the catalyst with quinoline was necessary to prevent the formation of the corresponding alkane. Therefore, the allylic alcohol **7** was obtained in quantitative yield from precursor **6**.

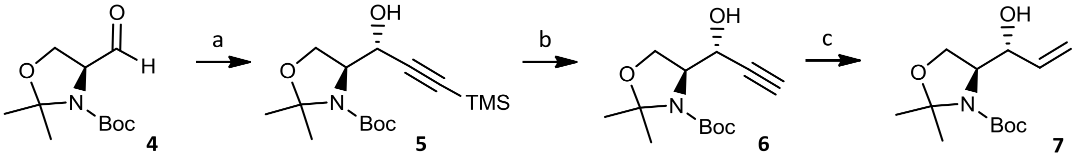

a) Ethynyltrimethylsilane, BuLi, HMPA, THF, -78 °C, 3 h, 73%; b) $K_2CO_3$, MeOH, rt, 3 h, 93%; c) $H_2$ (1 atm), Lindlar's catalyst, quinoline, EtOAc, rt, 1 h, quantitative.

**Figure 3.8** Synthesis of allylic alcohol **7**.

### 3.1.1.6 Synthesis of ω-azidosphingosine (RBM2-31) and *N*-acylated analogues (RBM2-32, RBM2-37, RBM2-46 and RBM2-77)

With building block **7** in hand, its CM reactivity with terminal alkenes bearing different functional groups was examined (Fig. 3.9). Thereby, allylic alcohol **7** was exposed to 4 equiv of the corresponding terminal alkene in the presence of 20 mol % of 0Grubb's 2nd generation catalyst (Fig 3.3).

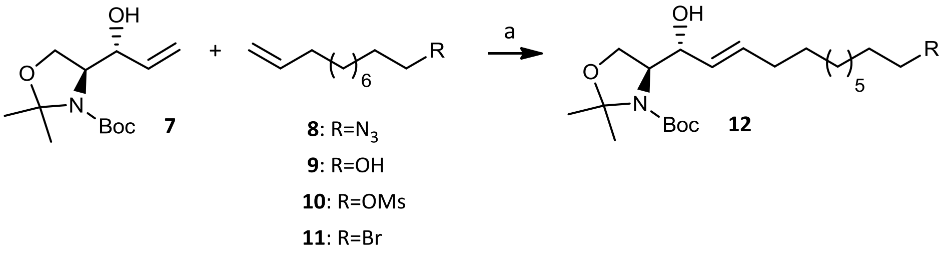

a) Grubb's 2nd generation catalyst, $CH_2Cl_2$, 45 °C, 5 h, 59%.

**Figure 3.9** CM of allylic alcohol **7** with terminal alkenes.

Alkene **8** provided an intractable mixture of compounds, in agreement with the reported failure of azides to undergo CM reactions.[33-35] CM with the ω-hydroxylalkene **9** or the ω-mesylalkene **10** was also examined. In both cases, inseparable mixtures of the desired cross-coupled compounds and the corresponding homodimerization by-products were obtained. Finally, CM of compound **7** with 11-bromoundec-1-ene (**11**) provided the desired olefin **12** in 59% yield, after an efficient chromatographic separation. Furthermore, compound **12** was obtained in excellent *E*-selectivity,[36] since no *Z*-isomer was observed by $^1$H NMR. The presence of the *trans* double bond at C4-C5 was unambiguously confirmed by the large $^1$H NMR coupling constant (> 15 Hz) between H4 and H5 protons.

The introduction of the azide functionality at ω position through nucleophilic displacement of the bromine atom in **12** was next required. With this purpose, we decided to use $NaN_3$, a very common azide source in organic synthesis, as depicted in Fig. 3.10. Therefore, bromide **12** was converted into the corresponding azide **13** with a 4-fold excess of $NaN_3$ in anhydrous DMF at 90 °C, in 84% yield. In the next step, deprotection of the oxazolidine and the *N*-Boc groups was required. Commonly, *N*-Boc removal can be accomplished with strong acids, such as neat trifluoroacetic acid (or a dichloromethane solution thereof), as well as with HCl in MeOH. We decided to use HCl, which was generated *in situ* by the addition of acetyl chloride to a methanolic solution of compound **13**. Thus, both oxazolidine and *N*-Boc groups were simultaneously deprotected under these conditions to afford the sphingosine analog **RBM2-31** in 84% yield. Lastly, selective *N*-acylations were carried out by activating the required carboxylic acid with EDC in the presence of a coupling reagent, such as HOBt in $CH_2Cl_2$. The corresponding *N*-acylated compounds **RBM2-32**, **RBM2-37**, **RBM2-46** and **RBM2-77** were obtained in 22-77% yield from **RBM2-31**, as illustrated in Fig. 3.10.

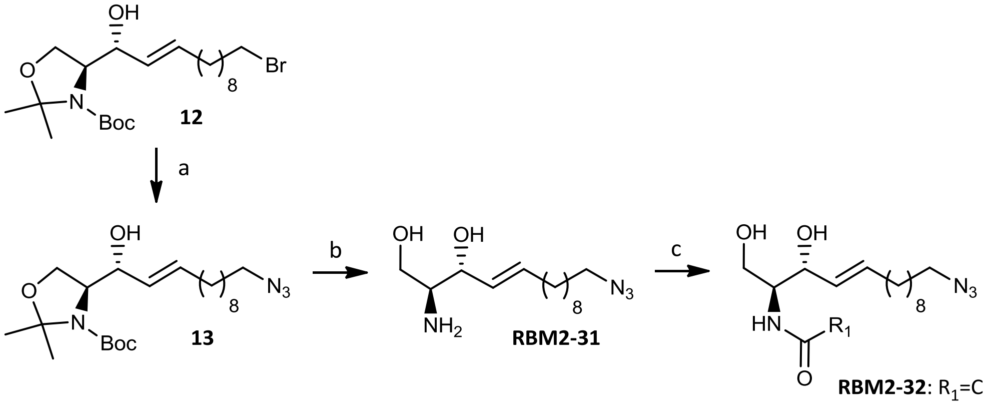

**RBM2-32**: $R_1$=$CH_2Br$, 22%
**RBM2-37**: $R_1$=$C_7H_{15}$, 59%
**RBM2-46**: $R_1$=$C(=CH_2)CH_3$, 77%
**RBM2-77**: $R_1$=$C_{15}H_{31}$, 36%

a) $NaN_3$, DMF, 80 °C, overnight, 93%; b) $ClCOCH_3$, MeOH, rt, 1 h, 84%; c) $R_1COOH$, EDC, HOBt, $Et_3N$, $CH_2Cl_2$, rt, 1 h, 22-77%.

**Figure 3.10** Synthesis of azide **RBM2-31** and *N*-acylated derivatives **RBM2-32**, **RBM2-37**, **RBM2-46** and **RBM2-77**.

## 3.1.2 Dihydrosphingosine and dihydroceramide analogues

### 3.1.2.1 Introduction

Dihydrosphingosine, also called sphinganine, is one of the major sphingoid bases found in many organisms as well as an early intermediate in the *de novo* biosynthesis of SLs (Fig. 3.11).[37]

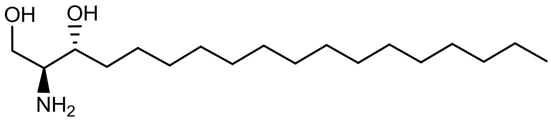

**Figure 3.11** Chemical structure of sphinganine.

### 3.1.2.2 Synthetic approaches to sphinganine

Although sphinganine can be obtained by reduction of sphingosine, other strategies have been reported. This SL has been prepared from sugars,[38-39] from the amino acid L-serine,[40-44] and from racemic precursors by a variety of asymmetric strategies.[45-48] Generally, the most common and straightforward synthesis uses serine derivatives.

### 3.1.2.3 Synthesis of ω-azidodihydrosphingosine (RBM2-40) and *N*-acylated analogues (RBM2-44, RBM2-45 and RBM2-87)

As discussed previously, the successful synthesis of sphingosine and its ω-azido derivatives prompted us to obtain the sphinganine skeleton by reduction of the C4-C5 double bond. This is a versatile, convenient and straightforward approach.

Starting from building block **12**, we decided to reduce the double bond at this step, as shown in Fig. 3.12. Otherwise, reduction in a more advanced stage might have not been compatible with the azide functionality, leading to amine formation. The synthesis started with the catalytic hydrogenation of **12** to give **14** in 77% yield, using a Rh catalyst in MeOH. Subsequently, bromide displacement by an azide group in **14** was carried out by reaction with $NaN_3$ in DMF at 90 °C, giving the azide **15** in 76% yield. Next, the oxazolidine and the *N*-Boc protecting groups were simultaneously removed with *in situ* generated HCl, by addition of acetyl chloride to a methanolic solution of compound **15**, to afford ω-azidosphinganine **RBM2-40** in 85% yield. Finally, *N*-acylated compounds **RBM2-44**, **RBM2-45**, and **RBM2-87** were obtained by the selective *N*-acylation of **RBM2-40** with suitable carboxylic acids, using EDC and HOBt as coupling reagents in yields ranging from 8-65%. The poor yield observed in the acylation with bromoacetic acid may be due to the high reactivity of this acid in the reaction conditions, leading to uncharacterized by-products.

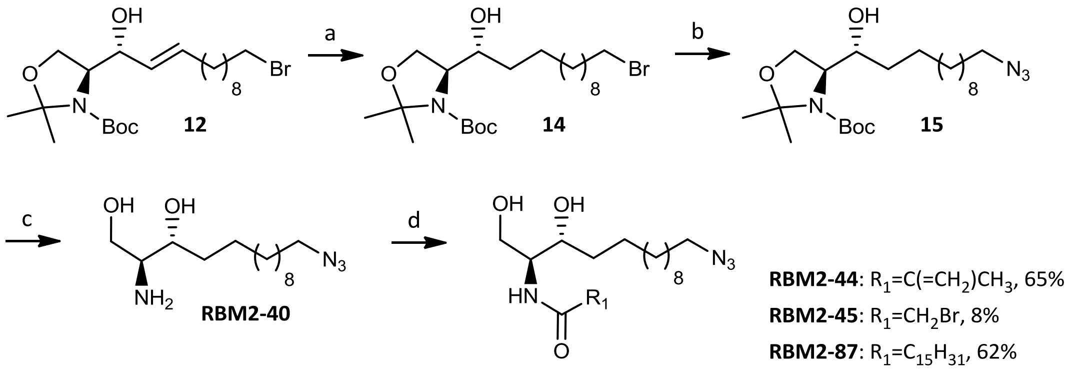

**12** **14** **15** **RBM2-40**

**RBM2-44**: $R_1$=C(=$CH_2$)$CH_3$, 65%
**RBM2-45**: $R_1$=$CH_2$Br, 8%
**RBM2-87**: $R_1$=$C_{15}H_{31}$, 62%

a) $H_2$ (1 atm), Rh catalyst, MeOH, rt, 6 h, 77%; b) $NaN_3$, DMF, 90 °C, overnight, 76%; c) $ClCOCH_3$, MeOH, rt, 1 h, 85%; d) $R_1COOH$, EDC, HOBt, $Et_3N$, $CH_2Cl_2$, rt, 1 h, 8-65%.

**Figure 3.12** Synthesis of azide **RBM2-40** and *N*-acylated derivatives **RBM2-44**, **RBM2-45** and **RBM2-87**.

### 3.1.3 ω-Azidosphingosine-1-phosphate and ω-azidodihydrosphingosine--1-phosphate

#### 3.1.3.1 Introduction

Sphingosine-1-phosphate or sphinganine-1-phosphate (Fig. 3.13), are biosynthesized from sphingosine and sphinganine by ATP-dependent phosphorylation at the primary hydroxyl group. This phosphorylation process is mediated by a specific sphingosine kinase (SK), which has been reported to be located in the cytoplasm.[49]

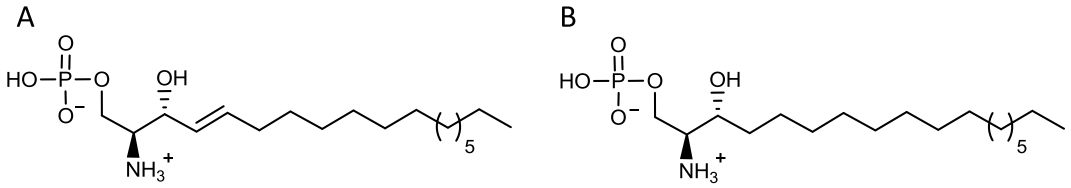

**Figure 3.13** Chemical structure of: (*A*) sphingosine-1-phosphate, and (*B*) sphinganine-1-phosphate.

Sphingosine-1-phosphate can be irreversibly degraded by the action of a pyridoxal phosphate-dependent lyase (S1PL) to ethanolamine-*O*-phosphate and (2*E*)-hexadecenal, as depicted in Fig. 3.14.[50] Analogously, this enzyme also degrades sphinganine-1-phosphate to hexadecanal.

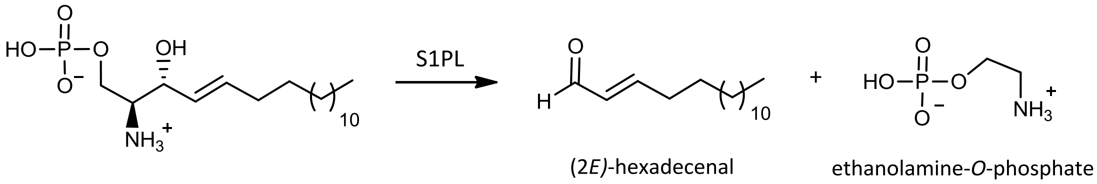

**Figure 3.14** The degradative pathway of sphingosine-1-phosphate mediated by S1PL.

In addition to its role as a catabolic intermediate, sphingosine-1-phosphate is believed to act both as an extracellular mediator and as an intracellular second messenger.[51-52] The cellular actions of sphingosine-1-phosphate include growth related effects, such as proliferation, differentiation and cell survival, and cytoskeletal effects, such as chemotaxis, aggregation, adhesion, morphological changes, and secretion. On the other hand, sphingosine-1-phosphate may be a component of the intracellular second messenger system that is involved in calcium release and the regulation of cell growth induced by sphingosine.[53-54]

### 3.1.3.2 Synthetic approaches to phosphorylated derivatives

Three types of phosphorus reagents are the most frequently used in the synthesis of phosphate esters (Fig. 3.15): (1) tetracoordinated P(V) compounds of type A (phosphates: oxidation state +5), (2) tricoordinated P(III) compounds of type B (phosphites) and type C (phosphoramidites), with oxidation state +3, and (3) tetracoordinated P(III) compounds of type D (*H*-phosphonates: oxidation state +3).

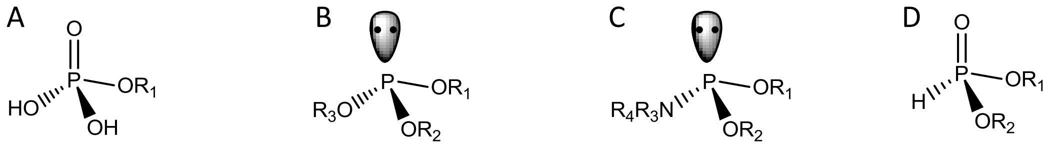

**Figure 3.15** Different types of phosphorus compounds: (*A*) phosphates; (*B*) phosphites; (*C*) phosphoramidites, and (*D*) *H*-phosphonates.

Phosphates have tetrahedral geometry and their chemistry is dominated by the presence of a very stable phosphoryl group (P=O). The phosphorus atom in A is an electrophilic center and is subject to reactions with hard nucleophiles. On the contrary, phosphites and phosphoramidites have a trigonal pyramidal geometry with a lone electron pair located on the phosphorus atom. Due to this electronic disposition, the phosphorus atom behaves as a basic, soft nucleophile center that may react with electrophiles. However, when the phosphorus atom is protonated or when it bears electron-withdrawing substituents, it may also react with nucleophiles. Lastly, albeit *H*-phosphonates show a close structural resemblance to phosphates, their reactivity is closer to that of related +3 oxidation state phosphites and phosphoramidites. Thus, *H*-phosphonates are also electrophilic compounds although less prone to oxidation than phosphites and phosphoramidites due to the lack of phosphorus atom lone pair electrons. It is worthy of mention that *H*-phosphonates exist as an equilibrium mixture of two tautomeric forms where the tetracoordinated phosphonate predominates over the tricoordinated phosphite tautomer (Fig. 3.16). Interestingly, the equilibrium can be shifted to the phosphite tautomer in the presence of silylating agents.

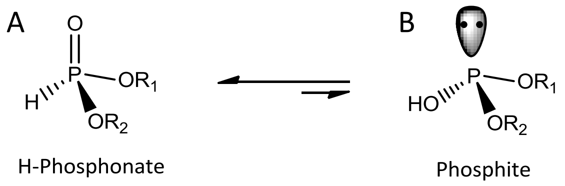

**Figure 3.16** *H*-phosphonate species exist as an equilibrium mixture of two tautomeric forms: (*A*) a tetracoordinated phosphonate form, and (*B*) a tricoordinated phosphite form.

In general, P(III) derivatives can be easily converted into P(V) derivatives using different oxidizing reagents (e.g. iodine/water, elemental sulfur, elemental selenium, etc.).

All the above phosphorus derivatives (phosphates,[55] phosphoramidites,[56-57] phosphites,[58] and *H*-phosphonates[59]) have been used to synthesize phosphorylated SLs, as depicted in Fig. 3.17.

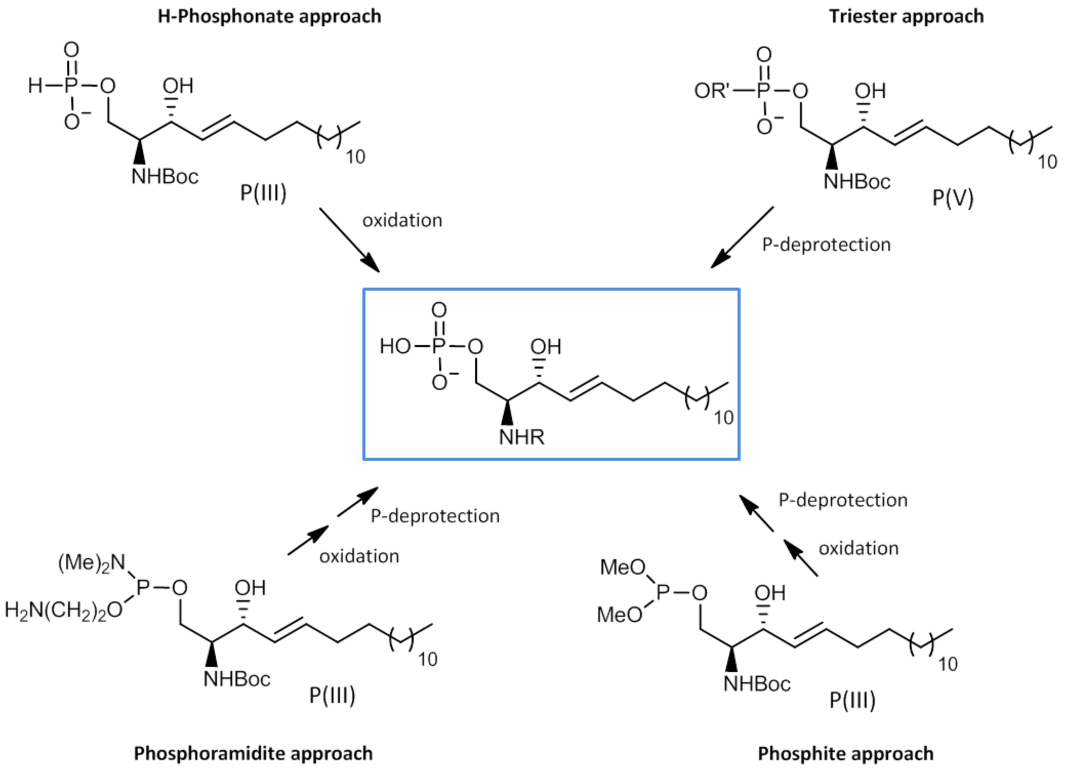
H-Phosphonate approach
Triester approach
P(III)
P(V)
oxidation
P-deprotection
NHBoc
NHR
10
P-deprotection
oxidation
P-deprotection
oxidation
P(III)
P(III)
Phosphoramidite approach
Phosphite approach

**Figure 3.17** Different synthetic approaches to phosphorylated SLs.

### 3.1.3.3 Synthesis of ω-azidosphingosine-1-phosphate (RBM2-35) and ω-azidodihydrosphingosine-1-phosphate (RBM2-43)

As a general approach, suitably protected phosphate moieties are required to provide ω-azidosphingosine-1-phosphate **RBM2-35** and its saturated analogue **RBM2-43**. Ideally, these protective groups should be easily removable in quantitative yields in the final synthetic step. The presence of an acid labile *N*-Boc group in the corresponding precursors, prompted us to choose a protecting group which could be easily cleaved under acidic conditions, such as the methyl ester group.

Starting from the ω-azido building block **13**, the selective cleavage of the oxazolidine moiety to liberate the primary hydroxyl group at C1 for further phosphorylation was envisaged. Thereby, the desired diol **16** was prepared in 87% yield under mild acidic conditions, using catalytic *p*-toluenesulfonic acid in MeOH, as shown in Fig. 3.18.

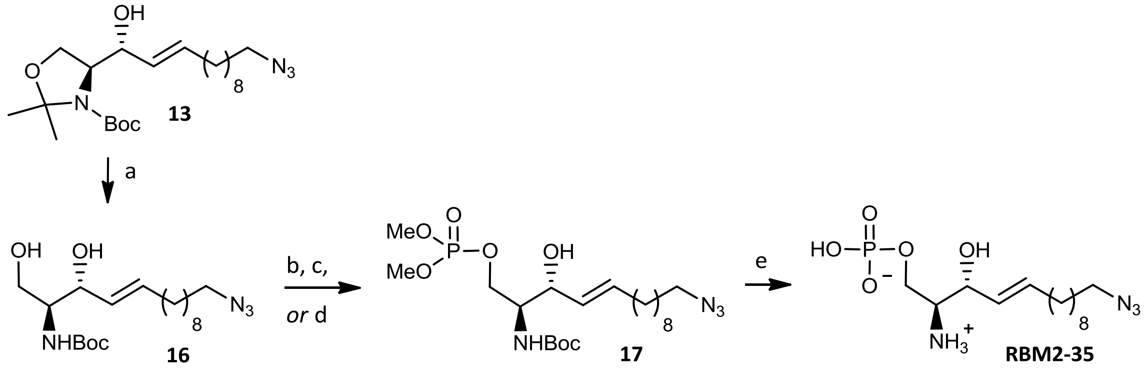

a) cat. TsOH, MeOH, rt, 6 h, 87%; b) $PO(OCH_3)_3$, proton sponge, $POCl_3$, 0 °C to rt, 2 h; c) $P(OCH_3)_3$, $CBr_4$, pyridine, 0 °C to rt, 3 h, 29%; d) $(CH_3O)_2P(O)Cl$, NMI, THF, 0 °C to rt, 5 h, 65%; e): 1) TMSBr, ACN, 0 °C to rt, 3 h; 2) MeOH, rt, 1 h, quantitative.

**Figure 3.18** Synthesis of phosphate **RBM2-35**.

Selective phosphorylation of the primary hydroxyl group was first attempted by means of the Yoshikawa's monophosphorylation method.[60] According to this methodology, diol **16** was treated with 2 equiv of $POCl_3$ and 1.5 equiv of 1,8-bis(dimethylamino)naphthalene, known as "proton sponge", using trimethyl phosphate as solvent. Unfortunately, phosphorylation under these conditions failed, obtaining undesired by-products.

In view of this result, the trimethyl phosphate/carbon tetrabromide method[61] was attempted next. Treatment of diol **16** with 1.3 equiv of $CBr_4$ and 1.4 equiv of $P(OCH_3)_3$ afforded the selective phosphorylation of the primary alcohol to give the protected phosphate **17**. Although no bisphosphate ester was detected, the reaction yield (29%) was moderate.

Fortunately, phosphorylation with dimethyl chlorophosphate in the presence of *N*-methylimidazole, afforded the required phosphate **17** in an acceptable 65% yield. Monophosphorylation was confirmed by the presence of two doublets in the $^1H$ NMR spectrum at 3.80 and 3.76 ppm ($J$ = 2.5 Hz, $^3J_{HP}$), each integrating for three protons and assigned to the $(OCH_3)_2$ moiety. The chemoselectivity of the phosphorylation step was determined by $^{13}C$ NMR, which confirmed the monophosphorylation of the primary hydroxyl group. The resonances for C1 and C2 at 66.79 and 54.71 ppm appeared as doublets due to the $^2J_{CP}$ and $^3J_{CP}$ couplings ($J_{C1\text{-}P}$ = 5.5 Hz, $J_{C2\text{-}P}$ = 6.0 Hz). Neither C3 nor the C4 resonances showed any C-P couplings, thus confirming the selective phosphorylation of the primary hydroxyl group.

Finally, the simultaneous phosphate ester and *N*-Boc removal in an "one-pot" two-step process with TMSBr in ACN, followed by methanolisis of the crude reaction mixture, gave **RBM2-35** in quantitative yield and good purity without further purification.

A similar synthetic route was followed to obtain the saturated phosphate **RBM2-43** (Fig. 3.19). The synthesis started with the selective cleavage of the oxazolidine moiety of **15** to give aminodiol **18** in 62% yield. Next, phosphorylation of the primary hydroxyl group with dimethyl chlorophosphate, as previously described, led to phosphate ester **19** in quantitative yield. Final simultaneous methyl ester and *N*-Boc deprotection with TMSBr, followed by methanolysis, gave **RBM2-43** in good overall yield and purity.

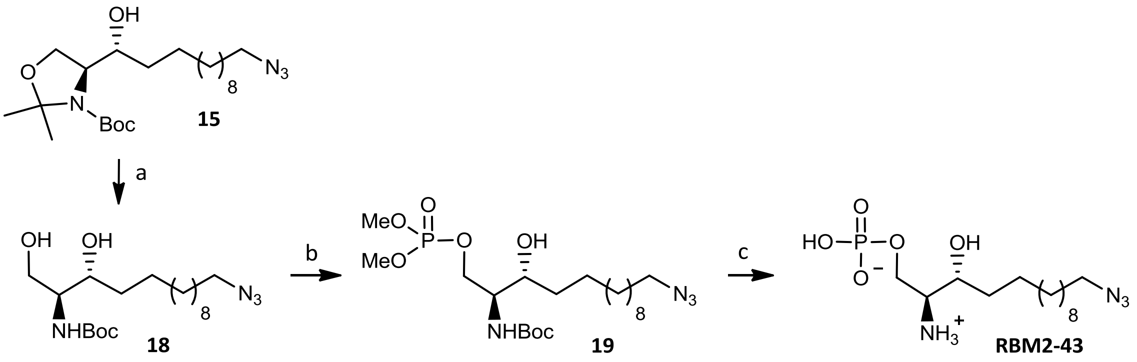

a) cat. TsOH, MeOH, rt, 6 h, 62%; b) $(CH_3O)_2P(O)Cl$, NMI, THF, 0 ºC to rt, 5 h, quantitative; c): 1) TMSBr, ACN, 0 ºC to rt, 3 h, 2) MeOH, rt, 1 h, quantitative.

**Figure 3.19** Synthesis of saturated phosphate **RBM2-43**.

### 3.1.4 ω-Azidoceramide-1-phosphate analogues

#### 3.1.4.1 Introduction

Ceramide-1-phosphate is a phosphorylated SL metabolite generated from ceramide by the action of ceramide kinase (CERK). The formation of ceramide-1-phosphate is critical for the regulation of ceramide levels. This SL has emerged as a bioactive molecule by its ability to regulate diverse cellular functions, such as arachidonic acid release, mast cell degranulation, $Ca^{2+}$ mobilization, translocation of lipid-metabolizing enzymes, vesicular trafficking, cell proliferation, and cell survival, among others.[62]

#### 3.1.4.2 Synthesis of ω-azidoceramide-1-phosphate (RBM2-47)

As indicated above, different phosphorylating agents have been reported to introduce a phosphate moiety into organic compounds (see Section 3.1.3.2).

The synthesis of ω-azidoceramide-1-phosphate **RBM2-47** was first attempted through a rapid and flexible method based on the *N*-acylation of ω-azidosphingosine-1-phosphate **RBM2-35**, as reported by Nussbaumer *et al.* for the synthesis of ceramide-1-phosphate from sphingosine-1-phosphate (Fig. 3.20).[63]

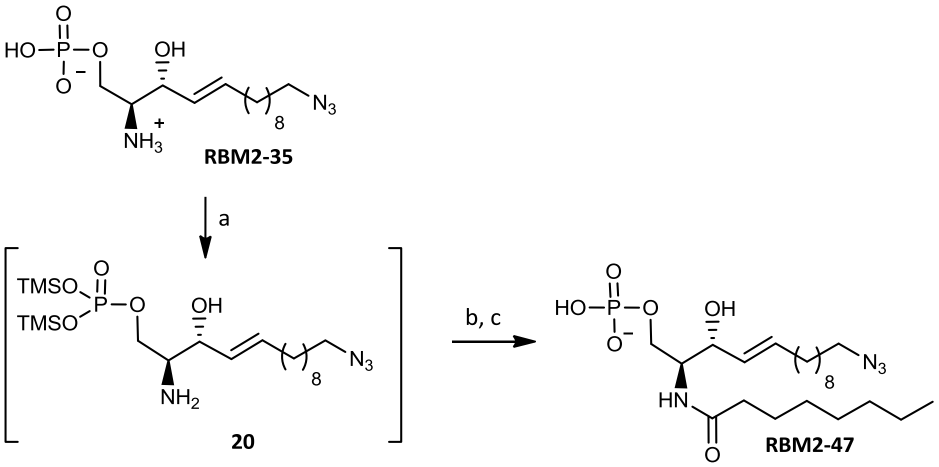

a) BSA, rt, overnight; b) DIPEA, octanoyl chloride, $CH_2Cl_2$, 0 °C to rt, 3 h.

**Figure 3.20** Synthetic approach to ω-azidoceramide-1-phosphate **RBM2-47** based on acylation of temporarily protected **RBM2-35**.

The synthesis started with the *in situ* hydroxyl protection of **RBM2-35** by silylation with an excess of neat BSA. The use of a TMS protecting group might significantly increase the solubility of the sphingoid base in organic solvents. After evaporation of the excess reagent, the silylated intermediate **20** was dissolved in dry $CH_2Cl_2$ and reacted with 1.2 equiv of octanoyl chloride in the presence of DIPEA. The crude reaction mixture was purified by reversed phase chromatography, and next analyzed by $^1H$ NMR spectroscopy. The presence of a new triplet at 0.91 ppm (*J*= 7.0 Hz) was attributed to a $CH_3$ group, whose integration largely exceeded that expected for a bis-(OTMS) phosphate ester. Moreover, the large aliphatic region between 1.20-1.45 ppm was not in agreement with the expected monoacylated compound, this confirming the failure of the method.

In a second strategy, we were prompted to use the dimethyl chlorophosphate method (see Section 3.1.3.3) to phosphorylate the ω-azidoceramide **RBM2-37**. We assumed that the subsequent silane-induced cleavage of the methyl ester groups would afford the desired ω-azidoceramide-1-phosphate **RBM2-47**, as indicated in Fig. 3.21. Thus, the synthesis started with the selective phosphorylation of compound **RBM2-37** with dimethyl chlorophosphate (see Section 3.1.3.3) to afford the corresponding dimethylphosphate ester **21** in quantitative yield. However, treatment of **21** with TMSBr, followed by methanolysis, did not afford the desired final product. The crude reaction mixture could not be satisfactorily purified by reversed phase chromatography, affording a complex mixture of compounds, as evidenced by the $^1H$ NMR and $^{13}C$ NMR spectra.

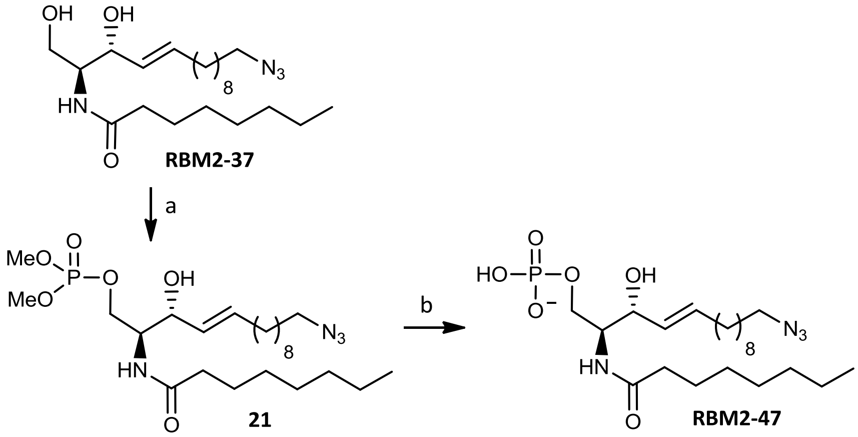

a) $(CH_3O)_2P(O)Cl$, NMI, THF, 0 °C to rt, 3 h, quantitative; b) TMSBr, ACN, 0 °C to rt, 3 h.

**Figure 3.21** Synthetic strategy to prepare ω-azidoceramide-1-phosphate **RBM2-47** based on phosphorylation **of RBM2-37**.

In consideration of the above results, we next attempted the preparation of ω-azidoceramide-1-phosphate **RBM2-47** *via* the *H*-phosphonate monoester approach, as reported by Bittman and coworkers (Fig. 3.22).[59] Thus, ω-azidoceramide **RBM2-37** was reacted with 3 equiv of 2-chloro-4*H*-1,3,2-benzodioxaphosphorin-4-one (**22**) in the presence of DIPEA in THF at -78 °C. Water addition was necessary to quench the excess reagent and also to hydrolyze the salicylic ester group in phosphite **23**, affording the *H*-phosphonate **24** in very good yield (83%). Initial attempts to oxidize this compound to the corresponding phosphate **RBM2-47** with *t*BuOOH were unsuccessful. However, the conversion of *H*-phosphonate monoesters into trivalent silyl phosphites, which are highly sensitive to oxidizing reagents, has been described (Fig. 3.16).[64-65] Thus, following a report by Garegg *et al.*,[64] silylation of *H*-phosphonate **24**, followed by *in situ* oxidation of the intermediate silyl phosphite **25** with 20 equiv of *t*BuOOH, afforded the desired phosphate **RBM2-47** in 21% yield. In this synthetic transformation, silylation is required in order to shift the tautomeric *H*-phosphonate/phosphite equilibrium (see section 3.1.3.2, Fig. 3.16) towards the phosphite species.

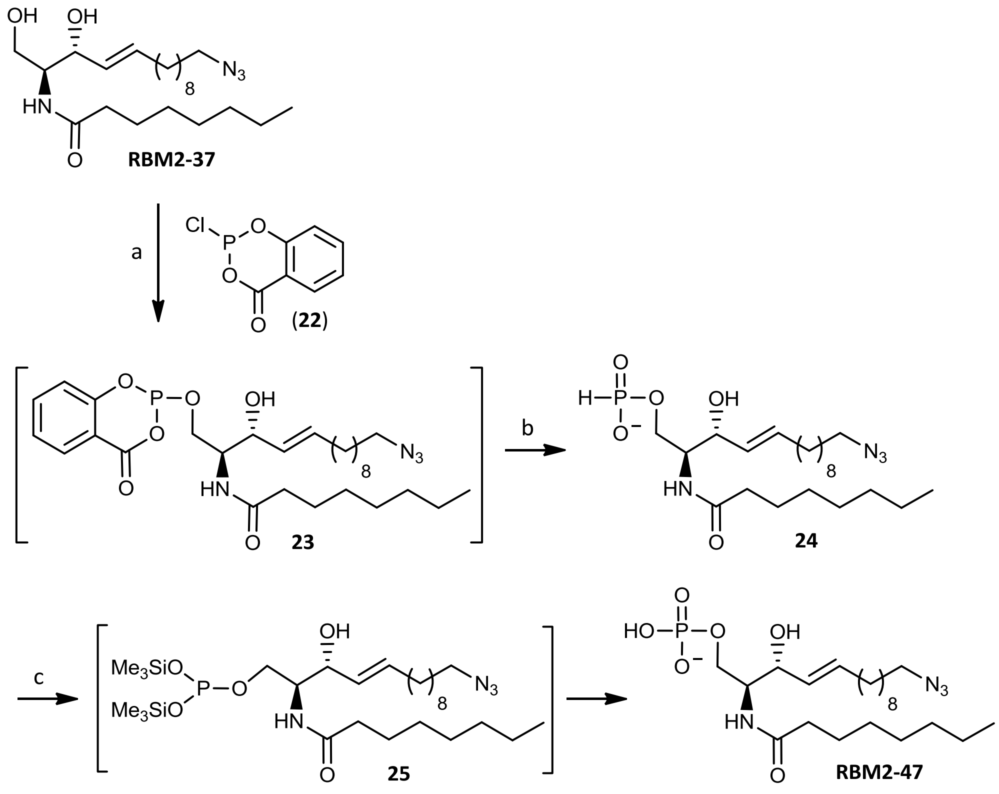

a) **22**, DIPEA, THF, -78 °C, 3 h; b) $H_2O$, -78 °C to rt, 83%; c): 1) TMSCl, $Et_3N$, $CH_2Cl_2$, rt, 30 min; 2) *t*BuOOH, rt, 1 h, 21%.

**Figure 3.22** Synthetis of ω-azidoceramide-1-phosphate **RBM2-47** *via H*-phosphonate.

## 3.1.5 Synthesis of ω-azido-3-ketodihydrosphingosine (RBM2-63)

### 3.1.5.1 Introduction

3-Ketosphinganine (Fig. 3.23) is the first product of the *de novo* SL biosynthesis and is often not detected in cells, due to its fast reduction to sphinganine.[66] Nonetheless, rat liver mitochondria have been reported to contain *N*-acylated and *O*-glycoslylated derivatives of 3-ketosphingoid bases,[67] and 3-ketosphinganine has been detected in cells when SPT activity is very high.[2]

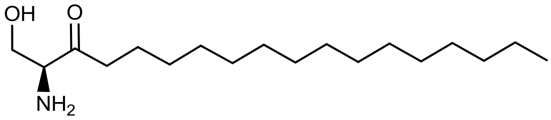

**Figure 3.23** Chemical structure of 3-ketosphinganine.

### 3.1.5.2 Selected approach for the synthesis of RBM2-63

Two synthetic approaches have been tested for the synthesis of this SL metabolite, as illustrated in Fig. 3.24. These are: (A) oxidation of *N*,*O*-diprotected ω-azidosphinganine (**15**), or (B) addition of various organometallic reagents to Weinreb amide **3**.[68]

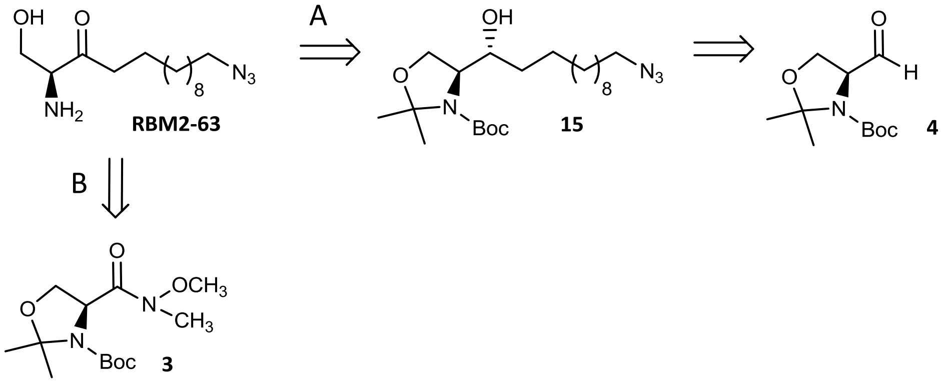

**Figure 3.24** Retrosynthetic strategies to ketone **RBM2-63**: (*A*) oxidation of intermediate **15**, and (*B*) addition of organometallic reagents to Weinreb amide **3**.

Since Weinreb amides cleanly react with Grignard and organolithium reagents to give ketones,[68] we first considered these routes as the most suitable ones to **RBM2-63**. However, several attempts to prepare the required Grignard reagent by reaction of a suitable iodo alkane with magnesium, and subsequent addition to Weinreb amide **3** resulted in failure.

In view of this result, we next considered the synthesis of **RBM2-63** by oxidation of the *N*,*O*-diprotected intermediate **15**. Although this scaffold had been prepared as described in Section 3.1.2.3, we envisaged an alternative, more practical approach for the synthesis of keto sphingolipids. As depicted in Fig. 3.25, **RBM2-63** can be obtained from protected ketone **29** by cleavage of both hydroxyl and amine protecting groups. The preparation of **29** can be carried out by oxidation of **15**, which, in turn, can be obtained by hydrogenation of **26**. The synthesis of intermediate **26** by diastereoselective addition of a suitable lithium-activated acetylide to Garner's aldehyde **4**, as reported by Herold,[69] becomes the key step of this synthetic approach.

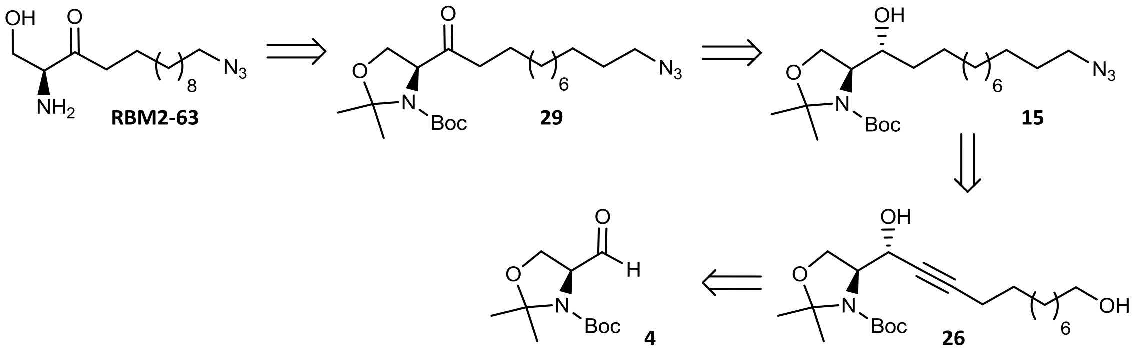

**Figure 3.25** Retrosynthetic analysis of 3-ketosphinganine **RBM2-63**.

### 3.1.5.3 Synthesis of ω-azido-3-ketodihydrosphingosine (RBM2-63)

Following the above retrosynthetic approach, addition of (11-hydroxyundec-1-yn-1-yl) lithium in THF/HMPA at -78 °C to aldehyde **4** afforded the *erythro* alkynol **26** in 50% yield, as depicted in Fig. 3.26. Hydrogenation of **26** in MeOH, in the presence of 10% Rh catalyst provided the saturated diol **27** in 89% yield. In order to introduce the azide group at the ω position, the selective activation of the primary hydroxyl group in **27** was required. With this purpose, the primary alcohol in **27** was transformed into the corresponding tosylate, using DMAP as catalyst, to afford compound **28** in 58% yield. Subsequent $S_N2$ tosylate displacement with sodium azide in DMF afforded azide **15** in 76% yield. The oxidation of the free hydroxyl group in **15** to the corresponding ketone **29** was accomplished with PCC as oxidizing agent in excellent yield (92%). The synthesis was successfully completed with the simultaneous cleavage of both oxazolidine and *N*-Boc protecting groups under acidic conditions, affording 3-ketosphinganine **RBM2-63** in 90% yield, which did not require any further chromatographic purification.

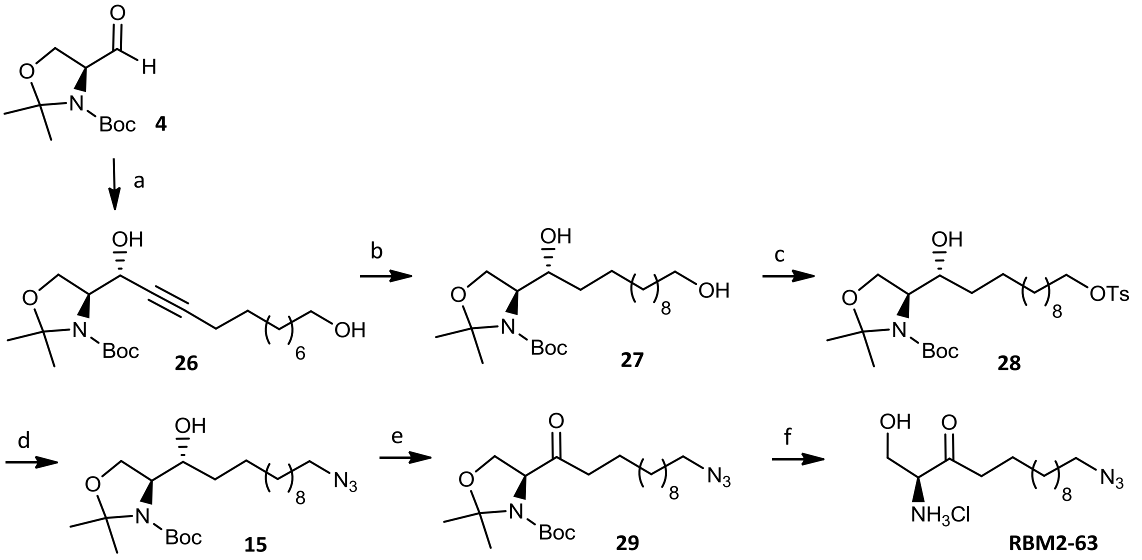

a) undec-10-yn-1-ol, BuLi, HMPA, THF, -78 °C, 3 h, 50%; b) Rh, MeOH, $H_2$ (AP), rt, 6 h, 89%; c) TsCl, DMAP, $Et_3N$, $CH_2Cl_2$, rt, 8 h, 58%; d) $NaN_3$, DMF, 90 °C, overnight, 76%; e) PCC, $CH_2Cl_2$, rt, overnight, 92%; f) $ClCOCH_3$, MeOH, rt, 1 h, 90%.

**Figure 3.26** Synthesis of ω-azido-3-ketosphinganine **RBM2-63**.

## 3.2 Synthesis of C1-azidoceramides

### 3.2.1 Introduction

Ceramides constitute the hydrophobic backbones of more complex SLs, such as sphingomyelin, cerebrosides, and gangliosides. They are also major components of the stratum corneum, which serves as a hydrophobic barrier to prevent water evaporation through the skin.[70] Besides, ceramides are known to exist in cell membranes as minor components,[71] where they are mainly found as biosynthetic intermediates of more complex SLs.[72-73] Ceramides are also able to regulate cell signaling through its ability to modulate the physical properties of the membranes, leading to membrane reorganization in response to stress signals.[74]

The most commonly found ceramides, those with a fatty acyl chain of 16 carbon or longer, are among the least polar, and more hydrophobic lipids in membranes. They have a strong propensity for hydrogen binding, functioning as both hydrogen donors and acceptors. All these properties contribute to the strong impact of ceramides on membrane properties, even at relatively low concentrations.[75]

When ceramides are part of phospholipid monolayers or bilayers, they show two main effects: (1) an increase of phospholipid molecular order, and (2) the promotion of lateral phase separation and domain formation. Other additional effects are also observed, such as enhancement of transmembrane lipid motion (flip-flop) leading to membrane permeabilization. In these scenarios, the use of specifically designed lipid probes has gained importance and become very useful for biophysical studies of cell membranes.

### 3.2.2 Synthetic approach to 1-azidoceramide (RBM2-79)

In order to synthesize the novel 1-azidoceramide **RBM2-79**, we decided to use CM as the key step to construct the ceramide skeleton possessing an *E*-double bond at C4-C5, as previously described in this dissertation (see Section 3.1.1.3).

The synthetic strategy for target ceramide **RBM2-79** is depicted in Fig. 3.27. We envisaged that **RBM2-79** could be obtained from protected azide **37** by removal of the *O*- and *N*-protecting groups, followed by *N*-acylation. The preparation of intermediate **37** would be feasible from scaffold **36** by $S_N2$ displacement with sodium azide of a suitable leaving group. Intermediate **36**, in turn, would be accessible from **30**, by protection of the secondary hydroxyl group, partial oxazolidine deprotection and subsequent activation of the primary hydroxyl group with an appropriate leaving group. Finally, the synthesis of **30** can be planned by CM reaction between allylic alcohol **7** and a terminal alkene.

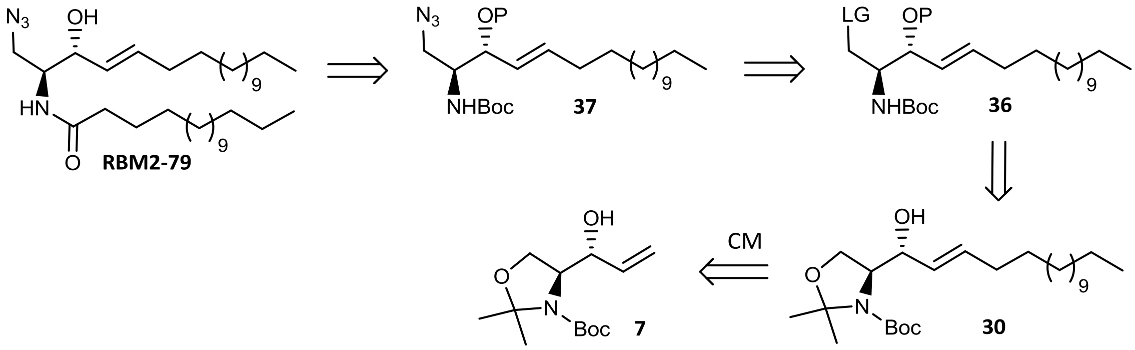

**Figure 3.27** Proposed retrosynthetic analysis of 1-azidoceramide **RBM2-79**. P represents a protecting group, and LG a leaving group.

### 3.2.3 Synthesis of 1-azidoceramide (RBM2-79)

According to the retrosynthetic scheme shown above, synthesis of ceramide **RBM2-79** started by CM reaction of alkene **7** with commercially available 1-pentadecene to give **30** in 59% yield with apparent total *E*-selectivity, since the corresponding *Z*-isomer was not observed by $^1$H NMR (Fig. 3.28). Compound **30** was next converted into mesylates **36a** (LG=OMs, P=H) or **36b** (LG=OMs, P=MOM) (Fig. 3.27), following standard protocols. However, introduction of the azide group by $S_N2$ displacement of the mesyloxy group with $NaN_3$ failed in both cases, giving several undefined by-products (data not shown). For this reason, we decided to block the C3 hydroxyl group with a constrained cyclic carbamate. Thus, **30** was quantitatively transformed into the bicyclic intermediate **31** by treatment with NaH in THF. Crude **31** was next treated under mild acidic conditions to afford alcohol **32** in 68% yield, which was converted into to the corresponding *O*-mesylate **33** in excellent yield (96%).

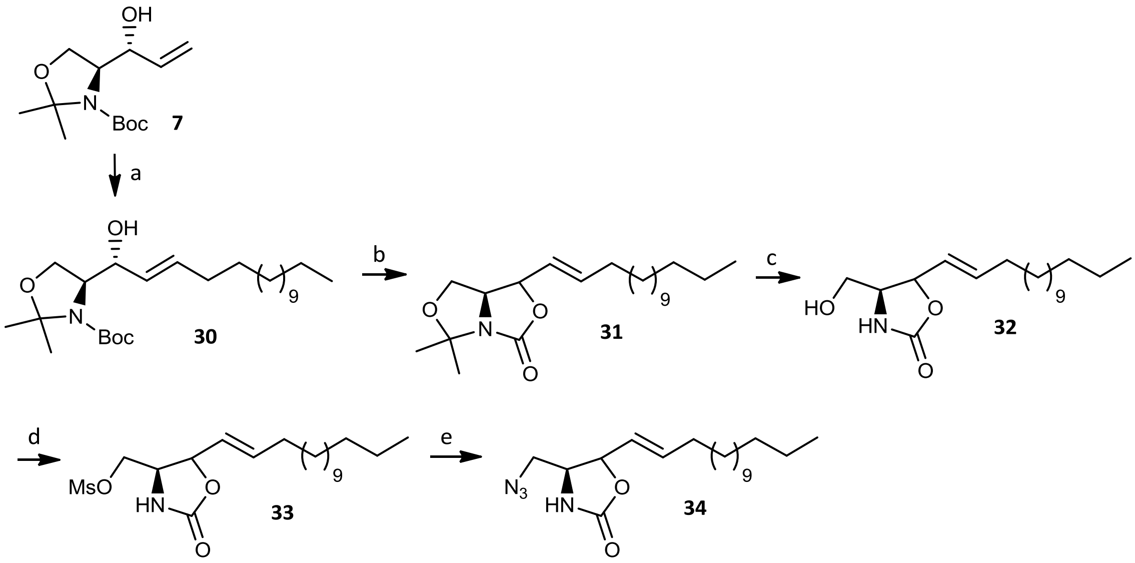

a) 1-Pentadecene, 2nd generation Grubb's catalyst, $CH_2Cl_2$, 45 °C, 5 h, 59%; b) NaH, THF, 0 °C to rt, overnight, quantitative; c) cat. TsOH, MeOH, rt, 2 h, 68%; d) MsCl, $Et_3N$, $CH_2Cl_2$, 0 °C to rt, 2 h, 96%; e) $NaN_3$, DMF, 45 °C, overnight, 68%.

**Figure 3.28** Synthesis of carbamate **34**.

We next evaluated the $S_N2$ displacement of the mesyloxy group in compound **33** by reaction with sodium azide in DMF at 85 °C. Surprisingly, pyrroline **35** was formed in 71% yield, instead of the expected azide **34** (Fig. 3.29). Formation of **35** was confirmed by MS, where a loss of molecular nitrogen was observed. Furthermore, $^1H$ NMR exhibited the disappearance of the olefinic C4-C5 protons (SL numbering), as well as a quartet at 2.10 ppm for the C6 protons. In addition, protons at C1, C2 and C3 appeared at 3.98 (multiplet), 4.41 (multiplet), and 6.10 ppm (singlet), respectively. In the $^{13}C$ NMR spectra, the resonance for C4 at 173.9 ppm was assigned to a new quaternary carbon. Gratifyingly, when the reaction temperature was lowered to 45 °C, a separable mixture of the desired azide **34** (68% yield) and pyrroline **35** (20%) was obtained. Formation of **35** can be interpreted as a result of an intramolecular azide-olefin 1,3-dipolar cycloaddition under thermal conditions.[76] Unlike their aromatic related 1,2,3-triazoles, the resulting 1,2,3-$\Delta^2$-triazolines are generally not isolable and evolve, by loss of molecular nitrogen, to the corresponding pyrrolines, as in **35** (Fig 3.29).

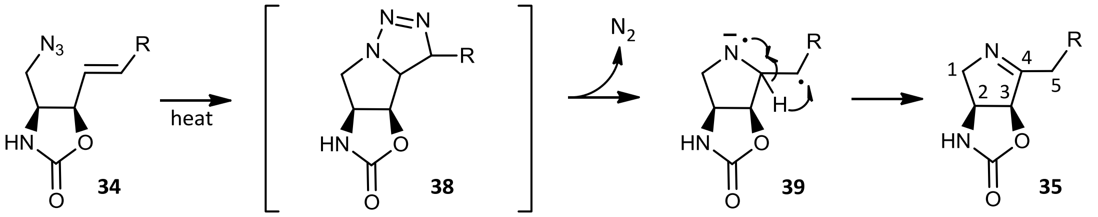

**Figure 3.29** Postulated mechanism to account for the formation of pyrroline **35** (sphingolipid numbering is used for this compound).

With oxazolidone **34** in hand, its cleavage under basic conditions was next studied, as shown in Table 3.1.

**Table 3.1** Cleavage of oxazolidone **34** under basic conditions.

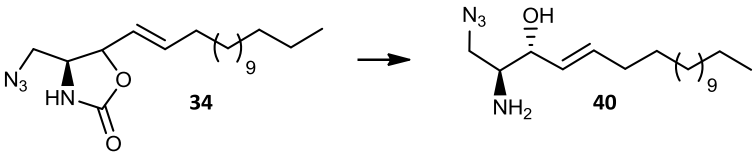

| Entry | Base | Solvent | Temperature (°C) | Time (h) | 40 (% yield) |
|---|---|---|---|---|---|
| 1 | LiOH | EtOH/$H_2O$ (7:3) | 75 | 24 | - |
| 2 | *t*-BuOK | DMF | 40 | 24 | - |
| 3 | $K_2CO_3$ | MeOH | 25 | 24 | - |
| 4 | NaOH | EtOH | 80 | 0.75 | - |
| 5 | NaOH | EtOH | 60 | 8 | **17** |

We tried to cleave oxazolidone **34** under a variety of basic conditions using different solvent mixtures and temperatures, as indicated in Table 3.1. Unfortunately, the use of LiOH, *t*-BuOK, and $K_2CO_3$ (entries 1-3) led to azide decomposition, as evidenced by the formation of several unidentified by-products. Similar results were obtained when oxazolidone **34** was treated with a 1:1 mixture of 2*N* NaOH in EtOH at 80 °C, even after 45 min (entry 4). However, azide **40** could be obtained under these conditions at lower temperature (60 °C) and prolonged reaction times (8 h), albeit in only 17% yield (entry 5).

Final *N*-acylation of compound **40** with palmitic acid and EDC/HOBt as coupling reagents in $CH_2Cl_2$ (Fig. 3.30) afforded the corresponding 1-azidoceramide **RBM2-79** in good yield (82%).

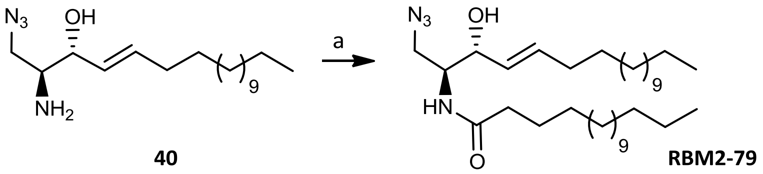

**40** **RBM2-79**

a) $CH_3(CH_2)_{14}COOH$, $Et_3N$, EDC, HOBt, $CH_2Cl_2$, 1 h, 82%.

**Figure 3.30** Synthesis of 1-Azidoceramide **RBM2-79**.

## 3.3 Applications of AzidoSLs as chemical probes

### 3.3.1 A new analytical method for the quantification of SL based on SPAAC

As previously mentioned, SLs are bioactive molecules that play important roles in a variety of cellular processes including apoptosis, senescence, differentiation, migration, angiogenesis, proliferation, infection, protein trafficking, autophagy and inflammation (see Section 1.3). Moreover, it has been suggested that many of the enzymes involved in SLs metabolism, and their products, are implicated in signal transduction and cell regulation.

Due to their physiological importance, the description of the complete SL profile within a cell or tissue has gained much attention in the last few years. This complete description, termed as sphingolipidome, contains information of the composition and abundance of SLs.

Several analytical approaches for the quantification of SLs have been described, including gas chromatography (GC),[77] and high performance liquid chromatography (HPLC).[78-80] In addition, advances in mass spectrometry (MS) have made this technique a widely used method for the quantitative measurement of SLs.[81-82] In this context, the simultaneous measurement of multiple ceramide and monohexosylceramide samples using an approach based on isobaric tags for relative and absolute quantitation has also been described.[83]

The growing interest in SLs detection and quantification led us to set up a new analytical method for SLs simultaneous analysis. The successful application of “Stable Isotope Labeling by Amino acids in Cell culture (SILAC)” as a quantitative method for proteomics,[84-85] in which differences of protein abundance among samples are detected by MS, prompted us to transfer this concept to the sphingolipidomics field. Instead of the isotopic labeling, we intended to explore click chemistry as a tool for the labeling of SLs mixtures. Thus, a novel approach consisting of the incorporation of $\omega$-azidoSLs on different cell populations for their subsequent chemical labeling with exogenous probes through click reactions was designed. These exogenous probes, bearing a reactive cyclooctyne moiety, have been designed as a homologous series differing in only one methylene unit mass. By optimization of this approach, the simultaneous quantification of SLs species in different samples would be possible based on mass differences among the cell populations to be analyzed (Fig. 3.31).

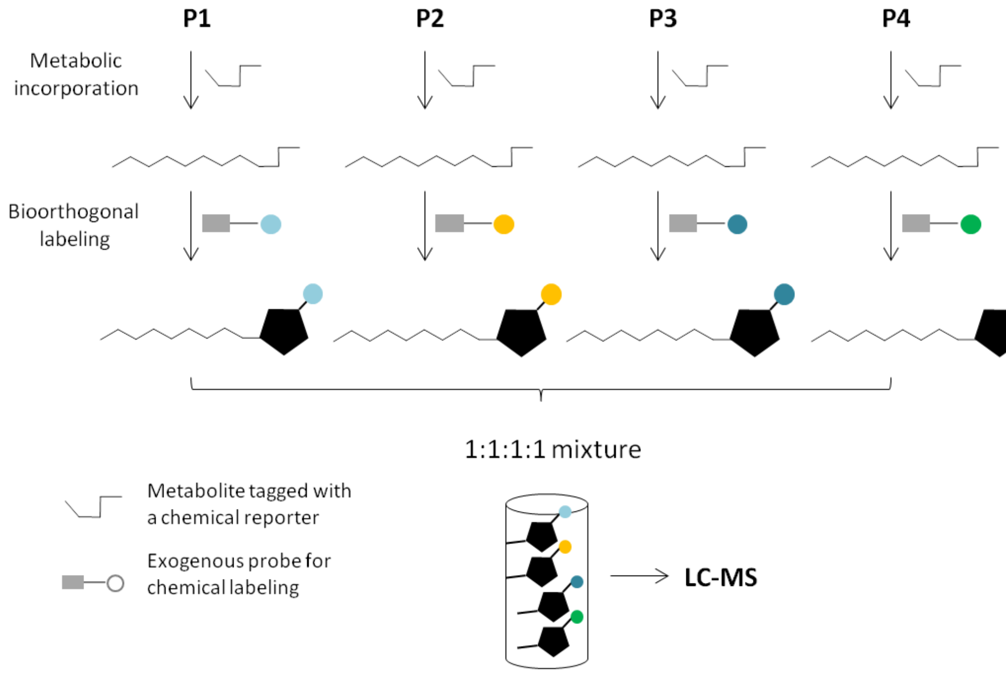
P1
P2
P3
P4
Metabolic incorporation
Bioorthogonal labeling
1:1:1:1 mixture
Metabolite tagged with a chemical reporter
Exogenous probe for chemical labeling
LC-MS

**Figure 3.31** Simultaneous analysis of labeled SLs through click reactions by LC-MS.

### 3.3.1.1 Effects of ω-azidoSLs on the sphingolipidome and metabolization

In order to test the above strategy, we selected some of the ω-azidoSLs described in Section 1.3 and shown in Fig. 3.32. The selected compounds are characterized by their structural similarity with the most relevant primary metabolites of the *de novo* biosynthesis of SLs (see Section 1.3.2).

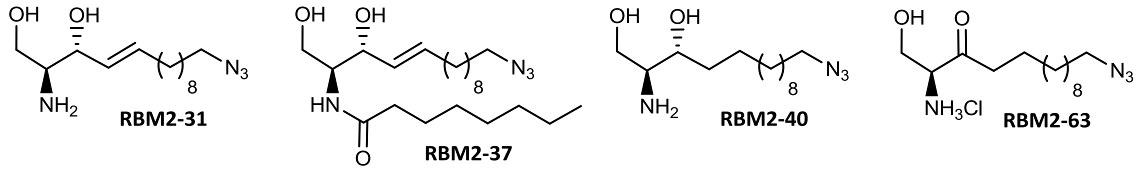

**Figure 3.32** Chemical structures of the selected ω-azidoSLs for SPAAC-based sphingolipidome analysis.

We first evaluated the cytotoxicity of these compounds in two cell lines: human lung adenocarcinoma A549, and human gastric carcinoma HGC-27 cells. Azides **RBM2-31**, **RBM2-40** and **RBM2-63** were not significantly toxic in A549 cells, with CC50 values of 74, 62, and 51 μM, respectively, after 24 h incubation. In contrast, these compounds turned out to be more cytotoxic in HGC-27 cells, with CC50 values of 10, 8, and 14 μM for **RBM2-31**, **RBM2-40** and **RBM2-63**, respectively.

We next studied the effect of these azides on the endogenous SL metabolism. Therefore, they were first tested in cancer A549 intact cells at 10 μM for 24 h. As depicted in Fig. 3.33*A*, compound **RBM2-31** produced a 0.6- and 0.7-fold decrease in total ceramides and dihydroceramides, respectively. This azide led to a 0.7-fold decrease in total sphingomyelins (not statistically significant at $p \leq 0.005$; unpaired two-tail *t*-test), while dihydrosphingomyelins were not affected. Azide **RBM2-37** exhibited a 0.7-fold decrease in both ceramides and dihydrosphingomyelins, while sphingomyelins decreased a 0.6-fold. However, any of these variations were statistically significant, according to the above criteria. On the other hand, compounds **RBM2-40** and **RBM2-63** did not display variations in comparison with control (Fig. 3.33*B*). Total sphingomyelins were slightly increased (1.1-fold) but with no statistical significance.

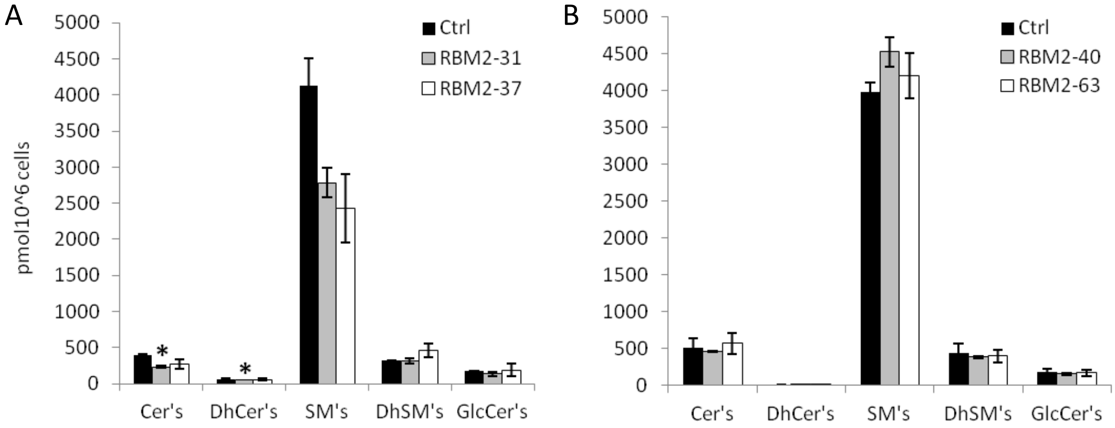

**Figure 3.33** Effect of compounds (*A*) **RBM2-31**, **RBM2-37**, and (*B*) **RBM2-40**, **RBM2-63** on the sphingolipidome. A549 cells were treated with 10 μM compounds for 24 h. SLs were extracted, and next analyzed as detailed in the Experimental Section. Data correspond to the mean ± SD of one representative experiment with triplicates. Asterisk indicates statistically significant difference from the mean ($p \leq 0.005$; unpaired two-tail *t*-test).

Analogously, the effect of compounds **RBM2-31**, **RBM2-40**, and **RBM2-63** on the sphingolipidome was also examined in HGC-27 cells at 5 μM of test compound, for different incubation times. As depicted in Fig. 3.34, our azides produced a decrease of ceramides, mainly at 3 and 6 h. **RBM2-40** and **RBM2-63** slightly increased the levels of cellular dihydroceramides at long incubation times (10 and 24 h), although this variation was not statistically significant. However, **RBM2-31** exhibited a 8-fold (significant) and 12-fold (not significant) increase of total dihydroceramides at 10 and 24 h, respectively. On the other hand, total sphingomyelins were not significantly modified and only **RBM2-31** decreased around 0.7-fold the levels of these species at 6 h. Moreover, **RBM2-40** and **RBM2-63** produced a 2-fold increase of the cellular dihydrosphingomyelins at 24 h, whereas **RBM2-31** significantly increased the levels of these species at 10h and 24 h. All compounds showed a slightly decrease in total glucosylceramides at 6 and 10 h, whereas this effect was higher (but not significant) for azide **RBM2-31** at 24 h.

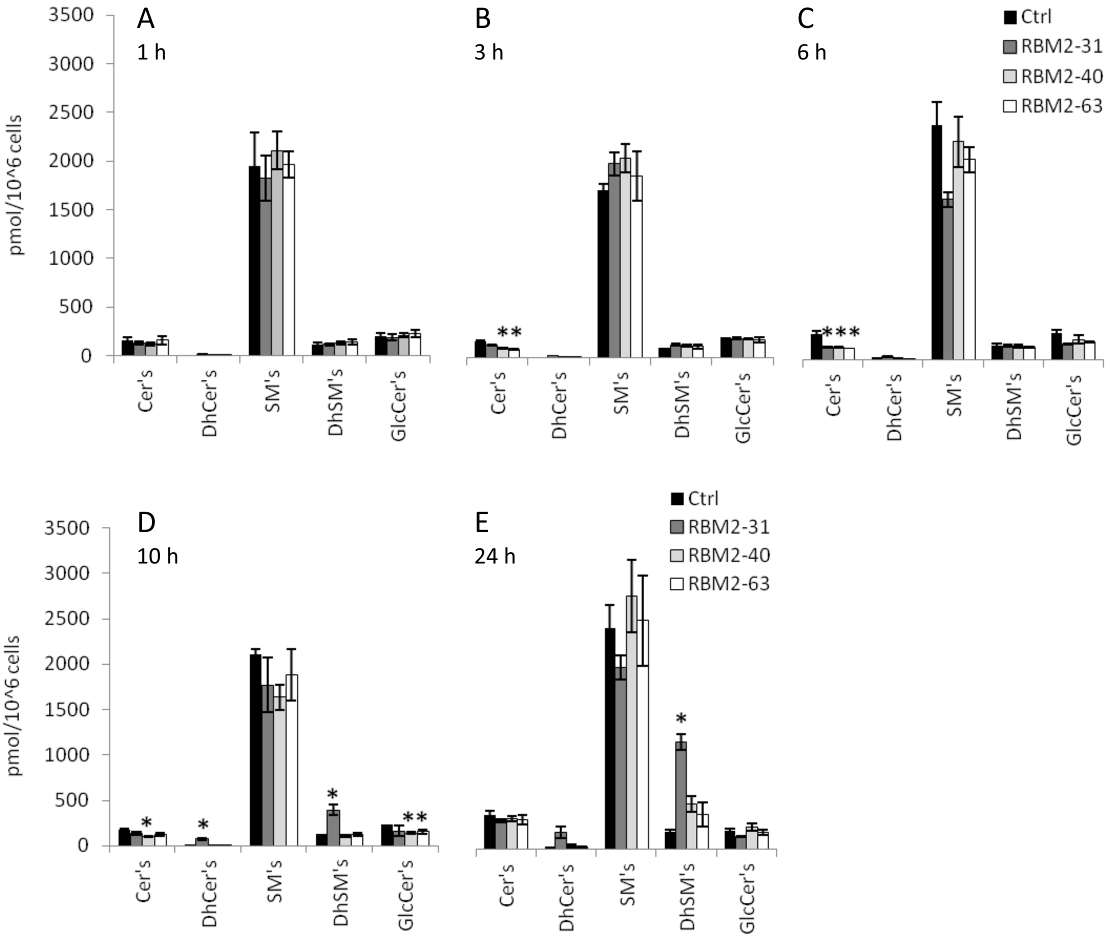

**Figure 3.34** Effect of compounds **RBM2-31, RBM2-40** and **RBM2-63** on the sphingolipidome. HGC-27 cells were treated with 5 μM compounds for: (*A*) 1 h; (*B*) 3 h; (*C*) 6 h; (*D*) 10 h, and (*E*) 24 h. SLs were extracted, and next analyzed as detailed in the Experimental Section. Data correspond to the mean ± SD of one representative experiment with triplicates. Asterisk indicates statistically significant difference from the mean ($p \leq 0.005$; unpaired two-tail *t*-test).

Moreover, the above extracts of A549 and HGC-27 cells used to characterize the sphingolipidomes revealed the metabolization of azides **RBM2-40** and **RBM2-63** *via* the *de novo* pathway (Fig. 3.35*A*). On the other hand, while **RBM2-31** was *N*-acylated by the action of CerS, **RBM2-37** resulted in trans-acylation by the sequential action of CDase and further CerS catalyzed *N*-acylation.

Compounds **RBM2-31** and **RBM2-37** were mainly metabolized to the corresponding ω-azidosphingomyelins in A549 cells (Fig. 3.35*B*), exhibiting high phosphocholine incorporation. The highest levels of ω-azidosphingomyelins were those of the C24 species in both compounds (mean equiv pmol/$10^6$ cells: **RBM2-31**, 55.6±7.27; **RBM2-37**, 61.3±13.96). Other species, such as ω-azidoceramides, were formed in lower levels. On the other hand, the saturated analog **RBM2-40** was metabolized to the corresponding ω-azidodihydroceramides, ω-azidosphingomyelins and ω-azidodihydrosphingomyelins. In this case, both ω-azidosphingomyelins and ω-azidodihydrosphingomyelins were the major metabolites, the C24 species being the most abundant ones (mean equiv pmol/$10^6$ cells: ω$N_3$C24-SM, 114.8±26.77; ω$N_3$C24-DhSM, 80.6±14.53). The low levels of ω-azidoceramides are in agreement with their extensive transformation into ω-azidosphingomyelins. Compound **RBM2-63** showed an extensive metabolism to ω-azidodihydroceramides, ω-azidoceramides, ω-azidosphingomyelins and ω-azidodihydrosphingomyelins. In this case, ω-azidodihydroceramides were the major species, with ω$N_3$C24-DhCer as the most abundant metabolite (mean equiv pmol/$10^6$ cells: 95.8±34.96).

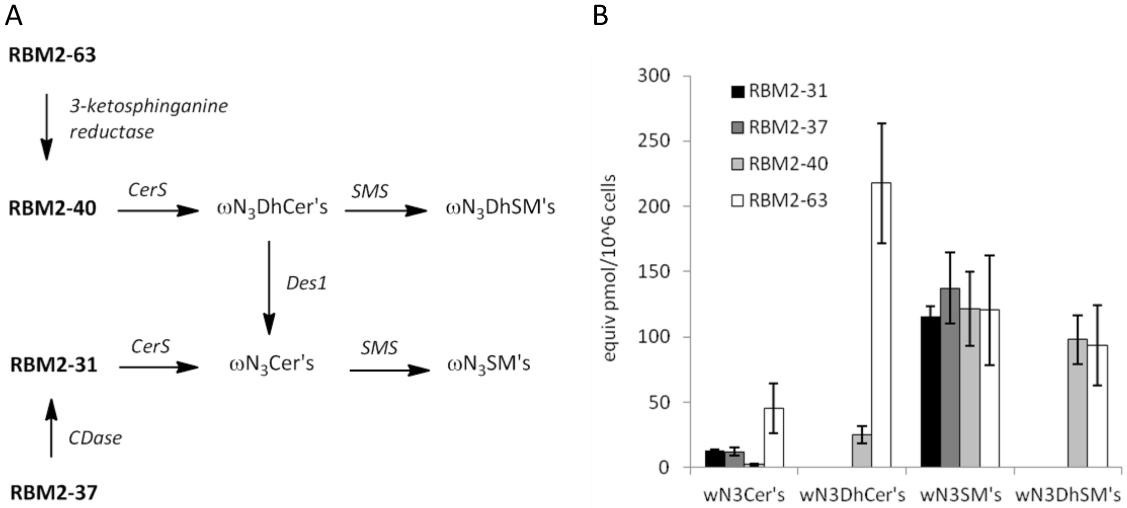

**Figure 3.35** Metabolization of **RBM2-31**, **RBM2-37**, **RBM2-40**, and **RBM2-63** after 24 h incubation in A549 cells. (*A*) Scheme of metabolic pathways, and (*B*) Levels of different metabolites labeled with an azide functionality. The amounts (mean pmol ± SD, n=3) of ω-azidoSL metabolites are relative to appropriate internal standards.

Metabolism in HGC-27 cells revealed the conversion of **RBM2-31** into the corresponding ω-azidoceramides and ω-azidosphingomyelins, as depicted in Fig. 3.36*A*. While the levels of ω-azidosphingomyelins were invariable between 6 and 24 h, ω-azidoceramides significantly decreased at 10 h. Compound **RBM2-40** (Fig. 3.36*B*) was rapidly metabolized to ω-azidoceramides and ω-azidodihydroceramides, as observed from their high levels at short incubation times. Both species decreased at long incubation times, at the expense of the observed increase of ω-azidodihydrosphingomyelins and ω-azidosphingomyelins.

Similarly, azide **RBM2-63** showed an extensive metabolization, similar to that of compound **RBM2-40** and also with a similar profile. However, all metabolites of **RBM2-63** decreased their levels at 24 h in comparison with those observed at shorter incubation times.

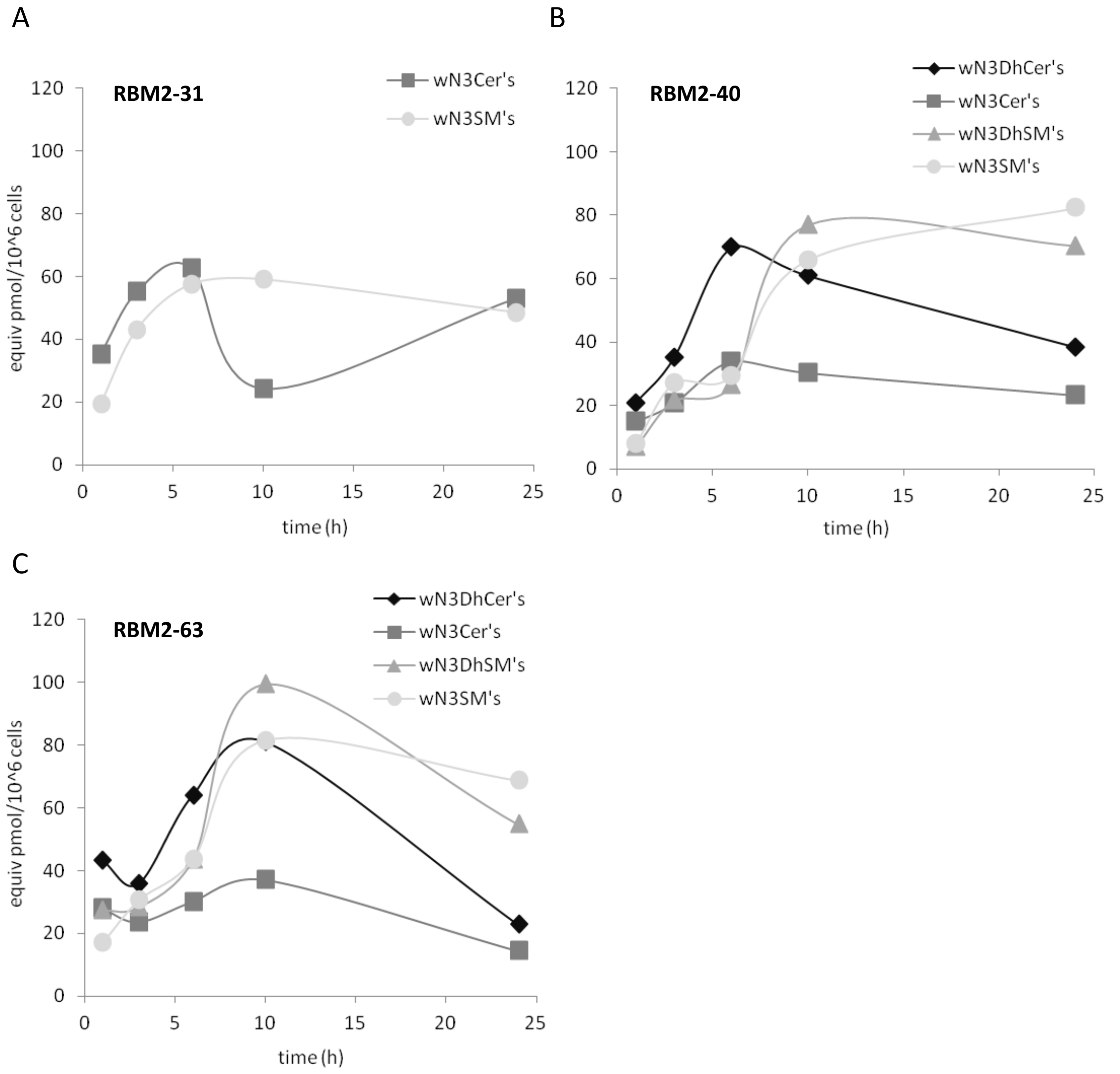

**Figure 3.36** Metabolization of probes (*A*) **RBM2-31**, (*B*) **RBM2-40**, and (*C*) **RBM2-63** in HGC-27 cells for different incubation times. All the detected metabolites are labelled with an azide functionality. The amounts (mean equiv pmol) of ω-azidoSL metabolites are relative to appropriate internal standards. To better visualize the graphics, the SD is not shown.

It is worthy of mention that the corresponding ω-aminoSL metabolites, arising from the enzymatic reduction of the azide group, were not detected in any of the two cell lines used in this study. This enzymatic transformation is known to take place in the presence of monothiols, such as glutathione at alkaline pH, but the rates of such reductions under physiological conditions are irrelevant on the time scale of our experiments.[86-87]

Collectively, the above results revealed the suitability of the selected ω-azidoSLs as appropriate probes to study SL metabolism, since they do not significantly alter the basal SL levels. In particular, the azido probe **RBM2-63** (a close analogue of 3-ketosphinganine, the first substrate of the *de novo* SL biosynthesis) showed a metabolic pattern for dihydrosphingomyelins similar to that of natural SLs, as illustrated in Fig. 3.37. Azido probes **RBM2-31**, **RBM2-37** and **RBM2-40**, despite they do not exhibit the same behaviour, might be also considered as suitable SL tracers.

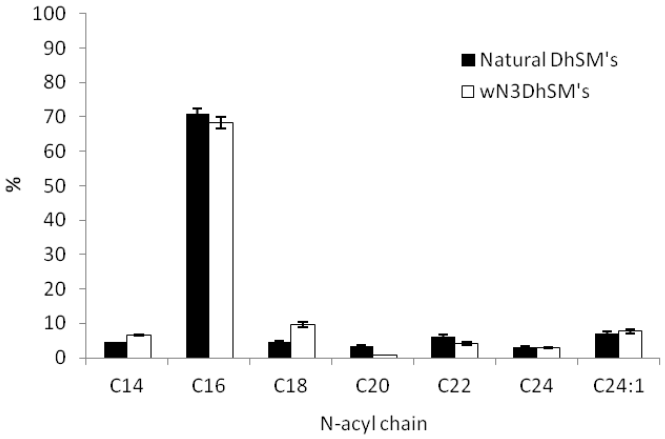

**Figure 3.37** Relative abundance of natural dihydrosphingomyelins and ω-azidodihydrosphingomyelins, containing different *N*-acyl chains, in HGC-27 cells incubated with the azido probe **RBM2-63** for 10 h.

### 3.3.1.2 Tags based on the azacyclooctyne moiety

As previously considered, various azacyclooctyne-based tags, differing in their mass, were required to selectively label different cell populations containing ω-azidoSLs through click chemistry reactions.

For this purpose, we decided to use commercially available dibenzocyclooctyne **41** (Fig. 3.38), bearing a suitable NHS ester for its reaction with amines and a highly reactive dibenzocyclooctyne moiety, due to its inherent ring strain.[88] The derivatization of this starting material was accomplished by acylation with different linear alkyl amines in DMF, using DIPEA as base. Therefore, amide tags **1-5** were obtained in a range of 73-80% yield.

The reasons to use an amide bond to functionalize the tags are twofold: first, the amide group offers an excellent chemical stability under the alkaline conditions required for the saponification step in the course of SL extraction (see Experimental Section); in addition, introduction of two nitrogen atoms has been described to enhance the sensitivity of the tag in the MS analysis.[83]

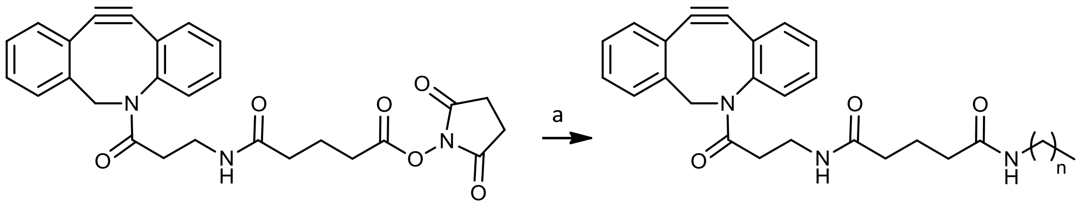

**41**

**tag 1-5**: n=1-5

a) $CH_3CH_2(CH_2)_nNH_2$, DIPEA, DMF, rt, overnight, 73-80%.

**Figure 3.38** Synthesis of tags **1**-**5** by acylation of starting material **41** with different alkyl amines.

### 3.3.1.3 Model click reactions between azide RBM2-37 and tags 1-5 in solution

With azacyclooctyne tags **1-5** in hand, we first examined their reactivity with probe **RBM2-37**, as shown in Table 3.2. Thus, azide **RBM2-37** was reacted with a 50-fold excess of tags **1-5** in MeOH at 37 °C overnight. Although the click reaction should be fast, we ensured the total disappearance of the starting azide by using long reaction times. In addition, we decided to use a concentration of azide probe (150 pmol) in the range of what should be expected in real cell assays for the total levels of ω-azidoSLs after cell incubation with the probes.

Although click reaction with tags **1-5** was expected to produce a 1:1 mixture of regioisomeric 1,2,3-triazoles, only single peaks for the triazole adducts were detected in all cases. Moreover, no starting azide **RBM2-37** was ever detected after the click reaction, this indicating the quantitative nature of this transformation. On the other hand, it is worthy of mention that the corresponding triazole adducts were detected with an approximate 8-fold higher sensitivity than the starting azide **RBM2-37**, as indicated by the relative peak areas shown in Table 3.2.

**Table 3.2** SPAAC between azide **RBM2-37** and tags **1**-**5**. MS-based assignments of click adducts.

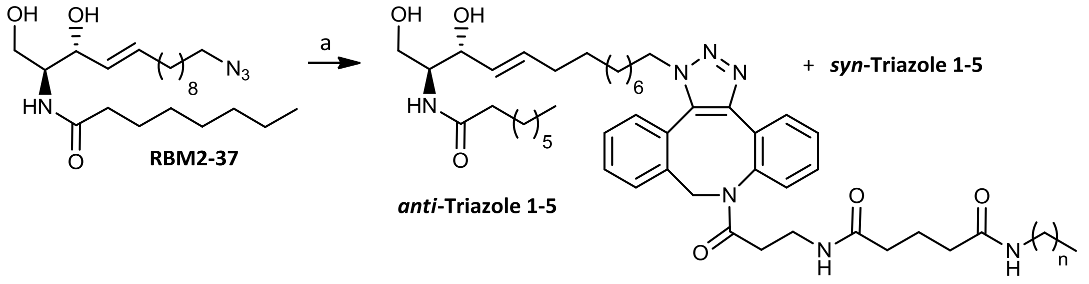

**RBM2-37**

***anti*-Triazole 1-5**

+ ***syn*-Triazole 1-5**

a) Tags **1**-**5**, MeOH, 37 °C, overnight.

| **Compound** | **RT (min)** | **Theoretical *m/z*** | **Measured *m/z* (error, ppm)** | **Relative peak areas**[a] |
|---|---|---|---|---|
| **RBM2-37** | 7.55 | 411.3335 | 411.3335 (0.0) | 1.0 |
| **Triazole 1** (n=1) | 5.83 | 828.5388 | 828.5380 (-1.0) | 7.3 |
| **Triazole 2** (n=2) | 6.25 | 842.5544 | 842.5545 (+0.1) | 8.4 |
| **Triazole 3** (n=3) | 6.75 | 856.5701 | 857.5701 (0.0) | 7.7 |
| **Triazole 4** (n=4) | 7.25 | 870.5857 | 870.5858 (+0.1) | 7.9 |
| **Triazole 5** (n=5) | 7.76 | 884.6014 | 884.6016 (+0.2) | 7.5 |

[a] Relative peak areas in relation to azide **RBM2-37**.

#### 3.3.1.4 Click reaction between ω-azidoSL metabolites and tag 1 in cell pellets

In a second optimization step, we next evaluated the selective labeling of ω-azidoSL metabolites with tag **1** in cell extracts.

Thus, ω-azidosphingosine (**RBM2-31**, 10 μM) was incubated for 6 h in A549 cells. This incubation time was considered optimal, as shown in Fig. 3.36. In order to examine the most efficient click reaction conditions for the sphingolipidome analysis, we added tag **1** at two different stages. First, tag **1** (7.5 nmol) was added prior to lipid solubilization, as shown in Fig 3.39*A*. Therefore, a suspension of cell pellets in the standard lipid extraction solvent mixture was treated with tag **1**, together with an internal standard mix (see below). The resulting mixture was gently agitated at 48 °C overnight, allowing click reaction to proceed smoothly. After SLs solubilization, subsequent saponification, neutralization and concentration steps were carried out prior to UPLC-TOF analysis, as detailed in the Experimental Section. In a parallel run (Fig. 3.39*B*), tag **1** was added after lipid solubilization. In this case, the click reaction was allowed to proceed at rt in a sonication bath for 2 h, prior to UPLC-TOF analysis.

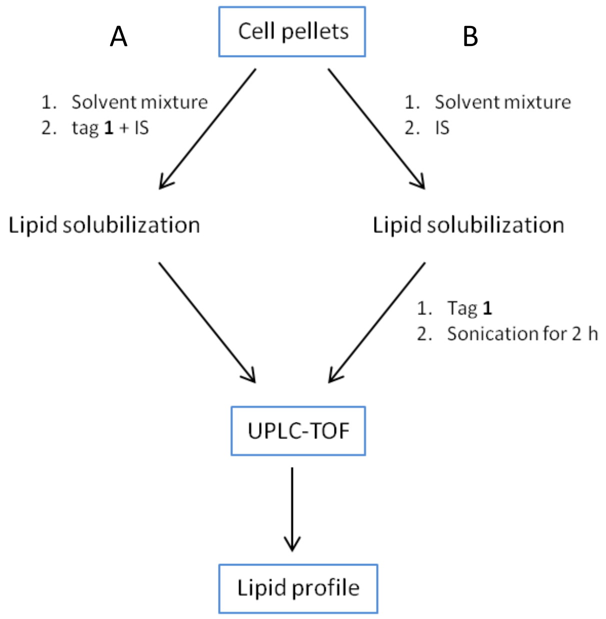
A
Cell pellets
B
1. Solvent mixture
2. tag 1 + IS
1. Solvent mixture
2. IS
Lipid solubilization
Lipid solubilization
1. Tag 1
2. Sonication for 2 h
UPLC-TOF
Lipid profile

**Figure 3.39** Labeling of ω-azidoSL metabolites through click reaction with tag **1**: (*A*) before, and (*B*) after lipid solubilization. IS: internal standard (standard mix).

When tag **1** was added before SL solubilization (path A), the total amounts of unreacted ω-azidoSL metabolites were 0, 20, 9, and 0% for ω-azidosphingosine, ω-azidoceramides, ω-azidosphingomyelins, and ω-azidoglucosylceramides, respectively, in relation to control (no click reaction, Table 3.3). In contrast, when tag **1** was added after SL solubilization (path B), the click reaction turned out to be much less efficient, resulting in higher levels of unreacted ω-azidoSL metabolites: 30, 75, 39, and 63% for ω-azidosphingosine, ω-azidoceramides, ω-azidosphingomyelins, and ω-azidoglucosylceramides, respectively (Table 3.3). These results indicate that the addition of tag **1** to the cell pellets before SL solubilization (path A) is more convenient for an efficient click reaction. However, it seems as if 7.5 nmol of tag **1** were not enough for a quantitative reaction, since no unreacted reagent could ever be detected and, moreover, some remaining ω-azidoSL metabolites were still observed, although in low levels. For this reason, 15 nmol tags were used in subsequent experiments (see below). The requirement of such an excess might be explained by nonspecific binding with some of the cell components during the click reaction.

**Table 3.3** % Amounts of remaining ω-azidoSL metabolites after click reaction with tag **1**. Percentages are calculated in relation to control (no click reaction).

| Species | % Click reaction (path A) | % Click reaction (path B) |
|---|---|---|
| ω$N_3$Sph | 0 | 30 |
| ω$N_3$Cer's | 20 | 75 |
| ω$N_3$SM's | 9 | 39 |
| ω$N_3$GlcCer's | 0 | 63 |

### 3.3.1.5 Labeling of ω-azidoSL metabolites with tags 1-5

We next decided to evaluate the suitability of tags **1-5** for sphingolipidome analysis using click chemistry. Therefore, azide **RBM2-31** (10 μM) was incubated with A549 cells for 6 h, followed by incorporation of tags (path A), as indicated above.

In order to properly quantify the resulting mixture of click adducts, the triazole **St1**, resulting from reaction of **RBM2-37** and tag **3** (Fig. 3.40, "Triazole 3" in Table 3.2) was used as internal standard, together with the commercial mixture of standards ("standard mix") currently used for SL analysis by UPLC-TOF.

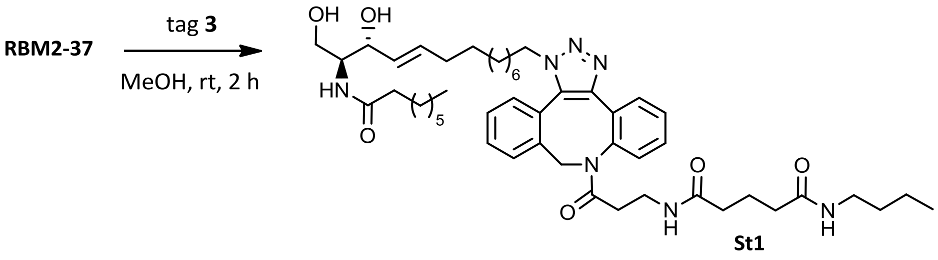

**Figure 3.40** Preparation of internal standard **St1**.

As indicated above, a large excess of azadibenzocyclooctyne tags (15 nmol) was added to the SL solubilization mixture to afford a quantitative labeling of target ω-azidoSLs. As illustrated in Fig. 3.41*A*, click reactions with tags **1-5** proceeded quantitatively, since unreacted ω-azidoSL metabolites were not detected or detected in very low amounts compared to control (non-tagged).

Moreover, the corresponding triazole SL metabolites arising from the click reactions (Tz-SLs) were detected with high sensitivity in all cases, as shown in Fig. 3.41*B*. Qualitatively, the metabolic profile of labeled ω-azidoSLs with tag **3** was similar to that of control (non-tagged), being sphingomyelins the species formed in highest levels (Fig 3.41*A*). Levels of both Tz-sphingosine and Tz-ceramides were lower than those of Tz-sphingomyelins, in agreement with that observed in the control (non-tagged). On the other hand, triazole SL metabolites of tags **1**, **2**, **4** and **5** were also formed in high amounts, as shown in Fig. 3.41*B*. In these cases, Tz-ceramides were the major species, while Tz-sphingosine and Tz-sphingomyelins were found in lower amounts. Surprisingly, this metabolic behavior did not parallel that observed in the control (non-tagged).

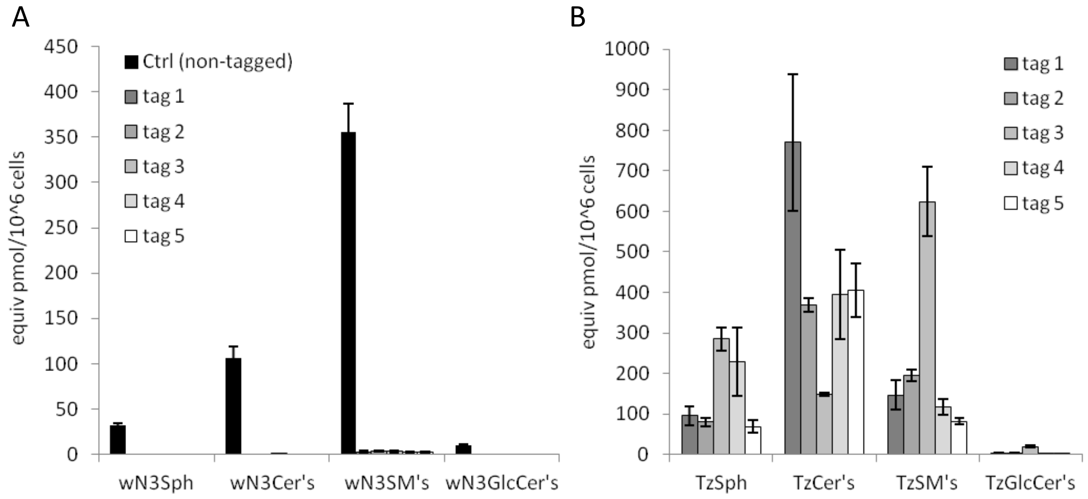

**Figure 3.41** Labeling of ω-azidoSL metabolites from A549 cells with tags **1**-**5**: (*A*) Levels of remaining ω-azidoSL metabolites after click reaction; and (*B*) Triazole SL metabolites formed by click reaction. Data correspond to the mean ± SD of one representative experiment with triplicates. Amounts of ω-azidoSL metabolites are relative to ”standard mix”, and triazole metabolites to **St1**.

It is worthy of mention that click chemistry labeling with tags **1**-**5** gives rise to changes in some of the physical properties of the resulting Tz-SL metabolites, such as mass, polarity, and ionization efficiency, among others. As shown in Table 3.4, significant changes in the retention times for the click adducts on reverse phase were also observed.

**Table 3.4** Effect of the click reaction labeling of ω-azidosphingoid bases on retention times in UPLC-TOF.

| | RT (min) | | | |
|---|---|---|---|---|
| | C24-Cer | C24:1-Cer | C24-SM | C24:1-SM |
| Non-labeled | 13.87 | 13.31 | 13.78 | 13.13 |
| Tag 1 | 12.52 | 11.94 | 12.10 | 11.62 |
| Δ | -1.35 | -1.37 | -1.68 | -1.51 |
| Tag 2 | 12.64 | 12.08 | 12.27 | 11.79 |
| Δ | -1.23 | -1.23 | -1.51 | -1.34 |
| Tag 3 | 12.83 | 12.30 | 12.47 | 11.93 |
| Δ | -1.04 | -1.01 | -1.31 | -1.20 |
| Tag 4 | 12.99 | 12.46 | 12.63 | 12.09 |
| Δ | -0.88 | -0.85 | -1.15 | -1.04 |
| Tag 5 | 13.21 | 12.69 | 12.87 | 12.33 |
| Δ | -0.66 | -0.62 | -0.91 | -0.80 |

In conclusion, this new methodology is suitable to properly quantify different SL metabolites when labeled with tag **3** with a substantial enhancement of sensitivity. However, quantification of SL levels derived from the click reaction of ω-azidoSLs with tags **1**, **2**, **4** and **5** did not parallel the results observed from non-tagged ω-azidoSLs, regardless of the close similarity between these tags and tag **3**. Despite we have not yet been able to find a satisfactory explanation for these results, we still believe that this methodology might be a convenient approach to directly analyze mixtures of different populations of SLs, reducing the time of instrument utilization.

In addition, ω-azidoSLs have revealed as suitable metabolic tracers. They are not cytotoxic, they do not give rise to significant modifications on the endogenous sphingolipidome and, moreover, their metabolic profile is similar to that of natural SLs. For these reasons, labeling of ω-azidoSL metabolites by click reactions could be an appropriate tool to enhance the sensitivity and, subsequently, the detection of minor species in specific assays.

### 3.3.2 Live cell labeling of ω-azidoSLs through click chemistry

#### 3.3.2.1 Introduction

Imaging biomolecules within living systems requires a reliable method to distinguish the target from the surrounding components by using a spectroscopic probe.

Along this line, the bioorthogonal chemical reporter strategy may offer an avenue for labeling and visualizing biomolecules *in vivo*, without the requirement of genetic manipulation. In this approach, the bioorthogonal reporter might be installed taking advantage of the cellular metabolic machinery.

As previously discussed, the azide group is one of the most widely used chemical reporters due to its small size, metabolic stability and lack of reactivity with natural biofunctionalities. Azides have been introduced into a wide variety of biomolecules with minimal physiological perturbation. Labeling with azides primes the target biomolecule for visualization by covalent attachment of an imaging probe. For dynamic *in vivo* imaging, the covalent reaction must be fast and not harmful to the cell. Considering these requirements, the strain-promoted azide-alkyne cycloaddition (SPAAC) may offer high reaction kinetics and the advantage of its negligible cytotoxicity.

The development of strategies that employ intracellular click reactions for the targeting of biomolecules requires the use of fluorophores with optimal cellular properties. Ideal fluorophores for such applications should possess three important characteristics. First, the fluorophore should readily enter the cells by passive diffusion and accumulate to a significant extent. The rate of the click reaction should be proportional to the concentration of each of the components in the subcellular site. Therefore, fluorophores with greater accumulation will show faster reaction rates and, as a result, the highest potential to yield products that can be detected in a reasonable time frame. Second, the intracellular distribution of the fluorophore is also important. This will facilitate the reactive fluorophore to reach its click partner easily. Lastly, it is critical that the reactive fluorophore is available to react with the intended click partner once it is in the immediate vicinity of the target.

As discussed in Section 1.3, SLs are important bioactive molecules, playing roles in a wide variety of cell functions. At the cell membrane level, SLs interact with cholesterol and other plasma components to form membrane microdomains.[89-90] The mode of action of SLs in cellular processes depends on their concentration in the various subcellular organelles and in the trans-bilayer and lateral distribution in these membranes. Since the mechanisms of these processes are unknown, the interest in the use of fluorescent lipid probes to visualize the way SLs are synthesized and delivered to their target organelles and membranes has grown in recent years.

### 3.3.2.2 Design and synthesis of a fluorescent azadibenzocyclooctyne (D1)

Dibenzocyclooctyne-based fluorophores, such as those derived from fluorescein (DBCO-Fluor 488), carboxyrhodamine (DBCO-Fluor 525), carboxytetramethylrhodamine (DBCO-Fluor 545), rhodamine (DBCO-Fluor 568) and sulforhodamine (DBCO-Fluor 585) have become commercially available for dynamic *in vivo* imaging. Preparation of cell permeable cyclooctynes based on a coumarin fluorophore, with a linker segment to improve water solubility has also been described.[91] On the other hand, cyclooctyne-functionalized quantum dots were also applied for imaging the metabolic incorporation of azido-modified sialic acids in cell membrane glycoconjugates.[92] In this study, the optical properties of the quantum dot nanocrystals provided very high detection sensitivity.

Along this line, we designed a new fluorescent dye **D1** (Fig. 3.42). It is based on an activated azadibenzocyclooctyne (suitable for *Cu*-free click chemistry reactions with azides) linked to a fluorescein moiety. The linker was designed to play the role of a spacer between the reactive azadibenzocyclooctyne moiety and the dye, in order to avoid: (1) any steric hindrance that could decrease the yield of the SPAAC reaction, and (2) any fluorescence quenching of the fluorophore in the conjugated dye with its target biomolecule, which might hamper the fluorescent signal. The choice of the azadibenzocyclooctyne as the reactive moiety was driven by the high reactivity of the cyclooctyne system, enhanced by the additional ring strain imposed by the two fused aromatic rings.[88] On the other hand, the use of fluorescein in fluorescent probes leads to highly bright molecules that absorb/emit at around 500 nm in aqueous media. This wavelength is suitable for fluorescence observation with classical microscopy tools, with reduced auto-fluorescence background in cell culture medium, in comparison with coumarin dyes. In addition, fluorescein is highly cell-permeable, which allows an efficient cell internalization, once incorporated into **D1**, and also an efficient washing of the non-conjugated dye after the SPAAC reaction has taken place, which reduces any non-specific signal.

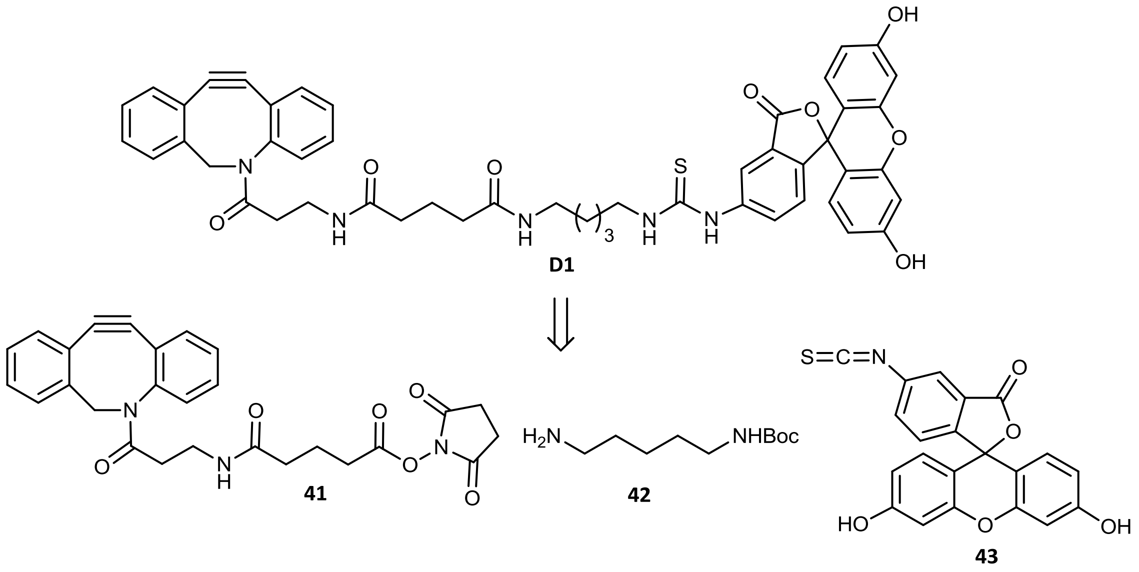

**Figure 3.42** Chemical structure of probe **D1** and building block precursors **41-43**.

Despite the outstanding optical properties of quantum dots, we preferred the use of an organic fluorescent dye in terms of cell internalization and labeling conditions. Based on the wealth of knowledge about mechanisms underlying the cellular uptake of nanoparticles and their subcellular distribution, we can assume that hydrophilic molecules, such as fluorescein conjugates, present higher mobility in the cytosol than quantum dots and, hence, they are able to rapidly diffuse through the entire cell.[93-94] Thus, the fluorescent dye can presumably reach all organelles and consequently their corresponding SL contents.

Based on their commercial availability, we considered building blocks **41-43** (Fig. 3.42) as the most suitable starting materials for the synthesis of **D1**. The fluorescein derivative **43**, with a reactive isothiocyanate group, allowed the introduction of the fluorescent moiety by reaction with monoprotected diamine **42**, followed by *N*-Boc removal from intermediate **44** and condensation with azadibenzocyclooctyne **41**, as shown in Fig 3.43. This synthetic approach led to the required cyclooctyne dye **D1** in 32% overall yield for three steps.

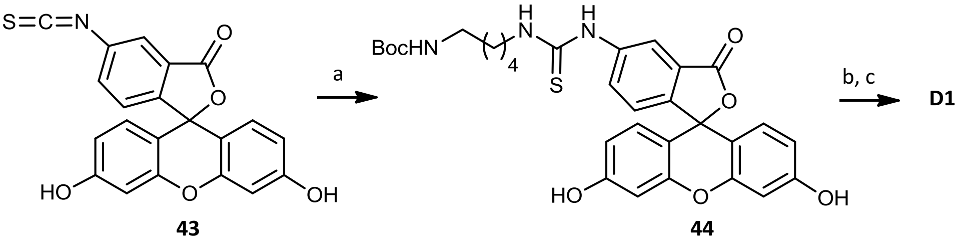

a) **42**, $Et_3N$, DMF, rt, overnight, 75%; b) $CH_3COCl$, MeOH, rt, 1 h, quantitative; c) **41**, DIPEA, DMF, rt, overnight, 42%.

**Figure 3.43** Synthesis of fluorescent azadibenzocyclooctyne **D1**.

As expected, **D1** displayed comparable optical properties to fluorescein **43** (absorption maximum: 491 nm, emission maximum 521 nm, in 0.1 M NaOH), constituting a highly fluorescent probe (fluorescence quantum yield of 0.20 ±0.04 in 0.1 M NaOH, referred to fluorescein in 0.1 M NaOH).

### 3.3.2.3 Evaluation of click reactions between D1 and the azido probe RBM2-87

With cyclooctyne **D1** in hand, we first examined the reactivity of this derivative with the azido probe **RBM2-87**, as depicted in Fig. 3.44.

Equimolar concentrations of both **RBM2-87** and **D1** (1mM) were mixed in MeOH at rt. In order to mimic the intracellular reaction conditions, the reaction was also carried out in two different standard culture media (MEM and DMEM) at 37 ºC.

In all cases, the reaction mixtures were analyzed by HPLC under the gradient conditions described in the Experimental Section. Cyclooctyne **D1** and the regioisomeric mixture of click adducts *syn*-**45** and *anti*-**45**, were monitored at different reaction times based on their retention times (5.01 for **D1**, and 12.64 and 13.02 min for each of the diastereomers). On the other hand, reaction conversions were calculated by measuring the disappearance of the starting cyclooctyne **D1** and comparison with a calibration curve.

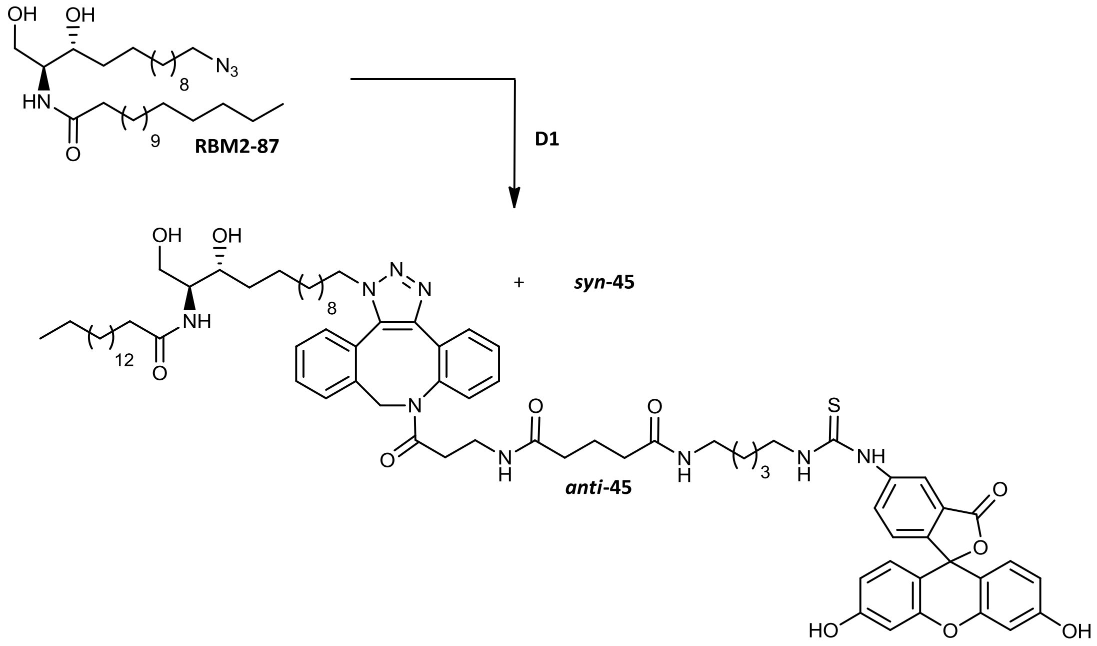

**Figure 3.44** SPAAC between fluorescent dye **D1** and azido probe **RBM2-87**.

Optimal conversion rates (84-87%) were achieved after 60 min reaction in the two cell culture media with no appreciable increase even at longer reaction times, as depicted in Fig 3.45. Comparable results were observed in reactions carried out in MeOH, accomplishing 100% reaction conversion at 105 min.

These results let us conclude that the SPAAC reaction between **D1** and ω–azidoSLs take place in cell culture media (37 °C in the presence of protein and salts) as efficiently as in MeOH.

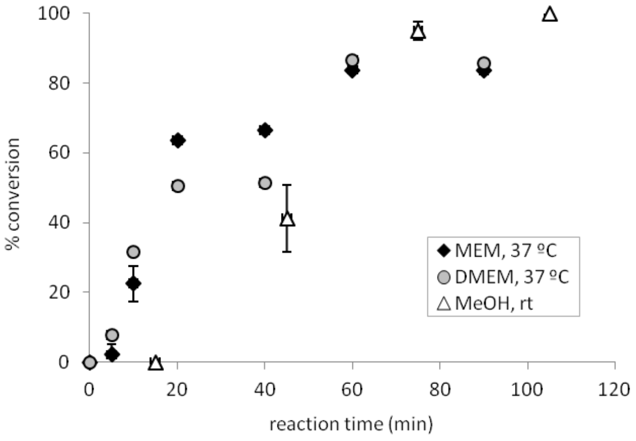

**Figure 3.45** % Conversion of SPAAC between azide **RBM2-87** and fluorescent dye **D1** in MeOH and in MEM and DMEM culture media.

#### 3.3.2.4 Studies of fluorescence sensitivity for dye D1

Human lung A549 and breast MCF-7 adenocarcinoma cell lines were used as model systems for internalization and fluorescent studies of dye **D1**.

First, we sought to explore the fluorescence sensitivity at various **D1** concentrations in both cellular models. Therefore, cells were treated with **D1** at different concentrations for a fixed time (30 min). Flow cytometry analysis showed a maximum fluorescence signal at 100 μM, which was considered as the optimal concentration (Fig. 3.46*A*). These results were reproducible for both cell lines. On the other hand, it is imperative that the reactive fluorophore not only enters the cells but also reaches the intracellular SL targets, regardless their cellular localization. As illustrated in Fig 3.46*B*-*C*, fluorophore **D1** exhibited a uniform distribution throughout the cell, showing no fluorescence within the nuclear space. Although nuclear membranes have numerous pore complexes that allow small molecules to diffuse across the membrane, pores become restrictive to bulk flow for cytosolic molecules over 30 KDa in size. Fluorophore **D1** showed an extensive cytosolic distribution across the entire cell. Despite SLs are synthesized in the ER[95] and Golgi, their accumulation in plasma membrane and endosomes require their traffic across organelles through the cytosol *via* vesicular and monomeric transport mechanisms. Thus, it is reasonable to assume that **D1** should be able to reach ω-azidoSLs for their specific labeling through the cytosol.

In addition, this optimal concentration (100 μM) did not result in any observable undesired effect (blebbing, detachment from plates, etc) in any of the two cell lines under study.

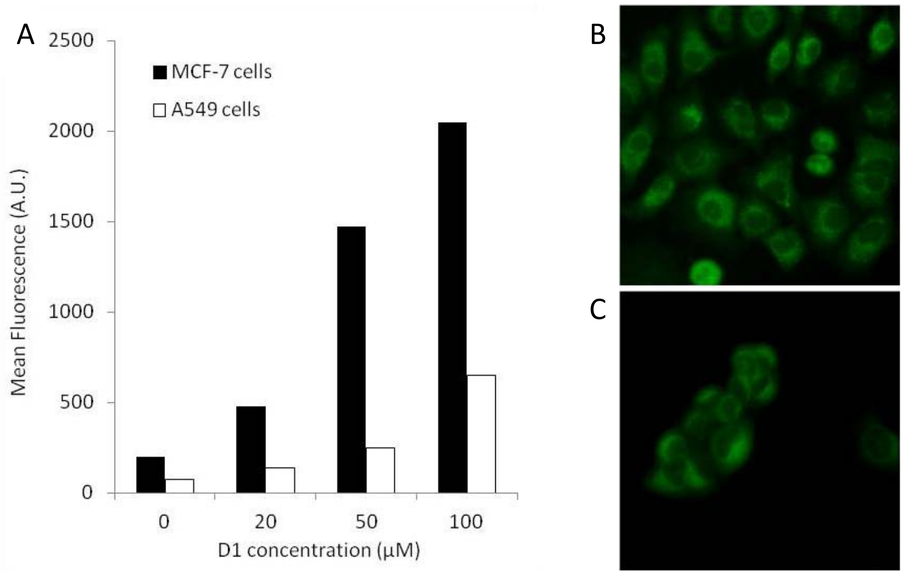

**Figure 3.46** (*A*) Flow cytometry plots of A549 and MCF-7 cells after treatment with **D1**. Comparison of fluorescence signals at different **D1** concentrations. Both cell lines were incubated with 0, 20, 50, and 100 μM **D1** for 30 min. Fluorescence was quantified by flow cytometry analysis. The level of fluorescence is reported in mean fluorescence intensity (arbitrary units). (*B*-*C*) Epifluorescence microscopy images for dye **D1**. Cells were treated with 100 μM **D1** for 30 min at 37 ºC. Green channel. (*A*) A549 cells, and (*B*) MCF-7 cells.

### 3.3.2.5 Internalization of dye D1 in cell membranes

In order to determine the optimal internalization time for dye **D1**, we next explored its kinetic behaviour in both cell lines. This study should be indicative of the optimal incubation time required for **D1** at the optimal concentration (100 μM) in order to maximize the efficiency of the click SPAAC reaction with the azido probes.

Cells were treated with 100 μM **D1** at 37 ºC for different incubation times, as shown in Fig. 3.47. Incubation for 30 min led to the maximum fluorescence, as determined by flow cytometry analysis. These conditions turned out to be optimal for both cell lines, since longer incubation times (60 min) led to a decrease of intracellular fluorescence, probably due to the passive diffusion of **D1** outside the cell.

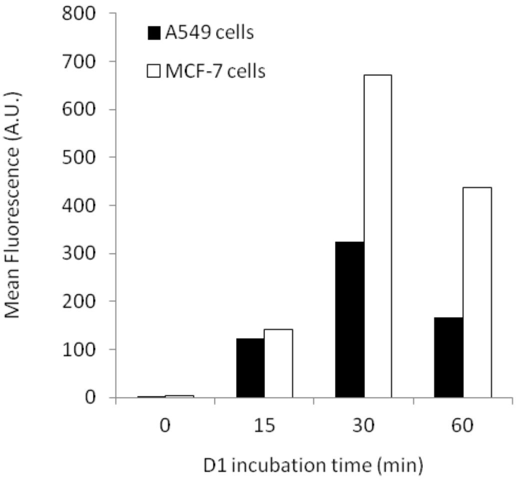

**Figure 3.47** Flow cytometry plots of A549 and MCF-7 cell treatment with **D1**. Comparison of **D1** accumulation in A549 and MCF-7 cells. Both cell lines were incubated with 100 μM **D1** for different times. The degree of accumulation was quantified by flow cytometry. The level of fluorescence is reported in mean fluorescence intensity (arbitrary units).

#### 3.3.2.6 Intracellular click reaction between dye D1 and ω-azidoSL metabolites

In order to evaluate the efficiency of the click reaction of **D1** in live cell labeling experiments with ω-azidoSL metabolites, we took advantage of our previous studies on the metabolization of the azido probe **RBM2-31** in A549 and MCF-7 cell lines (see Section 3.3.1.1). Cells were incubated with 10 μM **RBM2-31** for 16 h and labeled with excess (100 μM) fluorescent dye **D1** for different times (0.5, 1, and 2 h). After the indicated incubation times, a washing step, followed by addition of fresh medium and incubation for additional 30 min, was crucial to favor the passive diffusion of unreacted **D1** outside the cell subsequent to the SPAAC reaction. Flow cytometry analysis afforded the data shown in Fig. 3.48*B*-*C*.

Both cell lines showed a robust azide-specific labeling (Az+), since a significant fluorescence increase was observed in comparison with control experiments (Az-). A549 cells displayed a mean fluorescence 6, 10, and 12-fold higher than control when labeled for 0.5, 1, and 2 h, respectively (Fig. 3.48*B*). Gratifyingly, labeling of ω-azidoSL metabolites in MCF-7 cells showed a 22-fold higher mean fluorescence after 1 h SPAAC click reaction (Fig. 3.48*C*). These experiments showed that optimal results from click SPAAC require higher reaction times than those determined for the internalization of **D1**, as indicated in the above section.

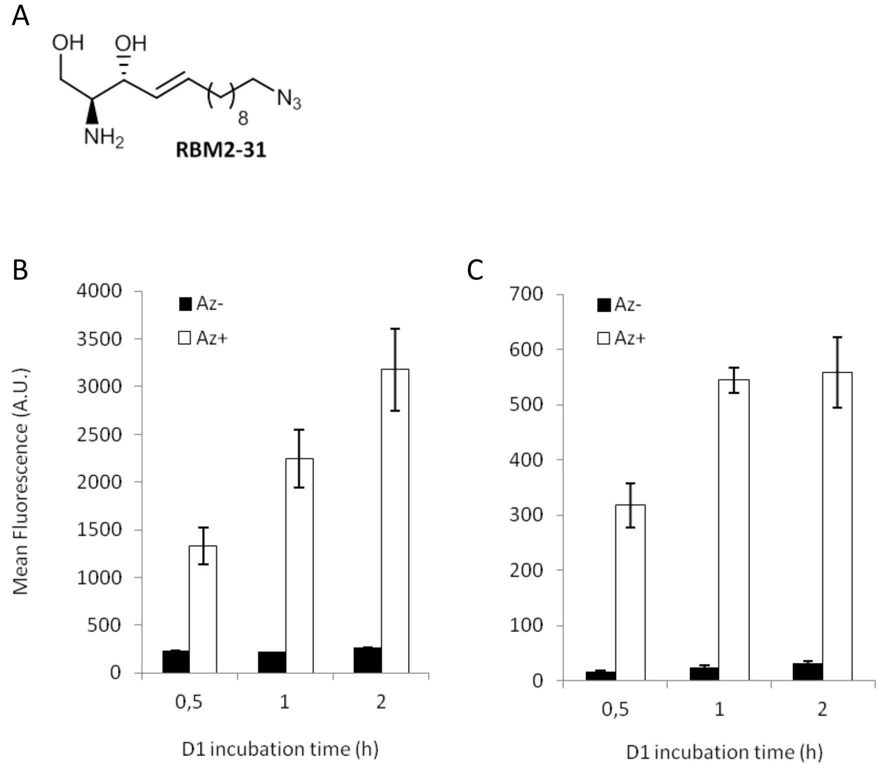

**Figure 3.48** (*A*) Chemical structure of the azido probe **RBM2-31**. (*B-C*) Flow cytometry plots of live cells labeling with dye **D1**. Both A549 (*B*) and MCF-7 (*C*) cells were incubated with (+Az) or without (-Az) 10 μM azide **RBM2-31** for 16 h. Cells were next labeled with 100 μM azacyclooctyne **D1** for different incubation times, followed by additional washings and incubation with fresh medium for additional 30 min. The degree of labeling was quantified by flow cytometry. The level of fluorescence is reported in mean fluorescence intensity (arbitrary units). Error bars represent the standard deviation of three replicate experiments.

Similar experiments were designed to evaluate the ability of fluorophore **D1** as reagent for direct fluorescence imaging. In this case, A549 cells were incubated with (Az+) or without (Az-) 10 μM **RBM2-31**, prior to the labeling with 100 μM **D1** for 2 h. Azide-pretreated cells showed a strong cytosolic fluorescence by confocal laser scanning microscopy (Fig. 3.49*B*), with major localization in the perinuclear area, possibly associated with membranes. As expected, non-containing azide cells (Fig. 3.49*A*) showed very weak cytosolic fluorescence. The observed background fluorescence might be due to either the nonspecific binding of **D1** or its sequestration by membranes.

Due to the similar metabolism of azido probe **RBM2-31** with that of natural SLs, it is reasonable to assume that the observed intracellular fluorescence is due to the different click adducts arising from SPAAC reaction between dye **D1** and ω-azidoSL metabolites.

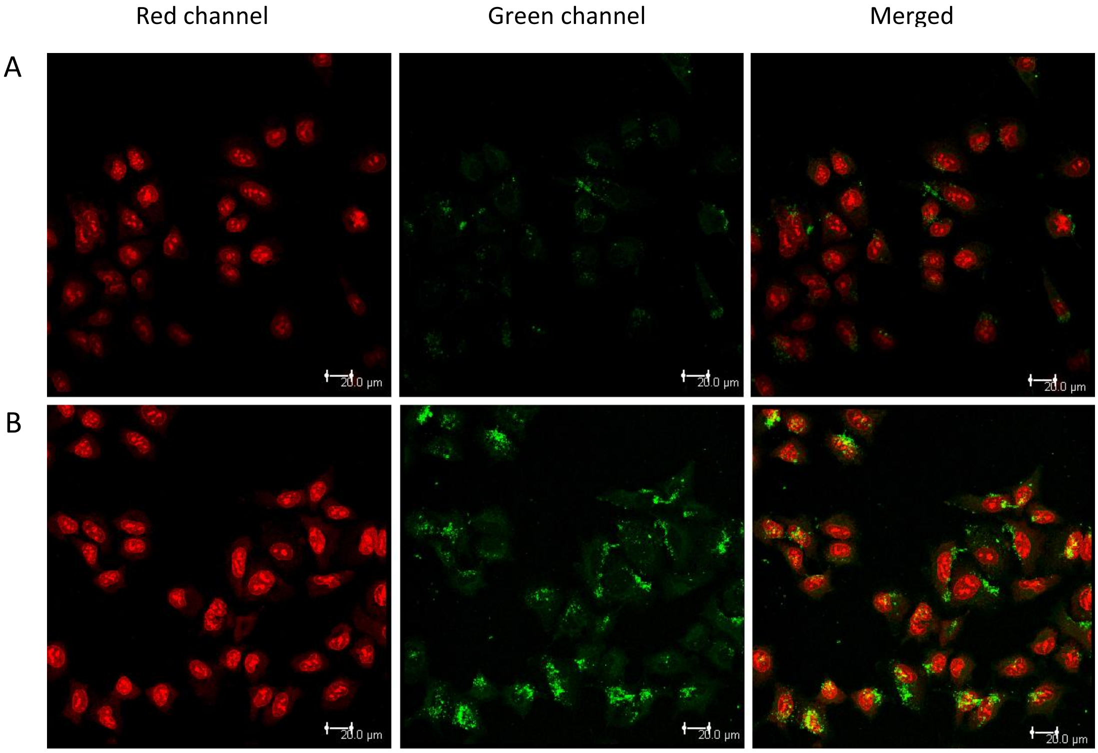

**Figure 3.49** Fluorescence analysis by confocal laser scanning microscopy. Representative labeling of A549 cells with 100 μM **D1** for 2 h. Cells were pretreated with (Az+) or without (Az-) 10 μM **RBM2-31** for 5 h. Nuclei were stained with propidium iodide (red). Labeling of cells lacking (*A*) (Az-) or containing (*B*) (Az+) ω-azidoSL metabolites.

## 3.3.3 Visualization of ceramides in artificial membranes using fluorogenic CuAAC

### 3.3.3.1 Introduction

Fluorescent lipid probes that mimic their natural counterparts have become useful tools to visualize the membrane architecture and its dynamic properties.[96] Fluorescent dyes that have been currently used in lipid derivatization, especially those emitting in the visible light region, are usually of hydrophilic nature. When chemically linked to a lipid molecule, they might alter the hydrophilic/hydrophobic balance of the resulting probe to give rise to a perturbation of some important cellular properties, such as trafficking, sorting and domain formation. Some of the mentioned fluorescent dyes used for coupling to lipidic structures are molecules such as BODIPY, rhodamine, NBD, coumarin, DPH and dansyl (fig. 3.50).

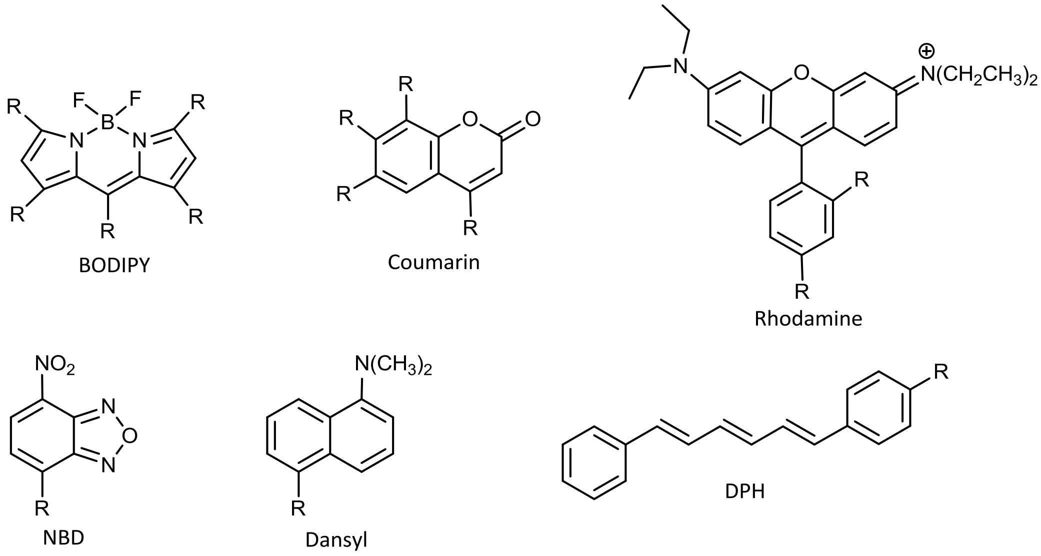

**Figure 3.50** Basic structures of fluorescent dyes. R represents either lipidic anchors or other functional groups.

Attempts to overcome these undesired effects have led to the design of minimally modified lipid probes that incorporate a small chemical reporter with negligible effects on the overall physical properties of the resulting probe. Once inside the cells, these probes should chemically react with a suitable fluorescent or fluorogenic dye to give rise to a detectable species for subsequent analysis. Among the most suitable reporters, the azide group has been extensively used by its ability to react through an alkyne-azide cycloaddition (click reaction) with appropriate dyes.

The use of the so-called “click-on” fluorogenic dyes, based on the use of reactive azides or alkynes with no or low baseline fluorescence and whose click conjugates become highly fluorescent, is a very reliable strategy for the direct visualization of lipid probes (see Section 1.2.1.2).

Among the objectives of this Doctoral Thesis, we were interested in the exploitation of the reactivity of some of our ω-azidoSL probes for the labeling of artificial membranes by means of a fluorogenic click reaction, as discussed in the following section.

### 3.3.3.2 *In situ* fluorogenic CuAAC of membrane azido ceramides

Sphingolipid probes **RBM2-77** and **RBM2-79** were used as fluorogenic membrane probes, allowing its visualization by labeling through *in situ* CuAAC with naphthalimide[97] **46** within a lipidic environment, as depicted in Fig. 3.51.[98]

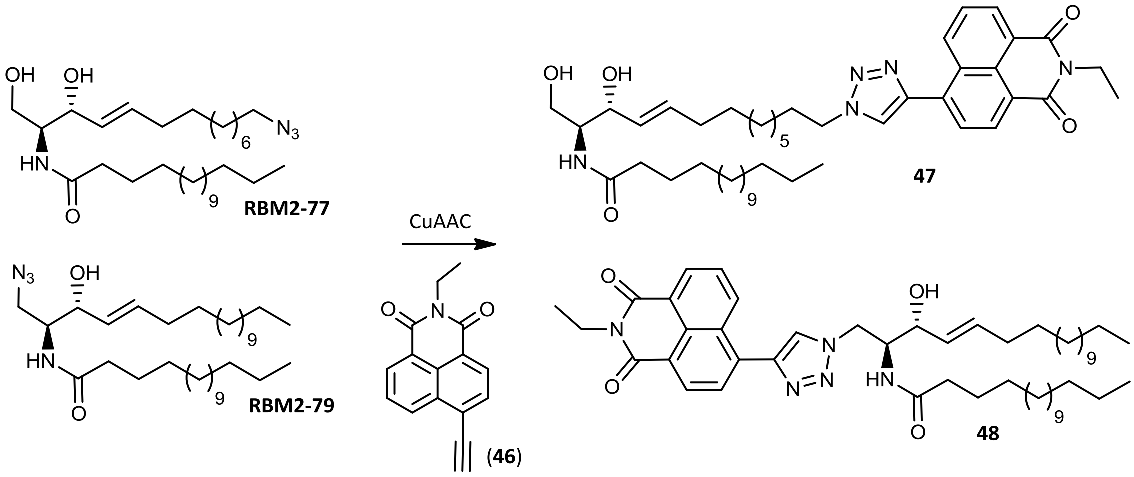

**Figure 3.51** Fluorogenic CuAAC between naphtalimide **46** and azido probes **RBM2-77** and **RBM2-79**.

Moreover, we have also explored the effect of the azide position on the reactivity and efficiency of the click reaction. Therefore, the azide group in probe **RBM2-77** is placed at ω-position of the sphingoid base, remaining immersed within the hydrophobic interphase of the lipidic artificial membranes. In contrast, in **RBM2-79**, the azide group is positioned at the polar head (C1) and might be placed towards the aqueous solvent.

In our case, the best reaction conditions for the CuAAC between the above azido probes and alkyne **46**, when incorporated into multilamellar vesicles (MLV), required the use of ascorbic acid and a 1:1 mixture of 0.1 mM $CuSO_4$ and the tris(triazolyl)amine ligand **49** (Fig. 3.52*A*) as "click cocktail". A high fluorescent signal for both probes was observed after 1.5 h incubation under these conditions. The fluorescent properties of the azido probes and those of their click adducts **47** and **48** in MLV were examined by fluorescence spectroscopy after excitation at 368 nm (Fig. 3.52*B-C*). In the absence of Cu(I), an emission maximum was observed at ≈400 nm after 1.5 h addition of alkyne **46**, whereas in the presence of the "click cocktail" a signal increase, together with a shift in the emission maximum to ≈440 nm, was observed.

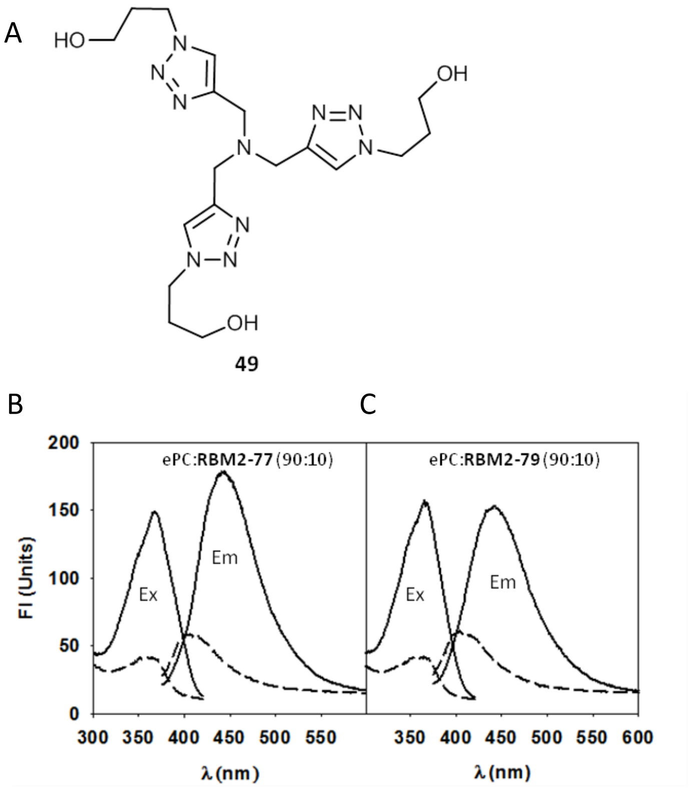

**Figure 3.52** (*A*) Chemical structure of tris(triazolyl)amine ligand **49**. (*B*-*C*) Fluorescence spectra of MLV composed of ePC, alkyne **46** (0.05 mM), and 10 mol% of either **RBM2-77** (*A*) or **RBM2-79** (*B*) in the presence (*solid lines*) or absence (*dashed lines*) of $CuSO_4$. 300-420 nm excitacion spectra was collected at 420 nm (*Ex*). 375-600 nm emission spectra was excited at 368 nm (*Em*).

To visualize the *in situ* formation of the fluorescent probes **47** and **48**, microscopy experiments using giant unilamellar vesicles (GUVs) containing alkyne **46** (0.05 mM) and 10% of azide probe, were performed. When GUVs were incubated with the "click cocktail" for 1.5 h, an intense fluorescence signal was observed between 450 and 500 nm (Fig. 3.53*A*-*B*, +Cu). However, when GUVs were incubated in the absence of Cu(I), no fluorescence signal was observed even at longer incubation times (Fig. 3.53*A*-*B*, -Cu).

To confirm the formation of the click adducts **47** and **48** in the artificial membranes, GUVs were treated with water, MeOH and $CHCl_3$, and the organic extracts were analyzed by UPLC-TOF, as described in the Experimental Section. As shown in Table 3.5, click adducts **47** and **48** were formed when GUVs-containing azides **RBM2-77** and **RBM2-79**, respectively, were incubated with alkyne **46** and the "click cocktail" in the above conditions (entries 3 and 5).

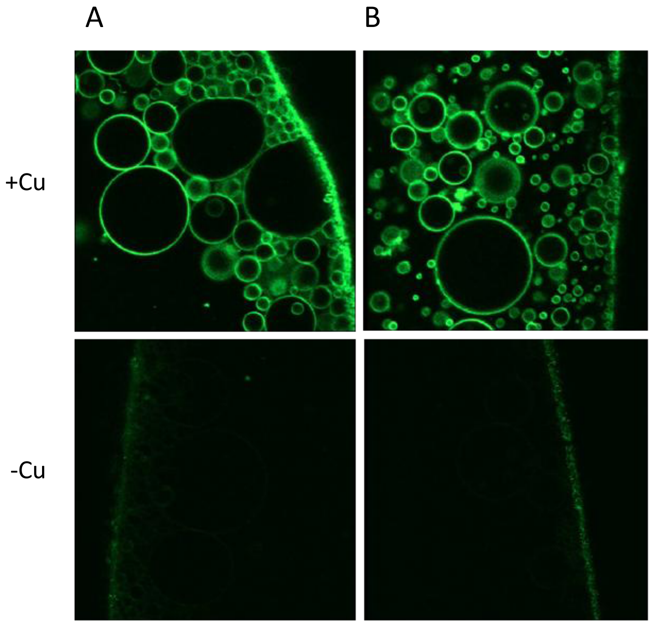

**Figure 3.53** Fluorescent images (false colour representation) of GUVs composed of alkyne **46** and ePC + 10 mol% of either (*A*) **RBM2-77** or (*B*) **RBM2-79**, treated with the "click cocktail" in the presence (+Cu) or in the absence (-Cu) of $CuSO_4$.

**Table 3.5** MS-based assignments of azido probes **RBM2-77** and **RBM2-79** and their corresponding click adducts **47** and **48**, after extraction from GUVs. Values correspond to the peak areas.

| **Entry** | **Samples** | **RBM2-77** *m/z* 523.4587 | Adduct **47** *m/z* 772.5377 | **RBM2-79** *m/z* 563.5264 | Adduct **48** *m/z* 812.6054 |
|---|---|---|---|---|---|
| **1** | ePC | 0 | 0 | 0 | 0 |
| **2** | ePC:RBM2-77 -Cu | 1998 | 0 | 0 | 0 |
| **3** | ePC:RBM2-77 +Cu | 1366 | **491** | 0 | 0 |
| **4** | ePC:RBM2-79 -Cu | 0 | 0 | 2963 | 0 |
| **5** | ePC:RBM2-79 +Cu | 0 | 0 | 2458 | **680** |

Despite the click reactions were not complete, as evidenced by the presence of unreacted probes in the crude extracts, the observed shift in the fluorescence emission and the increase of fluorescence intensity for the click adducts allowed their detection and visualization in the artificial membranes. As a result, we can conclude that fluorescent ceramide derivatives **47** and **48** can be formed within lipid membranes from non-fluorescent probes in the presence of alkyne **46**, thus offering a suitable approach for the study and visualization of ceramide-enriched domains in living cells.

## 3.4 New sphingolipid analogs as probes to determine Des1 activity

### 3.4.1 Introduction

Ceramide is involved as a mediator of apoptosis induced by either signaling molecules or stress events, which results in a transient increase of this bioactive SL. Intracellular generation of ceramide can occur by different routes (see Section 1). In the *de novo* pathway, ceramide is biosynthesized from L-serine in four steps, the last one being the $\Delta^4$-desaturation of dihydroceramide to ceramide by the action of dihydroceramide desaturase. This enzyme exhibits high dihydroceramide $\Delta^4$-desaturase activity and very low C4-hydroxylase activity, while Des2, another homologue found in mouse and humans, exhibits bifunctional sphingolipid C4 hydroxylase and $\Delta^4$-desaturase activities.[37] Des activity is influenced by different factors, such as (1) the alkyl chain length of both sphingoid base and fatty acid, (2) the stereochemistry of the sphingoid base, (3) the nature of the head group, and (4) the ability to use alternative reducing systems.[99]

Dihydroceramides have been regarded as biologically inactive biomolecules for years. This belief was sustained by the failure of exogenous short chain dihydroceramides to inhibit cell growth and to induce apoptosis, as the respective ceramides do.[100-101] However, recent studies have shown that dihydroceramides are bioactive molecules, though their effect may be different from those shown by ceramides. Inhibition of Des1, the major desaturase active in SMS-KCNR cells, and the subsequent accumulation of dihydroceramides led to cell cycle arrest.[102] On the other hand, it has been demonstrated that dihydroceramide inhibits the formation of ceramide channels, indicating its interference with ceramide nucleation of channel formation by using biophysical models.[103] Moreover, agents such as fenretinide, thought to cause large increases in ceramide, caused increases in dihydroceramides instead.[2]

These recent findings have grown the interest in the design and synthesis of new Des1 inhibitors, and more importantly, the determination of the resulting Des1 activity.

### 3.4.2 Assays to evaluate Des1 activity

Different assays to evaluate Des1 activity have been reported in the literature. Mainly, these methodologies rely on the quantification of the ceramide formed in the course of the enzymatic reaction.

Michel *et al*. first described an assay for the determination of Des1 in which the enzyme source was incubated with a radioactively labeled dihydroceramide analogue (Fig. 3.54*A*) as substrate and either NADH or NADHP as co-substrates. The resulting ceramide was detected by autoradiography after extraction and separation by TLC.[99] Besides, Des1 activity can be also determined by using D-*erythro*-*N*-octanoyldihydrosphingosine (Fig. 3.54*B*) as substrate, and monitoring the formation of ceramide by GC-MS of the volatile trimethylsilyl derivatives.[104] Analogously, the fluorescent analogue dhCerC6NBD (Fig. 3.54*C*) has been used as Des1 substrate, allowing the measurement of Des1 activity by HPLC-FD.[105]

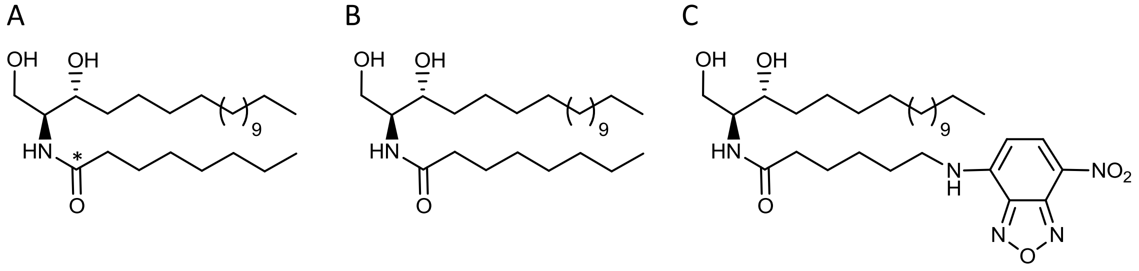

**Figure 3.54** Des1 substrates used in the different assays for Des1 activity reported to date: (*A*) *N*-[1-$^{14}$C]-Octanoyl-D-*erythro*-sphinganine, (*B*) D-*erythro*-*N*-octanoyldihydrosphingosine, and (*C*) 6-[*N*-(7-nitro-2,1,3-benzoxadiazol-4-yl)amino]hexanoylsphinganine (dhCerC6NBD).

An alternative way to determine Des1 activity was reported by Geeraert *et al*.[106] In this method, Des1 activity was determined by following the formation of the tritiated water that accompanied the 4,5-double bond formation of an appropriate labeled susbtrate, such as dihydroceramide *N*-hexanoyl-[4,5-$^{3}$H]-D-*erythro*-sphinganine.

### 3.4.3 Design of a high-throughput screening assay for Des1 activity

The discovery of new Des1 inhibitors with improved potency and selectivity would be greatly accelerated with the help of high-throughput screening (HTS) assays. These would allow the simultaneous screening of large libraries of compounds and the possibility of identifying new leads more efficiently. The most common format for a HTS protocol is the microtiter plate. Apparently, the adaptation to a HTS format of the above analytical methods for the evaluation of Des1 activity does not seem evident. For this reason, we were interested in the development of a new protocol suitable for the HTS screening of potential Des1 modulators.

We based our approach in the design of the $\Delta^6$-ceramide analogue **RBM2-85** (Fig 3.55*A*) as a potential Des1 substrate. Desaturation by Des1 would afford a conjugated diene, which could be trapped with a fluorescent dienophile, such as a suitable triazacyclopentadione (TAD), through a Diels-Alder (DA) reaction (Fig 3.55*A*). The excess reagent could be subsequently removed by reaction with a supported diene to afford the fluorescent DA adduct in solution for quantification. The adaptation of this approach for a HTS protocol would require a proper design of the supported diene quencher. However, the synthesis of **RBM2-85** and its suitability as Des1 substrate must be first guaranteed.

There are relatively few examples of fluorescent TADs in the literature. Specifically, the fluorescent labeling reagent DMEQ-TAD (Fig. 3.55*B*), developed by Shimizu *et al*,[107] has been used to target the diene moiety of the different vitamin $D_3$ congeners found in plasma. Since DMEQ-TAD is a highly reactive dienophile and a very sensitive fluorophore, the DA reaction between this reagent and vitamine D's has been reported as an efficient and rapid method for their quantification.[108]

Based on the above precedents, we considered commercially available DMEQ-TAD as a suitable fluorescent reagent for the development of our HTS assay for Des1 activity.

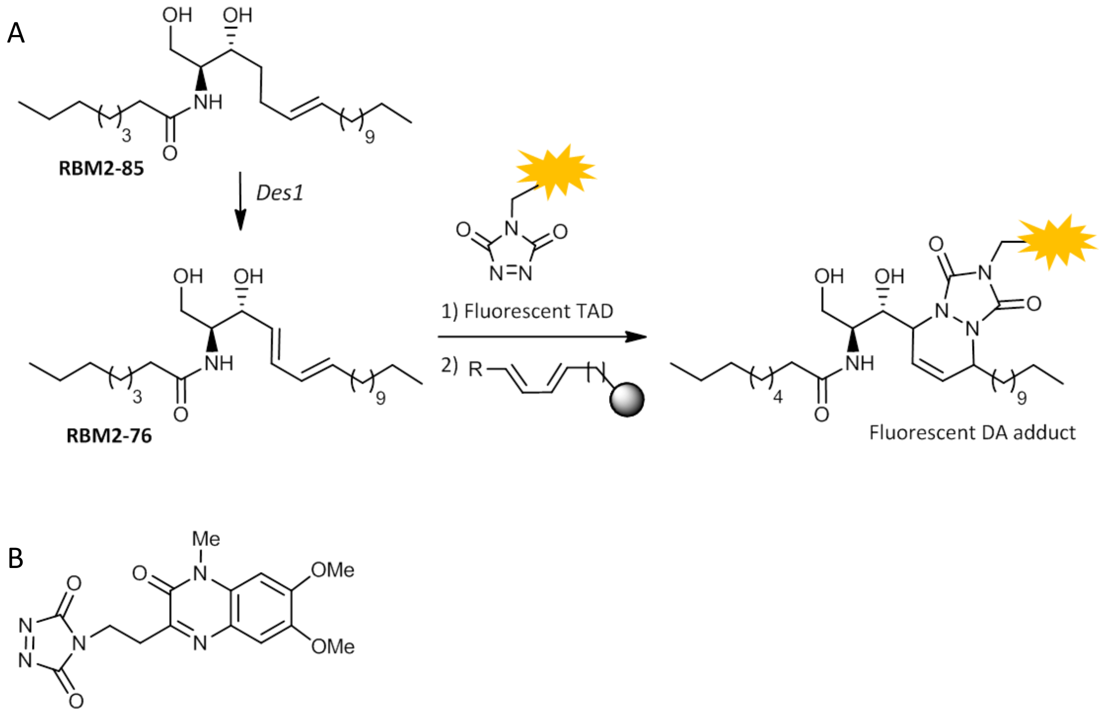

**Figure 3.55** (*A*) Designed HTS assay for Des1 activity using a $\Delta^{6}$-ceramide as substrate. (*B*) Chemical structure of the fluorescent reagent 4-[2-(6,7-dimethoxy-4-methyl-3-oxo-3,4-dihyroquinoxalyl)ethyl]-1,2,4-triazoline-3,5-dione (DMEQ-TAD).

## 3.4.4 Synthesis of (*E*)-$\Delta^{6}$-ceramide (RBM2-85) and (*E,E*)-$\Delta^{4,6}$-ceramide (RBM2-76)

### 3.4.4.1 (*E*)-$\Delta^{6}$-Ceramide RBM2-85

*Synthetic approach*

The development of our HTS assay requires the synthesis of (*E*)-$\Delta^{6}$-ceramide **RBM2-85** for its preliminary evaluation as Des1 substrate.

The preparation of this novel ceramide analogue was first reported by Bittman *et al.* in 2002 (Fig. 3.56).[109] The synthetic route consisted of the alkylation of an appropriate β-ketosulfone **51**, followed by its subsequent desulfonylation. The diastereoselective reduction of ketone **53**, followed by removal of the protecting groups and *N*-acylation provided the desired ceramide, in a 6:1 *erythro*/*threo* ratio, in 25% overall yield over six synthetic steps.

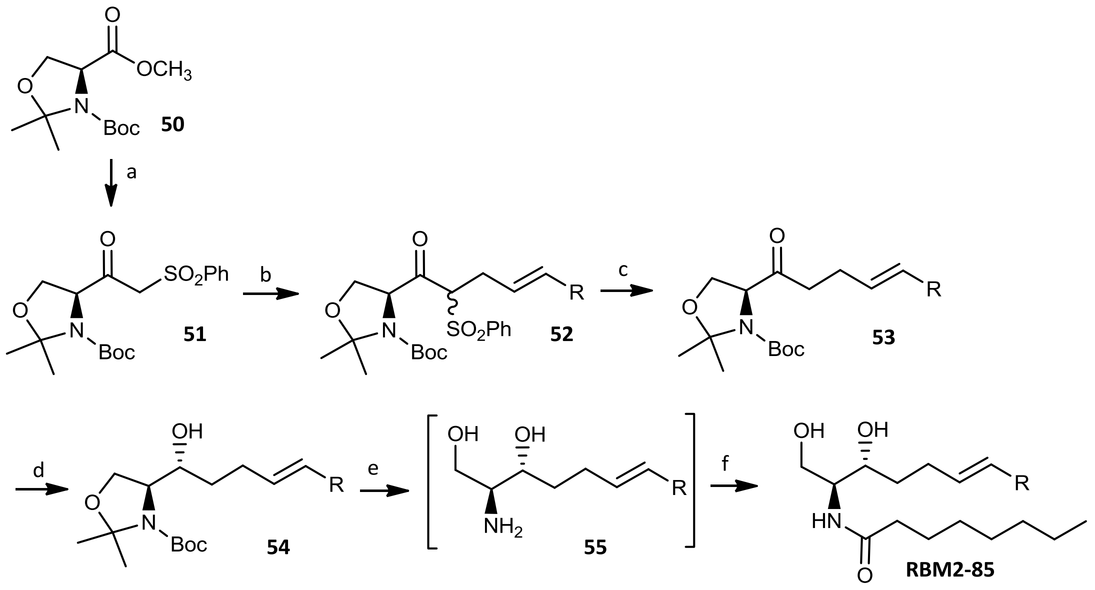

a) $MeSO_2Ph$, *n*BuLi, THF, -78 °C, 71%; b) $CH_3(CH_2)_{10}CH=CHCH_2Br$, DBU, benzene, rt, 74%; c) Al(Hg), 20:1 $THF/H_2O$, rt, 86%; d) $NaBH_4$, MeOH or DIBAL-H, THF, -15 °C, 88%; e) 1M HCl, THF, 70 °C; f) *p*-$O_2NC_6H_4CO_2C_7H_{15}$, THF, rt, 63%.

**Figure 3.56** Synthesis of $\Delta^6$-ceramide **RBM2-85** reported by Bittman and coworkers. R=$C_{11}H_{23}$.

In light of the above sequence, we were interested in a more convenient and direct synthetic approach for the preparation of the required $\Delta^6$-ceramide **RBM2-85**. As depicted in Fig. 3.57, compound **54** was also envisaged as an advanced intermediate in our synthetic route. However, in our case, the introduction of the *E*-double bond would be accomplished by olefin cross metathesis between **56** and a suitable terminal alkene. Retrosynthetically, the addition of 3-butenylmagnesium to aldehyde **4** at low temperature should provide scaffold **56** in high *erythro* selectivity.

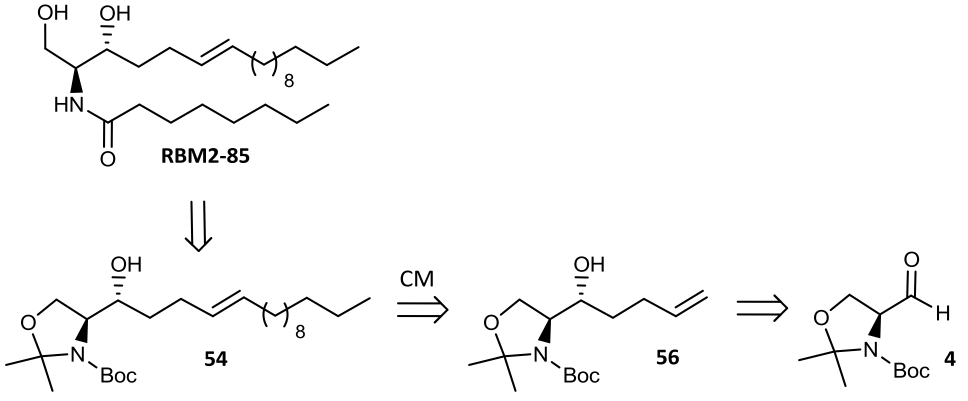

**Figure 3.57** Proposed retrosynthetic analysis of $\Delta^6$-ceramide **RBM2-85**.

### *Synthesis of $\Delta^6$-ceramide* ***RBM2-85***

In agreement with the above analysis, the synthetic route started with the addition of 3-butenylmagnesium bromide to aldehyde **4** in THF at -78 °C, giving the *erythro* alkenol **56** in 64% yield, as shown in Fig. 3.58.

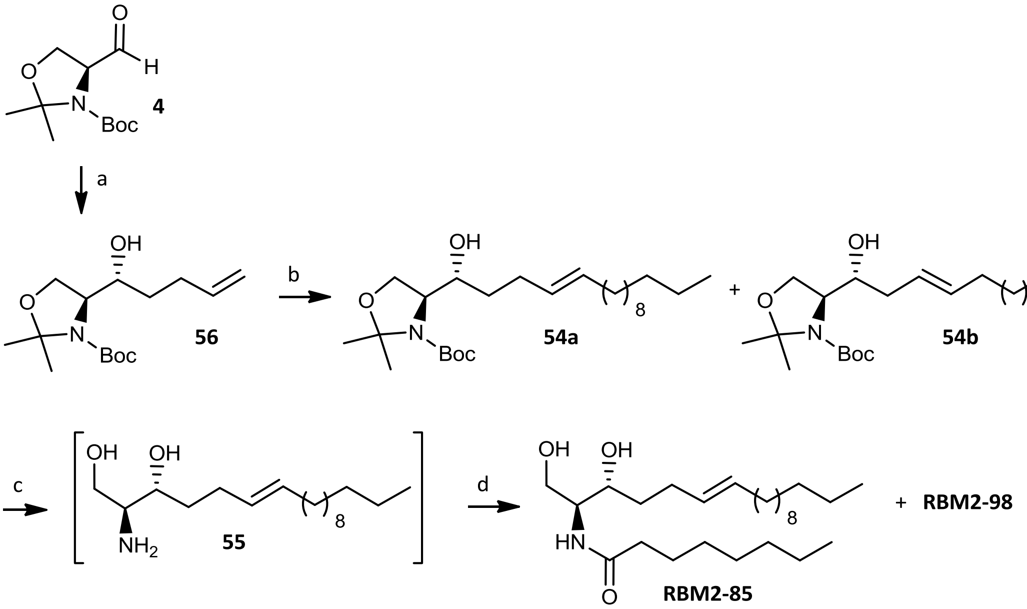

a) 3-Butenylmagnesium bromide, THF, -78 °C, 2 h, 64%; b) 1-Tridecene, Grubb's 2$^{nd}$ generation catalyst, $CH_2Cl_2$, 45 °C, 5 h, 62%; c) $CH_3COCl$, MeOH, rt, 1 h; d) octanoic acid, $Et_3N$, HOBt, EDC, $CH_2Cl_2$, rt, 1 h, 4%.

**Figure 3.58** Synthesis of $\Delta^6$-ceramide **RBM2-85**.

Next, a CM reaction between alkene **56** and a 4-fold excess of commercially available 1-tridecene, in the presence of Grubb's second generation catalyst, led to an inseparable mixture of two olefins, in 62% yield. This mixture was identified as the desired compound **54a** and an initially unknown compound, which was later identified as isomer **54b**. However, we decided to continue the synthetic route with the above mixture by carrying out the simultaneous deprotection of the oxazolidine and *N*-Boc groups under acidic conditions, and the subsequent *N*-acylation with octanoic acid in the presence of EDC and HOBt as coupling reagents. As expected, a mixture of two olefins was obtained, as confirmed by $^1H$ and $^{13}C$ NMR analysis of the crude reaction mixture. Attempts to separate this mixture by either flash chromatography, using $CH_2Cl_2$/MeOH as eluents, or Biotage Isolera flash purification with different mixtures of hexane/EtOAc, resulted fruitless. However, the separation of the two olefins was accomplished by flash chromatography using a mixture of hexane, EtOAc and MeOH as the mobile phase. Two different compounds were isolated, and subsequently characterized by NMR. The first one was identified as the desired $\Delta^6$-ceramide **RBM2-85** (10% yield) and the second one as the isomeric $\Delta^5$-ceramide **RBM2-98** (12% yield). In this isomer, the presence of the double bond at C5-C6 gave rise to a large chemical shift increment for the two diastereotopic protons at C4, appearing as multiplets in the $^1$H NMR spectrum at 2.21 and 2.11 ppm, respectively (Fig. 3.59). Moreover, comparison of the $^{13}$C resonances for C4 between **RBM2-85** and **RBM2-98** showed a shift from 26.0 to 29.4 ppm, an indication of the α position with respect to the double bond for this carbon.

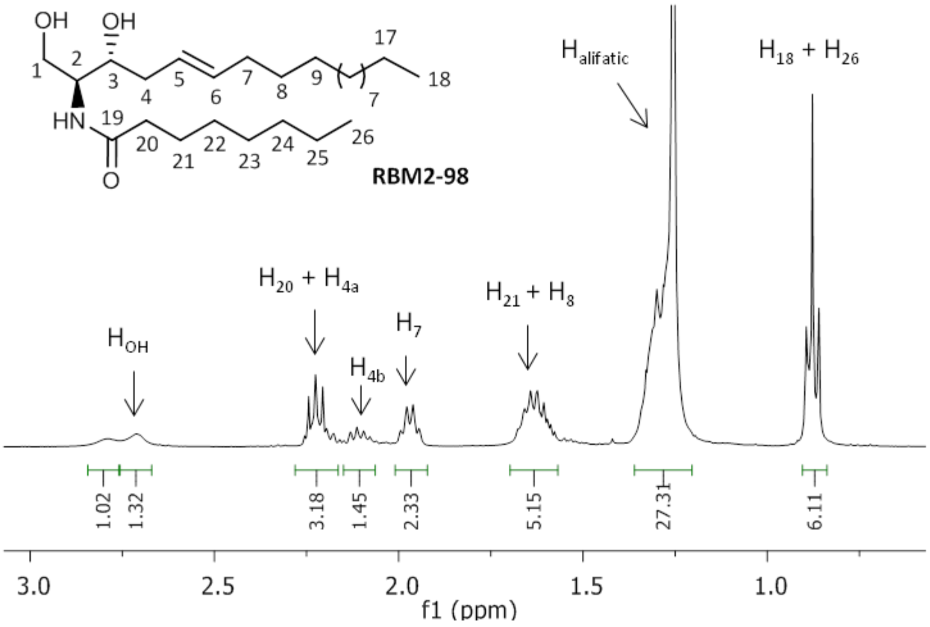

**Figure 3.59** $^1$H NMR spectra and chemical structure of **RBM2-98**.

Accordingly to the literature, olefin isomerization/migration is a known side reaction in CM when the catalysts are stressed by high temperatures and forced high turnovers. The resulting side products are usually difficult to remove by standard purification techniques.[110-111] While the exact mechanism for the isomerization remains unknown, it is believed that the ruthenium hydride species, formed from decomposition of ruthenium catalysts, catalyze the migration of olefins under the CM conditions.[112] Along this line, it has been described that 1,4-benzoquinones prevent olefin isomerization during CM with ruthenium catalysts.[113] In our case, however, addition of 1,4-benzoquinone not only did not prevent olefin isomerization, but decreased the reaction yield under the same conditions.

Although our synthetic approach to **RBM2--85** was initially designed to be more convenient and direct than the Bittman synthesis, the isomerization observed in the course of the CM reaction and the arduous chromatographic separation of the resulting isomeric mixture decreased considerably the overall yield of the route. To overcome these drawbacks, two possibilities can be considered for future work along this line: (1) to explore different reaction conditions in order to minimize the undesired isomerization during CM, or (2) to use an alternative approach for olefin formation as, for example, an *E*-selective Wittig reaction. This option, however, would require the design of a different synthetic approach.

#### 3.4.4.2 (*E*,*E*)-$\Delta^{4,6}$-Ceramide RBM2-76

*Synthetic approach*

The preparation of **RBM2-76**, the expected product of the enzymatic reaction of Des1 from substrate **RBM2-85**, was also considered of interest for its use as standard in the assay development process.

The synthetic route to this $\Delta^{4,6}$-ceramide was also described by Bittman *et al.*[109] in the same publication describing the synthesis of $\Delta^{6}$-ceramide **RBM2-85**. In this synthesis, $\alpha$-ketosulfoxide **57** was used as key intermediate, as depicted in Fig 3.60. The route continued with the alkylation of this intermediate, followed by sulfoxide elimination at high temperatures. Thus, the resulting ketone **59** was diastereoselectively reduced, deprotected under acidic conditions, and next *N*-acylated to the target $\Delta^{4,6}$-ceramide in 23% overall yield over six total steps.

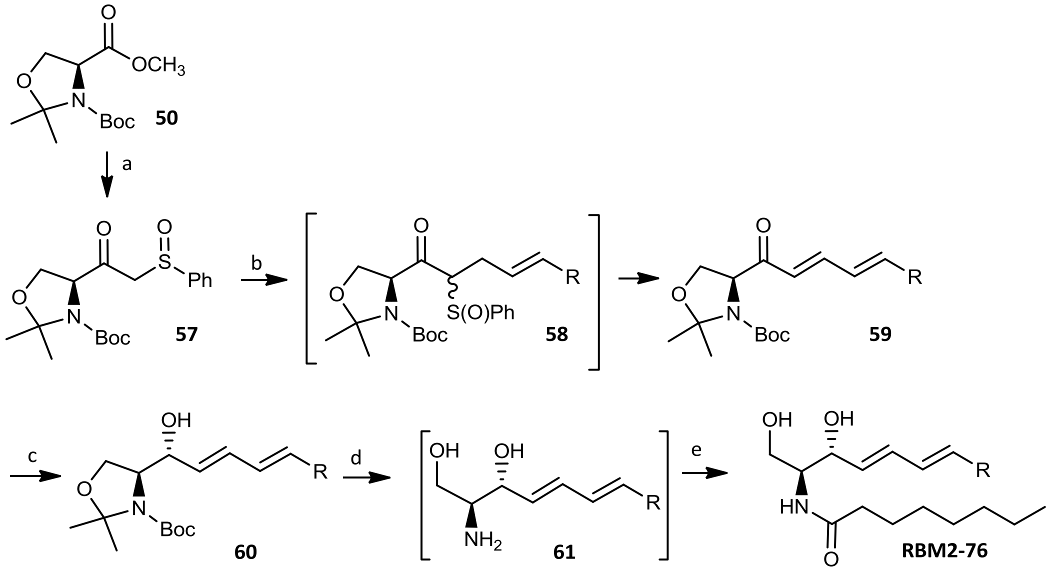
O
OCH3
O
N
Boc
50
a
O
O
S
Ph
O
N
Boc
57
b
O
R
O
N
S(O)Ph
Boc
58
O
R
O
N
Boc
59
c
OH
R
O
N
Boc
60
d
OH
OH
R
NH2
61
e
OH
OH
R
HN
O
RBM2-76

a) MeS(O)Ph, LDA, THF, -78 °C to rt, 71%; b) $CH_3(CH_2)_{10}CH=CHCH_2Br$, $K_2CO_3$, DMF, rt, 3 d, 60%; c) $NaBH_4$, $CeCl_3$, MeOH or DIBAL-H, THF, -15 °C to 0 °C, 88%; d) 1M HCl, THF, 70 °C; e) *p*-$O_2NC_6H_4CO_2C_7H_{15}$, THF, rt, 61%.

**Figure 3.60** Synthesis of $\Delta^{4,6}$-ceramide **RBM2-76**, as reported by Bittman and coworkers. R=$C_{11}H_{23}$.

In order to improve the above protocol, we decided to follow an apparently more direct synthetic approach to this diene. As illustrated in Fig. 3.61, we envisioned that ceramide **RBM2-76** could be obtained from an intermediate diene, such as **60**, which, in turn, could arisen from the *E*-selective Wittig reaction of aldehyde **62** with an appropriate phosphonium ylide. The acquired experience in C-C double bond formation by CM reactions along this doctoral thesis, prompted us to attempt the synthesis of α,β-unsaturated aldehyde **62** by CM reaction between scaffold **7** and acrolein.

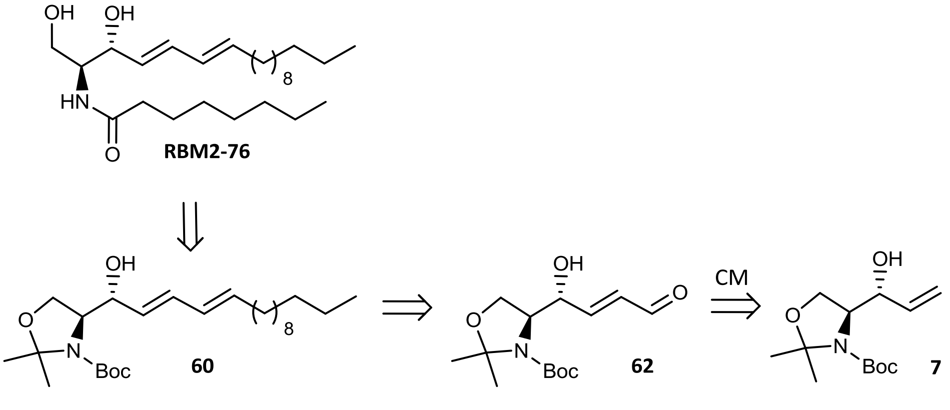
OH
OH
8
HN
O
RBM2-76
OH
8
O
N
Boc
60
OH
O
O
N
Boc
62
CM
OH
O
N
Boc
7

**Figure 3.61** Retrosynthetic analysis to $\Delta^{4,6}$-ceramide **RBM2-76**.

### *Synthetis of $\Delta^{4,6}$-ceramide (**RBM2-76**)*

As shown in Fig. 3.62, the synthesis of ceramide **RBM2-76** started by reaction between building block **7** and a 4-fold excess acrolein in $CH_2Cl_2$ at 45 °C, affording α,β-unsaturated aldehyde **62** in 53% yield. Efforts to improve the reaction yield by the slow addition of a 8-fold excess acrolein within 2 h failed. This low yield could be explained by the high reactivity of acrolein, probably arising from a self-coupling competing reaction.

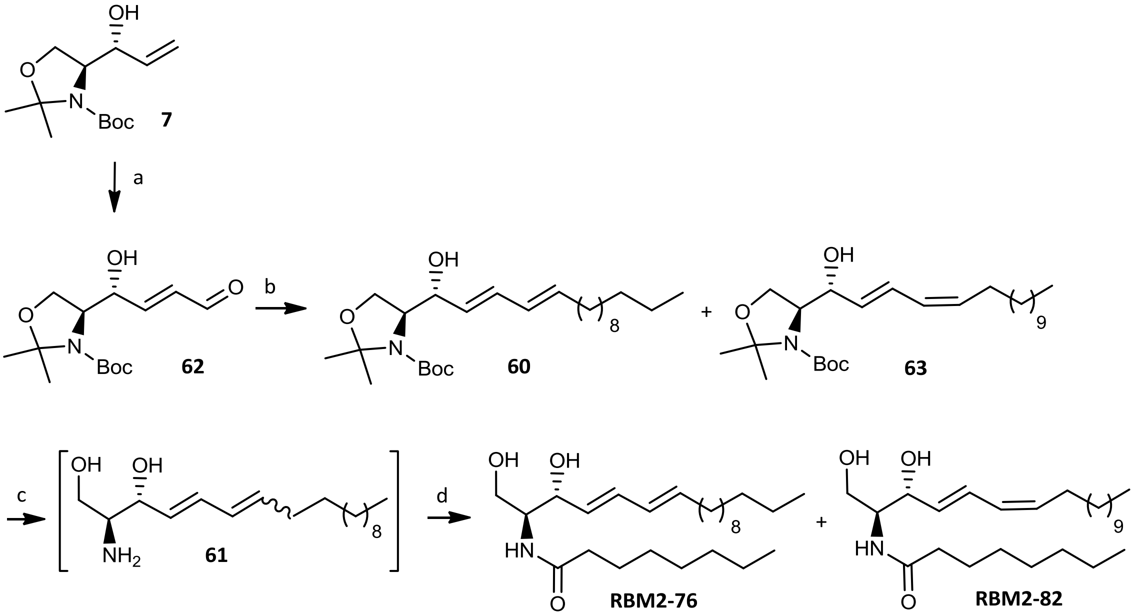

a) Acrolein, Grubb's 2nd generation cat., $CH_2Cl_2$, 45 °C, 5 h, 53%; b) $CH_3(CH_2)_{11}PPh_3Br$, *n*BuLi, THF, -78 °C, 4 h, 67%; c) $CH_3COCl$, MeOH, rt, 1 h; d) octanoic acid, $Et_3N$, HOBt, EDC, $CH_2Cl_2$, rt, 1 h, 22%.

**Figure 3.62** Synthesis of $\Delta^{4,6}$-Ceramide **RBM2-76**.

Using the classical Schlosser modification of the Wittig reaction for the preparation of *E*-alkenes,[114] aldehyde **62** was reacted with dodecyl triphenylphosphonium ylide in the presence of an excess of lithium salts at -75 °C, giving a complex reaction mixture. Although chromatographic separation was possible, an inseparable mixture of dienols (4*E*,6*E*)-**60** and (4*E*,6*Z*)-**63** was obtained in only 7% yield in a roughly 1:1 ratio. A more recent method to improve the *E*-selectivity in Wittig reactions is based on the quenching of the reaction mixture with MeOH at low temperatures.[115] In our case, the use of this modification afforded a mixture of dienes **60** and **63** in a 7:3 ratio and in substantially better yield (67%). In view of this result, we next tried to isomerize the mixture of dienes with a catalytic amount of iodine in $CH_2Cl_2$ for 1 h.[116] $^1H$ NMR data established that the ratio of dienes **60** and **63** remained unchanged, meaning that the isomerization failed even at longer reaction times. The synthetic route was continued from the above mixture of olefins with the removal of both oxazolidine and *N*-Boc protecting groups under acidic conditions, providing crude diene **61**, whose *N*-acylation with octanoic acid led to a mixture of two components, which were separated by flash chromatography. While the less polar component was identified as the by-product **64** (Fig 3.63)(14% yield), the most polar one consisted of an inseparable mixture of **RBM2-76** and the 4*E*,6*Z*-isomer **RBM2-82** in a roughly 2:3 ratio, and 22% overall yield.

Compound **64** was characterized by spectroscopic methods. Thus, MS analysis showed an increase of 14 units of mass with respect to **RBM2-76**. On the other hand, $^{1}H$ and $^{13}C$ NMR data confirmed the presence of a methoxy group as a singlet at 3.24 ppm, whose $^{13}C$ resonance appeared at 56.5 ppm. While C2 and C3 protons were shifted to a lower field (4.61 and 5.66 ppm, respectively), the C1 proton appeared at a higher field (3.72 ppm) compared to **RBM2-76**. In addition, the C7 proton appeared as an apparent quartet at 3.52 ppm, and correlated with the carbon atom at 82.1 ppm in HSQC spectra.

Formation of **64** can be interpreted as a result of a conjugated addition of MeOH to the mixture of dienes **60** and **63** in the course of the deprotection step under acidic conditions (Fig. 3.63). This result is indicative of the instability of conjugated dienes under acidic conditions.

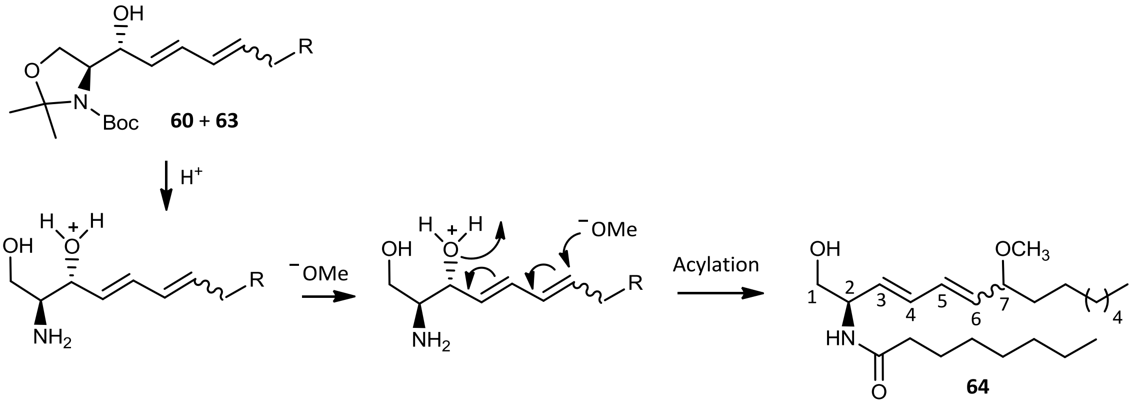

**Figure 3.63** Possible mechanism to account for the formation of compound **64** under acidic conditions in MeOH solution. R=$C_{10}H_{21}$.

In order to unambiguously characterize the desired *E,E*-isomer **RBM2-76** from the mixture with the *E,Z*-isomer **RBM2-82**, we decided to prepare this last isomer by an unambiguous route. Since the standard Wittig reaction shows a high stereoselection towards *Z* olefins, we reasoned that this approach should provide **63** as the major isomer from aldehyde **62**. Deprotection and *N*-acylation of diene **63** should provide **RBM2-82**, as shown in Fig 3.64.

In agreement with our expectations, condensation of **62** with dodecyl triphenylphosphonium ylide at rt afforded (4*E*,6*Z*)-**63** in 61% yield as a single stereoisomer. Deprotection to **65** under acidic conditions, followed by *N*-acylation with octanoic acid afforded a crude mixture from which the desired stereoisomerically pure **RBM2-82** could be isolated in 21% yield, as confirmed by its NMR data. As above, a small amount of the methanolysis by-product **64** was also obtained, albeit in a marginal 4% yield.

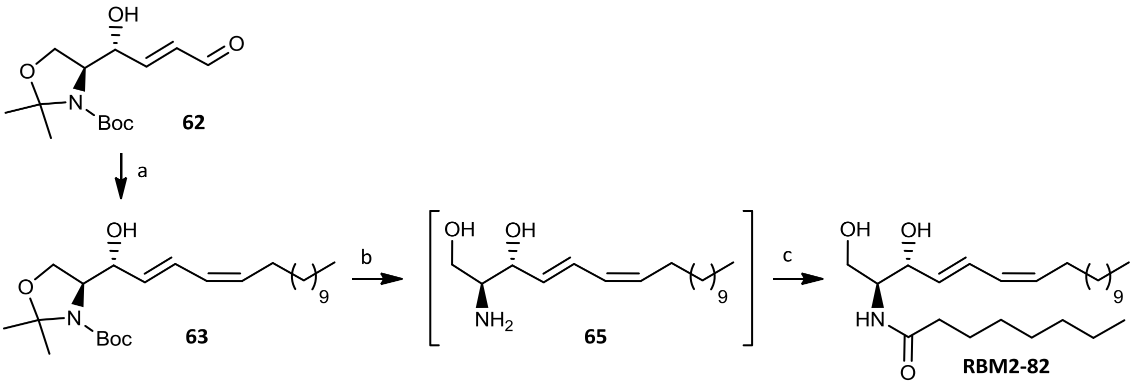

a) $CH_3(CH_2)_{11}PPh_3Br$, *n*BuLi, THF, -78 °C to rt, 2 h, 61%; b) $CH_3COCl$, MeOH, rt, 1 h; c) octanoic acid, $Et_3N$, HOBt, EDC, $CH_2Cl_2$, rt, 1 h, 21%.

**Figure 3.64** Synthesis of $\Delta^{4,6}$-ceramide **RBM2-82**.

### 3.4.5 Reactivity of RBM2-76 as dienophile against triazacyclopentadiones

To examine the efficiency of the Diels-Alder reaction between diene **RBM2-76** and the dienophile DMEQ-TAD, we carried out model reactions in the presence of an excess of this fluorophore in order to monitor the resulting DA adducts by HPLC with fluorescence detection. Since, apparently, DMEQ-TAD turned out to be non stable under the chromatographic conditions, the detection of **RBM2-76** DA adducts using this technique was troublesome. For this reason, we next sought to label **RBM2-76** with the non fluorescence dienophile PTAD, which had also been reported to rapidly form stable adducts with dienes through DA reaction (Fig. 3.65).[117] HRMS under flow injection analysis (FIA) of the DA adducts confirmed the formation of the expected adduct **67**, as indicated by the detection of a peak corresponding to $[M+H]^+$ 599.4184 (calculated: 599.4172). This result shows that TAD's may be suitable reagents for the labeling of diene **RBM2-76** and reinforces their use in a HTS Des1 assay.

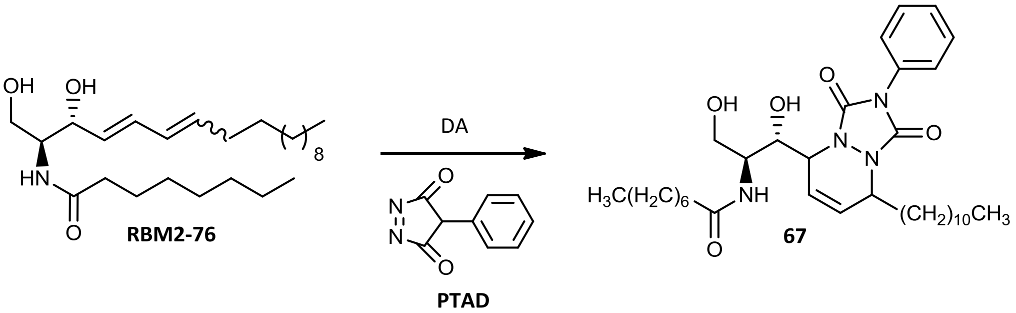

**Figure 3.65** DA reaction between diene **RBM2-76** and dienophile PTAD.

Although it is out of the scope of this Thesis Dissertation, future efforts along this line will be addressed at confirming the suitability of **RBM2-85** as Des1 substrate in cell lysates and also to set up a experimental protocol for the detection of diene **RBM2-76** after DA reaction with the fluorescent dienophile DMEQ-TAD.

## 3.5 References

1. Dickson, R. C., Thematic review series: sphingolipids. New insights into sphingolipid metabolism and function in budding yeast. *J. Lipid Res.* **2008,** 49, (5), 909-21.

2. Zheng, W.; Kollmeyer, J.; Symolon, H.; Momin, A.; Munter, E.; Wang, E.; Kelly, S.; Allegood, J. C.; Liu, Y.; Peng, Q.; Ramaraju, H.; Sullards, M. C.; Cabot, M.; Merrill Jr, A. H., Ceramides and other bioactive sphingolipid backbones in health and disease: Lipidomic analysis, metabolism and roles in membrane structure, dynamics, signaling and autophagy. *Biochim. Biophys. Acta, Biomembr.* **2006,** 1758, (12), 1864-1884.

3. Merrill, A. H., Jr.; Williams, R. D., Utilization of different fatty acyl-CoA thioesters by serine palmitoyltransferase from rat brain. *J. Lipid Res.* **1984,** 25, (2), 185-8.

4. Farwanah, H.; Pierstorff, B.; Schmelzer, C. E.; Raith, K.; Neubert, R. H.; Kolter, T.; Sandhoff, K., Separation and mass spectrometric characterization of covalently bound skin ceramides using LC/APCI-MS and Nano-ESI-MS/MS. *J. Chromatogr., B: Anal. Technol. Biomed. Life Sci.* **2007,** 852, (1-2), 562-70.

5. Shapiro, D.; Segal, K., The synthesis of sphingosine. *J. Am. Chem. Soc.* **1954,** 76, 5894-5.

6. Shapiro, D.; Segal, H.; Flowers, H. M., Total synthesis of sphingosine. *J. Am. Chem. Soc.* **1958,** 80, 1194-7.

7. Garner, P.; Park, J. M.; Malecki, E., A stereodivergent synthesis of D-erythro-sphingosine and D-threo-sphingosine from L-serine. *J. Org. Chem.* **1988,** 53, 4395-8.

8. Nimkar, S.; Menaldino, D.; Merrill, A. H.; Liotta, D., A stereoselective synthesis of sphingosine, a protein kinase C inhibitor. *Tetrahedron Lett.* **1988,** 29, 3037-40.

9. Herold, P., Synthesis of D-Erythro- and D-Threo-Sphingosine Derivatives From L-Serine. *Helv. Chim. Acta* **1988,** 71, (2), 354-362.

10. Koskinen, A. M. P.; Krische, M. J., γ-Amino-β-keto phosphonates in synthesis: synthesis of the sphingosine skeleton. *Synlett* **1990**, 665-6.

11. Li, Y.-L.; Sun, X.-L.; Wu, Y.-L., Synthetic study on chiral building block of vicinal diol, chiron approach to the precursors of all sphingosine stereoisomers. *Tetrahedron* **1994,** 50, 10727-38.

12. Murakami, T.; Minamikawa, H.; Hato, M., Regio- and stereocontrolled synthesis of D-erythro-sphingosine and phytosphingosine from D-glucosamine. *Tetrahedron Lett.* **1994,** 35, 745-8.

13. Murakami, T.; Hato, M., Synthetic studies on sphingolipids. 3. Efficient stereo controlled synthesis of D-erythro-sphingosine from N-benzoyl-D-glucosamine. *J. Chem. Soc., Perkin Trans. 1* **1996**, 823-7.

14. Mori, K.; Umemura, T., Stereochemistry of aplidiasphingosine as proposed by the asymmetric synthesis and carbon-13 NMR study of sphingosine relatives. *Tetrahedron Lett.* **1981,** 22, 4433-6.

15. Roush, W. R.; Adam, M. A., Directed openings of 2,3-epoxy alcohols via reactions with isocyanates: synthesis of (+)-erythro-dihydrosphingosine. *J. Org. Chem.* **1985,** 50, 3752-7.

16. Bernet, B.; Vasella, A., Enantioselective synthesis of D-erythro-sphingosine. *Tetrahedron Lett.* **1983,** 24, 5491-4.

17. Hino, T.; Nakakyama, K.; Taniguchi, M.; Nakagawa, M., A new to racemic erythro-sphingosine and ceramides. The 1,2- versus 1,4-addition reaction of hexadec-2-enal with 2-nitroethanol. *J. Chem. Soc., Perkin Trans. 1* **1986**, 1687-90.

18. Groth, U.; Schoellkopf, U.; Tiller, T., Asymmetric synthesis via heterocyclic intermediates. 43. Asymmetric synthesis of D-erythro-sphingosine. *Tetrahedron* **1991,** 47, 2835-42.

19. Ito, Y.; Sawamura, M.; Hayashi, T., Asymmetric synthesis of threo- and erythro-sphingosines by asymmetric aldol reaction of α-isocyanoacetate catalyzed by a chiral ferrocenylphosphine gold(I) complex. *Tetrahedron Lett.* **1988,** 29, 239-40.

20. Solladie-Cavallo, A.; Koessler, J. L., A Four-Step Diastereoselective Synthesis of D-erythro-Sphingosine by an Enantioselective Aldol Reaction Using a Titanium Enolate Derived from a Chiral Iminoglycinate. *J. Org. Chem.* **1994,** 59, 3240-2.

21. Ullrich, T.; Ghobrial, M.; Peters, C.; Billich, A.; Guerini, D.; Nussbaumer, P., Synthesis and immobilization of erythro-C14-ω-aminosphingosine-1-phosphate as a potential tool for affinity chromatography. *ChemMedChem* **2008,** 3, 356-360.

22. Rai, A. N.; Basu, A. In *Synthesis of sphingolipids: A cross metathesis approach*, 2005; American Chemical Society: 2005; pp ORGN-816.

23. Torssell, S.; Somfai, P. In *A practical synthesis of D-erythro-Sphingosine using a cross-metathesis approach*, 2004; American Chemical Society: 2004; pp ORGN-108.

24. Jean-Louis Hérisson, P.; Chauvin, Y., Catalyse de transformation des oléfines par les complexes du tungstène. II. Télomérisation des oléfines cycliques en présence d'oléfines acycliques. *Die Makromolekulare Chemie* **1971,** 141, (1), 161-176.

25. Garner, P., Stereocontrolled addition to a penaldic acid equivalent: an asymmetric synthesis of threo-β-hydroxy-L-glutamic acid. *Tetrahedron Lett.* **1984,** 25, 5855-8.

26. McKillop, A.; Taylor, R. J. K.; Watson, R. J.; Lewis, N., An improved procedure for the preparation of the Garner aldehyde and its use for the synthesis of N-protected 1-halo-2-(R)-amino-3-butenes. *Synthesis* **1994**, 31-3.

27. Moriwake, T.; Hamano, S.; Saito, S.; Torii, S., A straightforward synthesis of allyl amines from α-amino acids without racemization. *Chem. Lett.* **1987**, 2085-8.

28. Yanagida, M.; Hashimoto, K.; Ishida, M.; Shinozaki, H.; Shirahama, H., Syntheses of acyclic analogs of kainoids and neuroexcitatory activity. *Tetrahedron Lett.* **1989,** 30, 3799-802.

29. Dondoni, A.; Perrone, D., Synthesis of N-(tert-butoxycarbonyl)-N,O-isopropylideneserinal from serine methyl ester by a reduction-oxidation sequence. *Synthesis* **1997**, 527-529.

30. Jurczak, J.; Gryko, D.; Kobrzycka, E.; Gruza, H.; Prokopowicz, P., Effective and mild method for preparation of optically active α-amino aldehydes via TEMPO oxidation. *Tetrahedron* **1998,** 54, 6051-6064.

31. Bold, G.; Allmendinger, T.; Herold, P.; Moesch, L.; Schaer, H. P.; Duthaler, R. O., Stereoselective synthesis of (2S,6S)-2,6-diaminoheptanedioic acid and of unsymmetrical derivatives of meso-2,6-diaminoheptanedioic acid. *Helv. Chim. Acta* **1992,** 75, 865-82.

32. Campbell, A. D.; Raynham, T. M.; Taylor, R. J. K., A simplified route to the (R)-Garner aldehyde and (S)-vinylglycinol. *Synthesis* **1998**, 1707-1709.

33. Kanemitsu, T.; Seeberger, P. H., Use of olefin cross-metathesis to release azide-containing sugars from solid support. *Org. Lett.* **2003,** 5, (24), 4541-4.

34. Barrett, A. G.; Beall, J. C.; Braddock, D. C.; Flack, K.; Gibson, V. C.; Salter, M. M., Asymmetric allylboration and ring closing alkene metathesis: a novel strategy for the synthesis of glycosphingolipids. *J. Org. Chem.* **2000,** 65, (20), 6508-14.

35. Randl, S.; Blechert, S., Concise enantioselective synthesis of 3,5-dialkyl-substituted indolizidine alkaloids via sequential cross-metathesis-double-reductive cyclization. *J. Org. Chem.* **2003,** 68, (23), 8879-82.

36. Chatterjee, A. K.; Choi, T.-L.; Sanders, D. P.; Grubbs, R. H., A General Model for Selectivity in Olefin Cross Metathesis. *J. Am. Chem. Soc.* **2003,** 125, (37), 11360-11370.

37. Ternes, P.; Franke, S.; Zahringer, U.; Sperling, P.; Heinz, E., Identification and characterization of a sphingolipid delta 4-desaturase family. *J. Biol. Chem.* **2002,** 277, (28), 25512-8.

38. Reist, E. J.; Christie, P. H., Synthesis of D-dihydrosphingosine. *J. Org. Chem.* **1970,** 35, 3521-4.

39. Wild, R.; Schmidt, R. R., Synthesis of sphingosines. 11. Convenient synthesis of phytosphingosine and sphinganine from D-galactal and D-arabitol. *Liebigs Ann.* **1995**, 755-64.

40. Cook, G. R.; Pararajasingham, K., Stereoselective synthesis of D-erythro- and L-threo-sphinganines via Palladium-catalyzed equilibration and Suzuki coupling. *Tetrahedron Lett.* **2002,** 43, 9027-9029.

41. Azuma, H.; Tamagaki, S.; Ogino, K., Stereospecific Total Syntheses of Sphingosine and Its Analogues from L-Serine. *J. Org. Chem.* **2000,** 65, 3538-3541.

42. De, J. S.; Van, O. I.; Poulton, S.; Hendrix, C.; Busson, R.; Van, C. S.; De, K. D.; Spiegel, S.; Herdewijn, P., Structure-activity relationship of short-chain sphingoid bases as inhibitors of sphingosine kinase. *Bioorg. Med. Chem. Lett.* **1999,** 9, 3175-3180.

43. Thum, O.; Hertweck, C.; Simon, H.; Boland, W., (6R,7R)-[4,5,6,7-2H4]-Palmitate and (8S,9R)-[8,9-2H2]-L-erythro-sphinganine. Probes for the analysis of the stereochemical course of Δ6-desaturases from plants and insects. *Synthesis* **1999**, 2145-2150.

44. Hoffman, R. V.; Tao, J., A Synthesis of D-erythro- and L-threo-Sphingosine and Sphinganine Diastereomers via the Biomimetic Precursor 3-Ketosphinganine. *J. Org. Chem.* **1998,** 63, 3979-3985.

45. Fernandes, R. A.; Kumar, P., A stereoselective synthesis of dihydrosphingosine. *Eur. J. Org. Chem.* **2000**, 3447-3449.

46. Kobayashi, S.; Furuta, T., Use of heterocycles as chiral ligands and auxiliaries in asymmetric syntheses of sphingosine, sphingofungins B and F. *Tetrahedron* **1998,** 54, 10275-10294.

47. Masui, M.; Shioiri, T., Stereoselective synthesis of sphinganine by means of modified asymmetric borane reduction. *Tetrahedron Lett.* **1998,** 39, 5199-5200.

48. Ishizuka, T.; Morooka, K.; Ishibuchi, S.; Kunieda, T., Synthetic application of chiral 4-methoxy-2-oxazolidinone synthons to 2-amino alcohols of biological interest. *Heterocycles* **1996,** 42, 837-48.

49. Buehrer, B. M.; Bell, R. M., Sphingosine kinase: properties and cellular functions. *Adv. Lipid Res.* **1993,** 26, 59-67.

50. van Veldhoven, P. P.; Mannaerts, G. P., Sphingosine-phosphate lyase. *Adv. Lipid Res.* **1993,** 26, 69-98.

51. Spiegel, S.; Milstien, S., Sphingosine-1-phosphate: signaling inside and out. *FEBS Lett.* **2000,** 476, (1-2), 55-7.

52. Spiegel, S.; Milstien, S., Sphingosine-1-phosphate: an enigmatic signalling lipid. *Nat. Rev. Mol. Cell Biol.* **2003,** 4, 397-407.

53. Olivera, A.; Spiegel, S., Sphingosine-1-phosphate as second messenger in cell proliferation induced by PDGF and FCS mitogens. *Nature* **1993,** 365, (6446), 557-60.

54. Ghosh, T. K.; Bian, J.; Gill, D. L., Intracellular calcium release mediated by sphingosine derivatives generated in cells. *Science (Washington, DC, U.S.)* **1990,** 248, (4963), 1653-6.

55. Ruan, F.; Sadahira, Y.; Hakomori, S.; Igarashi, Y., Chemical synthesis of D-erythro-sphingosine-1-phosphate, and its inhibitory effect on cell motility. *Bioorg. Med. Chem. Lett.* **1992,** 2, 973-8.

56. Boumendjel, A.; Miller, S. P. F., Synthesis of sphingosine-1-phosphate and dihydrosphingosine-1-phosphate. *J. Lipid Res.* **1994,** 35, 2305-11.

57. Clemens, J. J.; Davis, M. D.; Lynch, K. R.; Macdonald, T. L., Synthesis of benzimidazole based analogues of sphingosine-1-phosphate: discovery of potent, subtype-selective S1P4 receptor agonists. *Bioorg. Med. Chem. Lett.* **2004,** 14, 4903-4906.

58. Blot, V.; Jacquemard, U.; Reissig, H.-U.; Kleuser, B., Practical syntheses of sphingosine-1-phosphate and analogues. *Synthesis* **2009**, 759-766.

59. Byun, H.-S.; Erukulla, R. K.; Bittman, R., Synthesis of Sphingomyelin and Ceramide 1-Phosphate from Ceramide without Protection of the Allylic Hydroxyl Group. *J. Org. Chem.* **1994,** 59, 6495-8.

60. Yoshikawa, M.; Kato, T.; Takenishi, T., A novel method for phosphorylation of nucleosides to 5'-nucleotides. *Tetrahedron Lett.* **1967,** 50, 5065-8.

61. Oza, V. B.; Corcoran, R. C., A Mild Preparation of Protected Phosphate Esters From Alcohols. *J. Org. Chem.* **1995,** 60, 3680-4.

62. Chalfant, C. E.; Spiegel, S., Sphingosine 1-phosphate and ceramide 1-phosphate: expanding roles in cell signaling. *J. Cell Sci.* **2005,** 118, (20), 4605-12.

63. Nussbaumer, P.; Hornillos, V.; Ghobrial, M.; Ullrich, T., An efficient, one-pot synthesis of various ceramide 1-phosphates from sphingosine 1-phosphate. *Chem Phys Lipids* **2008,** 151, (2), 125-8.

64. Garegg, P. J.; Regberg, T.; Stawinski, J.; Stroemberg, R., Nucleoside phosphonates. Part 7. Studies on the oxidation of nucleoside phosphonate esters. *J. Chem. Soc., Perkin Trans. 1* **1987**, 1269-73.

65. Wada, T.; Mochizuki, A.; Sato, Y.; Sekine, M., A convenient method for phosphorylation involving a facile oxidation of H-phosphonate monoesters via bis(trimethylsilyl)phosphites. *Tetrahedron Lett.* **1998,** 39, 7123-7126.

66. Merrill, A. H., Jr., De novo sphingolipid biosynthesis: a necessary, but dangerous, pathway. *J. Biol. Chem.* **2002,** 277, 25843-25846.

67. Ardail, D.; Popa, I.; Alcantara, K.; Pons, A.; Zanetta, J. P.; Louisot, P.; Thomas, L.; Portoukalian, J., Occurrence of ceramides and neutral glycolipids with unusual long-chain base composition in purified rat liver mitochondria. *FEBS Lett.* **2001,** 488, (3), 160-4.

68. Singh, J.; Satyamurthi, N.; Aidhen, I. S., The growing synthetic utility of Weinreb's amide. *J. Prakt. Chem. (Weinheim, Ger.)* **2000,** 342, 340-347.

69. Herold, P., Synthesis of D-erythro- and D-threo-sphingosine derivatives from L-serine. *Helv. Chim. Acta* **1988,** 71, 354-62.

70. Bouwstra, J. A.; Ponec, M., The skin barrier in healthy and diseased state. *Biochim. Biophys. Acta* **2006,** 1758, (12), 2080-95.

71. Stoffel, W., Sphingolipids. *Annu. Rev. Biochem.* **1971,** 40, 57-82.

72. Kolesnick, R. N.; Goni, F. M.; Alonso, A., Compartmentalization of ceramide signaling: physical foundations and biological effects. *J. Cell. Physiol.* **2000,** 184, (3), 285-300.

73. Futerman, A. H.; Hannun, Y. A., The complex life of simple sphingolipids. *EMBO Rep.* **2004,** 5, 777-782.

74. Grassme, H.; Riethmuller, J.; Gulbins, E., Biological aspects of ceramide-enriched membrane domains. *Prog. Lipid Res.* **2007,** 46, (3-4), 161-70.

75. Goñi, F. M.; Alonso, A., Biophysics of sphingolipids I. Membrane properties of sphingosine, ceramides and other simple sphingolipids. *Biochim. Biophys. Acta, Biomembr.* **2006,** 1758, (12), 1902-1921.

76. de Miguel, I.; Herradón, B.; Mann, E., Intramolecular Azide-Alkene 1,3-Dipolar Cycloaddition/Enamine Addition(s) Cascade Reaction: Synthesis of Nitrogen-Containing Heterocycles. *Adv. Synth. Catal.* **2012,** 354, (9), 1731-1736.

77. Vieu, C.; Terce, F.; Chevy, F.; Rolland, C.; Barbaras, R.; Chap, H.; Wolf, C.; Perret, B.; Collet, X., Coupled assay of sphingomyelin and ceramide molecular species by gas liquid chromatography. *J. Lipid Res.* **2002,** 43, (3), 510-22.

78. Snada, S.; Uchida, Y.; Anraku, Y.; Izawa, A.; Iwamori, M.; Nagai, Y., Analysis of ceramide and monohexaosyl glycolipid derivatives by high-performance liquid chromatography and its application to the determination of the molecular species in tissues. *J. Chromatogr.* **1987,** 400, 223-31.

79. Previati, M.; Bertolaso, L.; Tramarin, M.; Bertagnolo, V.; Capitani, S., Low nanogram range quantitation of diglycerides and ceramide by high-performance liquid chromatography. *Anal. Biochem.* **1996,** 233, (1), 108-14.

80. Yano, M.; Kishida, E.; Muneyuki, Y.; Masuzawa, Y., Quantitative analysis of ceramide molecular species by high performance liquid chromatography. *J. Lipid Res.* **1998,** 39, (10), 2091-8.

81. Kasumov, T.; Huang, H.; Chung, Y. M.; Zhang, R.; McCullough, A. J.; Kirwan, J. P., Quantification of ceramide species in biological samples by liquid chromatography electrospray ionization tandem mass spectrometry. *Anal. Biochem.* **2010,** 401, (1), 154-61.

82. Scherer, M.; Leuthauser-Jaschinski, K.; Ecker, J.; Schmitz, G.; Liebisch, G., A rapid and quantitative LC-MS/MS method to profile sphingolipids. *J. Lipid Res.* **2010,** 51, (7), 2001-11.

83. Nabetani, T.; Makino, A.; Hullin-Matsuda, F.; Hirakawa, T. A.; Takeoka, S.; Okino, N.; Ito, M.; Kobayashi, T.; Hirabayashi, Y., Multiplex analysis of sphingolipids using amine-reactive tags (iTRAQ). *J. Lipid Res.* **2011,** 52, (6), 1294-302.

84. Mann, M., Functional and quantitative proteomics using SILAC. *Nat. Rev. Mol. Cell Biol.* **2006,** 7, 952-958.

85. Ong, S.-E.; Mann, M., Stable isotope labeling by amino acids in cell culture for quantitative proteomics. *Methods Mol. Biol. (Totowa, NJ, U. S.)* **2007,** 359, 37-52.

86. Cartwright, I. L.; Hutchinson, D. W.; Armstrong, V. W., The reaction between thiols and 8-azidoadenosine derivatives. *Nucleic Acids Res.* **1976,** 3, (9), 2331-9.

87. Duckworth, B. P.; Zhang, Z.; Hosokawa, A.; Distefano, M. D., Selective labeling of proteins by using protein farnesyltransferase. *Chembiochem* **2007,** 8, (1), 98-105.

88. Ning, X.; Guo, J.; Wolfert, M. A.; Boons, G.-J., Visualizing metabolically labeled glycoconjugates of living cells by copper-free and fast huisgen cycloadditions. *Angew. Chem., Int. Ed.* **2008,** 47, 2253-2255.

89. Parton, R. G.; Richards, A. A., Lipid rafts and caveolae as portals for endocytosis: new insights and common mechanisms. *Traffic* **2003,** 4, (11), 724-38.
90. Simons, K.; Vaz, W. L., Model systems, lipid rafts, and cell membranes. *Annu. Rev. Biophys. Biomol. Struct.* **2004,** 33, 269-95.

91. Beatty, K. E.; Fisk, J. D.; Smart, B. P.; Lu, Y. Y.; Szychowski, J.; Hangauer, M. J.; Baskin, J. M.; Bertozzi, C. R.; Tirrell, D. A., Live-cell imaging of cellular proteins by a strain-promoted azide-alkyne cycloaddition. *ChemBioChem* **2010,** 11, 2092-2095.

92. Bernardin, A.; Cazet, A.; Guyon, L.; Delannoy, P.; Vinet, F.; Bonnaffe, D.; Texier, I., Copper-Free Click Chemistry for Highly Luminescent Quantum Dot Conjugates: Application to in Vivo Metabolic Imaging. *Bioconjugate Chem.* **2010,** 21, 583-588.

93. Stepensky, D., Quantitative aspects of intracellularly-targeted drug delivery. *Pharm. Res.* **2010,** 27, (12), 2776-80.

94. Glauner, H.; Ruttekolk, I. R.; Hansen, K.; Steemers, B.; Chung, Y. D.; Becker, F.; Hannus, S.; Brock, R., Simultaneous detection of intracellular target and off-target binding of small molecule cancer drugs at nanomolar concentrations. *Br. J. Pharmacol.* **2010,** 160, (4), 958-70.

95. Hakomori, S., Bifunctional role of glycosphingolipids. Modulators for transmembrane signaling and mediators for cellular interactions. *J. Biol. Chem.* **1990,** 265, 18713-16.

96. Maier, O.; Oberle, V.; Hoekstra, D., Fluorescent lipid probes: some properties and applications (a review). *Chem. Phys. Lipids* **2002,** 116, (1–2), 3-18.

97. Sawa, M.; Hsu, T.-L.; Itoh, T.; Sugiyama, M.; Hanson, S. R.; Vogt, P. K.; Wong, C.-H., Glycoproteomic probes for fluorescent imaging of fucosylated glycans in vivo. *Proc. Natl. Acad. Sci. U.S.A.* **2006,** 103, 12371-12376.

98. Garrido, M.; Abad, J.; Alonso, A.; Goñi, F.; Delgado, A.; Montes, L. R., In situ synthesis of fluorescent membrane lipids (ceramides) using click chemistry. *J. Chem. Biol.* **2012,** 5, (3), 119-123.

99. Michel, C.; van, E.-D. G.; Rother, J.; Sandhoff, K.; Wang, E.; Merrill, A. H., Jr., Characterization of ceramide synthesis. A dihydroceramide desaturase introduces the 4,5-trans-double bond of sphingosine at the level of dihydroceramide. *J. Biol. Chem.* **1997,** 272, 22432-22437.

100. Bielawska, A.; Crane, H. M.; Liotta, D.; Obeid, L. M.; Hannun, Y. A., Selectivity of ceramide-mediated biology. Lack of activity of erythro-dihydroceramide. *J. Biol. Chem.* **1993,** 268, (35), 26226-26232.

101. Ahn, E. H.; Schroeder, J. J., Sphingoid Bases and Ceramide Induce Apoptosis in HT-29 and HCT-116 Human Colon Cancer Cells. *Exp. Biol. Med.* **2002,** 227, (5), 345-353.

102. Kraveka, J. M.; Li, L.; Szulc, Z. M.; Bielawski, J.; Ogretmen, B.; Hannun, Y. A.; Obeid, L. M.; Bielawska, A., Involvement of Dihydroceramide Desaturase in Cell Cycle Progression in Human Neuroblastoma Cells. *J. Biol. Chem.* **2007,** 282, (23), 16718-16728.

103. Stiban, J.; Fistere, D.; Colombini, M., Dihydroceramide hinders ceramide channel formation: Implications on apoptosis. *Apoptosis* **2006,** 11, (5), 773-80.

104. Raith, K.; Darius, J.; Neubert, R. H., Ceramide analysis utilizing gas chromatography-mass spectrometry. *J. Chromatogr., A* **2000,** 876, (1-2), 229-33.

105. Kok, J. W.; Nikolova-Karakashian, M.; Klappe, K.; Alexander, C.; Merrill, A. H., Jr., Dihydroceramide biology. Structure-specific metabolism and intracellular localization. *J. Biol. Chem.* **1997,** 272, (34), 21128-36.

106. Geeraert, L.; Mannaerts, G. P.; van Veldhoven, P. P., Conversion of dihydroceramide into ceramide: involvement of a desaturase. *Biochem. J.* **1997,** 327 ( Pt 1), 125-32.

107. Shimizu, M.; Kamachi, S.; Nishii, Y.; Yamada, S., Synthesis of a reagent for fluorescence-labeling of vitamin D and its use in assaying vitamin D metabolites. *Anal. Biochem.* **1991,** 194, (1), 77-81.

108. Shimizu, M.; Wang, X. X.; Iwasaki, Y.; Yamada, S., First fluorometric method for the assay of plasma 1α,25-dihydroxyvitamin D3. *J. Fluoresc.* **1997,** 7, 235S-237S.

109. Chun, J.; Li, G.; Byun, H. S.; Bittman, R., Synthesis of new trans double-bond sphingolipid analogues: Delta(4,6) and Delta(6) ceramides. *J. Org. Chem.* **2002,** 67, (8), 2600-5.

110. Lehman, S. E.; Schwendeman, J. E.; O'Donnell, P. M.; Wagener, K. B., Olefin isomerization promoted by olefin metathesis catalysts. *Inorg. Chim. Acta* **2003,** 345, 190-198.

111. Schmidt, B., Catalysis at the interface of ruthenium carbene and ruthenium hydride chemistry: Organometallic aspects and applications to organic synthesis. *Eur. J. Org. Chem.* **2004**, 1865-1880.

112. Hong, S. H.; Day, M. W.; Grubbs, R. H., Decomposition of a Key Intermediate in Ruthenium-Catalyzed Olefin Metathesis Reactions. *J. Am. Chem. Soc.* **2004,** 126, 7414-7415.

113. Hong, S. H.; Sanders, D. P.; Lee, C. W.; Grubbs, R. H., Prevention of undesirable isomerization during olefin metathesis. *J. Am. Chem. Soc.* **2005,** 127, (49), 17160-1.

114. Schlosser, M.; Huynh, B. T.; Schaub, B., The betaine-ylide route to trans-alkenols. *Tetrahedron Lett.* **1985,** 26, 311-14.

115. Oh, J. S.; Hyun Kim, B.; Gyu Kim, Y., (E)-Selective Wittig reactions of Garner's aldehyde with nonstabilized ylides. *Tetrahedron Lett.* **2004,** 45, (20), 3925-3928.

116. Hepperle, S. S.; Li, Q.; East, A. L. L., Mechanism of Cis/Trans Equilibration of Alkenes via Iodine Catalysis. *J. Phys. Chem. A* **2005,** 109, 10975-10981.

117. Higashi, T.; Shibayama, Y.; Fuji, M.; Shimada, K., Liquid chromatography-tandem mass spectrometric method for the determination of salivary 25-hydroxyvitamin D3: a noninvasive tool for the assessment of vitamin D status. *Anal Bioanal Chem* **2008,** 391, (1), 229-38.

# 4. Summary & Conclusions

- Garner's aldehyde **4** has been used as chiral building block to construct the 2-amino-1,3-diol head of the sphingoid backbone in scaffolds **7** and **56**. Diastereoselective addition of metal-activated carbon nucleophiles (either lithium or organomagnesium compounds) to **4** was a convenient approach for the preparation of the above scaffolds with high *erythro* selectivity and good overall yields. Likewise, ω-azido-3-ketodihydrosphingosine **RBM2-63** was obtained by the diastereoselective addition of lithium 1-pentadecylacetylide to aldehyde **4**, followed by triple bond reduction and selective oxidation of the secondary hydroxyl group.

- A synthetic methodology based on an olefin cross-methatesis (CM) reaction was devised to prepare a series of sphingolipid analogues. This approach has been used to introduce a double bond at the sphingoid backbone with high *E*-selectivity from the starting 2-amino-1,3-diols **7** and **56**.

- ω-Azidosphingosine (**RBM2-31**) and a series of ω-azidoceramides (**RBM2-32**, **RBM2-37**, **RBM2-46** and **RBM2-77**) have been synthesized from a common intermediate **12** resulting from CM reaction between scaffold **7** and 11-bromoundec-1-ene (**11**). Likewise, the catalytic hydrogenation of the C4-C5 double bond in **12** led to the saturated ω-azidodihydrosphingosine **RBM2-40** and the corresponding ω-azidodihydroceramides **RBM2-44**, **RBM2-45** and **RBM2-87** by *N*-acylation.

- Appreciable double bond migration was observed from CM reaction of **56** with a terminal alkene. This side reaction hampered olefin purification and reduced the overall yield of the final (*E*)-$\Delta^6$-ceramide **RBM2-85**. However, reaction of **7** with a terminal alkene or with the highly reactive acrolein, led to the required adducts **12** and **62**, respectively, in acceptable yields as the only isolable compounds after chromatographic purification.

- Attempts to obtain $\Delta^{4,6}$-ceramide **RBM2-76** based on the Wittig reaction of aldehyde **62** with a suitable triphenylphosphonium ylide met with limited success, since mixtures of (4*E*,6*E*) and (4*E*,6*Z*) isomers were obtained in an approximate 4:6 ratio. Moreover, formation of an additional methoxydiene by-product **64** was also observed in the course of the final deprotection step under acidic conditions.

- The introduction of an azide group at C1 position of the sphingoid backbone was better carried out by nucleophilic substitution of azide from mesylate **33**. Special care was taken to minimize the formation of pyrroline **35**. The formation of this by-product has been interpreted as a result of an intramolecular thermal azide-olefin 1,3-dipolar cycloaddition in the course of the $S_N$ reaction.

- Phosphorylated ω-azidosphingosine **RBM2-35** and ω-azidodihydrosphingosine **RBM2-43** were obtained in high yield by selective monophosphorylation of the corresponding primary hydroxyl groups of the corresponding *N*-Boc precursors with dimethyl chlorophosphate and TMSBr-MeOH promoted methanolysis of the intermediate *N*-Boc phosphate esters.

- The *H*-phosphonate approach was the method of choice for the synthesis of ω-azidoceramide-1-phosphate **RBM2-47**. The method is based on the formation of an intermediate phosphite triester, hydrolysis to the *H*-phosphonate **24** and silylation followed by oxidation to the corresponding phosphate. Attempts to obtain **RBM2-47** by either *N*-acylation of **RBM2-35** or selective C1-OH phosphorylation of **RBM2-37** with dimethyl chlorophosphate proved unsatisfactory.

- Azido probes **RBM2-31**, **RBM2-37**, **RBM2-40** and **RBM2-63** were selected to examine their effect on the sphingolipidome on cancer A549 and HGC-27 cell lines. The above azido probes did not show any relevant variations on the sphingolipidomes of both cell lines. Furthermore, **RBM2-31** and **RBM2-37** showed metabolization to ω-azidoceramides and ω-azidosphingomyelins, while **RBM2-40** and **RBM2-63** were metabolized to ω-azidoceramides, ω-azidodihydroceramides, ω-azidosphingomyelins and ω-azidodihydrosphingomyelins after different incubation times. Several *N*-acyl chains of different lengths and unsaturations were also detected in all ω-azido metabolites. These results revealed the suitability of these ω-azido SLs as chemical probes to study SL metabolism.

- A series of five homologous azadibenzocyclooctyne tags have been synthesized and tested in the SPAAC reaction with the azido probe **RBM2-37** at low concentrations (~0.2 μM). The resulting click adducts were formed in quantitative yields and were detected by UPLC-TOF with a sensitivity around 8-fold higher than that of the parent azide **RBM2-37**. These results allowed the development of a SPAAC-based methodology for the labeling of cell extracts containing ω-azido SL metabolites for their detection by UPLC-TOF analysis.

- A new fluorescent dye (**D1**), consisting of a strained azadibenzocyclooctyne linked to fluorescein, has been prepared. This new dye was able to internalize into the two cancer cell lines used in the study (A549 and MCF-7 cells). Moreover, the efficiency of the SPAAC reaction between **D1** and the ω-azidodihydroceramide probe **RBM2-87**, which was taken as a model, was evaluated in both organic solvent and culture media to establish the optimum reaction parameters.

- A methodology for the labeling of live cells containing ω-azido SL metabolites with the fluorescent probe **D1** has been developed. Labeling of live cells containing ω-azido SL metabolites with dye **D1** was examined in A549 and MCF-7 cells at different times. The best results showed between 12 and 17-fold fluorescence enhancements in comparison with control experiments. In addition, the SPAAC reaction could be evidenced by confocal laser scanning microscopy, showing a strong fluorescence associated to membranes.

- Sphingolipid probes **RBM2-77** and **RBM2-79** were incorporated in GUVs (10%) and next labeled by CuAAC reaction with the fluorogenic naphtalamide **46**. The resulting fluorescent click adducts **47** and **48** were visualized by confocal laser microscopy (450-500 nm) in the presence of Cu(I). Furthermore, the formation of these click adducts was also confirmed by UPLC-TOF after their extraction from GUVs.

# 5. Experimental Section

## 5.1 Synthesis and product characterization

### 5.1.1 Chemistry: general methods

All chemicals were purchased from Aldrich® or Fluka® and used as received unless otherwise noted. Starting material **41** was purchased from Click Chemistry Tools®.

Most of the reactions were performed under argon atmosphere, and the anhydrous solvents were prepared as follows: $Et_2O$ and THF by distillation at atmospheric pressure over sodium and benzophenone under $N_2$ atmosphere; MeOH, $CH_2Cl_2$, $CH_3CN$ and $Et_3N$ by distillation at atmospheric pressure over calcium hydride under $N_2$ atmosphere; DMF by distillation under reduced pressure over calcium hydride, and stored over 4Å molecular sieves and argon atmosphere. Molecular sieves were previously dried in a dry flask, heated to 120 °C under high vacuum for 5 h, and refilled with argon.

Progression of the the reactions was monitored by thin layer chromatographic (TLC) analysis, using $SiO_2$ ALUGRAM® SIL G/$UV_{254}$ aluminum sheets (0.2 mm-thickness). Compounds were detected by using ultraviolet light ($\lambda$=254 nm) and the following staining solutions: ninhydrin (0.1% in EtOH), phosphomolibdic acid (5.7% in EtOH), and anisaldehyde (2% in EtOH, with 2% sulfuric acid).

Compounds were purified by flash column chromatography, using silica gel 60 Å (35-75 μm) Chromagel as stationary phase, unless otherwise noted.

NMR spectra were recorded in $CDCl_3$ or $CD_3OD$ as solvents. $^1H$ and $^{13}C$ chemical shifts of deuterated solvents were used as internal standards. NMR spectra were recorded on the following spectrometers:

- Varian Unity-300 ($^{31}P$ NMR at 121.4 MHz, $^1H$ NMR at 300 MHz and $^{13}C$ NMR at 75 MHz)
- Bruker-400 ($^{31}P$ NMR at 162 MHz, $^1H$ NMR at 400 MHz, $^{13}C$ NMR at 100.6 MHz and bidimensional spectra)
- Inova-500 ($^1H$ NMR at 500 MHz and $^{13}C$ NMR at 126 MHz)

Chemical shifts are given in parts per million (ppm) and coupling constants (*J*) in Hertz (Hz). Splitting patterns have been described as singlet (s), broad singlet (brs), doublet (d), triplet (t), quartet (q), quintuplet (quint), sextuplet (sext), multiplet (m) or combinations of these descriptive names.

Specific optical rotations were determined on a digital Perkin-Elmer 34 at 25 °C in 1-dm 1-mL cell, using a sodium light lamp (λ=589 nm). Specific optical rotations ($[\alpha]_D$) are expressed in $10^{-1}$ deg $cm^3$ $g^{-1}$, and concentrations (*c*) are reported in g/100 mL of solvent.

High-resolution mass spectra were recorded on a Waters Micromass LCT Premier apparatus equipped with a dual electrospray (ESI) LockSpray ion source. Data were acquired in positive ESI. Samples were analyzed by FIA (Flow Injection Analysis), using ACN/water (70:30) as mobile phase. Samples were analyzed using a 10 μL volume injection.

### 5.1.2 Synthesis of chiral aldehyde 4

**(*S*)-2-((*tert*-Butoxycarbonyl)amino)-3-hydroxypropanoic acid (1)**

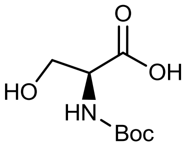

To a solution of *L*-serine (5.0 g, 47.51 mmol) in aqueous 1 *N* NaOH (100 mL) was added a solution of $Boc_2O$ (12.3 g, 56.32 mmol) in dioxane at 0 °C. After vigorous stirrring at this temperature for 30 min, the reaction mixture was allowed to warm to rt and stirred overnight. Next, the reaction mixture was concentrated under reduced pressure to half volume and acidified to pH = 2 by addition of aqueous 1 *N* HCl. The aqueous phase was extracted with EtOAc (3 x 100 mL). The combined organic layers were dried over $MgSO_4$, filtered, and evaporated *in vacuo*. Compound **1** (9.7 g, 47.5 mmol, quantitative) was obtained as a white solid, which was used without further purification. The physical and spectroscopic data of compound **1** were identical to those reported in the literature.[1]

$^1$H NMR (δ, 400 MHz, $CDCl_3$): 1.47 (s, 9H), 3.82-3.92 (m, 1H), 3.95-4.23 (m, 2H), 4.36 (brs, 1H), 5.59 (brs, 1H).

### (*S*)-*tert*-Butyl (3-hydroxy-1-(methoxy(methyl)amino)-1-oxopropan-2-yl)carbamate (2)

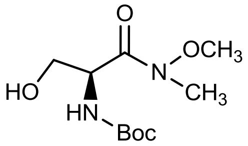

A solution of compound **1** (8.1 g, 39.77 mmol) in anhydrous $CH_2Cl_2$ (70 mL) was treated successively with *N*,*O*-DMHA (4.0 g, 40.56 mmol), and NMM (4.5 mL, 40.56 mmol) at -15 °C under argon atmosphere. To the resulting mixture EDC (7.8 g, 40.56 mmol) was slowly added. After vigorous stirrring at -15 °C for 2 h, the reaction mixture was quenched with aqueous 1 *N* HCl (50 mL). The aqueous phase was extracted with $CH_2Cl_2$ (3 x 70 mL). The combined organic layers were washed with brine, dried over $MgSO_4$, and filtered. Evaporation under reduced pressure afforded compound **2** (9.3 g, 37.48 mmol, 94%) as a white solid, which was used without further purification. The physical and spectroscopic data of compound **2** were identical to those reported in the literature.[2-3]

$^1$H NMR (δ, 300 MHz, $CDCl_3$): 1.45 (s, 9H), 3.23 (s, 3H), 3.78 (s, 3H), 3.80-3.85 (m, 2H), 4.80 (brs, 1H), 5.58 (d, *J*=5.7 Hz, 1H).

### (*S*)-*tert*-Butyl 4-(methoxy(methyl)carbamoyl)-2,2-dimethyloxazolidine-3-carboxylate (3)

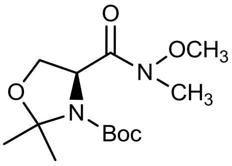

To a solution of Weinreb's amide **2** (8.5 g, 34.10 mmol) in DMP/acetone (25:75 mL) was added dropwise $BF_3 \cdot OEt_2$ (240 μL, 1.33 mmol). The resulting red solution was next vigorously stirred at rt for 2 h and quenched next with $Et_3N$ (500 μL) to give a colorless solution. The crude reaction mixture was concentrated *in vacuo* and purified by flash chromatography (7:3 hexane/EtOAc) to afford compound **3** (9.8 g, quantitative) as a pale yellow oil. The physical and spectroscopic data of compound **3** were identical to those reported in the literature.[2-3]

$^1$H NMR (δ, 500 MHz, $CDCl_3$) (mixture of rotamers): 1.41 (s, 4.5H), 1.50 (s, 4.5H), 1.52 (s, 1.5H), 1.57 (s, 1.5H), 1.68 (s, 1.5H), 1.71 (s, 1.5H), 3.21 (s, 3H), 3.70 (s, 1.5H), 3.75 (s, 1.5H), 3.93 (dd, *J*=9.0, 4.0 Hz, 0.5H), 3.97 (dd, *J*=9.5, 3.0 Hz, 0.5H), 4.15-4.22 (m, 1H), 4.72 (dd, *J*=7.5, 3.5 Hz, 0.5H), 4.80 (dd, *J*=7.0, 3.0 Hz, 0.5H).

### (*S*)-*tert*-Butyl 4-formyl-2,2-dimethyloxazolidine-3-carboxylate (4)

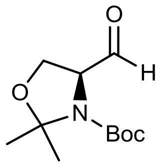

To a solution of $LiAlH_4$ (1.0 g, 26.0 mmol) in dry THF (20 mL) was added dropwise a solution of **3** (7.5, 26.0 mmol) in dry THF (30 mL) under argon atmosphere at 0 °C. After stirring for 1.5 h at rt, the reaction mixture was cooled down to -15 °C, and quenched by dropwise addition of aqueous saturated $NaHCO_3$. After stirring for 30 min, the resulting white solid was taken up in water (10 mL), and the aqueous phase was extracted with $Et_2O$ (2 x 20 mL). The combined organic layers were successively washed with 2 x 20 mL aqueous 0.5 *N* HCl and brine, dried over $MgSO_4$, and filtered. Concentration under reduced pressure and purification by flash chromatography (8:2 hexane/EtOAc) of the resulting residue yielded compound **4** (4.2 g, 18.46 mmol, 71%) as a colorless oil. The physical and spectroscopic data of compound **4** were identical to those reported in the literature.[1]

$[\alpha]_D$ -98.3 (*c* 1.6, $CHCl_3$); lit[1] $[\alpha]_D$ -91.7 (*c* 1.34, $CHCl_3$); $^1H$ NMR (δ, 500 MHz, $CDCl_3$) (mixture of rotamers): 1.43 (s, 4.5H), 1.47 (s, 4.5H), 1.56 (s, 3H), 1.60 (s, 1.5H), 1.65 (s, 1.5H), 4.03-4.16 (m, 2H), 4.17-4.22 (m, 0.5H), 4.32-4.37 (m, 0.5H), 9.55 (d, *J*=2.5 Hz, 0.5H), 9.61 (brs, 0.5H).

### 5.1.3 Synthesis of synthon 7

**(*S*)-*tert*-Butyl 4-((*R*)-1-hydroxy-3-(trimethylsilyl)prop-2-yn-1-yl)-2,2-dimethyloxazolidine-3-carboxylate (5)**

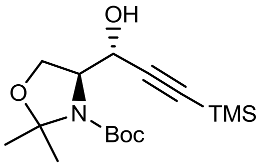

To a solution of ethynyltrimethylsilane (2.0 mL, 14.15 mmol) in dry THF (20 mL) was added dropwise *n*BuLi (6.9 mL, 17.16 mmol, 2.5 M in hexanes) at -78 °C under argon atmosphere. After vigorous stirring at -78 °C for 1 h, was added HMPA (2.8 mL, 16.09 mmol), followed by a solution of aldehyde **4** (2.0 g, 8.72 mmol) in dry THF (8 mL). After stirred at -78 °C for 2 h, the reaction mixture was quenched with dropwise addition of aqueous saturated $NH_4Cl$, and next allowed to warm to rt. The resulting white residue was taken up in water, and the aqueous phase was extracted with $Et_2O$ (3 x 20 mL). The combined organic layers were washed successively with 0.5 *N* HCl and brine, filtered, and dried over $MgSO_4$. Solvent was removed *in vacuo*, and the resulting residue was purified by flash chromatography (6:0 to 5:1 hexane/EtOAc gradient) to afford compound **5** (2.09 g, 6.37 mmol, 73%) as a colorless oil. The physical and spectroscopic data of compound **5** were identical to those reported in the literature.[4]

$^1$H NMR (δ, 400 MHz, $CDCl_3$): 0.16 (s, 9H), 1.50 (s, 9H), 1.52 (s, 3H), 1.59 (brs, 3H), 3.81-3.89 (m, 1H), 4.06-4.20 (m, 2H), 4.46 (d, *J*=6.0 Hz, 1H).

**(*S*)-*tert*-Butyl 4-((*R*)-1-hydroxyprop-2-yn-1-yl)-2,2-dimethyloxazolidine-3-carboxylate (6)**

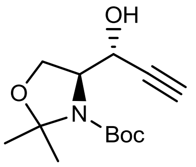

To a solution of compound **5** (2.09 g, 6.37 mmol) in MeOH (80 mL) was added solid $K_2CO_3$ (10.0 g, 72.36 mmol). After vigorous stirring at rt for 3 h, the reaction mixture was concentrated *in vacuo*. The resulting residue was taken up in water (25 mL), and the aqueous phase was extracted with EtOAc (3 x 30 mL). The combined organic layers were dried over $MgSO_4$, and filtered. Concentration under reduced pressure afforded compound

**6** (1.51 g, 5.92 mmol, 93%) as a yellow oil, which was used without further purification. The physical and spectroscopic data of compound **6** were identical to those reported in the literature.[4]

$^1$H NMR (δ, 400 MHz, $CDCl_3$): 1.50 (s, 9H), 1.57 (s, 3H), 1.61 (s, 3H), 3.85-3.95 (m, 1H), 4.05-4.23 (m, 3H), 4.47-4.57 (m, 1H), 5.04 (d, *J*=6.8 Hz, 1H).

### (*S*)-*tert*-Butyl 4-((*R*)-1-hydroxyallyl)-2,2-dimethyloxazolidine-3-carboxylate (7)

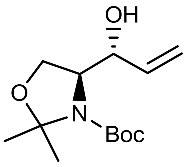

To a solution of compound **6** (1.51 g, 5.92 mmol) and quinoline (11 μL, 5% weight in relation to the catalyst) in previously degassed EtOAc (80 mL), Lindlar catalyst (226 mg, 15% weight) was added. The resulting mixture was vigorously stirred at rt for 2 h under $H_2$ atmosphere (1 atm). The reaction mixture was next filtered through a plug of Celite, and the solid washed with 3 x 5 mL EtOAc. The filtrate and the combined washings were concentrated *in vacuo* to afford **7** (1.52 g, 5.92 mmol, quantitative) as a colorless oil, which was used without further purification. The physical and spectroscopic data of compound **7** were identical to those reported in the literature.[4]

$[\alpha]_D$ -22.0 (*c* 1.2, $CHCl_3$); lit[4] $[\alpha]_D$ -19.1 (*c* 0.8, $CHCl_3$); $^1$H NMR (δ, 500 MHz, $CDCl_3$): 1.48 (brs, 15H), 1.58 (brs, 1H), 3.80-4.31 (m, 3H), 5.22 (d, *J*=10.5 Hz, 1H), 5.38 (d, *J*=17.0 Hz, 1H), 5.80-5.91 (m, 1H).

### 5.1.4 Synthesis of sphingosine RBM2-31 and ceramides RBM2-32, RBM2-37, RBM2-46 and RBM2-77

**General procedure 1: synthesis of azides by $SN_2$ nucleophilic displacement**

To a two necked round bottom flask fitted with a reflux condenser was added a solution of the starting bromide, mesylate or tosylate (1.00 mmol) in anhydrous DMF (20 mL). To the resulting solution, $NaN_3$ (4.00 mmol) was added portionwise under argon atmosphere, and the resulting mixture was vigorously stirred at 80 °C overnight. After cooling down to rt, the reaction mixture was quenched by addition of water (100 mL), and the aqueous phase was extracted with $Et_2O$ (3 x 50 mL). The combined organic phases were dried over $MgSO_4$, filtered and evaporated *in vacuo* to give a crude mixture, which was purified as indicated below.

**11-Azidoundec-1-ene (8)**

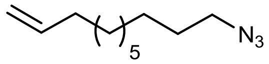

512 mg (2.62 mmol, 88%) of compound **8** were obtained, as a colorless oil, from mesylate **10** (740 mg, 2.98 mmol), and $NaN_3$ (775 mg, 11.92 mmol) in DMF (40 mL), according to *general procedure 1*. Purification was carried out by flash chromatography (hexane).

$^1H$ NMR (δ, 400 MHz, $CDCl_3$): 1.24-1.43 (m, 12H), 1.54-1.65 (m, 2H), 2.00-2.08 (m, 2H), 3.25 (t, *J*=7.0 Hz, 2H), 4.90-5.04 (m, 2H), 5.75-5.88 (m, 1H); $^{13}C$ NMR (δ, 101 MHz, $CDCl_3$): 26.9, 28.9, 29.0, 29.2, 29.3, 29.5, 29.6, 33.9, 51.62, 114.3, 139.3. HRMS calculated for $C_{11}H_{21}N_3Na$: 218.1633 $[M+Na]^+$. Found: 218.1630.

**Undec-10-en-1-yl methanesulfonate (10)**

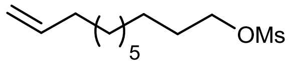

To a solution of commercially available 10-undec-1-ol (**9**) (600 μL, 2.98 mmol) in dry $CH_2Cl_2$ (25 mL), neat $Et_3N$ (620 μL, 4.47 mmol) was added at 0 °C. The resulting mixture was vigorously stirred for 10 min, followed by dropwise addition of neat MsCl (330 μL, 4.47 mmol). After stirring at 0 °C for 2 h, the reaction mixture was diluted by addition of

$CH_2Cl_2$ (10 mL). The organic layer was successively washed with 0.5 *N* HCl (15 mL), aqueous sat. $NaHCO_3$ (15 mL), and brine (15 mL), dried over $MgSO_4$ and filtered. Concentration under reduced pressure afforded 740 mg (2.98 mmol, quantitative) of compound **10**, as a yellow pale oil. This compound was used without further purification.

$^1H$ NMR (δ, 400 MHz, $CDCl_3$): 1.23-1.44 (m, 12H), 1.74 (quint, *J*=8.0 Hz, 2H), 2.03 (q, *J*=7.6 Hz, 2H), 3.00 (s, 3H), 4.22 (t, *J*=6.6 Hz, 2H), 4.90-5.03 (m, 2H), 5.75-5.88 (m, 1H). $^{13}C$ NMR (δ, 101 MHz, $CDCl_3$): 25.5, 29.02, 29.1, 29.2, 29.3, 29.4, 29.5, 33.9, 37.5, 70.3, 114.3, 139.3. HRMS calculated for $C_{12}H_{24}NaO_3S$: 271.1344 $[M+Na]^+$. Found: 271.1347.

### 11-Bromoundec-1-ene (11)

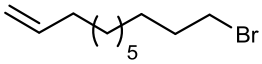

To a solution of mesylate **10** (500 mg, 2.01 mmol) in acetone (60 mL) solid LiBr (373 mg, 4.30 mmol) was added portionwise. After vigorous stirring at 55 °C overnight, the reaction mixture was allowed to cool down to rt. After concentration under reduced pressure, the resulting residue was purified by flash chromatography (hexane) to afford 390 mg (1.67 mmol, 83%) of compound **11**, as a colorless oil.

$^1H$ NMR (δ, 400 MHz, $CDCl_3$): 1.24-1.48 (m, 12H), 1.85 (quint, *J*=7.6 Hz, 2H), 2.04 (q, *J*=7.2 Hz, 2H), 3.41 (t, *J*=6.9 Hz, 2H), 4.90-5.04 (m, 2H), 5.74-5.87 (m, 1H); $^{13}C$ NMR (δ, 101 MHz, $CDCl_3$): 28.3, 28.9, 29.1, 29.2, 29.5, 33.0, 33.9, 34.2, 114.3, 139.3. HRMS calculated for $C_{11}H_{21}BrNa$: 255.0724 $[M+Na]^+$. Found: 255.0730.

### General procedure 2: olefin cross metathesis reactions

A two necked round bottom flask fitted with a reflux condenser under argon atmosphere, was charged with solutions of the starting olefins (1.00 or 4.00 mmol) in previously degassed $CH_2Cl_2$ (10 mL). Next, Grubb's 2nd generation catalyst (14% weight in relation to the limiting reagent) was added portionwise, and the resulting mixture was stirred at reflux temperature for 5 h. The mixture was next allowed to cool down to rt and concentrated *in vacuo* to afford a crude, which was purified as indicated below.

### (*S*)-*tert*-Butyl 4-((*R,E*)-12-bromo-1-hydroxydodec-2-en-1-yl)-2,2-dimethyloxazolidine-3-carboxylate (12)

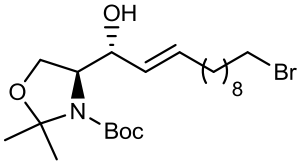

770 mg (1.66 mmol, 59%) of compound **12** were obtained, as a colorless oil, from alkene **7** (730 mg, 2.80 mmol), bromide **11** (2.6 g, 11.20 mmol) and Grubb's 2nd generation catalyst (102 mg) in $CH_2Cl_2$ (20 mL), according to *general procedure 2.* The compound was purified by flash chromatography (10:0 to 7:3 hexane/EtOAc gradient).

$[\alpha]_D$ -26.3 (*c* 1.0, $CHCl_3$); $^1H$ NMR (δ, 400 MHz, $CDCl_3$) (major rotamer): 1.27 (brs, 9H), 1.33-1.55 (m, 18H), 1.85 (quint, *J*=6.8 Hz, 2H), 2.04 (q, *J*=6.8 Hz, 2H), 3.41 (t, *J*=6.9 Hz, 2H), 3.77-4.23 (m, 4H), 5.44 (dd, *J*=15.2, 6.0 Hz, 1H), 5.72 (dt, *J*=14.5, 7.2 Hz, 1H); $^{13}C$ NMR (δ, 101 MHz, $CDCl_3$) (major rotamer): 24.7, 26.4, 28.2, 28.4, 28.5, 28.8, 28.9, 29.0, 29.2, 29.3, 29.4, 29.5, 32.5, 32.9, 34.2, 62.4, 65.0, 74.2, 81.1, 94.5, 98.7, 128.3, 133.4, 154.3. HRMS calculated for $C_{22}H_{40}NNaO_4$: 484.2038 $[M+Na]^+$. Found: 484.2037.

### (*S*)-*tert*-Butyl 4-((*R,E*)-12-azido-1-hydroxydodec-2-en-1-yl)-2,2-dimethyloxazolidine-3-carboxylate (13)

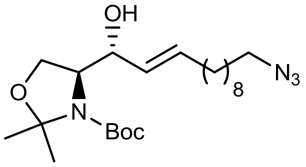

470 mg (1.11 mmol, 93%) of azide **13** were obtained, as a colorless oil, from bromide **12** (550 mg, 1.19 mmol) and $NaN_3$ (311 mg, 4.78 mmol) in DMF (20 mL), according to the *general procedure 1*. The compound was purified by flash chromatography (10:0 to 8:2 hexane/EtOAc gradient).

$[\alpha]_D$ -30.9 (*c* 0.9, $CHCl_3$); $^1H$ NMR (δ, 400 MHz, $CDCl_3$) (major rotamer): 1.24-1.41 (m, 11H), 1.45-1.63 (m, 16H), 2.04 (q, *J*=6.8 Hz, 2H), 3.25 (t, *J*=7.0 Hz, 2H), 3.76-4.22 (m, 4H), 5.44 (dd, *J*=15.2, 5.2 Hz, 1H), 5.73 (dt, *J*=15.2, 7.2 Hz, 1H); $^{13}C$ NMR (δ, 101 MHz, $CDCl_3$) (major rotamer): 24.7, 26.4, 26.8, 28.5, 29.0, 29.2, 29.3, 29.3, 29.4, 29.5, 29.6, 32.5, 51.6, 62.4, 65.1, 74.3, 81.2, 94.6, 128.3, 133.5. HRMS calculated for $C_{22}H_{40}N_4NaO_4$: 447.2947 [M+Na]$^+$. Found: 447.2960.

### General procedure 3: "one pot" deprotection of oxazolidine and *N*-Boc protecting groups

To a solution of the corresponding protected aminodiols (1.00 mmol) in MeOH (16 mL) was added neat acetyl chloride (960 μL, 6%). The resulting mixture was vigorously stirred at rt for 1 h. Concentration under reduced pressure afforded crude compounds, which were purified as indicated below.

### (2*S*,3*R*,*E*)-2-Amino-14-azidotetradec-4-ene-1,3-diol (RBM2-31)

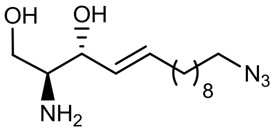

190 mg (0.67 mmol, 84%) of aminodiol **RBM2-31** were obtained, as a waxy white solid, from **9** (335 mg, 0.80 mmol), and acetyl chloride (900 μL) in MeOH (15 mL), according to *general procedure 3*. Purification was carried out by flash chromatography (9:0.9:0.1 $CH_2Cl_2$/MeOH/$NH_3$).

$[\alpha]_D$ -1.2 (*c* 0.5, $CHCl_3$); $^1$H NMR (δ, 400 MHz, $CDCl_3$): 1.22-1.41 (m, 12H), 1.58 (quint, *J*=7.2 Hz, 2H), 2.05 (q, *J*=8.0 Hz, 2H), 2.77 (brs, 5H), 3.24 (t, *J*=6.9 Hz, 2H), 3.64 (d, *J*=4.8 Hz, 2H), 4.03 (t, *J*=6.2 Hz, 1H), 5.44 (dd, *J*=15.4, 7.1 Hz, 1H), 5.72 (dt, *J*=15.6, 6.8 Hz, 1H). $^{13}$C NMR (δ, 101 MHz, $CDCl_3$): 26.8, 28.9, 29.2, 29.3, 29.3-29.5 (m), 32.5, 51.6, 56.3, 63.8, 75.2, 129.4, 134.6. HRMS calculated for $C_{14}H_{29}N_4O_2$: 285.2291 [M+H]$^+$. Found: 285.2274.

### General procedure 4: *N*-acylation reactions

To a solution of EDC (1.62 mmol) and HOBt (1.19 mmol) in anhydrous $CH_2Cl_2$ (5 mL) was added the corresponding carboxylic acid (1.08 mmol) under argon atmosphere. The resulting mixture was vigorously stirred at rt for 10 min, and next added dropwise to a solution of the corresponding deprotected aminodiol (1.00 mmol) and $Et_3N$ (3.90 mmol) in anhydrous $CH_2Cl_2$ (5 mL). The reaction mixture was stirred at rt for 1 h under argon atmosphere. The mixture was next diluted by addition of $CH_2Cl_2$ (20 mL), and washed successively with water (20 mL) and brine (20 mL). The organic layer was dried over $MgSO_4$, and filtered. Concentration under reduced pressure afforded crude compounds, which were purified as indicated below.

### ***N*-((2*S*,3*R*,*E*)-14-Azido-1,3-dihydorxytetradec-4-en-2-yl)-2-bromoacetamide (RBM2-32)**

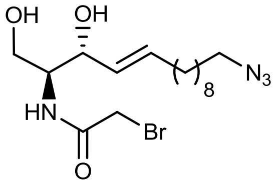

27 mg (0.07 mmol, 22%) of ceramide **RBM2-32** were obtained, as a white waxy solid, from aminodiol **RBM2-31** (90 mg, 0.32 mmol), $Et_3N$ (174 μL, 1.25 mmol), bromoacetic acid (49 mg, 0.35 mmol), HOBt (51 mg, 0.38 mmol), and EDC (100 mg, 0.52 mmol) in $CH_2Cl_2$ (4 mL), according to *general procedure 4*. The compound was purified by flash chromatography (10:0 to 4:6 hexane/EtOAc gradient, followed by 100:0 to 96:4 $CH_2Cl_2$/MeOH gradient).

$[\alpha]_D$ +2.7 (*c* 1.1, $CHCl_3$); $^1H$ NMR (δ, 400 MHz, $CDCl_3$): 1.24-1.42 (m, 12H), 1.59 (quint, *J*=7.6 Hz, 2H), 2.07 (q, *J*=7.2 Hz, 2H), 3.25 (t, *J*=6.9 Hz, 2H), 3.73 (dd, *J*=11.2, 3.6 Hz, 1H), 3.93 (dt, *J*=11.6, 3.6 Hz, 1H), 4.01 (dd, *J*=11.5, 3.3 Hz, 1H), 4.09 (s, 2H), 4.36 (t, *J*=5.6 Hz, 1H), 5.54 (dd, *J*=15.4, 6.4 Hz, 1H), 5.81 (dt, *J*=15.2, 7.2 Hz, 1H), 7.31 (d, *J*=7.1 Hz, 1H); $^{13}C$ NMR (δ, 101 MHz, $CDCl_3$): 26.8, 28.9, 29.1, 29.2, 29.3, 29.4, 29.5, 32.4, 42.8, 51.6, 54.8, 62.0, 74.2, 128.6, 134.8, 166.6. HRMS calculated for $C_{16}H_{29}BrN_4NaO_3$: 427.1321 $[M+Na]^+$. Found: 427.1335.

### ***N*-((2*S*,3*R*,*E*)-14-Azido-1,3-dihydroxytetradec-4-en-2-yl)octanamide (RBM2-37)**

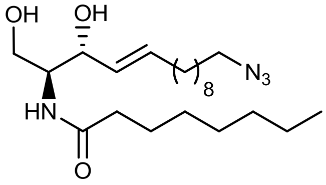

89 mg (0.22 mmol, 59%) of ceramide **RBM2-37** were obtained, as a white waxy solid, from aminodiol **RBM2-31** (105 mg, 0.37 mmol), $Et_3N$ (201 μL, 1.44 mmol), octanoic acid (63 μL, 0.40 mmol), HOBt (59 mg, 0.44 mmol), and EDC (116 mg, 0.60 mmol) in $CH_2Cl_2$ (5

mL), according to *general procedure 4*. The compound was purified by flash chromatography (100:0 to 95:5 $CH_2Cl_2$/MeOH gradient).

$[\alpha]_D$ -3.6 (*c* 1.1, $CHCl_3$); $^1H$ NMR (δ, 400 MHz, $CDCl_3$): 0.87 (t, *J*=7.2 Hz, 3H), 1.21-1.41 (m, 20H), 1.57-1.67 (m, 4H), 2.04 (q, *J*=7.0 Hz, 2H), 2.21 (t, *J*=7.6 Hz, 2H), 2.91 (brs, 2H), 3.25 (t, *J*=7.2 Hz, 2H), 3.68 (dd, *J*=10.8, 2.4 Hz, 1H), 3.85-3.96 (m, 2H), 4.28 (t, *J*=4.4 Hz, 1H), 5.51 (dd, *J* = 15.4, 6.4 Hz, 1H), 5.76 (dt, *J* = 15.6, 6.8 Hz, 1H), 6.35 (d, *J* = 6.5 Hz, 1H); $^{13}C$ NMR (δ, 101 MHz, $CDCl_3$): 22.7, 25.9, 26.8, 28.9, 29.2-29.5 (m), 31.8, 32.4, 36.9, 51.6, 54.7, 62.5, 74.5, 129.0, 134.2, 174.2. HRMS calculated for $C_{22}H_{42}N_4NaO_3$: 433.3155 $[M+Na]^+$. Found: 433.3153.

### ***N*-((2*S*,3*R*,*E*)-14-Azido-1,3-dihydroxytetradec-4-en-2-yl)methacrylamide (RBM2-46)**

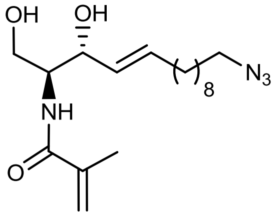

34 mg (0.10 mmol, 77%) of ceramide **RBM2-46** were obtained, as a yellow pale oil, from aminodiol **RBM2-31** (36 mg, 0.13 mmol), $Et_3N$ (71 µL, 0.51 mmol), methacrylic acid (12 µL, 0.14 mmol), HOBt (20 mg, 0.15 mmol), and EDC (41 mg, 0.21 mmol) in $CH_2Cl_2$ (5 mL), according to *general procedure 4*. Purification was carried out by flash chromatography (7:3 hexane/*t*-BuOMe, followed by 100:0 to 95:5 $CH_2Cl_2$/MeOH gradient).

$[\alpha]_D$ -1.2 (*c* 0.8, $CHCl_3$); $^1H$ NMR (δ, 400 MHz, $CDCl_3$): 1.23-1.42 (m, 12H), 1.59 (quint, *J*=7.2 Hz, 2H), 1.98 (s, 3H), 2.06 (q, *J*=7.2 Hz, 2H), ), 2.70 (brs, 2H), 3.26 (t, *J*=6.9 Hz, 2H), 3.74 (dd, *J*=11.1, 3.1 Hz, 1H), 3.91-4.02 (m, 2H), 4.36 (t, *J*=5.2 Hz, 1H), 5.54 (dd, *J*=15.5, 6.4 Hz, 1H), 5.75-5.84 (m, 3H), 6.63 (d, *J*=7.2 Hz, 1H); $^{13}C$ NMR (δ, 101 MHz, $CDCl_3$): 18.7, 26.8, 28.9, 29.2-29.5 (m), 32.4, 51.6, 54.8, 62.4, 74.4, 120.5, 128.9, 134.2, 139.7, 169.0. HRMS calculated for $C_{18}H_{33}N_4O_3$: 353.2553 $[M+H]^+$. Found: 353.2567.

### ***N*-((2*S*,3*R*,*E*)-14-Azido-1,3-dihydroxytetradec-4-en-2-yl)palmitamide (RBM2-77)**

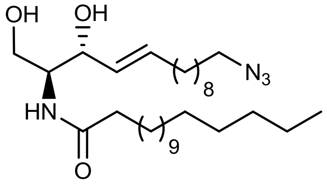

38 mg (0.07 mmol, 36%) of ceramide **RBM2-77** were obtained, as a white waxy solid, from aminodiol **RBM2-31** (56 mg, 0.20 mmol), $Et_3N$ (109 µL, 0.78 mmol), palmitic acid (66 µL, 0.22 mmol), HOBt (32 mg, 0.24 mmol), and EDC (63 mg, 0.32 mmol) in $CH_2Cl_2$ (5 mL), according to *general procedure 4*. Purification was carried outby flash chromatography (7:3 hexane/*t*-BuOMe, followed by 100:0 to 97:3 $CH_2Cl_2$/MeOH gradient).

$[\alpha]_D$ -0.7 (*c* 0.9, $CHCl_3$); $^1H$ NMR (δ, 500 MHz, $CDCl_3$): 0.88 (t, *J*=6.9 Hz, 3H), 1.22-1.41 (m, 36H), 1.55-1.69 (m, 4H), 2.06 (q, *J*=7.0 Hz, 2H), 2.23 (t, *J*=7.5 Hz, 2H), 3.26 (t, *J*=7.0 Hz, 2H), 3.71 (dd, *J*=11.3, 3.2 Hz, 1H), 3.91 (sext, *J*=4.0 Hz, 1H), 3.96 (dd, *J*=11.3, 3.7 Hz, 1H), 4.33 (t, *J*=4.5 Hz, 1H), 5.54 (dd, *J*=15.4, 6.4 Hz, 1H), 5.78 (dt, *J*=16.0, 6.5 Hz, 1H), 6.25 (d, *J*=6.8 Hz, 1H); $^{13}C$ NMR (δ, 101 MHz, $CDCl_3$): 14.3, 22.9, 25.9, 26.9, 29.0, 29.2, 29.3, 29.5 (m), 29.7, 29.8 , 29.8 (m), 29.9, 32.1, 32.4, 37.0, 51.7, 54.7, 62.7, 74.9, 129.1, 134.4, 174.0. HRMS calculated for $C_{30}H_{58}N_4NaO_3$: 545.4407 $[M+Na]^+$. Found: 545.4415.

## 5.1.5 Synthesis of dihydrosphingosine RBM2-40 and dihydroceramides RBM2-44, RBM2-45 and RBM2-87

### General procedure 5: reduction of double and triple bonds by catalytic hydrogenation

Rhodium catalyst (18% weight in relation to the starting material, rhodium on alumina, Sigma Aldrich, ref. 212857) was added to a solution of the starting unsaturated compound (1.00 mmol) in freshly degassed MeOH (30 mL). The resulting mixture was vigorously stirred at rt for 6 h under $H_2$ (1 atm). The mixture was next filtered through a plug of Celite, and the solid was rinsed with MeOH (3 x 10 mL). The combined filtrates were concentrated *in vacuo* to afford a crude, which was purified as indicated below.

### (*S*)-*tert*-Butyl 4-((*R*)-12-bromo-1-hydroxydodecyl)-2-2-dimethyloxazolidine-3-carboxylate (14)

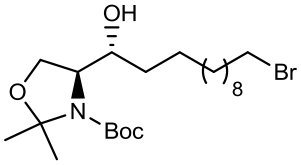

250 mg (0.54 mmol, 77%) of compound **14** were obtained, as a colorless oil, from dienol **12** (322 mg, 0.70 mmol), and rhodium catalyst (58 mg) in MeOH (20 mL), according to *general procedure 5*. Purification was carried out by flash chromatography (8:2 hexane/EtOAc).

[α]$_D$ -7.3 (*c* 1.0, $CHCl_3$); $^1$H NMR (δ, 400 MHz, $CDCl_3$) (mixture of rotamers): 1.22-1.43 (m, 16H), 1.45-1.62 (m, 15H), 1.85 (quint, *J*=7.6 Hz, 2H), 3.40 (t, *J*=6.9 Hz, 2H), 3.65-4.13 (m, 4H); $^{13}$C NMR (δ, 101 MHz, $CDCl_3$) (mixture of rotamers): 26.2, 26.6, 28.3, 28.5, 28.6, 28.9, 29.5, 29.6, 29.7, 29.8, 32.8, 33.0, 34.0, 34.6, 50.04, 55.1, 62.3, 62.8, 63.7, 64.6, 72.9, 74.4, 79.7, 80.9, 94.4, 98.9, 155.4. HRMS calculated for $C_{22}H_{42}BrNNaO_4$: 486.2195 [M+Na]$^+$. Found: 486.2190.

### (*S*)-*tert*-Butyl 4-((*R*)-12-azido-1-hydroxydodecyl)-2,2-dimethyloxazolidine-3-carboxylate (15)

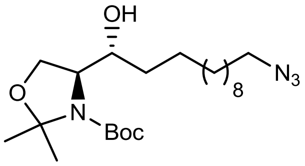

137 mg (0.32 mmol, 78%) of azide **15** were obtained, as a colorless oil, from bromide **14** (190 mg, 0.41 mmol), and $NaN_3$ (101 mg, 1.64 mmol) in DMF (10 mL), according to *general procedure 1*. When using tosylate **28** (110 mg, 0.20 mmol) as starting material and $NaN_3$ (52 mg, 0.80 mmol) in DMF (10 mL), 65 mg (0.15 mmol, 76%) of azide **15** were obtained. Purification was carried out by flash chromatography (8:2 hexane/EtOAc).

[α]$_D$ -2.6 (*c* 0.9, $CHCl_3$); $^1$H NMR (δ, 400 MHz, $CDCl_3$) (major rotamer): 1.23-1.40 (m, 17H), 1.49 (brs, 12H), 1.54-1.63 (m, 6H), 3.25 (t, *J*=7.0 Hz, 2H), 3.67-4.14 (m, 4H); $^{13}$C NMR (δ, 101 MHz, $CDCl_3$) (major rotamer): 26.2, 26.5, 26.8, 28.4, 28.5, 29.8, 29.2, 29.5, 29.6 (m), 29.8, 32.9, 51.5, 62.5, 64.8, 73.0, 81.1, 94.3, 154.1. HRMS calculated for $C_{22}H_{43}N_4O_4$: 427.3284 $[M+H]^+$. Found: 427.3293.

### (2*S*,3*R*)-2-Amino-14-azidotetradecane-1,3-diol (RBM2-40)

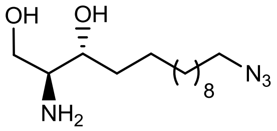

79 mg (0.27 mmol, 85%) of aminodiol **RBM2-40** were obtained, as a waxy solid, from **15** (137 mg, 0.32 mmol), and acetyl chloride (600 μL) in MeOH (10 mL), according to *general procedure 3*. Purification was carried out by flash chromatography (8:1.9:0.1 $CH_2Cl_2$/MeOH/$NH_3$).

$[\alpha]_D$ +3.9 (*c* 0.9, $CHCl_3$); $^1H$ NMR (δ, 400 MHz, $CDCl_3$): 1.24-1.40 (m, 16H); 1.43-1.52 (m, 2H), 1.59 (quint, *J*=7.6 Hz, 2H), 2.33 (brs, 4H), 2.83 (brs, 1H), 3.25 (t, *J*=7.0 Hz, 1H), 3.56-3.64 (m, 1H), 3.70 (d, *J*=4.8 Hz, 2H); $^{13}C$ NMR (δ, 101 MHz, $CDCl_3$): 26.2, 26.8, 28.9, 29.3, 29.6 (m), 29.7 (m), 29.8, 34.0, 51.6, 55.8, 63.5, 74.6. HRMS calculated for $C_{14}H_{31}N_4O_2$: 287.2447 $[M+H]^+$. Found: 287.2442.

### *N*-((2*S*,3*R*)-14-Azido-1,3-dihydroxytetradecan-2-yl)methacrylamide (RBM2-44)

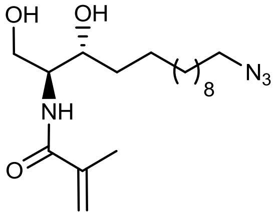

38 mg (0.11 mmol, 65%) of ceramide **RBM2-44** were obtained, as a yellow pale oil, from **RBM2-40** (48 mg, 0.17 mmol), $Et_3N$ (92 μL, 0.66 mmol), methacrylic acid (15 μL, 0.18 mmol), HOBt (27 mg, 0.20 mmol), and EDC (53 mg, 0.28 mmol) in $CH_2Cl_2$ (5 mL), according to *general procedure 4*. Purification was carried out by flash chromatography (100:0 to 96:4 $CH_2Cl_2$/MeOH gradient).

$[\alpha]_D$ +11.2 (*c* 1.0, $CHCl_3$); $^1H$ NMR (δ, 400 MHz, $CDCl_3$): 1.22-1.41 (m, 16H); 1.50-1.65 (m, 4H), 1.99 (s, 3H), 2.48 (brs, 2H), 3.26 (t, *J*=6.9 Hz, 2H), 3.72-3.92 (m, 3H), 4.05 (dd, *J*=11.4, 3.2 Hz, 1H), 5.38 (s, 1H), 5.77 (s, 1H), 6.76 (d, *J*=7.5 Hz, 1H); $^{13}$C NMR (δ, 101 MHz, CDCl$_3$): 18.7, 26.1, 26.8, 28.9, 29.4, 29.6, 29.60, 29.6, 29.6, 29.7, 34.6, 51.6, 54.0, 62.3, 74.0, 120.5, 139.7, 168.8. HRMS calculated for $C_{18}H_{35}N_4O_3$: 355.2709 [M+H]$^+$. Found: 355.2708.

### ***N*-((2*S*,3*R*)-14-Azido-1,3-dihydroxytetradecan-2-yl)-2-bromoacetamide (RBM2-45)**

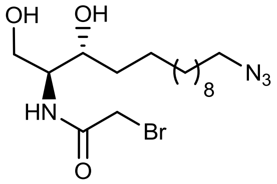

5 mg (0.01 mmol, 8%) of ceramide **RBM2-45** were obtained, as a white waxy solid, from aminodiol **RBM2-40** (71 mg, 0.12 mmol), Et$_3$N (65 µL, 0.45 mmol), bromoacetic acid (18 mg, 0.13 mmol), HOBt (19 mg, 0.14 mmol), and EDC (38 mg, 0.19 mmol) in CH$_2$Cl$_2$ (4 mL), according to *general procedure 4*. Purification was carried out by flash chromatography (10:0 to 4:6 hexane/EtOAc gradient, followed by 100:0 to 97:3 CH$_2$Cl$_2$/MeOH gradient).

[α]$_D$ +3.5 (*c* 0.5, CHCl$_3$); $^1$H NMR (δ, 500 MHz, CDCl$_3$): 1.24-1.37 (m, 16H), 1.55-1.62 (m, 4H), 2.36-2.48 (m, 2H), 3.26 (t, *J*=7.0 Hz, 2H), 3.46-3.89 (m, 3H), 4.05-4.15 (m, 3H), 7.43 (d, *J*=7.5 Hz, 1H); $^{13}$C NMR (δ, 101 MHz, CDCl$_3$): 29.0, 29.3, 29.6 (m), 34.7, 42.8, 51.6, 53.9, 54.0, 62.2, 74.2, 166.3. HRMS calculated for $C_{16}H_{31}BrN_4NaO_3$: 429.1477 [M+Na]$^+$. Found: 429.1490.

### ***N*-((2*S*,3*R*)-14-Azido-1,3-dihydroxytetradecan-2-yl)palmitamide (RBM2-87)**

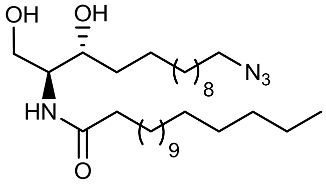

65 mg (0.12 mmol, 62%) of ceramide **RBM2-87** were obtained, as a white waxy solid, from **RBM2-40** (57 mg, 0.20 mmol), Et$_3$N (109 µL, 0.78 mmol), palmitic acid (66 µL, 0.22 mmol), HOBt (32 mg, 0.24 mmol), and EDC (63 mg, 0.32 mmol) in CH$_2$Cl$_2$ (5 mL), according to *general procedure 4*. Purification was carried out by flash chromatography (7:3 hexane/*t*-BuOMe, followed by 100:0 to 97:3 CH$_2$Cl$_2$/MeOH gradient).

[α]$_D$ +7.1 (*c* 0.9, $CHCl_3$); $^1$H NMR (δ, 500 MHz, $CDCl_3$): 0.88 (t, *J*=7.0 Hz, 3H), 1.21-1.38 (m, 40H), 1.48-1.69 (m, 6H), 2.23 (t, *J*=7.5 Hz, 2H), 3.25 (t, *J*=7.0 Hz, 2H), 3.74-3.81 (m, 2H), 3.83 (hexaplet, *J*=4.0 Hz, 1H), 4.02 (dd, *J*= 11.3, 3.4 Hz, 1H), 6.35 (d, *J*=8.1 Hz, 1H); $^{13}$C NMR (δ, 101 MHz, $CDCl_3$): 14.2, 22.8, 25.9, 26.1, 26.9, 29.0, 29.3, 29.5 (m), 29.6 (m), 29.7 (m), 29.8 (m), 32.1, 34.7, 37.0, 51.6, 54.0, 62.6, 74.3, 173.8. HRMS calculated for $C_{30}H_{60}N_4NaO_3$: 547.4563 [M+Na]$^+$. Found: 547.4572.

## 5.1.6 Synthesis of phosphorylated derivatives RBM2-35, RBM2-43, and RBM2-47

### General procedure 6: partial deprotection of oxazolidines

Solid TsOH (0.20 mmol) was added portionwise to a solution of the starting oxazolidine (1.00 mmol) in MeOH (20 mL). After vigorous stirring at rt for 2 h, the reaction mixture was quenched with sat. aqueous $NaHCO_3$ and concentrated *in vacuo*. The resulting residue was taken up in EtOAc (20 mL), and the organic layer was successively washed with a mixture of 1:1 $HCO_3^-/H_2O$ (20 mL), and brine (20 mL). The organic layer was dried over $MgSO_4$, filtered and evaporated under reduce pressure. Crude compounds were obtained and next purified as indicated below.

### *tert*-Butyl[(2*S*,3*R*,*E*)-14-azido-1,3-dihydroxytetradec-4-en-2-yl]carbamate (16)

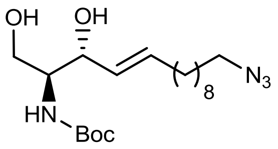

180 mg (0.47 mmol, 87%) of compound **16** were obtained, as a colorless oil, from **13** (233 mg, 0.54 mmol), and TsOH (13 mg, 0.11 mmol) in MeOH (10 mL), according to the *general procedure 6*. Purification was carried out by flash chromatography (6:4 hexane/EtOAc).

[α]$_D$ -2.1 (*c* 0.8, $CHCl_3$); $^1$H NMR (δ, 400 MHz, $CDCl_3$): 1.23-1.40 (m, 12H), 1.45 (brs, 9H), 1.59 (quint, *J*=7.6 Hz, 2H), 2.05 (q, *J*=6.8 Hz, 2H), 2.40 (brs, 2H), 3.25 (t, *J*=7.0 Hz, 2H), 3.59 (brs, 1H), 3.70 (dd, *J*=11.4, 3.5 Hz, 1H), 3.93 (dd, *J*=11.4, 3.6 Hz, 1H), 4.31 (t, *J*=5.2 Hz, 1H), 5.52 (dd, *J*=15.5, 6.4 Hz, 1H), 5.77 (dt, *J*=15.6, 6.4 Hz, 1H); $^{13}$C NMR (δ, 101 MHz, $CDCl_3$):

26.8, 28.5, 28.9, 29.2 (m), 29.3 (m), 29.5 (m), 32.4, 51.6, 55.4, 62.8, 75.1, 129.1, 134.3. HMRS calculated for $C_{19}H_{36}N_4NaO_4$: 407.2634 $[M+Na]^+$. Found: 407.2656.

### General procedure 7: synthesis of phosphate triesters

Neat NMI (4.50 mmol) was added dropwise to a solution of the starting alcohol (1.00 mmol) in anhydrous THF (20 mL). The resulting mixture was cooled down to 0 °C, followed by dropwise addition of dimethylchlorophosphate (4.00 mmol) under argon atmosphere. The reaction mixture was allowed to warm to rt, and vigorously stirred for 5 h. The reaction was next quenched by addition of water (10 mL), and the aqueous phase was extracted with EtOAc (3 x 10 mL). The combined organic extracts were dried over $MgSO_4$, filtered and concentrated *in vacuo*. The resulting crude was purified as indicated below.

### *tert*-Butyl ((2*S*,3*R*,*E*)-14-azido-1-((dimethoxyphosphoryl)oxy)-3-hydroxytetradec-4-en-2-yl)carbamate (17)

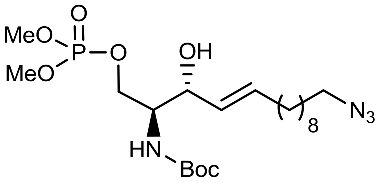

83 mg (0.17 mmol, 65%) of compound **17** were obtained, as a colorless oil, from **16** (100 mg, 0.26 mmol), NMI (93 μL, 1.17 mmol), and dimethylchlorophosphate (112 μL, 1.04 mmol) in THF (5 mL), according to *general procedure 7*. Purification was carried out by flash chromatography (4:6 hexane/EtOAc).

$[\alpha]_D$ +3.8 (*c* 1.0, $CHCl_3$); $^{31}P$ NMR (δ, 121 MHz, $CDCl_3$): 2.33; $^1H$ NMR (δ, 400 MHz, $CDCl_3$): 1.24-1.38 (m, 12H), 1.43 (brs, 9H), 1.59 (quint, *J*=7.6 Hz, 2H), 2.03 (q, *J*=7.6 Hz, 2H), 3.25 (t, *J*=6.9 Hz, 2H), 3.76-3.83 (m, 7H), 4.09-4.16 (m, 2H), 4.30-4.37 (m, 1H), 5.02 (d, *J*=7.6 Hz, 1H), 5.50 (dd, *J*=15.3, 7.0 Hz, 1H), 5.75 (dt, *J*=15.6, 6.4 Hz, 1H); $^{13}C$ NMR (δ, 101 MHz, $CDCl_3$): 15.4, 26.8, 28.5, 29.0, 29.1, 29.2 (m), 29.3 (m), 29.4, 29.5, 29.5, 32.4, 51.6, 54.7 (d, $^2J_{C\text{-}P}$=6.0 Hz), 55.0, 66.0, 66.8 (d, $^2J_{C\text{-}P}$=5.7 Hz), 72.5, 79.9, 128.6, 134.9, 155.8. HRMS calculated for $C_{21}H_{42}N_4O_7P$: 493.2791 $[M+H]^+$. Found: 493.2808. HRMS calculated for $C_{21}H_{41}N_4NaO_7P$: 515.2611 $[M+Na]^+$. Found: 515.2638.

### General procedure 8: TMSBr mediated deprotection

The starting *N*-Boc phosphate methyl ester (0.10 mmol) was kept under reduced pressure for 2 h, dissolved in anhydrous ACN (5 mL), and cooled down to 0 °C under argon atmosphere. To the resulting solution, neat TMSBr (0.98 mmol) was added dropwise and the reaction mixture was vigorously stirred at rt for 3 h and concentrated under reduced pressure. The crude residue was taken up in a 95:5 MeOH/$H_2O$ mixture (9 mL), and vigorously stirred for 1 h. Evaporation under reduced pressure afforded the desired compounds, without further purification.

### (2*S*,3*R*,*E*)-2-Amino-14-azido-3-hydroxytetradec-4-en-1-yl dihydrogen phosphate (RBM2-35)

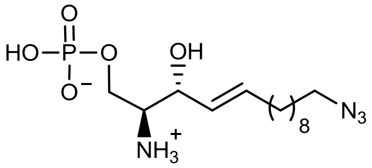

62 mg (0.17 mmol, quantitative) of **RBM2-35** were obtained, as a pale yellow oil, from **17** (86 mg, 0.17 mmol), and TMSBr (220 μL, 1.67 mmol) in ACN (8 mL), according to *general procedure 8*.

$[\alpha]_D$ -3.3 (*c* 1.1, MeOH); $^{31}P$ NMR (δ, 162 MHz, $CD_3OD$): 1.31; $^1H$ NMR (δ, 500 MHz, $CD_3OD$): 1.31-1.48 (m, 12H), 1.59 (quint, *J*=7.0 Hz, 2H), 2.11 (q, *J*=7.0 Hz, 2H), 3.25 (t, *J*=7.0 Hz, 2H), 3.39-3.44 (m, 1H), 4.04-4.12 (m, 1H), 4.16-4.23 (m, 1H), 4.32 (t, *J*=5.7 Hz, 1H), 5.49 (dd, *J*=15.4, 6.7 Hz, 1H), 5.89 (dt, *J*=15.5, 7.5 Hz, 1H); $^{13}C$ NMR (δ, 101 MHz, $CD_3OD$): 27.8, 29.9, 30.1, 30.3, 30.4, 30.5, 30.6, 33.4, 52.5, 57.1 (d, $^2J_{C-P}$=7.3 Hz), 64.0 (d, $^3J_{C-P}$=4.6 Hz), 70.7, 128.1, 137.0. HRMS calculated for $C_{14}H_{29}N_4NaO_5P$: 387.1773 $[M+Na]^+$. Found: 387.1778.

### *tert*-Butyl ((2*S*,3*R*)-14-azido-1,3-dihydroxytetradecan-2-yl)carbamate (18)

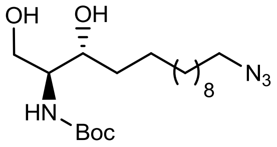

36 mg (0.09 mmol, 62%) of compound **18** were obtained, as a white waxy solid, from **15** (64 mg, 0.15 mmol), and TsOH (3.5 mg, 0.03 mmol) in MeOH (5 mL), according to *general procedure 6*. This compound was used in the next step without further purification.

$[\alpha]_D$ +9.5 (*c* 0.8, $CHCl_3$); $^1H$ NMR (δ, 400 MHz, $CDCl_3$): 1.23-1.40 (m, 16H), 1.45 (s, 9H), 1.49-1.63 (m, 4H), 2.42 (brs, 2H), 3.25 (t, *J*=7.0 Hz, 2H), 3.52 (brs, 1H), 3.71-3.82 (m, 2H), 3.99 (dd, *J*=11.4, 3.3 Hz, 1H), 5.41 (brs, 1H); $^{13}C$ NMR (δ, 101 MHz, $CDCl_3$): 26.1, 26.8, 28.5, 29.0, 29.3, 29.6, 29.6 (m), 29.7 (m), 34.6, 51.6, 54.8, 62.7, 74.5, 79.9, 156.2. HRMS calculated for $C_{19}H_{38}N_4NaO_4$: 409.2791 $[M+Na]^+$. Found: 409.2780.

### *tert*-Butyl [(2*S*,3*R*)-14-azido-1-[(dimethoxyphosphoryl)oxy]-3-hydroxytetradecan-2-yl]carbamate (19)

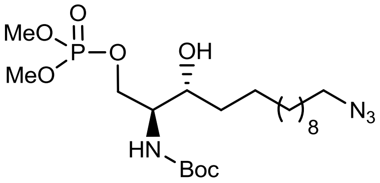

44 mg (0.09 mmol, quantitative) of compound **19** were obtained, as a colorless oil, from **18** (36 mg, 0.09 mmol), NMI (32 μL, 0.41 mmol), and dimethylchlorophosphate (39 μL, 0.36 mmol) in THF (3 mL), according to *general procedure 7*. Purification was carried out by flash chromatography (4:6 hexane/EtOAc).

$[\alpha]_D$ +21.3 (*c* 0.5, $CHCl_3$); $^1H$ NMR (δ, 400 MHz, $CDCl_3$): 1.24-1.34 (m, 16H), 1.45 (brs, 9H), 1.52-1.64 (m, 4H), 3.26 (t, *J*=7.0 Hz, 2H), 3.57-3.64 (m, 1H), 3.68 (brs, 1H), 3.78 (d, *J*=3.4 Hz, 1H), 3.81 (d, *J*=3.4 Hz, 3H), 4.11 (t, *J*=7.1 Hz, 1H), 4.41 (d, *J*=8.2 Hz, 1H), 5.05 (d, *J*=8.1 Hz, 1H); $^{13}C$ NMR (δ, 101 MHz, $CDCl_3$): 26.8, 28.5, 28.9, 29.3, 29.6, 29.6, 29.6, 29.7, 33.8, 51.6, 54.6 (d, $^2J_{C-P}$ =6.0 Hz), 55.0 (d, $^2J_{C-P}$=5.0 Hz), 67.1 (d, $^3J_{C-P}$=5.7 Hz), 71.4, 80.0, 155.7. $C_{21}H_{43}N_4NaO_7P$: 517.2767 $[M+Na]^+$. Found: 517.2770.

### (2*S*,3*R*)-2-Amino-14-azido-3-hydroxytetradecyl dihydrogenphosphate (RBM2-43)

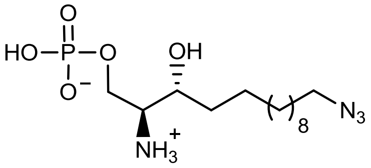

33 mg (0.09 mmol, quantiative) of phosphate **RBM2-43** were obtained, as a pale yellow oil, from **19** (44 mg, 0.09 mmol), and TMSBr (116 μL, 0.88 mmol) in ACN (5 mL), according to *general procedure 8*.

[α]D -5.3 (*c* 0.9, MeOH); $^{31}$P NMR (δ, 162 MHz, $CD_3OD$): 1.28; $^{1}$H NMR (δ, 500 MHz, $CD_3OD$): 1.26-1.44 (m, 18H), 1.46-1.64 (m, 6H), 3.28 (t, *J*=6.5 Hz, 2H), 3.34-3.46 (m, 1H), 3.77-3.86 (m, 1H), 4.09-4.18 (m, 1H); 4.20-4.29 (m, 1H); $^{13}$C NMR (δ, 101 MHz, $CD_3OD$): 27.0, 27.8, 29.9, 30.3, 30.5, 30.6, 30.7, 30.8, 34.2, 52.4, 57.0 (d, $^{2}J_{C\text{-}P}$=7.4 Hz), 63.8 (d, $^{3}J_{C\text{-}P}$=2.6 Hz), 70.0. HRMS calculated for $C_{14}H_{32}N_4O_5P$: 367.2110 [M+H]$^+$. Found: 367.2096.

### (2*S*,3*R*)-14-Azido-3-hydroxy-2-octanamidotetradecyl dimethylphosphate (21)

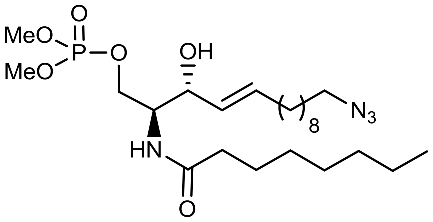

200 mg (0.38 mmol, quantitative) of compound **21** were obtained, as a white waxy solid, from ceramide **RBM2-37** (158 mg, 0.39 mmol), NMI (140 μL, 1.76 mmol), and dimethylchlorophosphate (168 μL, 1.56 mmol) in THF (5 mL), according to *general procedure 7*. Purification was carried out by flash chromatography (100:0 to 97:3 $CH_2Cl_2$/MeOH gradient).

[α]D -4.8 (*c* 1.0, $CHCl_3$); $^{31}$P NMR (δ, 162 MHz, $CDCl_3$): 2.49; $^{1}$H NMR (δ, 400 MHz, $CDCl_3$): 0.87 (t, *J*=7.2 Hz, 3H), 1.21-1.40 (m, 20H), 1.54-1.66 (m, 4H), 2.03 (q, *J*=7.2 Hz, 2H), 2.20 (t, *J*=7.2 Hz, 2H), 3.25 (t, *J*=7.0 Hz, 2H), 3.77 (d, *J*=2.4 Hz, 3H), 3.80 (d, *J* = 2.4 Hz, 3H), 4.09-4.19 (m, 3H), 4.28-4.38 (m, 1H), 5.48 (dd, *J*=15.2, 6.3 Hz, 1H), 5.74 (dt, *J*=15.2, 6.4 Hz, 1H), 6.24 (d, *J*=6.4 Hz, 1H); $^{13}$C NMR (δ, 101 MHz, $CDCl_3$): 14.2, 22.8, 25.8, 26.8, 29.0, 29.2 (m), 29.3 (m), 29.4, 29.5 (m), 31.8, 32.4, 36.9, 51.6, 54.0 (d, $^{2}J_{C\text{-}P}$=5.2 Hz), 54.8 (d, $^{2}J_{C\text{-}P}$=6.1 Hz), 66.7

(d, $^{3}J_{C\text{-}P}$=5.7 Hz), 72.6, 128.6, 134.9, 173.9. HRMS calculated for $C_{24}H_{47}N_{4}NaO_{6}P$: 541.3131 $[M+Na]^{+}$. Found: 541.3138.

### (2*S*,3*R*)-14-Azido-3-hydroxy-2-octanamidotetradecyl hydrogenphosphonate diisopropylethylamine salt (24)

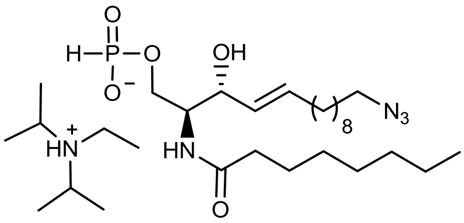

To a solution of ceramide **RBM2-37** (76 mg, 0.19 mmol) and DIPEA (152 μL, 0.91 mmol) in anhydrous THF (30 mL) was added dropwise a solution of 2-chloro-4-*H*-1,3,2-benzodioxaphosphorin-4-one (**22**) (112 mg, 0.56 mmol) in anhydrous THF (4 mL) at -78 °C under argon atmosphere. After vigourous stirring at -78 °C for 3 h, the reaction mixture was quenched by dropwise addition of water (4 mL), and allowed to warm to rt. The mixture was concentrated *in vacuo*, and the resulting residue was next purified by flash chromatography (99.75:0:0.25 to 74.75:25:0.25 $CH_{2}Cl_{2}$/MeOH/$NH_{4}OH$ gradient). *H*-Phosphonate **24** (95 mg, 0.16 mmol, 83%) was obtained as a DIPEA salt (yellow pale wax).

$[\alpha]_{D}$ -22.6 (*c* 0.2, $CHCl_{3}$); $^{31}P$ NMR (δ, 121 MHz, $CDCl_{3}$): 5.18 (d, $J_{P\text{-}H}$= 33.3 Hz); $^{1}H$ NMR (δ, 400 MHz, $CDCl_{3}$): 0.86 (t, *J*=6.8 Hz, 3H), 1.20-1.34 (m, 20H), 1.36-1.41 (m, 6H), 1.42-1.51 (m, 9H), 1.58 (quint, *J*=6.4 Hz, 2H), 1.98 (q, *J*=6.4 Hz, 2H), 2.15 (t, *J*=7.6 Hz, 2H), 2.99-3.08 (m, 2H), 3.24 (t, *J*=6.8 Hz, 2H), 3.54-3.65 (m, 2H), 3.82-3.91 (m, 2H), 3.97–4.08 (m, 1H), 4.47 (brs, 1H), 5.41 (dd, *J*=15.2, 5.2 Hz, 1H), 5.72 (dt, *J*=14.8, 7.2 Hz, 1H), 6.55 (brs, 1H), 6.82 (d, $J_{P\text{-}H}$=625.2 Hz, 1H); $^{13}C$ NMR (δ, 101 MHz, $CDCl_{3}$): 12.1, 14.2, 17.4, 19.6, 22.7, 26.0, 26.8, 28.9, 29.2, 29.3, 29.4, 29.5, 29.6, 31.0, 31.8, 32.5, 36.8, 41.89, 51.6, 53.4, 53.7 (d, $^{2}J_{C\text{-}P}$=4.0 Hz), 62.1 (d, $^{3}J_{C\text{-}P}$=4.0 Hz), 69.5, 129.2, 132.2, 174.1. HRMS calculated for $C_{22}H_{43}N_{4}NaO_{5}P$: 497.2869 $[M+Na]^{+}$. Found: 497.2873.

### (2*S*,3*R*)-14-Azido-3-hydroxy-2-octanamidotetradecyl dihydrogen phosphate triethylamine salt (RBM2-47)

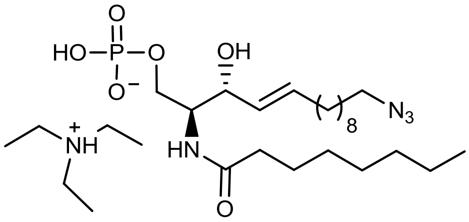

To a solution of *H*-phosphonate salt **24** (95 mg, 0.16 mmol) and $Et_3N$ (100 μL, 0.72 mmol) in dry $CH_2Cl_2$ (5 mL) was added dropwise TMSCl (81 μL, 0.64 mmol) under argon atmosphere. After vigorous stirring at rt for 30 min, *t*-BuOOH (347 μL, 3.2 mmol, 5.5 M in decane) was added dropwise. Once the reaction was completed (within 1 h, as monitored by TLC (7:3 $CH_2Cl_2$/MeOH)), it was quenched by dropwise addition of MeOH (3 mL) and concentrated *in vacuo*. The resulting residue was purified by flash chromatography (99.8:0:0.2 to 79.8:20:0.2 $CH_2Cl_2$/MeOH/$Et_3N$ gradient) to afford compound **RBM2-47** (20 mg, 0.03 mmol, 21%) as a $Et_3N$ salt.

$[\alpha]_D$ -6.3 (*c* 0.5, MeOH); $^{31}P$ NMR (δ, 162 MHz, $CD_3OD$): 1.94; $^1H$ NMR (δ, 400 MHz, $CD_3OD$): 0.91 (t, *J*=6.8 Hz, 3H), 1.26-1.43 (m, 29H), 1.52-1.65 (m, 4H), 2.04 (q, *J*=6.8 Hz, 2H), 2.16-2.26 (m, 2H), 3.19 (q, *J*=7.6 Hz, 6H), 3.28 (t, *J*=6.8 Hz, 2H), 3.81-4.08 (m, 3H), 4.32-4.38 (m, 1H), 5.46 (dd, *J*=15.2, 6.0 Hz, 1H), 5.73 (dt, *J*=15.6, 6.0 Hz, 1H); $^{13}C$ NMR (δ, 101 MHz, $CD_3OD$): 14.5, 23.8, 27.2, 27.9, 29.9, 30.28, 30.3, 30.4, 30.6, 30.7, 33.0, 33.5, 37.2, 47.7, 52.4, 55.3 (d, $^2J_{C\text{-}P}$=7.6 Hz), 64.8 (d, $^3J_{C\text{-}P}$ =4.8 Hz), 71.1, 74.0, 130.7, 133.6, 176.4. HRMS calculated for $C_{22}H_{43}N_4NaO_6P$: 513.2818 $[M+Na]^+$. Found: 513.2825.

### 5.1.7 Synthesis of ketone RBM2-63

**(*S*)-*tert*-Butyl 4-[(*R*)-1,12-dihydroxydodec-2-yn-1-yl]-2,2-dimethyloxazolidine-3-carboxylate (26)**

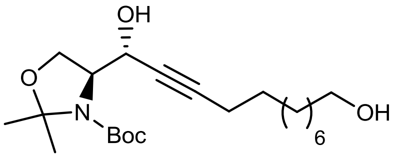

To a solution of undec-10-yn-1-ol (225 mg, 1.34 mmol) in anhydrous THF (15 mL) was added dropwise *n*BuLi (1.29 mL, 3.22 mmol, 2.5 M in hexanes) at -20 °C. After vigorous stirring at -20 °C for 30 min, neat HMPA (350 µL, 2.01 mmol) was added dropwise. The reaction mixture was cooled down to -78 °C, followed by dropwise addition of a solution of aldehyde **4** (236 mg, 1.03 mmol) in anhydrous THF (2 mL). After stirring at −78 °C for 1 h, the reaction mixture was allowed to warm to -20 °C within 2 h, and next quenched by addition of saturated aqueous $NH_4Cl$ (10 mL). After dilution by addition of water, the aqueous phase was extracted with $Et_2O$ (3 x 20 mL). The combined organic layers were successively washed with 0.5 *N* HCl and brine, dried over $MgSO_4$, filtered and concentrated *in vacuo*. The resulting residue was purified by flash chromatography (10:0 to 6:4 hexane/EtOAc gradient) to afford 205 mg (0.52 mmol, 50%) of compound **24**, as a colorless oil.

$[\alpha]_D$ -30.3 (*c* 1.2, $CHCl_3$); $^1H$ NMR (δ, 400 MHz, $CDCl_3$): 1.21-1.38 (m, 10H), 1.42–1.51 (m, 15H), 1.51-1.63 (m, 4H), 2.17 (t, *J*=7.1 Hz, 2H), 3.61 (t, *J*=6.6 Hz, 2H), 3.85–4.15 (m, 3H), 4.50 (brs, 1H); $^{13}C$ NMR (δ, 101 MHz, $CDCl_3$): 18.8, 25.5, 25.8, 25.9, 28.5, 28.8, 29.0, 29.4, 29.5, 32.8, 62.8, 63.0, 64.1, 65.14, 78.0, 81.3, 86.7, 95.0, 154.2. HRMS calculated for $C_{22}H_{39}NNaO_5$: 420.2726 $[M+Na]^+$. Found: 420.2712.

### (*S*)-*tert*-Butyl 4-[(*R*)-1,12-dihydroxydodecyl]-2,2-dimethyloxazolidine-3-carboxylate (27)

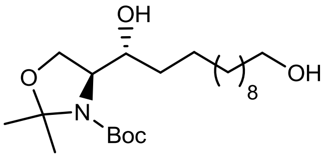

136 mg (0.34 mmol, 89%) of compound **27** were obtained, as a white solid, from alkyne **26** (150 mg, 0.38 mmol), and rhodium catalyst (27 mg) in MeOH (10 mL), according to *general procedure 5*. Compound **27** was used in the next step without further purification.

[α]$_D$ -11.0 (*c* 1.0, $CHCl_3$); $^1$H NMR (δ, 500 MHz, $CDCl_3$) (major rotamer): 1.19-1.37 (m, 16H), 1.41-1.65 (m, 19H), 3.62 (t, *J*=6.6 Hz, 2H), 3.66-4.11 (m, 4H); $^{13}$C NMR (δ, 101 MHz, $CDCl_3$) (major rotamer): 25.8, 26.2, 26.5, 28.5, 29.5, 29.6, 29.7, 29.8, 32.9, 62.5, 63.0, 64.8, 73.0, 81.1, 94.3, 154.2. HRMS calculated for $C_{22}H_{45}NO_5$: 402.3219 [M+H]$^+$. Found: 402.3229. HRMS calculated for $C_{22}H_{44}NNaO_5$: 424.3039 [M+Na]$^+$. Found: 424.3031.

### (*S*)-*tert*-Butyl 4-[(*R*)-1-hydroxy-12-(tosyloxy)dodecyl]-2,2-dimethyloxazolidine-3-carboxylate (28)

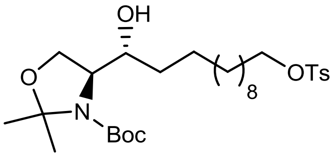

A solution of **27** (136 mg, 0.34 mmol) and $Et_3N$ (47 μL, mmol) in dry $CH_2Cl_2$ (7 mL) was added dropwise to a solution of tosyl chloride (65 mg. 0.34 mmol) and DMAP (21 mg, 0.17 mmol) in dry $CH_2Cl_2$ (3 mL) under argon atmosphere. After vigorous stirring at rt for 8 h, the reaction mixture was diluted by addition of $CH_2Cl_2$ (10 mL). The organic layer was washed with brine (2 x 10 mL), dried over $MgSO_4$, filtered and concentrated under reduced pressure. Purification of the resulting residue by flash chromatography (10:0 to 5:5 hexane/EtOAc gradient) gave 110 mg (0.20 mmol, 58%) of tosylate **28**, as a colorless wax.

[α]$_D$ -6.7 (*c* 1.0, $CHCl_3$); $^1$H NMR (δ, 400 MHz, $CDCl_3$) (major rotamer): 1.16–1.34 (m, 17H), 1.48 (brs, 13H), 1.53-1.70 (m, 6H), 2.44 (s, 3H), 3.69-4.11 (m, 6H), 7.34 (d, *J*=8.0 Hz, 2H), 7.78 (d, *J*=8.2, 2H); $^{13}$C NMR (δ, 101 MHz, $CDCl_3$) (major rotamer): 21.8, 25.4, 26.2, 26.5, 28.5, 28.9, 29.0, 29.5, 29.6 (m), 29.7, 29.8, 32.9, 62.5, 64.8, 70.8, 73.1, 81.1, 94.3, 128.0, 129.

9, 133.3, 144.7, 154.2. HRMS calculated for $C_{29}H_{50}NO_7S$: 556.3308 [M+H]$^+$. Found: 556.3325. HRMS calculated for $C_{29}H_{49}NnaO_7S$: 578.3127 [M+Na]$^+$. Found: 578.3132.

### (*S*)-*tert*-Butyl 4-(12-azidododecanoyl)-2,2-dimethyloxazolidine-3-carboxylate (29)

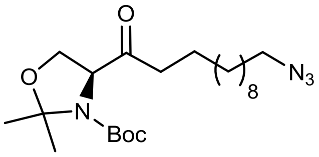

To a solution of compound **15** (55 mg, 0.13 mmol) in dry $CH_2Cl_2$ (4 mL) was added PCC (72 mg, 0.33 mmol) under argon atmosphere. After vigorous stirring at rt overnight, the reaction mixture was filtered through a plug of Celite and concentrated *in vacuo*. The residue was purified by flash chromatography (10:0 to 9:1 hexane/EtOAc gradient) to afford 51 mg (0.12 mmol, 92%) of compound **29**, as a colorless wax.

$[\alpha]_D$ -30.0 (*c* 1.0, $CHCl_3$); $^1H$ NMR (δ, 500 MHz, $CDCl_3$) (rotameric mixture): 1.24-1.38 (m, 15H), 1.41 (brs, 5H), 1.46-1.63 (m, 13H), 2.40-2.55 (m, 2H), 3.25 (t, *J*=7.0 Hz, 2H), 3.88 (dd, *J*=9.5, 2.5 Hz, 0.6H), 3.93 (dd, *J*=9.0, 2.5 Hz, 0.4H), 4.09-4.18 (m, 1H), 4.31 (dd, *J*=7.5, 2.5 Hz, 0.6H), 4.44 (dd, *J*=7.0, 2.5 Hz, 0.4H); $^{13}C$ NMR (δ, 101 MHz, $CDCl_3$) (rotameric mixture): 23.2, 23.2, 23.8, 25.0, 25.5, 26.3, 26.8, 28.5 (m), 29.0, 29.3, 29.4, 29.5 (m), 29.6, 29.7, 38.6, 39.2, 51.6, 65.3, 65.5, 65.5, 65.9, 80.7, 81.0, 94.6, 95.3, 151.6, 152.2, 208.4, 208.9. HRMS calculated for $C_{22}H_{40}N_4NaO_2$: 447.2947 [M+Na]$^+$. Found: 447.2957.

### (*S*)-2-Amino-14-azido-1-hydroxytetradecan-3-one (RBM2-63)

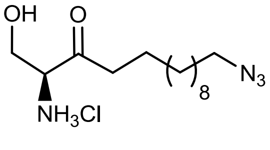

Ketone **RBM2-63** (30 mg, 0.09 mmol, 90%) was obtained, as a yellow pale wax, from **29** (41 mg, 0.10 mmol) and acetyl chloride (300 μL) in MeOH (5 mL), according to *general procedure 3*. Compound **RBM2-63** was used without further purification.

$[\alpha]_D$ +23.9 (*c* 0.6, $CHCl_3$); $^1H$ NMR (δ, 400 MHz, $CD_3OD$): 1.28-1.41 (m, 14H), 1.54-1.67 (m, 2H), 2.64 (t, *J*=7.2 Hz, 2H), 3.28 (t, *J*=6.8 Hz, 2H), 3.97 (dd, *J*=12.0, 3.4 Hz, 1H), 4.10 (dd, *J*=2.0, 4.3 Hz, 1H), 4.16 (t, *J*=4.0, 1H); $^{13}C$ NMR (δ, 101 MHz, $CD_3OD$): 24.2, 27.8, 29.9, 30.1, 30.3, 30.5, 30.6 (m), 39.6, 52.4, 60.3, 62.2, 205.2. HRMS calculated for $C_{14}H_{29}N_4O_2$: 285.2291 $[M+H]^+$. Found: 285.2278.

### 5.1.8 Synthesis of 1-azidoceramide RBM2-79

***tert*-Butyl 4-[(*R*,*E*)-1-hydroxyhexadec-2-en-1-yl]-2,2-dimethyloxazolidine-3-carboxylate (30)**

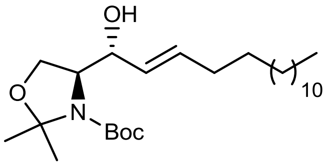

Compound **30** (1.51 g, 3.43 mmol, 59%) was obtained, as a white solid, from alkene **7** (1.5 g, 5.8 mmol), 1-pentadecene (4.9 g, 23.3 mmol), and Grubb's 2nd generation catalyst (210 mg) in $CH_2Cl_2$ (75 mL), according to *general procedure 2.* Purification was carried out by flash chromatography (100:0 to 85:15 hexane/EtOAc gradient).

$[\alpha]_D$ -10.4 (*c* 1.1, $CHCl_3$); $^1H$ NMR (δ, 400 MHz, $CDCl_3$) (major rotamer): 0.88 (t, *J*=6.6 Hz, 3H), 1.25 (brs, 20H), 1.33-1.40 (m, 2H), 1.43-1.57 (m, 15H), 2.03 (q, *J*=7.2 Hz, 2H), 3.73-4.22 (m, 4H), 5.44 (dd, *J*=16.0, 4.0 Hz, 1H), 5.73 (dt, *J*=14.8, 7.3 Hz, 1H), $^{13}C$ NMR (δ, 101 MHz, $CDCl_3$) (major rotamer): 14.3, 22.8, 24.8, 26.4, 28.5, 29.2-30.0 (m), 32.1, 32.6, 62.4, 65.1, 74.2, 76.8, 77.2, 77.5, 81.2, 94.6, 128.2, 133.6, 154.4. HRMS calculated for $C_{26}H_{49}NNaO_4$: 462.3559 [M+Na]+. Found: 462.3552.

**(1*S*,7a*S*)-5,5-dimethyl-1-[(*E*)-pentadec-1-en-1-yl]dihydro-1*H*-oxazolo[3,4-*c*]oxazol-3(5*H*)-one (31)**

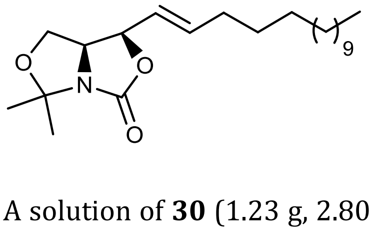

A solution of **30** (1.23 g, 2.80 mmol) in anydrous THF (10 mL) was added to a suspension of NaH (1.12 g, 28.00 mmol) in anhydrous THF (30 mL) at 0 °C. The reaction mixture was vigorously stirred at rt overnight under argon atmosphere. The reaction was next quenched by dropwise addition of aqueous sat. $NaHCO_3$ at 0 °C, until $H_2$ evolution was not observed. The aqueous phase was next extracted with EtOAc (3 x 40 mL). The combined organic layers were dried over $MgSO_4$, and filtered. Concentration under reduced pressure afforded 1.03 g (2.80 mmol, quantitative) of crude carbamate **31**, as a white solid. This compound was used in the next step without further purification.

[α]$_D$ -7.7 (*c* 1.2, $CHCl_3$); $^1$H NMR (δ, 500 MHz, $CDCl_3$): 0.88 (t, *J*=5.0 Hz, 3H), 1.25 (brs, 22H), 1.44 (s, 6H), 2.03-2.11 (m, 2H), 3.68-3.79 (m, 2H), 3.87 (t, *J*=7.5 Hz, 1H), 4.40 (q, *J*=7.5 Hz, 1H), 5.02 (t, *J*=7.8 Hz, 1H), 5.40 (dd, *J*=15.2, 7.2 Hz, 1H), 5.89 (dt, *J* =16.0, 6.5 Hz, 1H); $^{13}$C NMR (δ, 75 MHz, $CDCl_3$): 14.21, 22.79, 23.47, 27.94, 28.81, 29.20, 29.27, 29.46, 29.52, 29.68, 29.76, 32.02, 32.30, 53.51, 61.76, 64.31, 75.44, 95.11, 122.40, 138.03, 156.95. HRMS calculated for $C_{22}H_{39}NNaO_3$: 388.2828 [M+Na]$^+$. Found: 388.2832.

### (4*S*,5*S*)-4-(Hydroxymethyl)-5-((*E*)-pentadec-1-en-1-yl)oxazolidin-2-one (32)

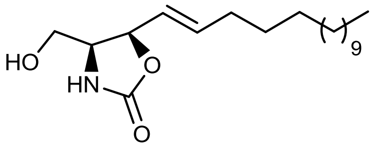

According to *general procedure 6,* 617 mg (1.74 mmol, 68%) of compound **32** were obtained, as a white solid, from **31** (1.03 g, 2.80 mmol), and TsOH (112 mg, 0.59 mmol) in MeOH (60 mL). Purification was carried out by flash chromatography (100:0 to 95:5 $CH_2Cl_2$/MeOH gradient).

[α]$_D$ -6.5 (*c* 0.9, $CHCl_3$); $^1$H NMR (δ, 500 MHz, $CDCl_3$): 0.88 (t, *J*=6.9 Hz, 3H), 1.22-1.34 (m, 20H), 1.34-1.42 (m, 2H), 2.09 (q, *J*=7.0 Hz, 2H), 3.60-3.71 (m, 2H), 3.85-3.92 (m, 1H), 5.08 (t, *J*=8.2 Hz, 1H), 5.57 (dd, *J*=15.3, 8.2 Hz, 1H), 5.80 (brs, 1H), 5.92 (dt, *J*=15.5, 7.0 Hz, 1H). $^{13}$C NMR (δ, 75 MHz, $CDCl_3$): 13.3, 21.9, 27.9, 28.3, 28.4, 28.5, 28.6, 28.7, 28.8, 31.1, 31.4, 43.9, 56.3, 61.2, 79.1, 121.1, 138.2, 158.6. HRMS calculated for $C_{19}H_{35}NNaO_3$: 348.2515 [M+Na]$^+$. Found: 348.2503.

### (4*S*,5*S*) 2-Oxo-5-[(*E*)-pentadec-1-en-1-yl]oxazolidin-4-ylmethyl methanesulfonate (33)

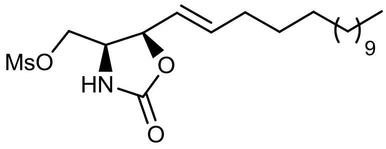

A solution of compound **32** (895 mg, 2.75 mmol) and $Et_3N$ (660 µL, 4.67 mmol) in anhydrous $CH_2Cl_2$ (50 mL) was cooled down to 0 °C. After vigorous stirring at this temperature for 10 min, MsCl (320 µL, 4.13 mmol) was added dropwise. The reaction mixture was next allowed to warm to rt, and stirred for 2 h under argon atmosphere. The mixture was diluted by addition of $CH_2Cl_2$ (20 mL), and the organic layer was successively washed with 0.5 *N* HCl (50 mL), aqueous sat. $NaHCO_3$ (50 mL), and brine (50 mL). The washed organic layer was dried over $MgSO_4$, and filtered. Concentration *in vacuo* gave 1.07 g (2.65 mmol, 96%) of crude compound **33**, as a white solid, which was used in the next step without further purification.

$[\alpha]_D$ -3.8 (*c* 0.5, $CHCl_3$); $^1H$ NMR (δ, 500 MHz, $CDCl_3$): 0.88 (t, *J*=7.0 Hz, 3H), 1.22-1.32 (m, 20H), 1.34-1.44 (m, 2H), 2.12 (q, *J*=7.1 Hz, 2H), 3.09 (s, 3H), 4.10-4.18 (m, 2H), 4.24-4.30 (m, 1H), 5.10-5.15 (m, 1H), 5.48 (dd, *J*=15.4, 8.1 Hz, 1H), 5.82-5.94 (m, 1H), 5.96 (dt, *J*=14.9, 7.3 Hz, 1H); $^{13}C$ NMR (δ, 75 MHz, $CDCl_3$): 14.3, 22.8, 28.8, 29.1-30.1 (m), 32.1, 32.4, 37.8, 54.7, 67.6, 78.9, 120.8, 140.2, 158.9. HRMS calculated for $C_{20}H_{37}NNaO_5S$: 426.2290 $[M+Na]^+$. Found: 426.2297.

### (4*S*,5*S*)-4-Azidomethyl-5-[(*E*)-pentadec-1-en-1-yl]oxazolidin-2-one (34)

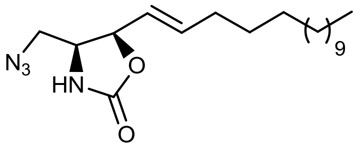

In a two necked round bottom flask fitted with a reflux condenser, $NaN_3$ (495 mg, 7.62 mmol) was added portionwise to a solution of **33** (510 mg, 1.27 mmol) in anhydrous DMF (25 mL). The reaction mixture was heated at 45 °C, and vigorously stirred overnight. The mixture was next allowed to cool down to rt, and concentrated under reduced pressure. The resulting residue was purified by flash chromatography (10:0 to 5:5 hexane/EtOAc gradient). 300 mg (0.86 mmol, 68%) of azide **34**, as a brown solid, and by-product pyrroline **35** (82 mg, 0.25 mmol, 20%), as an orange solid, were obtained.

$[\alpha]_D$ -4.5 (*c* 0.7, $CHCl_3$); $^1H$ NMR (δ, 500 MHz, $CDCl_3$): 0.88 (t, *J*=6.8 Hz, 3H), 1.21-1.32 (m, 20H), 1.34-1.43 (m, 2H), 2.10 (q, *J*=7.5 Hz, 2H), 3.33-3.41 (m, 1H), 3.47 (dd, *J*=12.2, 4.3 Hz, 1H), 3.90 (dt, *J*=12.4, 6.2 Hz, 1H), 5.08 (t, *J*=8.0 Hz, 1H), 5.49 (dd, *J*=15.2, 7.8 Hz, 1H), 5.79-5.88 (m, 1H), 5.93 (dt, *J*=15.5, 7.0 Hz, 1H); $^{13}C$ NMR (δ, 75 MHz, $CDCl_3$): 14.3, 22.8, 28.8, 29.1–30.0 (m), 32.1, 32.5, 52.2, 55.2, 79.4, 121.3, 139.5, 158.7. HRMS calculated for $C_{19}H_{34}N_4NaO_2$: 373.2579 $[M+Na]^+$. Found: 373.2564.

Data for **35**:

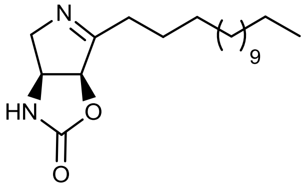

$[\alpha]_D$ +10.2 (*c* 1.1, $CHCl_3$); $^1H$ NMR (δ, 400 MHz, $CDCl_3$): 0.88 (t, *J*=6.8 Hz, 3H), 1.21-1.39 (m, 22H), 1.58-1.74 (m, 2H), 2.37-2.58 (m, 2H), 3.93-4.07 (m, 2H), 4.38-4.44 (m, 1H), 5.30 (d, *J*=7.8 Hz, 1H), 5.59 (brs, 1H); $^{13}C$ NMR (δ, 75 MHz, $CDCl_3$): 14.1, 22.7, 25.6, 29.1-29.9 (m), 30.9, 31.9, 53.6, 67.1, 85.4, 158.5, 173.9. HRMS calculated for $C_{19}H_{35}N_2O_2$: 323.2699 $[M+H]^+$. Found: 323.2700.

### (2*S*,3*R*,*E*)-2-Amino-1-azidooctadec-4-en-3-ol (40)

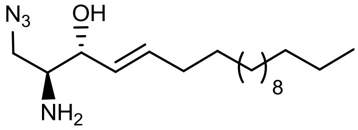

Carbamate **34** (480 mg, 1.37 mmol) was dissolved in a 1:1 EtOH/2 *N* NaOH mixture (50 mL), and the resulting mixture was heated at 60 °C. After vigorous stirring at this temperature for 8 h, the reaction mixture was concentrated under reduced pressure, and the aqueous phase was extracted with $CH_2Cl_2$ (3 x 40 mL). The combined organic layers were dried over $MgSO_4$, filtered and concentrated *in vacuo*. The resulting residue was purified by flash column chromatography (10:0 to 4:6 hexane/EtOAc gradient, followed by 100:0 to 97:3 $CH_2Cl_2$/MeOH gradient) to afford 75 mg (0.23 mmol, 17%) of compound **40**, as a yellow oil.

$[\alpha]_D$ -6.5 (*c* 0.9, MeOH); $^1$H NMR (δ, 500 MHz, $CD_3OD$): 0.90 (t, *J*=6.9 Hz, 3H), 1.23-1.37 (m, 20H), 1.38-1.48 (m, 2H), 2.12 (q, *J*=7.1 Hz, 2H), 3.26-3.30 (m, 1H), 3.57-3.63 (m, 1H), 3.75 (dd, *J*=13.3, 4.0 Hz, 1H), 4.29 (t, *J*=5.5 Hz, 1H), 5.47 (dd, *J*=15.5, 8.0 Hz, 1H), 5.89 (dt, *J*=15.5, 6.5 Hz, 1H); $^{13}$C NMR (δ, 75 MHz, $CDCl_3$): 14.3, 22.8, 29.0-30.3 (m), 32.1, 32.5, 54.1, 55.1, 74.1, 128.3, 135.6. HRMS calculated for $C_{18}H_{36}N_4NaO$: 347.2787 $[M+Na]^+$. Found: 347.2790.

### ***N*- (2*S*,3*R*,*E*)-1-Azido-3-hydroxyoctadec-4-en-2-ylpalmitamide (RBM2-79)**

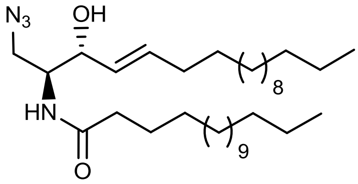

According to *general procedure 4*, 22 mg (0.05 mmol, 82%) of ceramide **RBM2-79** were obtained, as a white solid, from aminodiol **33** (20 mg, 0.06 mmol), $Et_3N$ (33 μL, 0.23 mmol), octanoic acid (10 μL, 0.06 mmol), HOBt (10 mg, 0.07 mmol), and EDC (19 mg, 0.10 mmol) in $CH_2Cl_2$ (5 mL). Purification was carried out by flash chromatography (100:0 to 98:2 $CH_2Cl_2$/MeOH gradient).

$[\alpha]_D$ -2.4 (*c* 0.5, $CHCl_3$); $^1$H NMR (δ, 400 MHz, $CDCl_3$): 0.88 (t, *J*=6.8 Hz, 6H), 1.19-1.42 (m, 46H), 1.62 (quint, *J*=7.2 Hz, 2H), 2.05 (q, *J*=6.8 Hz, 2H), 2.16-2.24 (m, 2H), 2.47 (brs, 1H), 3.52 (dd, *J*=12.5, 4.0 Hz, 1H), 3.63 (dd, *J*=13.0, 5.0 Hz, 1H), 4.01-4.09 (m, 1H), 4.18 (t, *J*=6.0 Hz, 1H), 5.45 (dd, *J*=15.5, 6.5 Hz, 1H), 5.76 (dt, *J*=15.0, 7.0 Hz, 1H), 5.83 (d, *J*=8.5 Hz, 1H); $^{13}$C NMR (δ, 101 MHz, $CDCl_3$): 14.3, 22.8, 28.8, 29.3, 29.4 (m), 29.5, 29.7-29.9 (m), 32.1, 32.4, 37.0, 51.0, 53.0, 73.5, 128.6, 135.1, 173.6. HRMS calculated for $C_{34}H_{66}N_4NaO_2$: 585.5083 $[M+Na]^+$. Found: 585.5086.

## 5.1.9 Synthesis of $\Delta^6$ and $\Delta^{4,6}$-ceramides RBM2-85, RBM2-76 and RMB2-82

### (*S*)-*tert*-Butyl 4-[(*R*)-1-hydroxypent-4-en-1-yl]-2,2-dimethyloxazolidine-3-carboxylate (56)

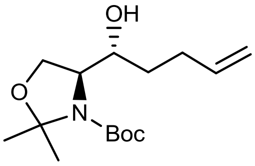

3-Butenylmagnesium bromide (12.36 mL, 6.18 mmol, 0.5 M in THF) was added dropwise to a solution of aldehyde **4** (945 mg, 4.12 mmol) in anhydrous THF (15 mL) at -78 ºC under argon atmosphere. After vigorous stirring at this temperature for 2 h, the reaction mixture was allowed to warm to rt. The reaction was next quenched by dropwise addition of $NH_4Cl$, and the aqueous phase was extracted with $Et_2O$ (3 x 15 mL). The combined organic layers were dried over $MgSO_4$, filtered and concentrated under reduced pressure. The resulting residue was purified by flash chromatography (10:0 to 8:2 hexane/EtOAc gradient) to give 750 mg (2.63 mmol, 64%) of compound **56**, as a colorless oil.

$[\alpha]_D$ -1.7 (*c* 1.1, $CHCl_3$); $^1H$ NMR ($\delta$, 500 MHz, $CDCl_3$): 1.44-1.63 (m, 17H), 2.08-2.22 (m, 1H), 2.26-2.39 (m, 1H), 3.67-4.15 (m, 4H), 4.97 (d, *J*=9.5 Hz, 1H), 5.05 (d, *J*=17.0 Hz, 1H), 5.78-5.90 (m, 1H); $^{13}C$ NMR ($\delta$, 101 MHz, $CDCl_3$): 28.5, 29.03, 29.9, 30.9, 33.7, 65.5, 70.6, 74.0, 79.5, 99.2, 115.2, 138.1, 155.8. HRMS calculated for $C_{15}H_{27}NNaO_4$: 308.1838 $[M+ Na]^+$. Found: 308.1823.

### (*S*)-*tert*-Butyl 4-[(1*R*,4*E*)-1-hydroxyhexadec-4-en-1-yl]-2,2-dimethyloxazolidine-3-carboxylate (54a)

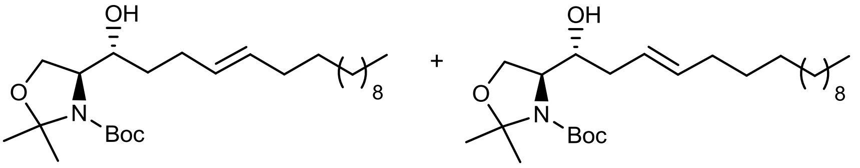

According to *general procedure 2*, compound **54a** was obtained from alkene **56** (265 mg, 0.93 mmol), 1-tridecene (880 μL, 3.72 mmol), and Grubb's 2$^{nd}$ generation catalyst (39 mg) in $CH_2Cl_2$ (20 mL). After flash chromatographic purification (10:0 to 7:3 hexane/EtOAc gradient), 180 mg (0.41 mmol, 44%) of compounds **54a** and **54b** were isolated as an inseparable mixture (colorless oil).

Data for the mixture of **54a** and **54b**:

$^1$H NMR ($\delta$, 500 MHz, $CDCl_3$)(mixture of isomers): 0.88 (t, *J*=7.0 Hz, 3H), 1.21-1.35 (m, 20H), 1.38-1.53 (m, 15H), 1.54-1.63 (m, 4H), 2.17-2.31 (m, 1H), 2.00-2.15 (m, 1H), 3.64-4.12 (m, 5H), 5.36-5.48 (m, 2H); $^{13}$C NMR ($\delta$, 101 MHz, $CDCl_3$) (mixture of isomers): 14.3, 22.8, 26.6, 28.5, 29.2, 29.4, 29.5, 29.7, 29.7, 29.8, 29.8, 32.1, 32.8, 62.5, 65.1, 72.7, 73.9, 81.2, 94.4, 129.7, 131.1. HRMS calculated for $C_{26}H_{49}NNaO_4$: 462.3559 [M+Na]$^+$. Found: 462.3566.

### *N*-(2*S*,3*R*,*E*)-(1,3-Dihydroxyoctadec-6-en-2-yl)octanamide (RBM2-85)

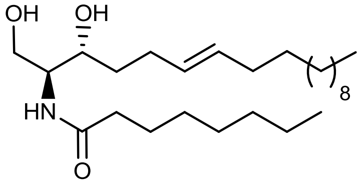

According to *general procedure 3*, crude **55** was obtained from the isomeric mixture **54a** and **54b** (165 mg, 0.38 mmol), and acetyl chloride (600 μL) in MeOH (10 mL). Concentration under reduced pressure gave crude compound, as a white solid, which was used without further purification.

*N*-Acylation of **55** (0.38 mmol) was carried out from octanoic acid (66 μL, 0.42 mmol), HOBt (61 mg, 0.45 mmol), EDC (116 mg, 0.61 mmol), $Et_3N$ (106 μL, 0.76 mmol) in $CH_2Cl_2$ (6 mL), according to *general procedure 4*. After flash chromatographic purification (79.75:20:0.25 to 49.75:50:0.25 hexane/EtOAc/MeOH gradient), 16 mg (0.04 mmol, 10%) of desired compound **RBM2-85**, and 19 mg (0.05 mmol, 12%) of isomer **RBM2-98** were obtained. Both compounds were isolated as white solids. The physical and spectroscopic data of **RBM2-85** were identical to those reported in the literature.[5]

$[\alpha]_D$ -1.3 (*c* 1.2, $CHCl_3$); lit[5] $[\alpha]_D$ -2.4 (*c* 2.20, $CHCl_3$); $^1$H NMR ($\delta$, 400 MHz, $CDCl_3$): 0.88 (t, *J*=7.0 Hz, 6H), 1.14-1.41 (m, 26H), 1.49-1.70 (m, 4H), 1.97 (q, *J*=8.5 Hz, 2H), 2.10 (q, *J*=7.0 Hz, 2H), 2.24 (t, *J*=8.0 Hz, 2H), 2.59 (brs, 1H), 2.66 (brs, 1H), 3.75-3.88 (m, 2H), 3.89-3.95 (m, 1H), 3.98 (t, *J*=6.0 Hz, 1H), 5.34-5.52 (m, 2H), 6.15 (d, *J*=8.0 Hz, 1H); $^{13}$C NMR ($\delta$, 101 MHz, $CDCl_3$): 14.2, 14.3, 22.8, 22.9, 26.0, 29.0, 29.2, 29.4, 29.5, 29.7, 29.7, 29.8, 29.9, 31.9, 32.1, 32.7, 34.2, 37.1, 53.3, 65.8, 73.0, 129.2, 132.0, 174.1. HRMS calculated for $C_{26}H_{52}NO_3$: 426.3947 [M+H]$^+$. Found: 426.3954. HRMS calculated for $C_{26}H_{51}NNaO_3$: 448.3767 [M+Na]+. Found: 448.3777.

Data for **RBM2-98**:

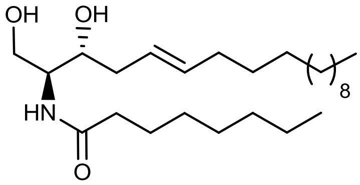

$[\alpha]_D$ +7.5 (*c* 0.8, $CHCl_3$); $^1H$ NMR (*δ*, 400 MHz, $CDCl_3$): 0.88 (t, *J*=7.0 Hz, 6H), 1.17-1.44 (m, 26H), 1.57-1.71 (m, 4H), 1.97 (q, *J*=7.0 Hz, 2H), 2.08-2.28 (m, 4H), 2.71 (brs, 1H), 2.79 (brs, 1H), 3.71-3.86 (m, 3H), 4.01 (dd, *J*= 11.0, 3.0 Hz, 1H), 5.36-5.53 (m, 2H), 6.35 (d, *J*=7.5 Hz, 1H); $^{13}C$ NMR (*δ*, 101 MHz, $CDCl_3$): 14.2, 14.3, 22.8, 22.9, 25.9, 29.2, 29.4, 29.4, 29.5, 29.6, 29.7, 29.8, 29.9, 31.8, 32.1, 32.7, 34.3, 37.0, 54.0, 62.7, 74.1, 129.2, 132.1, 173.7. HRMS calculated for $C_{26}H_{52}NO_3$: 426.3947 $[M+H]^+$. Found: 426.3966. HRMS calculated for $C_{26}H_{51}NNaO_3$: 448.3767 $[M+Na]^+$. Found: 448.3784.

### (*S*)-*tert*-Butyl 4-[(*R*,*E*)-1-hydroxy-4-oxobut-2-en-1-yl]-2,2-dimethyloxazolidine-3-carboxylate (62)

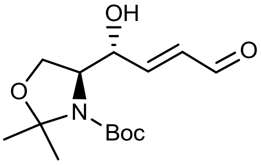

Compound **62** (146 mg, 0.51 mmol, 53%) was obtained, as a yellow oil, from alkene **7** (250 mg, 0.97 mmol), acrolein (260 μL, 3.89 mmol), and Grubb's 2nd generation catalyst (50 mg) in $CH_2Cl_2$ (20 mL), according to *general procedure 2*. Purification was carried out by flash chromatography (6:4 hexane/EtOAc).

$[\alpha]_D$ -7.4 (*c* 0.9, $CHCl_3$); $^1H$ NMR (*δ*, 500 MHz, $CDCl_3$): 1.45-1.51 (m, 15H), 3.91 (d, *J*=9.5 Hz, 1H), 4.14 (t, *J*=8.5 Hz, 1H), 4.32 (d, *J*=6.5 Hz, 1H), 4.54 (brs, 1H), 4.99 (d, *J*=7.0 Hz, 1H), 6.47 (dd, *J*=15.5, 7.5 Hz, 1H), 6.88 (dd, *J*=15.5, 3.2 Hz, 1H), 9.64 (d, *J*=8.0 Hz, 1H); $^{13}C$ NMR (*δ*, 101 MHz, $CDCl_3$): 24.1, 26.6, 28.4, 53.5, 62.0, 65.2, 74.2, 82.1, 94.9, 132.6, 155.8, 193.3. HRMS calculated for $C_{14}H_{23}NNaO_5$: 308.1474 $[M+Na]^+$. Found: 308.1489.

### Dodecyl(triphenyl)phosphonium bromide (66)

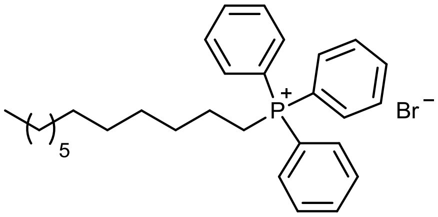

To a 25 mL two necked round bottom flask fitted with a reflux condenser, $PPh_3$ (3.16 g, 12.04 mmol) was added portionwise to neat 1-bromododecane (1.00 g, 4.01 mmol). The reaction mixture was heated at 85 °C, and allowed to stir at this temperature overnight. After cooling down to rt, the resulting precipitate was taken up $CH_2Cl_2$ and flash chromatographed (95:5 $CH_2Cl_2$/MeOH) to give 2.01 g (3.93 mmol, 98%) of compound **66**, as a colorless foam.

$^1$H NMR ($\delta$, 500 MHz, $CDCl_3$): 0.85 (t, J=7.0 Hz, 3H), 1.14-1.29 (m, 16H), 1.55-1.68 (m, 4H), 3.73-3.86 (m, 2H), 7.66-7.72 (m, 6H), 7.75-7.81 (m, 3H), 7.81-7.88 (m, 6H); $^{13}$C NMR ($\delta$, 75 MHz, $CDCl_3$): 14.3, 22.6, 22.8, 23.2, 29.2-29.9 (m), 30.54 (d, $J_{C\text{-}P}$=15.4 Hz), 32.0, 118.7 (d, $^1J_{C\text{-}P}$=85.7 Hz), 130.6 (d, $^2J_{C\text{-}P}$=12.5 Hz), 133.9 (d, $^3J_{C\text{-}P}$ =9.9 Hz), 135.05 (d, $^4J_{C\text{-}P}$=3.0 Hz).

### (*S*)-*tert*-Butyl 4-[(*R*,2*E*,4*E*)-1-hydroxyhexadeca-2,4-dien-1-yl]-2,2-dimethyloxazolidine-3-carboxylate (60)

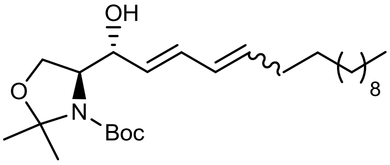

A solution of bromide **66** (1.20 g, 2.37 mmol) in anhydrous THF (20 mL) was cooled down to -78 °C, followed by dropwise addition of *n*BuLi (1.14 mL, 2.84 mmol, 2.5 M in hexane) over ~15 min period under argon atmosphere. The resulting orange solution was allowed to warm to 0 °C, and next stirred for 30 min. After cooling down to -78 °C, a solution of aldehyde **62** (286 mg, 1.00 mmol) in anhydrous THF (2 mL) was added dropwise. After vigorous stirring at -78 °C for 4 h, the reaction mixture was quenched by addition of MeOH (10 mL) at this temperature. The mixture was allowed to slowly warm to rt, and concentrated under reduced pressure. The resulting residue was taken up in EtOAc (25 mL), and the organic layer was successively washed with water and brine. The combined organic layers were dried over $MgSO_4$, filtered and concentrated *in vacuo*. Purification by flash chromatography (100:0 to 85:15 hexane/EtOAc gradient) gave 293 mg (0.67 mmol, 67%) of an inseparable mixture of (4*E*,6*E*)-**60** and (4*E*,6*Z*)-**63** in a ~7:3 ratio, as a colorless oil.

Data for the mixture of (4*E*,6*E*)-**60** and (4*E*,6*Z*)-**63**:
$^1$H NMR ($\delta$, 500 MHz, $CDCl_3$): 0.87 (t, *J*=7.0 Hz, 4H), 1.20-1.32 (m, 22H), 1.32-1.40 (m, 3H), 1.43-1.56 (m, 19H), 1.56-1.67 (m, 2H), 2.06 (q, *J*=7.0 Hz, 2H), 2.16 (q, *J*=7.5 Hz, 0.8H), 3.80-4.45 (m, 6H), 5.37-5.75 (m, 2.5H), 5.95-6.06 (m, 1.3H), 6.26 (t, *J*=12.5 Hz, 0.8H), 6.61 (t, *J*=13.5 Hz, 0.4H); $^{13}$C NMR ($\delta$, 101 MHz, $CDCl_3$): 14.3, 22.8, 24.7, 26.4, 28.5, 29.3, 29.4, 29.5, 29.6, 29.7, 29.7-29.8 (m), 32.1, 32.8, 62.5, 65.0, 74.0, 81.3, 94.6, 127.0, 129.0, 129.6, 132.1, 135.6. HRMS calculated for $C_{26}H_{47}NNaO_4$: 460.3403 $[M+Na]^+$. Found: 460.3410.

### ***N*-[(2*S*,3*R*,4*E*,6*E*)-1,3-Dihydroxyoctadeca-4,6-dien-2-yl]octanamide (RBM2-76)**

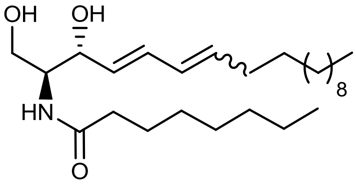

Crude **61** was obtained from the mixture of olefins **60** and **63** (80 mg, 0.18 mmol), using acetyl chloride (300 μL) in MeOH (5 mL), according to *general procedure 3*. Concentration under reduced pressure gave **61**, as a white solid, which was used without further purification.

*N*-acylation of **61** (0.18 mmol) was carried out from octanoic acid (31 μL, 0.20 mmol), HOBt (29 mg, 0.22 mmol), EDC (56 mg, 0.29 mmol), and $Et_3N$ (50 μL, 0.36 mmol) in $CH_2Cl_2$ (5 mL), according to *general procedure 4*. Purification by flash chromatography (8:2 hexane/*t*-BuOMe, followed by 100:0 to 97:3 $CH_2Cl_2$/MeOH gradient) afforded 17 mg (0.04 mmol, 22%) of an inseparable mixture of (4*E*,6*E*)-**RBM2-76** and (4*E*,6*Z*)-**RBM2-82** in a ~4:6 ratio, and 11 mg (0.03 mmol, 14%) of compound **64**. Both compounds were isolated as a white solid.

Data for the mixture of (4*E*,6*E*)-**RBM2-76** and (4*E*,6*Z*)-**RBM2-82**:

$^1$H NMR (*δ*, 500 MHz, $CDCl_3$): 0.88 (t, *J*=7.0 Hz, 10H), 1.20-4.42 (m, 45.5H), 1.60-1.68 (m, 3.8H), 2.08 (q, *J*=7.0 Hz, 1.3H), 2.18 (q, *J*=7.5 Hz, 2H), 2.21-2.27 (m, 2.8H), 3.68-3.74 (m, 1.5H), 3.91-4.01 (m, 2.6H), 4.41 (t, *J*=4.5 Hz, 0.5H), 4.46 (t, *J*=4.5 Hz, 0.7H), 5.50 (dd, *J*=18.0, 7.5, 0.9H), 5.61 (dd, *J*=15.5, 6.5, 0.7H), 5.67-5.78 (m, 1.5H), 5.95-6.08 (m, 1.6H), 6.21-6.34 (m, 2H), 6.62 (dd, *J*=15.0, 11.0 Hz, 0.8H). HRMS calculated for $C_{26}H_{49}NNaO_3$: 446.3610 $[M+Na]^+$. Found: 446.3603.

Data for **64**:

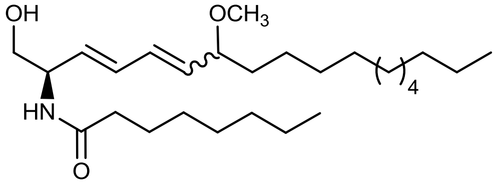

$^1$H NMR (δ, 500 MHz, $CDCl_3$): 0.88 (t, *J* = 6.8 Hz, 6H), 1.21-1.48 (m, 26H), 1.53-1.61 (m, 2H), 1.65 (quint, *J*=7.0 Hz, 2H), 2.23 (t, *J*=7.6 Hz, 2H), 3.25 (s, 3H), 3.53 (q, *J*=6.8 Hz, 1H), 3.72 (qd, *J*=11.1, 4.5 Hz, 2H), 4.62 (quint, *J*=5.5 Hz, 1H), 5.53 (dd, *J*=15.0, 7.9 Hz, 1H), 5.65 (dd, *J*=15.2, 6.0 Hz, 1H), 5.79 (d, *J*=7.2 Hz, 1H), 6.11-6.27 (m, 2H); $^{13}$C NMR (δ, 101 MHz, $CDCl_3$): 14.2, 14.3, 22.7, 22.8, 25.5, 25.9, 29.2, 29.4, 29.5, 29.7, 29.8, 29.9, 31.8, 32.1, 35.8, 37.0, 53.2, 56.4, 62.8, 82.2, 129.7, 131.1, 131.9, 135.5, 173.7. HRMS calculated for $C_{27}H_{51}NNaO_3$: 460.3767 $[M+Na]^+$. Found: 460.3770.

### (*S*)-*tert*-Butyl 4-[(*R*,2*E*,4*Z*)-1-hydroxyhexadeca-2,4-dien-1-yl]-2,2-dimethyloxazolidine-3-carboxylate (63)

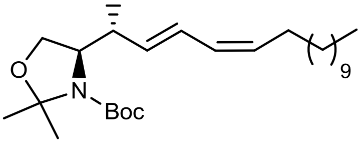

A solution of bromide **66** (297 mg, 0.59 mmol) in anhydrous THF (8 mL) was cooled down to -78 °C, followed by dropwise addition of *n*BuLi (280 μL, 2.84 mmol, 2.5 M in hexane) over a ~30 min period under argon atmosphere. The resulting orange solution was allowed to warm to 0 °C, and next stirred for 30 min. After cooling down to -78 °C, a solution of aldehyde **62** (50 mg, 0.18 mmol) in anhydrous THF (2 mL) was added dropwise. After vigorous stirring at -78 °C for 15 min, the reaction mixture was allowed to warm gradually to rt kept at this temperature for 2 h under stirring. The reaction mixture was quenched by addition of aqueous sat. $NH_4Cl$ (4 mL), and stirred for 30 min. The aqueous phase was extracted with EtOAc (3 x 10 mL), and the combined organic layers were dried over $MgSO_4$ and filtered. Concentration under reduced pressure afforded a crude, which was purified by flash chromatography (10:0 to 8:2 hexane/EtAcO gradient) to give 47 mg (0.11 mmol, 61%) of **63**, as a colorless wax.

$[\alpha]_D$ -2.8 (*c* 0.9, $CHCl_3$) ; $^1H$ NMR (*δ*, 500 MHz, $CDCl_3$): 1.22-1.38 (m, 21H), 1.44-1.55 (m, 15H), 2.16 (q, *J*=7.5 Hz, 2H), 3.81-4.47 (m, 4H), 5.39-5.50 (m, 1H), 5.64 (dd, *J*=14.5, 3.5 Hz, 1H), 5.99 (t, *J*=11.0 Hz, 1H), 6.61 (t, *J* = 13.5 Hz, 1H); $^{13}C$ NMR (*δ*, 126 MHz, $CDCl_3$): 14.3, 22.8, 26.4, 28.0, 28.5, 29.4, 29.5, 29.7, 29.7-29.8 (m), 32.1, 62.5, 65.1, 74.1, 81.3, 94.6, 127.0, 127.8, 131.3, 133.0. HRMS calculated for $C_{26}H_{47}NNaO_4$: 460.3403 $[M+Na]^+$. Found: 460.3400.

### ***N*-[(2*S*,3*R*,4*E*,6*Z*)-1,3-Dihydroxyoctadeca-4,6-dien-2-yl]octanamide (RBM2-82)**

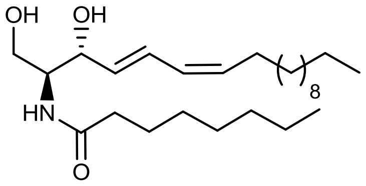

Crude **65** (0.10 mmol) was obtained from **63** (44 mg, 0.10 mmol), and acetyl chloride (300 μL) in MeOH (5 mL), according to *general procedure 3*. Concentration *in vacuo* afforded **65** as a white solid, which was used without further purification.

According to *general procedure 4*, *N*-acylation of **65** was carried out from octanoic acid (18 μL, 0.11 mmol), HOBt (16 mg, 0.12 mmol), EDC (31 mg, 0.16 mmol), and $Et_3N$ (28 μL, 0.20 mmol) in $CH_2Cl_2$ (5 mL). After flash chromatographic purification, 9 mg (0.02 mmol, 21%) of **RBM2-82**, and 4 mg (0.01 mmol, 4%) of **64** were obtained. Both compounds were isolated as white solids.

$[\alpha]_D$ -3.3 (*c* 0.4, $CHCl_3$); $^1H$ NMR (*δ*, 500 MHz, $CDCl_3$): 0.88 (t, *J*=7.0 Hz, 6H), 1.22-1.40 (m, 26H), 1.64 (quint, *J*=7.5 Hz, 2H), 2.18 (q, *J*=7.5 Hz, 2H), 2.24 (t, *J*=7.5 Hz, 2H), 3.72 (dd, *J*=11.0, 3.0 Hz, 1H), 3.92-4.00 (m, 2H), 4.45 (t, *J*=4.0 Hz, 1H), 5.50 (dd, *J*=18.0, 8.0 Hz, 1H), 5.70 (dd, *J*=15.5, 6.2 Hz, 1H), 5.99 (t, *J*=11.0 Hz, 1H), 6.29 (d, *J*=7.5 Hz, 1H), 6.61 (dd, *J*=15.0, 11.0 Hz, 1H), $^{13}$C NMR (*δ*, 101 MHz, $CDCl_3$): 14.2, 14.3, 22.8, 22.5, 25.9, 28.0, 29.2, 29.4, 29.5, 29.6, 29.7, 29.8-29.9 (m), 31.8, 32.1, 37.0, 54.7, 62.6, 74.7, 127.4, 127.8, 131.4, 134.2, 174.1. HRMS calculated for $C_{26}H_{49}NNaO_3$: 446.3610 [M+Na]$^+$. Found: 446.3614.

### 5.1.10 Synthesis of tags 1-5 and St1

**General procedure 9: acylation of azadibenzocyclooctyne 41**

To a solution of commercially available azadibenzocyclooctyne **41** (5 mg, 0.010 mmol), and DIPEA (5 µL, 0.025 mmol) in anhydrous DMF (2 mL), the corresponding alkyl amine (0.02 mmol) was added under argon atmosphereand stirred at rt overnight. Concentration under reduced pressure gave crude tags, which were flash chromatographed (100:0 to 96:4 $CH_2Cl_2$/MeOH gradient) to give the corresponding pure compounds.

***N*$^1$-Ethyl-*N*$^5$-[3-oxo-3-(7-azadibenzo[b,f]cyclooctyn-7-yl)propyl]glutaramide (tag1)**

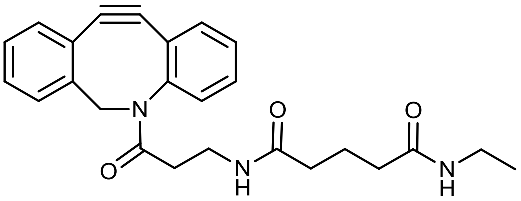

3.1 mg (0.01 mmol, 74%) of tag **1** were obtained, as a colorless oil, from **41** (5 mg, 0.01 mmol), and ethylamine (1.6 µL, 0.02 mmol) in DMF (2 mL), according to *general procedure 9*.

$^1$H NMR (δ, 400 MHz, $CD_3OD$): 1.11 (t, *J*=7.2 Hz, 3H), 1.74 (quint, *J*=7.2 Hz, 2H), 1.99-2.12 (m, 5H), 2.41-2.51 (m, 1H), 3.13-3.24 (m, 4H), 3.72 (d, *J*=14.0 Hz, 1H), 5.15 (d, *J*=14.0 Hz, 1H), 7.27 (dd, *J*=7.4, 1.6 Hz, 1H), 7.29-7.50 (m, 6H), 7.66 (d, *J*=6.9 Hz, 1H). HRMS calculated for $C_{25}H_{27}N_3NaO_3$: 440.1950 [M+Na]$^+$. Found: 440.1965.

### ***N***$^1$-Propyl-***N***$^5$-[3-oxo-3-(7-azadibenzo[b,f]cyclooctyn-7-yl)propyl]glutaramide (tag2)

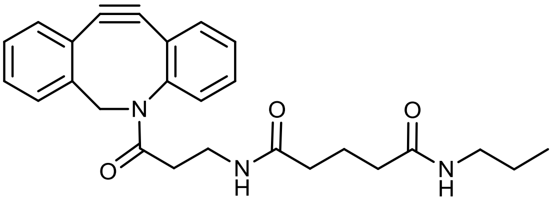

3.4 mg (0.01 mmol, 80%) of tag **2** were obtained, as a colorless oil, from **41** (5 mg, 0.01 mmol), and propylamine (1.3 μL, 0.02 mmol) in DMF (2 mL), according to *general procedure 9*.

$^1$H NMR (δ, 400 MHz, CDCl$_3$): 0.93 (t, *J*=7.6 Hz, 3H), 1.54 (sext, *J*=7.2 Hz, 2H), 1.83 (quint, *J*=7.2 Hz, 2H), 1.94-2.10 (m, 3H), 2.16 (t, *J*=6.8 Hz, 2H), 2.47 (ddd, *J*=16.6, 7.4, 4.0 Hz, 1H), 2.87 (t, *J*=5.6 Hz, 1H), 3.17-3.27 (m, 3H), 3.27-3.41 (m, 1H), 3.71 (d, *J*=13.9 Hz, 1H), 5.14 (d, *J*=13.9 Hz, 1H), 7.27-7.44 (m, 7H), 7.66 (d, *J*=7.3 Hz, 1H). HRMS calculated for $C_{26}H_{30}N_3NaO_3$: 454.2107 [M+Na]$^+$. Found: 454.2106.

### ***N***$^1$-Butyl-***N***$^5$-[3-oxo-3-(7-azadibenzo[b,f]cyclooctyn-7-yl)propyl]glutaramide (tag3)

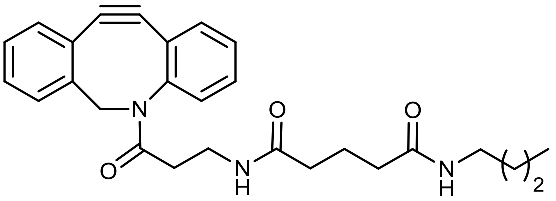

According to *general procedure 9*, 3.3 mg (0.01 mmol, 75%) of tag **3** were obtained, as a colorless oil, from **41** (5 mg, 0.01 mmol), and butylamine (1.5 μL, 0.02 mmol) in DMF (2 mL).

$^1$H NMR (δ, 400 MHz, CD$_3$OD): 0.94 (t, *J*=7.2 Hz, 3H), 1.33-1.41 (m, 2H), 1.48 (quint, *J*=8.0 Hz, 2H), 1.74 (quint, *J*=7.6 Hz, 2H), 1.99-2.14 (m, 5H), 2.42-2.51 (m, 1H), 3.10-3.28 (m, 4H), 3.72 (d, *J*=14.0 Hz, 1H), 5.14 (d, *J*=14.0 Hz, 1H), 7.27 (dd, *J*=7.2, 1.6 Hz, 1H), 7.30-7.52 (m, 6H), 7.66 (d, *J*=7.0 Hz, 1H). HRMS calculated for $C_{27}H_{31}N_3NaO_3$: 468.2263 [M+Na]$^+$. Found: 468.2277.

### *N*¹-Pentyl-*N*⁵-[3-oxo-3-(7-azadibenzo[b,f]cyclooctyn-7-yl)propyl]glutaramide (tag4)

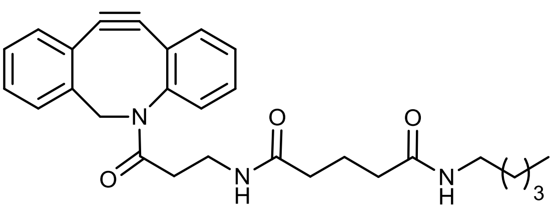

According to *general procedure 9*, 3.4 mg (0.01 mmol, 73%) of tag **4** were obtained, as a colorless oil, from **41** (5 mg, 0.01 mmol) and pentylamine (1.8 μL, 0.02 mmol) in DMF (2 mL).

$^1$H NMR (δ, 400 MHz, $CDCl_3$): 0.90 (t, *J*=7.2 Hz, 3H), 1.28-1.34 (m, 4H), 1.45-1.53 (m, 2H), 1.82 (quint, *J*=7.2 Hz, 2H), 1.95-2.11 (m, 5H), 2.46 (ddd, *J*=16.6, 7.3, 3.8 Hz, 1H), 3.17-3.26 (m, 3H), 3.29-3.39 (m, 1H), 3.71 (d, *J*=13.9 Hz, 1H), 5.14 (d, *J*=13.9 Hz, 1H), 7.27-7.44 (m, 7H), 7.66 (d, *J*=7.2 Hz, 1H). HRMS calculated for $C_{28}H_{33}N_3NaO_3$: 482.2420 [M+Na]$^+$. Found: 482.2412.

### *N*¹-Hexyl-*N*⁵-[3-oxo-3-(7-azadibenzo[b,f]cyclooctyn-7-yl)propyl]glutaramide (tag5)

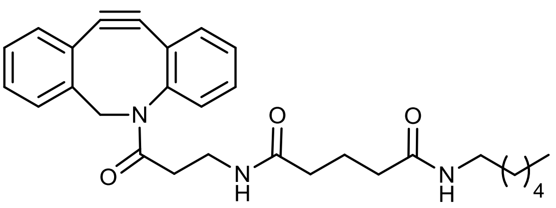

3.7 mg (0.01 mmol, 78%) of tag **5** were obtained, as a colorless oil, from **41** (5 mg, 0.01 mmol), and hexylamine (2.0 μL, 0.02 mmol) in DMF (2 mL), according to *general procedure 9*.

$^1$H NMR (δ, 400 MHz, $CD_3OD$): 0.91 (t, *J*=6.8 Hz, 3H), 1.27-1.38 (m, 6H), 1.43-1.54 (m, 2H), 1.74 (quint, *J*=7.2 Hz, 2H), 1.98-2.13 (m, 5H), 2.41-2.51 (m, 1H), 3.09-3.18 (m, 3H), 3.20-3.29 (m, 1H), 3.72 (d, *J*=14.0 Hz, 1H), 5.14 (d, *J*=14.0 Hz, 1H), 7.27 (dd, *J*=7.4, 1.6 Hz, 1H), 7.30-7.51 (m, 6H), 7.66 (dd, *J*=7.3, 1.2 Hz, 1H). HRMS calculated for $C_{29}H_{36}N_3O_3$: 474.2757 [M+H]$^+$. Found: 474.2783.

**Triazole standard (St1)**

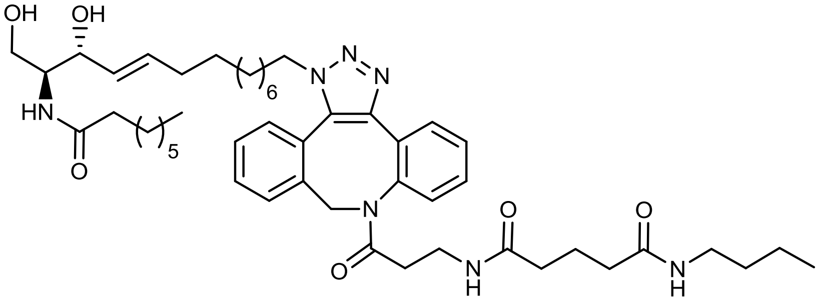

To a solution of **RBM2-37** (1.6 mg, 4 μmol) in MeOH (0.5 mL), a solution of **tag 3** (1.7 mg, 4 μmol) in MeOH (0.5 mL) was added. After vigorously stirring for 2 h at rt, the reaction mixture was concentrated under reduced pressure. The resulting residue was purified by flash column chromatography (100:0 to 90:10 $CH_2Cl_2$/MeOH gradient) to obtain 3.4 mg (4 μmol, quantitative) of **St1** as a mixture of regioisomers (colorless oil).

HRMS calculated for $C_{49}H_{73}N_7NaO_6$: 878.5520 $[M+Na]^+$. Found: 878.5500.

## 5.1.11 Synthesis of fluorescent dye D1

***tert*-Butyl [5-[3-(3',6'-dihydroxy-3-oxo-3*H*-spiro[isobenzofuran-1,9'-xanthen]-5-yl)thioureido]pentyl]carbamate (44)**

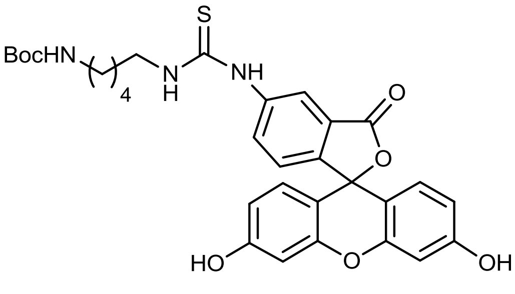

A solution of fluorescein isothiocyanate **43** (61 mg, 0.16 mmol) in anhydrous DMF (2.5 mL) was added to a solution of *N*-Boc-cadaverine **42** (66 μL, 0.32 mmol) and $Et_3N$ (56 μL, 0.40 mmol) in anhydrous DMF (2.5 mL) under argon atmosphere. The reaction mixture was stirred at rt overnight and protected from light. Concentration under reduced pressure afforded a crude, which was purified by flash chromatography (99.9:0:0.1 to 94.9:5:0.1 $CH_2Cl_2$/MeOH/$CH_3COOH$ gradient) to give 70 mg (0.12 mmol, 75%) of **44** as an orange oil.

$^1$H NMR ($\delta$, 400 MHz, $CD_3OD$): 1.37-1.47 (m, 11H), 1.54 (q, $J$=7.5 Hz, 2H), 1.68 (q, $J$=7.0 Hz, 2H), 3.06 (t, $J$=7.0 Hz, 2H), 3.56-3.65 (m, 2H), 6.53 (d, $J$=2.5 Hz, 1H), 6.56 (d, $J$=2.5 Hz, 1H), 6.65-6.70 (m, 4H), 7.15 (d, $J$= 8.0 Hz, 1H), 7.76 (dd, $J$=8.5, 1.5 Hz, 1H), 8.11 (d, $J$=1.5 Hz, 1H). $^{13}$C NMR ($\delta$, 101 MHz, $CD_3OD$): 25.2, 28.8, 29.6, 30.6, 41.2, 45.5, 79.9, 103.5, 111.6, 113.7, 119.9, 125.6, 128.9, 130.3, 131.8, 142.3, 149.5, 154.1, 158.5, 161.4, 171.1, 175.2, 182.5. HRMS calculated for $C_{31}H_{33}N_3NaO_7S$: 614.1937 $[M+Na]^+$. Found: 614.1935.

### Dibenzocyclooctyne-fluorescein dye ( D1)

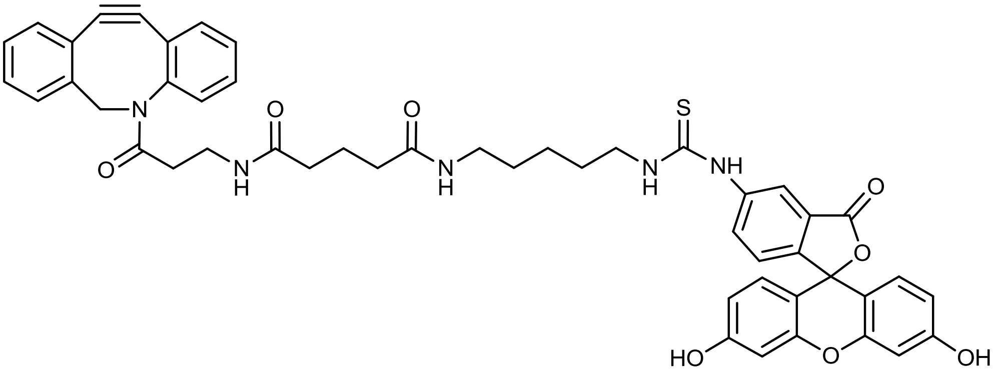

Near acetyl chloride (720 μL) was added dropwise over a solution of compound **44** (70 mg, 0.12 mmol) in MeOH (12.0 mL). After vigorous stirring at rt for 2 h in the dark, the reaction mixture was concentrated *in vacuo*. The resulting orange solid was taken up in DMF (2 mL) and added dropwise to a solution of azadibenzocyclooctyne **41** (40 mg, 0.08 mmol) and DIPEA (66 μL, 0.36 mmol) in anhydrous DMF (2 mL). After vigorous stirring at rt overnight in the dark, the reaction mixture was concentrated *in vacuo.* The resulting residue was purified with Amberlite XAD-4 resin (100:0 to 0:100 water/ACN gradient) to afford 30 mg (0.04 mmol, 42%) of fluorescent dye **D1**, as an orange solid.

$^1$H NMR ($\delta$, 400 MHz, $CD_3OD$): 1.14 (dd, $J$=6.0, 3.0 Hz, 1H), 1.26-1.49 (m, 4H), 1.58 (q, $J$=8.0 Hz, 2H), 1.64-1.80 (m, 4H), 2.00-2.23 (m, 6H), 2.39-2.49 (m, 1H), 3.08-3.25 (m, 3H), 3.59-3.66 (m, 2H), 3.69 (d, $J$=14.0 Hz, 1H), 5.13 (d, $J$=14.0 Hz, 1H), 6.52-6.56 (m, 2H), 6.55-6.70 (m, 2H), 7.11-7.16 (m, 1H), 7.20–7.78 (m, 10H), 7.86-7.95 (m, 1H), 8.12 (s, 1H); $^{13}$C NMR ($\delta$, 101 MHz, $CD_3OD$): 23.2, 25.3, 29.6, 30.1, 35.4, 36.1, 36.3, 36.7, 40.2, 56.6, 58.3, 103.5, 108.9, 111.7, 113.9, 115.6, 125.9, 126.5, 128.1, 128.9, 129.2, 129.7, 129.9, 130.4, 133.4, 149.5, 152.2, 171.2, 173.2, 175.1, 175.3. HRMS calculated for $C_{49}H_{46}N_5O_8S$: 864.3067 $[M+H]^+$. Found: 864.3053. HRMS calculated for $C_{49}H_{45}N_5NaO_8S$: 886.2887 $[M+Na]^+$. Found: 886.2900.

UV-vis (0.1 M NaOH): $\lambda_{max}$ (abs)=491 nm, $\lambda_{max}$ (em)=521 nm, $\varphi_f$=0.20±0.04 (reference: fluorescein in 0.1 M NaOH, $\varphi_f$=0.95 ± 0.03).

## 5.2 Evaluation of click reactions in solution

### 5.2.1 SPAAC between azido probe RBM2-37 and tags 1-5

Azide **RBM2-37** (150 pmol from 15 μL of a 10 μM MeOH solution) was placed in a 7 mL glass vial and treated with the corresponding tag (7.5 nmol, from 15 μL of a 500 μM MeOH solution). The resulting mixture was diluted with MeOH (470 μL), stirred at 48 ºC overnight, and next transferred to an UPLC vial. After concentration under a stream of nitrogen, the resulting residue was taken up in MeOH (130 μL) and analyzed by UPLC-TOF.

### 5.2.2 SPAAC between dye D1 and azido probe RBM2-87

#### Click reactions in MeOH

Azide **RBM2-87** (35 μL of a 4.5 mM MeOH solution) and dye **D1** (20 μL of a 7.5 mM MeOH solution) were placed in a glass vial and diluted with MeOH (95 μL) to obtain final substrate concentrations around 1 mM for each component. The reaction mixture was stirred at rt for different reaction times, prior to HPLC sample analysis.

#### Click reactions in growth media

Azide **RBM2-87** (35 μL of a 4.5 mM MeOH solution) and dye **D1** (10 μL of a 15 mM MeOH solution) were successively added to a glass vial containing the culture media (105 μL of DMEM or MEM) for a final concentration of around 1 mM each. The reaction mixture was incubated at 37 ºC for different reaction times and each sample was next centrifuged in a Nanosep Centrifugal Device 10K OMEGA at 14 rpm for 15 min. The filtered fluids were recovered and analyzed by HPLC.

### Stantard solutions and standard curves

Fluorescent dye **D1** was identified at 5.03 min by mass and absorbance detection (220 nm). Calibration curves were obtained by linear least-square regression analysis of **D1** peak area versus **D1** concentrations for 0.125, 0.25, 0.5 and 1 mM **D1** in MeOH, DMEM or MEM medium. Percent reaction conversion was monitored by disappearance of fluorescent dye **D1**, as determined by integration of the corresponding peak for each reaction time.

### 5.2.3 Diels-Alder reaction between RBM2-76 and PTAD

A solution of **RBM2-76** (100 μL of a 2mg/mL MeOH solution) was transferred to a 5-mL glass vial, followed by addition of a solution of PTAD (100 μL of a 0.8 mg/mL MeOH solution). After 30 min, adduct formation was analyzed by FIA, as described in Section 4.1.1.

### 5.2.4 Mass spectrometry

A Waters Aquity UPLC system coupled to a Waters LCT Premier orthogonal accelerated time-of-flight mass spectrometer (Waters, Millford, MA) was used to analyze the reaction click samples. The samples were injected onto a reversed-phase C18 column (1.7 μm C18 Acquity UPLC BEH, 2.1 x 100 mm, Waters) at 0.3 mL/min. Solvent A [methanol-formic acid (99.8:0.2, v/v) with 1mM ammonium formate] and solvent B [water-formic acid (99.8:0.2, v/v) with 2mM ammonium formate] were used as eluents. The samples were eluted through the following linear gradient conditions: 0.0 min, 65% A; 8.0 min, 90% A; 13.0 min, 99% A; 15.0 min, 99% A; 18.0 min, 65% A. The mass spectrometer was run in the positive electrospray ionization mode. Full scan spectra from 50 to 1,500 Da were acquired, and individual spectra were summed to produce data points each 0.2 s. Mass accuracy and reproducibility were maintained by using an independent reference spray by the LockSpray interference. The column was held at 30 ºC. The injection volume was set at 10 μL. Positive identification of compounds was based on the accurate mass measurement with an error <5 ppm.

### 5.2.5 High-performance liquid chromatography

HPLC analysis were performed at 20 °C using a Supelcosil LC-18 column (25 cm x 4.6 mm inner diameter, 5 μm particle size) and a Waters HPLC system equipped with a 515 HPLC pump, a 2545 binary gradient module, a 3100 mass detector and a 2998 photodiode array detector. Solvent A (water) and solvent B (ACN) were used as eluent. The samples were eluted through the following logarithmic gradient conditions: 0.0 min, 50% B; 6.0 min, 90% B; followed by an isocratic elution: 6.1 to 20.0 min, 90% B. After each run, the column was thoroughly washed with ACN and equilibrated with the initial conditions. The mobile phase was degassed and pumped at a flow rate of 1.0 mL/min. The injection volume was set at 20 μL.

## 5.3 Biological assays

### 5.3.1 Materials and methods for cell culture

Cell culture was carried out in a sterile environment, using laminar flow cabinets provided with a UV-C germicidal lamp. Cells were grown in flasks by adherent culture system, in an incubator which maintained optimal temperature (37 °C), humidity and $CO_2$ atmosphere (5%).

A549 human lung adenocarcinoma epithelial cells were obtained from the America type Culture Collection (ATCC), and grown in DMEM (GIBCO) media supplemented with 10% Fetal Bovine Serum, and 100 ng/mL each of penicillin and streptomycin. This cell line was maintained to a maximum confluence of 80%. They were used between passages 15 and 30.

MCF-7 human cancerous breast tissue cells were obtained from the American type Culture Collection (ATCC), and grown in MEM (GIBCO) media supplemented with 10% fetal bovine serum, 0.01 mg/mL of insulin and 100 ng/mL each of penicillin and streptomycin. The cells were maintained to a maximum confluence of 70%.

As cells reached confluency (3-4 days), they were subcultured. Then, growth medium was removed by aspiration, and cells were rinsed with PBS. Cells were detached by treatment with trypsin at 37 °C (incubator) for 2-3 minutes. Cellular suspension was recovered by addition of growth medium. Cellular counting was performed in Neubauer hematocytometer, using trypan blue to selectively stain. Appropriate dilutions were performed by addition of growth medium to achieve the desired cellular suspension.

### 5.3.2 Cell viability

Cells were seeded at a density of $10^5$ cells/well in 96-well plates in fresh media (100 μL/well) and grown overnight at 37 °C and 5% $CO_2$-water saturated atmosphere. The media was next removed and replaced with fresh media (100 μL), containing the test compounds. Cells were incubated at 37 °C and 5% of $CO_2$ for 24/72 h. The number of viable cells was quantified by the estimation of its dehydrogenase activity, which reduces the 3-(4,5-dimethylthiazol-2-yl)-2,5-diphenyltetrazolium bromide (MTT) to water-insoluble formazan, which was dissolved in DMSO (100 μL/well) and measured at 570 nm with a Spectramax Plus (Molecular Device Corporation). All compounds were dissolved in EtOH and control experiments were performed with EtOH (0.1%).

### 5.3.3 Labeling of cell extracts containing ω-azido SLs through SPAAC

#### Sphingolipidomics

Cells were seeded at a density of $2.5x10^5$ cells/well in 6 well-plates, in fresh media (1 mL) and grown overnight at 37 °C and 5% $CO_2$-water saturated atmosphere. The media was next replaced with fresh media (1 mL) containing EtOH or 10 μM of the test compounds (**RBM2-31**, **RBM2-37**, **RBM2-40** or **RBM2-63**). After the specified time of incubation at 37 °C and 5% $CO_2$, cells were washed with PBS, trypsinized (trypsin-EDTA, 0.4 mL) and collected with fresh media (0.6 mL) in eppendorfs. The corresponding cellular suspensions were stored at 4 °C prior SL extraction.

#### Extraction of sphingolipids

Cells (10 μL of cellular suspension) were counted in a Countess® Automated Cell Counter, using trypan blue (10 μL). Cells were next sedimented at 9.3 x g at 4 °C for 3 min. After supernatant removal, pellets were washed twice with 4 °C PBS (200 μL), and sedimented again. The resulting pellets were resuspended in water (100 μL), followed by MeOH (500 μL), and transferred to 5-mL glass vials. $CHCl_3$ (250 μL) was added, followed by addition of internal standards (*N*-lauroyl-D-*erythro*-sphingosine, *N*-lauroyl-D-*erythro*-sphingosylphosphorylcholine, D-glucosyl-ß-1,1' *N*-lauroyl-D-*erythro*-sphingosine, and D-*erythro*-sphinganine, 0.2 nmol each). The resulting mixtures were dispersed by sonication, and SLs were extracted at 48 °C overnight. After cooling down to rt, 1 M KOH in MeOH (75 μL) was added, followed by dispersion and incubation at 37 °C for 2 h. The samples were neutralized by addition of 1 M acetic acid (75 μL), and concentrated under a stream of nitrogen. The resulting residues were taken up in MeOH (500 μL), transferred to eppendorfs, concentrated under a $N_2$ stream, and taken up in MeOH (150 μL). The resulting mixtures were centrifuged (9.3 x g, 3 min), and supernatants (130 μL) were transferred to glass vials. Samples were dried and stored at -20 °C until UPLC-TOF analysis.

### "One pot" sphingolipid extraction and SPAAC with tags 1-5

Cells were counted and pelleted as indicated above. The washed pellets were next resuspended in water (100 μL), followed by MeOH (500 μL) and transferred to 5-mL glass vials. Next, $CHCl_3$ (250 μL) was added, followed by addition of standard **St1** (0.15 nmol), internal standards (0.2 nmol of each SL indicated above), and the corresponding tags (15 nmol). Controls were treated similarly except that tags were not added. The resulting mixtures were dispersed by sonication, and incubated at 48 °C overnight. The SL extraction procedure was next continued as indicated above.

### Mass spectrometry

To determine the effect on the sphingolipidome and metabolization of ω-azidoSLs in different cell lines, samples were analyzed as described in Section 4.2.4. To analyze endogenous SL and ω-azidoSL metabolites, the following linear gradient conditions were used: 0.0 min, 80% A; 3.0 min, 90% A; 6.0 min, 90% A; 15.0 min, 99% A; 18.0 min, 99% A; 20.0 min, 80% A.

Cell extracts containing ω-azidoSL metabolites and labeled through SPAAC were analyzed by UPLC-TOF, using the same conditions described in Section 5.2.4.

### 5.3.4 Live cells labeling through SPAAC

#### Assay of fluorescence sensitivity

Cells were seeded at a density of 2.5 x $10^5$ cells/mL in 6-well plates and grown overnight at 37 ºC and 5% $CO_2$-water saturated atmosphere. The media was next removed and cells were treated with fresh media (1 mL) containing 0, 20, 50, and 100 μM **D1** for 30 min at 37 ºC and 5% $CO_2$. Next, growth media was poured off, and cells were rinsed twice with PBS.

#### Assay of dye internalization

Cells lines were seeded at a density of 2.5 x $10^5$ cells/mL in 6-well plates and grown overnight at 37 ºC and 5% $CO_2$-water saturated atmosphere . Then, media was removed and cells were treated with fresh media (1 mL) containing 100 μM **D1** for 0, 15, 30, and 60 min at 37 ºC and 5% $CO_2$.

#### Intracellular SPAAC between fluorescent dye D1 and ω-azidoSL metabolites

Cell lines were seeded at a density of 2.5 x $10^5$ cells/mL in 6-well plates and grown overnight at 37 ºC and 5% $CO_2$-water saturated atmosphere. Then, the media was poured off, and cells were treated with fresh media (1 mL) containing EtOH (vehicle) or 10 μM azido probe **RBM2-31**. After 16 h incubation, the media was poured off and cells were rinsed twice with PBS. Cells were next treated with fresh media (1 mL) containing 100 μM **D1** for 0.5, 1 and 2 h. After the corresponding incubation times, the media was poured off, and cells were rinsed with PBS and incubated with fresh media for 30 min.

#### Cell fixation for imaging by epifluorescence microscopy

Growth media was poured off, and cells were rinsed twice with PBS. Cell fixation was carried out by addition of cold (-20 ºC) MeOH, and incubation at rt for 5 min. MeOH was poured off, cells were rinsed twice with PBS, and next analyzed by epifluorescence microscopy in PBS.

### Cell fixation for FACS analysis

Cells were collected by brief trypsinization and concentrated by centrifugation (250 x g, 7 min, 4 °C). Cells were next washed twice with cold (4 °C) PBS and resuspended in cold (-20 °C) MeOH (1 mL). After incubation at rt for 5 min, cells were concentrated by centrifugation (250 x g, 7 min, 4 °C), and washed twice with cold (4 °C) PBS. Next, cells were resuspended in PBS (500 μL), containing 3% BSA and incubated at rt for 10 min. The resulting cellular suspension was stored at 4 °C until FACS analysis. Flow cytometry data on at least 10,000 cells per sample were acquired on a BD LSR2 flow cytometer (Becton Dickinson) using a 488 nm argon laser and a 530 ± 30 nm emission filter, or on 5,000 cells per sample on a Guava® Flow Cytometry easyCyte Systems using a blue laser (488 nm).

### Confocal microscopy

Cells were seeded at a density of 2.0 x $10^5$ cells/mL on coverslips in 6-well plates, and grown overnight at 37 °C and 5% $CO_2$-water saturated atmosphere. After pre-incubation with 10 μM **RBM2-31** for 5 h, cells were treated with 100 μM **D1** for 2 h at 37 °C. Next cells were rinsed twice with PBS, and incubated with fresh media for 30 min. Growth media was poured off, and cells were rinsed twice with PBS, followed by fixation with cold MeOH (-20 °C) for 5 min at rt. Next, MeOH was poured off and cells were rinsed twice with PBS, incubated with 2,5 μg/ml of propidium iodide at rt for 15 min, and rinsed 4 times with PBS (5 min each wash). All preparations were mounted in Fluoprep (Biomérieux, Marcy l'Etoile, France), and analyzed by confocal laser scanning microscopy with Leica TSC-SPE (Leica, Wetzlar, Germany).

## 5.4 Extraction and detection of click adducts from GUVs

### Extraction of click adducts from GUVs

Liposomes (10 μL) were transferred to 5 mL glass vials, followed by addition of water (100 μL), MeOH (500 μL), and $CHCl_3$ (250 μL). The resulting mixtures were incubated at 48 °C overnight. After cooling down to rt, 1 M KOH in MeOH (75 μL) was added, followed by dispersion, and incubation at 37 °C for 2 h. The samples were neutralized by addition of 1 M acetic acid (75 μL), concentrated under a stream of nitrogen, and resuspended in MeOH (500 μL). The samples were next transferred to eppendorfs, concentrated and resuspended again in MeOH (150 μL). After centrifugation (9.3 x g, 3 min), supernatants (130 μL) were transferred to glass vials and stored at -20 °C until UPLC-TOF analysis.

### Mass spectrometry

Samples were analyzed by UPLC-TOF as described in Section 5.2.4.

## 5.5 References

1. Garner, P.; Park, J. M., 1,1-Dimethylethyl (S)- or (R)-4-formyl-2,2-dimethyl-3-oxazolidinecarboxylate: a useful serinal derivative. *Org. Synth.* **1992,** 70.

2. Bold, G.; Allmendinger, T.; Herold, P.; Moesch, L.; Schaer, H. P.; Duthaler, R. O., Stereoselective synthesis of (2S,6S)-2,6-diaminoheptanedioic acid and of unsymmetrical derivatives of meso-2,6-diaminoheptanedioic acid. *Helv. Chim. Acta* **1992,** 75, 865-82.

3. Campbell, A. D.; Raynham, T. M.; Taylor, R. J. K., A simplified route to the (R)-Garner aldehyde and (S)-vinylglycinol. *Synthesis* **1998**, 1707-1709.

4. Herold, P., Synthesis of D-erythro- and D-threo-sphingosine derivatives from L-serine. *Helv. Chim. Acta* **1988,** 71, 354-62.

5. Chun, J.; Li, G.; Byun, H. S.; Bittman, R., Synthesis of new trans double-bond sphingolipid analogues: Delta(4,6) and Delta(6) ceramides. *J. Org. Chem.* **2002,** 67, (8), 2600-5.

# 6. Spanish Summary

## Introducción

El estudio de procesos biológicos mediante reacciones químicas que permitan conjugar específicamente biomoléculas de interés ha cobrado un creciente auge en los últimos años. Para que una reacción química pueda tener lugar en un sistema biológico, tiene que ser compatible con las condiciones fisiólogicas de dicho sistema, como, por ejemplo, temperaturas moderadas, pH neutro, diversidad de grupos funcionales, concentración elevada de iones y, por último, la presencia de agua como disolvente.

Desde hace una década, Sharpless y colaboradores desarrollaron el concepto de "click chemistry", [1] término que abarca una serie de procesos químicos que reúnen las siguientes características: (1) alto rendimiento y velocidad de reacción rápida a bajas concentraciones; (2) condiciones de reacción sencillas; (3) fácil aislamiento del producto de reacción; (4) disolventes benignos (agua); (5) formación de subproductos inofensivos; (6) ser de amplio alcance y modular; (7) estereoespecificidad y (8) que el producto de reacción sea estable en condiciones fisiológicas.

Además de satisfacer los requisitos de "click chemistry", para que una reacción química sea apropiada para el estudio de sistemas biológicos debe ser bioortogonal. Esta propiedad implica que los reactivos involucrados en el proceso químico no reaccionen con otros nucleófilos/electrófilos presentes en las células, sino que reaccionen selectivamente entre sí.

Una de las estrategias más utilizadas para alcanzar bioortogonalidad es la incorporación de una funcionalidad específica, conocida como "chemical reporter", ya sea por modificación química o incorporación metabólica en la biomolécula de interés. Dichos "chemical reporters" no son propios de la célula y pueden ser modificados mediante reacciones selectivas en sistemas vivos. Entre estos procesos selectivos, la ligación de Staudinger, las ciclaciones de tipo 1,3-dipolar y de Diels-Alder, la ligación de oximas y el acoplamiento de hidrazonas son los más representativos.

Concretamente, la cicloadición de Diels-Alder cumple todos los requisitos de una reacción "click". Dicha reacción consiste en una cicloadición [4+2] entre un dieno rico en electrones y un dienófilo pobre en electrones para formar un sistema de ciclohexeno (Fig. 6.1).

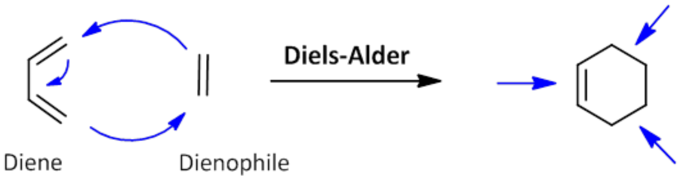

**Figura 6.1** Mecanismo general de la reacción de Diels-Alder entre un dieno y un dienófilo.

En la literatura se pueden encontrar una gran variedad de "chemical reporters", entre estos el grupo funcional azida es uno de los más ampliamente utilizados debido a sus características adecuadas, tales como: (1) pequeño tamaño; (2) naturaleza abiótica; (3) no reacciona con agua, es resistente a la oxidación y, además, (4) es un electrófilo suave y no reacciona con nucleófilos presentes en sistemas biológicos. Asimismo, el grupo azida puede ser introducido fácilmente en las biomoléculas, ya sea mediante incorporación metabólica o por modificación química. Por otro lado, esta funcionalidad interviene en procesos selectivos y bioortogonales como la ligación de Staudinger[2-4] y las cicloadiciones 1,3-dipolares con alquinos. En la presente tesis, nos hemos centrado en procesos químicos como las cicloadiciones, debido a la biocompatibilidad que ofrecen y a su amplia aplicación en el estudio de sistemas biológicos.

La funcionalidad azida, además de ser un electrófilo que reacciona con nucleófilos suaves, es un dipolo 1,3 que da lugar a reacciones con dipolarófilos como los alquinos terminales. El hecho de que los alquinos no se encuentren en los sistemas biológicos aumenta la bioortogonalidad de la azida. Las cicloadiciones[3+2] entre azidas y alquinos terminales, descritas por primera vez por Huisgen en 1963,[5] generan triazoles estables como productos de reacción. Los alquinos terminales son sistemas muy poco reactivos y, por este motivo, dichas cicloadiciones requieren el empleo de presiones o temperaturas elevadas, que no son compatibles con los sistemas biológicos (Fig. 6.2*B*). Sin embargo, la presencia de catalizadores basados en Cu(I)[6-7] promueve la activación del alquino, acelerando la velocidad de estos procesos unas $10^6$ veces. Este tipo de cicloadiciones alquino-azida catalizadas por Cu(I) (CuAAC) se han convertido en el paradigma de las reacciones click ("click chemistry"), dando lugar a triazoles 1,4-disubstituidos con una alta regioselectividad (Fig. 6.2*A*).

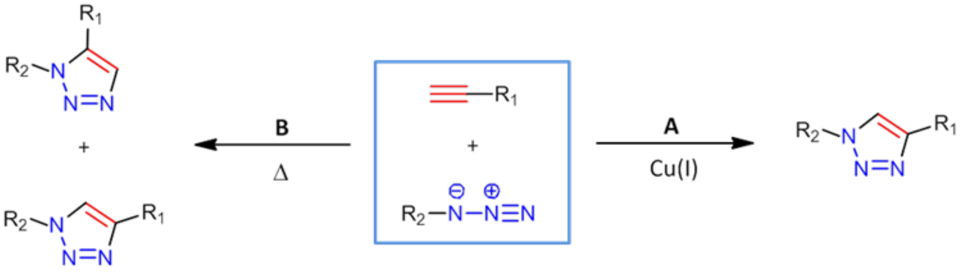

**Figura 6.2** (*A*) La 1,3-cicloadición catalizada por Cu(I) forma el regioisómero 1,4-disubstituido a temperatura ambiente con elevados rendimientos. (*B*) La cicloadición térmica entre alquinos y azidas requiere temperaturas elevadas y genera mezclas de los dos posibles regioisómeros.

A pesar de que la CuAAC ofrece las características requeridas para su aplicación en la bioconjugación de sistemas biológicos, el Cu(I) posee la desventaja de ser citotóxico, incluso a bajas concentraciones. Con el propósito de minimizar la toxicidad y de aumentar la velocidad de reacción, en los últimos años se han desarrollado una serie de ligandos y sistemas catalíticos que permiten el uso de sistemas de Cu(I) en procesos biológicos.[8] De este modo, la CuAAC ha sido utilizada en la bioconjugación de proteínas de membrana[9-10] y ADN,[11-12] entre otros.

Una variante de la CuAAC con interesantes aplicaciones, conocida por el término de reacción "click" fluorogénica, permite la visualización *in vivo* de biomoléculas por fluorescencia mediante su conjugación selectiva. Las reacciones "click" fluorogénicas son posibles gracias al desarrollo de marcadores basados en azidas/alquinos no fluorescentes, capaces de dar lugar, tras la reacción "click", a sistemas de triazol altamente conjugados y fluorescentes debido a la extensa deslocalización del sistema de electrones π. De este modo, el marcador remanente no interfiere con la señal de fluorescencia generada a partir de la biomolécula de conjugada de interés. Esta variante ha sido ampliamente utilizada en la bioconjugación *in vivo* de proteínas,[13-14] de glicanos fucosilados,[15-16] de ADN[17] y de virus.[18-19]

Otra estrategia para la activación de alquinos en las cicloadiciones[3+2] con azidas consiste en el uso de anillos tensionados. Esta posibilidad fue explorada por vez primera por Wittig y Krebs,[20] quienes demostraron que el ciclooctino, el cicloalquino estable más pequeño, reacciona con azidas para formar mezclas regioisoméricas 1:1 de 1,2,3-triazoles. El ángulo de enlace en los átomos sp del ciclooctino es de 160º, lo que distorsiona el estado de transición de la reacción y conduce a un aumento de la velocidad (Fig. 6.3). A este proceso se le conoce con el nombre de "strain promoted alkyne-azide cycloaddition" (SPAAC).

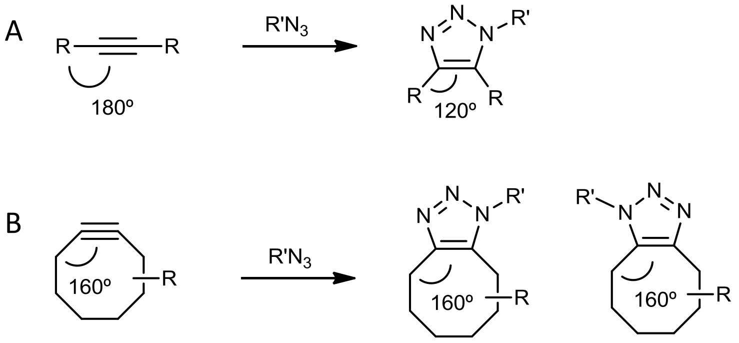

**Figura 6.3** Cicloadiciones 1,3-dipolares entre azidas y alquinos. (*A*) Cicloadición entre azidas y alquinos terminales. (*B*) La cicloadición [3+2] entre cicloalquinos y azidas genera mezclas regioisoméricas 1:1 de 1,2,3-triazoles.

Con el objetivo de mejorar la cinética de estas cicloadiciones, en los últimos años se han desarrollado diversos sistemas de cicloalquino altamente reactivos. Destacan los trabajos de Bertozzi y colaboradores, que diseñaron sistemas de ciclooctino con uno o dos átomos de fluor en el anillo, lo que aumenta la velocidad de reacción 2 y 40 veces, respectivamente, debido al efecto atrayente de electrones de los átomos de flúor.[21-22] Por otro lado, el grupo de Boons diseñó sistemas de dibenzociclooctino, altamente tensionados.[23] El hecho de que estas reacciones no requieran Cu(I) las hace muy adecuadas para procesos de bioconjugación en sistemas vivos. De este modo, estos ciclooctinos reactivos han sido utilizados en la bioconjugación selectiva de glicoproteínas,[24] proteínas de membrana de *Escherichia Coli*,[25] proteínas celulares,[26] así como de ADN.[27]

Los esfingolípidos (SLs) son lípidos estructurales ampliamente distribuidos en las membranas de las células eucariotas. Durante años se ha creído que su función era meramente estructural. Sin embargo, la intensa investigación durante las dos últimas décadas en este campo ha establecido que algunos SLs, como la ceramida, la esfingosina-1-fosfato o la ceramida-1-fosfato, son moléculas bioactivas que desempeñan funciones fundamentales en la célula, desde la regulación de vías de señalización celular[28] hasta los procesos de comunicación y reconocimiento célula-célula. Además, se ha descubierto que los SLs se ensamblan dinámicamente con esteroles en las membranas, formando microdominios especializados que están íntimamente asociados con la señalización celular.[29] Asimismo, las alteraciones del metabolismo de estas especies son responsables del establecimiento y la progresión de enfermedades de tipo neurodegenerativo, cardiovascular, procesos inflamatorios crónicos crónicos o cáncer.[30-33]

Estructuralmente, los SLs contienen una base esfingoide, que se halla unida a un ácido graso mediante un enlace amida y, en ocasiones, a una cabeza polar mediante un enlace ester. Las bases esfingoides son 2-amino-1,3-dihidroxialcanos, o los correspondientes alquenos, con estereoquímica (2*S*,3*R*)-eritro y las más abundantes son la esfingosina y la esfinganina. Las cabezas polares en el grupo hidroxilo de C1 definen las diversas clases de SLs (Fig. 6.4).

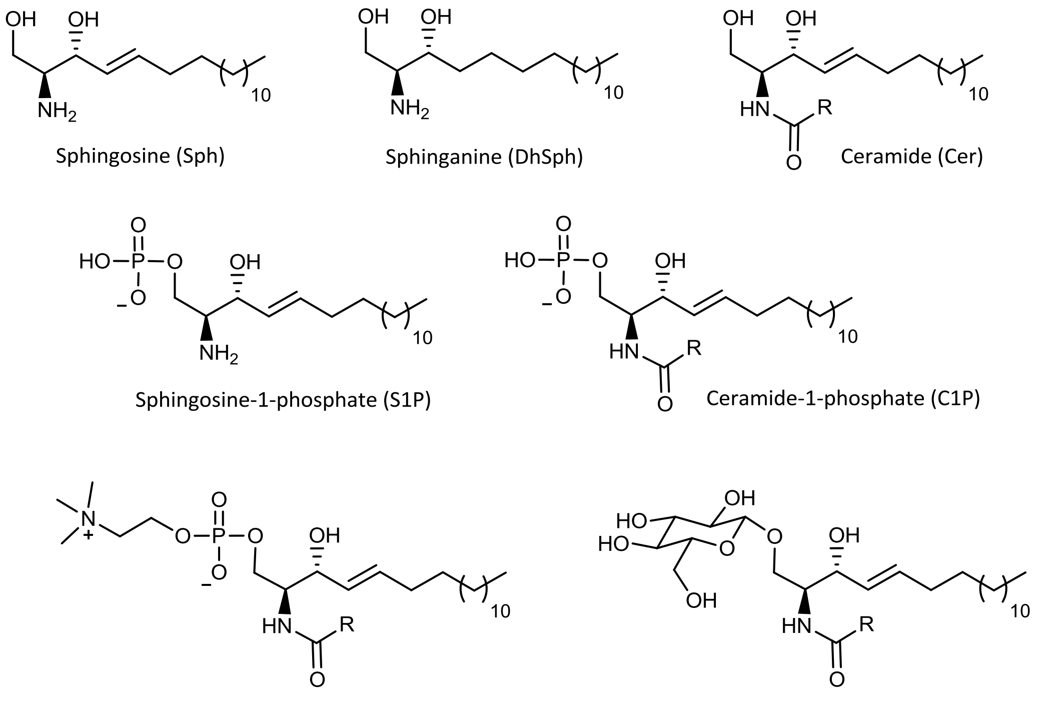

Sphingosine (Sph)

Sphinganine (DhSph)

Ceramide (Cer)

Sphingosine-1-phosphate (S1P)

Ceramide-1-phosphate (C1P)

Sphingomyelin (SM)

Glucosylceramide (GlcCer)

**Figura 6.4** Estructura de diversas clases de SLs. R representa diferentes cadenas acilo.

La ceramida es la molécula central en la biosíntesis de SLs, que pueden biosintetizase mediante cuatro vías diferentes: (1) la biosíntesis *De novo*, (2) el ciclo de la esfingomielina, (3) la hidrólisis de glicoesfingolípidos y (4) la vía de reciclaje.

## Objetivos

Tal y como se ha indicado en el apartado anterior, los SLs son moléculas bioactivas esenciales en los procesos de regulación del crecimiento celular, diferenciación, senescencia y apoptosis. Para ser capaces de entender y conocer las numerosas funciones reguladoras de los diferentes SLs, es necesario un conocimiento exacto de cómo y dónde se generan, transforman o degradan estas biomoléculas en el interior de la célula. Por este motivo, la síntesis de marcadores de SLs y el desarrollo de herramientas químicas para estudiar el metabolismo y la localización de estas especies constituye un tema de creciente interés.

Por otro lado, el desarrollo de las reacciones bioortogonales ha estimulado una gran variedad de aplicaciones en biología química. Concretamente, aquellas reacciones que implican cicloadiciones entre azidas y alquinos permiten la conjugación selectiva de moléculas en sistemas biológicos, ayudando a su estudio.

Teniendo en cuenta estas consideraciones, se contemplaron los siguientes objetivos en la presente tesis doctoral:

1. Diseño y síntesis de SLs marcados ("sondas") con una funcionalidad azida en la posición ω (Fig. 6.5*A*), o en posición C1 (Fig. 6.5*B*) de la base esfingoide. Asimismo, la síntesis de los ω-azido SLs comprende modificaciones en la posición C1 y en el enlace amida.

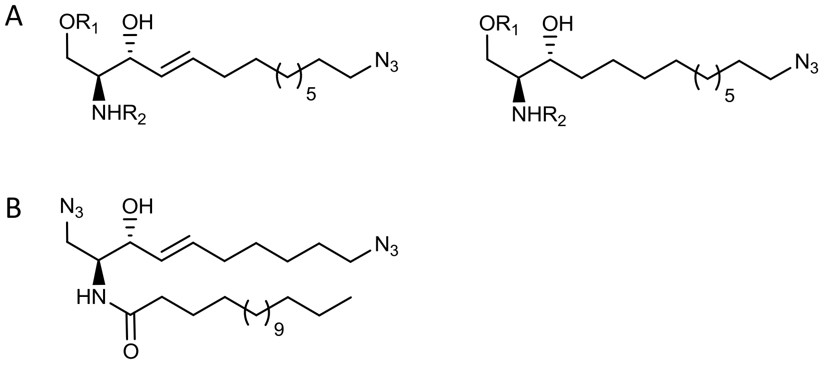

**Figura 6.5** SL propuestos como sondas funcionalizadas con un grupo azida en: (*A*) posición ω y (*B*) posición C1 de la base esfingoide. $R_1$ representa un grupo fosfato o H, y $R_2$ diferentes grupos acilo o H.

2. Desarrollo de nuevas metodologías para estudiar el metabolismo y la localización intracelular de los SLs mediante reacciones de cicloadición azida-alquino.

    2.1 Nueva aproximación para la cuantificación del esfingolipidoma basada en reacciones SPAAC.

    2.2 Desarrollo de marcador fluorescente para la conjugación y localización intracelular de esfingolípidos mediante el empleo de sondas de tipo ω-azido en reacciones SPAAC.

    2.3 Nueva metodología para la visualización de ceramidas fluorescentes en membranas lipídicas mediante reacciones de tipo CuAAC. Este objetivo específico incluye la evaluación de las propiedades fluorescentes de las azido-ceramidas en un entorno lipídico artificial en presencia de un alquino fluorogénico.

3. Nuevas aproximaciones sintéticas para la preparación de ceramidas artificiales como sondas con potencial aplicación en un nuevo ensayo fluorogénico para la determinación de la actividad Des1 (Fig. 6.6).

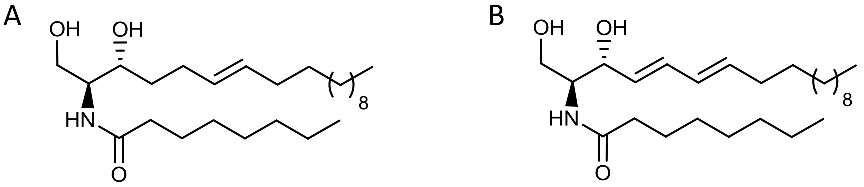

**Figura 6.6** Estructura química las ceramidas artificiales propuestas como sondas para la determinación de la actividad Des1: (*A*) $\Delta^{6}$-ceramida, y (*B*) $\Delta^{4,6}$-ceramida.

## Resultados y discusión

En el apartado 3.1 se presenta la síntesis de una serie de nuevas sondas de SLs, caracterizadas por la incorporación de una funcionalidad azida en la posición ω de la base esfingoide, tal y como se muestra en la Fig. 6.7:

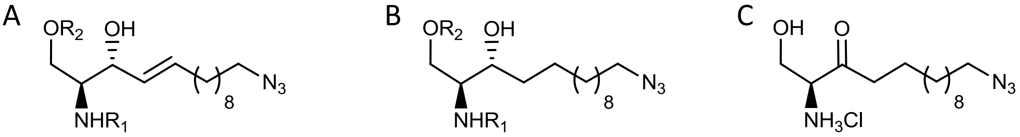

**RBM2-31**: $R_1$=H, $R_2$=H
**RBM2-32**: $R_1$=$CH_2Br$, $R_2$=H
**RBM2-35**: $R_1$=H, $R_2$=$P(O)(OH)_2$
**RBM2-37**: $R_1$=$C_7H_{15}$, $R_2$=H
**RBM2-46**: $R_1$=$C(=CH_2)CH_3$, $R_2$=H
**RBM2-47**: $R_1$=$C_7H_{15}$, $R_2$=$P(O)(OH)_2$
**RBM2-77**: $R_1$=$C_{15}H_{31}$, $R_2$=H

**RBM2-40**: $R_1$=H, $R_2$=H
**RBM2-43**: $R_1$=H, $R_2$=$P(O)(OH)_2$
**RBM2-44**: $R_1$=$C(=CH_2)CH_3$, $R_2$=H
**RBM2-45**: $R_1$=$CH_2Br$, $R_2$=H
**RBM2-87**: $R_1$=$C_{15}H_{31}$, $R_2$=H

**RBM2-63**

**Figura 6.7** Estructura química general de las nuevas sondas con un grupo azida sintetizadas. Derivados de: (*A*) esfingosina; (*B*) dihidroesfingosina, y (*C*) 3-cetoesfinganina.

Desde la publicación de la primera síntesis de la esfingosina por Shapiro,[34] se han descrito numerosas rutas sintéticas para la preparación de este compuesto en forma enantioméricamente pura. Mientras que unas utilizan precursores quirales como la L-serina o los carbohidratos, otras aproximaciones se basan, entre otros métodos, en epoxidaciones asimétricas y reacciones aldólicas. Por otro lado, el conocimiento de reacciones de metátesis cruzada para la formación de dobles enlaces con total selectividad *E*, nos alentó a utilizar esta reacción para la formación del doble enlace *trans* en C4-C5 de la base esfingoide. Asimismo, esta estrategia sintética resulta tolerante con la funcionalidad aminodiol presente en las bases esfingoides. Para poder llevar a cabo la ruta sintética seleccionada, primero se requirió la preparación de un precursor quiral (**7**), que poseyera la unidad 2-amino-1,3-diol junto con un doble enlace terminal. De este modo, el compuesto **7** se preparó a partir del aldehído de Garner (**4**),[35] *building block* quiral ampliamente utilizado en síntesis asimétrica y que permite obtener la configuración adecuada de los centros esterogénicos C2 y C3 requerida para la síntesis de SLs.

De la reacción de metátesis cruzada de **7** con el bromoalqueno **11** se pudo obtener el intermedio avanzado **12**, que fue transformado en la esfingosina **RBM2-31** tras su reacción con azida sódica y la subsiguiente desprotección de los grupos *N*-Boc y oxazolidina. Los derivados *N*-acilados de **RBM2-31** (**RBM2-32**, **RBM2-37**, **RBM2-46** y **RBM2-77**) se obtuvieron a partir de los correspondientes ácidos carboxílicos, utilizando EDC y HOBt como agentes de acoplamiento.

Con el propósito de obtener los derivados de la dihidroesfingosina (Fig. 6.7*B*), se procedió a la hidrogenación catalítica del doble enlace en el intermedio común **12**. Con esta aproximación sintética se obtuvo la dihidroesfingosina **RBM2-40** y sus derivados *N*-acilados **RBM2-44**, **RBM2-45** y **RBM2-87**.

Con el objetivo de obtener los derivados fosforilados **RBM2-35** y **RBM2-43** se ensayaron diferentes metodologías descritas en la literatura para la fosforilación selectiva de alcoholes primarios. En primer lugar, se utilizó el método de Yoshikawa,[36] sin que proporcionara el producto deseado. Seguidamente se probó la metodología fosfato de trimetilo/tetrabromuro de carbono,[37] lo que dio lugar al producto monofosforilado deseado, pero con bajo rendimiento (29%). Afortunadamente, la reacción de monofosforilación pudo ser optimizada mediante el uso de clorofosfato de dimetilo en presencia de *N*-metilimidazol, aumentando el rendimiento hasta un 65%. La posterior desprotección de ésteres metílicos y del grupo *N*-Boc en los intermedios **17** y **19** con TMSBr, proporcionó los fosfatos **RBM2-35** y **RBM2-43**, respectivamente, con elevados rendimientos. Para la obtención del derivado de ceramida-1-fosfato **RBM2-47**, se empleó una aproximación basada en un intermedio del tipo *H*-fosfonato, lo que condujo al producto deseado. En esta ruta sintética se utilizó como producto de partida la ω-azidoceramida **RBM2-37**, que fue transformada en *H*-fosfonato. La introducción de una etapa de sililación *in situ* de la especie *H*-fosfonato fue necesaria para poder oxidar el fosfito correspondiente y, de este modo, obtener el compuesto **RBM2-47**.

Para la obtención del derivado de 3-cetoesfinganina **RBM2-63** (Fig. 6.7*C*) se decidió llevar a cabo la oxidación del alcohol secundario del intermedio **15**. En esta ocasión se decidió sintetizar este intermedio mediante una ruta sintética basada en la adición diastereoselectiva de un acetiluro de litio sobre el aldehído quiral (**4**) y la posterior oxidación del alcohol secundario a cetona. La desprotección de los grupos oxazolidina y *N*-Boc proporcionó la cetona deseada con un rendimiento del 90% en esta última etapa.

En el apartado 3.2 se describe la síntesis de un análogo de ceramida, que se caracteriza por poseer una funcionalidad azida en la posición C1 de la base esfingoide (Fig. 6.8):

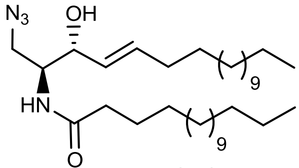

**RBM2-79**

**Figura 6.8** Estructura química de 1-azidoceramida **RBM2-79**.

Para la preparación de esta nueva ceramida, se decidió utilizar nuevamente la reacción de metátesis cruzada para la formación del doble enlace *trans* en C4-C5. Para ello se hizo reaccionar el compuesto **7** con 1-pentadeceno, generando el intermedio **30**. En ensayos preliminares, se probó la reacción de substitución con azida sódica en C1 a partir de un intermedio con el hidróxilo primario (C1) activado y el grupo hidroxilo secundario (C3) con o sin proteger. En ninguno de los dos casos se pudo aislar la azida deseada, sino una mezcla de productos secundarios sin identificar. Por este motivo, se decidió bloquear el grupo hidroxilo en C3 mediante su protección en forma de carbamato. A partir del carbamato **31** se pudo activar el grupo hidroxilo (C1) en forma del correspondiente mesilato y, posteriormente, su substitución nucleófila con azida sódica dio lugar a la azida deseada **34**, aunque solamente a bajas temperaturas. La desprotección del grupo carbamato se ensayó utilizando diferentes condiciones, de entre las que únicamente una mezcla de EtOH/NaOH a 60 °C condujo a **40**, aunque con bajos rendimientos (17%). Finalmente, la *N*-acilación de **40** proporcionó la ceramida **RBM2-79** con rendimiento elevado (82%).

Debido a la importancia fisiológica de los SLs, la descripción de los mapas de SLs (denominados esfingolipidomas) de una determinada línea celular o tejido es de gran importancia. Por este motivo, en el apartado 3.3.1 se describe una nueva aproximación para el análisis simultáneo y la cuantificación de estas especies basada en el etiquetaje de diferentes poblaciones de SLs mediante reacciones "click". Para ello se escogieron algunas de las azidas sintetizadas en el apartado 3.1, en concreto **RBM2-31**, **RBM2-37**, **RBM2-40** y **RBM2-63**. En primer lugar, se examinó la citotoxicidad de estas azidas en las líneas celulares A549 y MCF-7, sin obtener valores de toxicidad significativos. Seguidamente se evaluó el efecto de estos compuestos sobre el esfingolipidoma de ambas líneas celulares. En células intactas A549 se ensayaron los compuestos a una concentración 10 μM durante 24 h. Después de analizar los diferentes SLs mediante UPLC-TOF, se observó que

**RBM2-31** y **RBM2-37** habían disminuido levemente los niveles celulares de esfinogomielinas sin que se produjeran otras alteraciones. Paralelamente, se trataron células intactas HGC-27 con **RBM2-31**, **RBM2-40** y **RBM2-63** a una concentración de 5 μM durante diferentes tiempos de incubación. En esta ocasión, tampoco se observaron variaciones significativas de los SLs celulares a los diferentes tiempos de incubación. Por otro lado, el análisis de las mismas muestras también reveló que las azidas ensayadas se metabolizaron de forma análoga a un SL natural, dando lugar a especies tales como ω-azidoceramidas, ω-azidodihidroceramidas, ω-azidoesfingomielinas y ω-azidodihidroesfingomielinas, todas ellas con diferentes cadenas acilo. Las variaciones en los niveles de los diferentes metabolitos dependieron de los tiempos de incubación (por ejemplo, a tiempos de incubación largos los niveles de ω-azidoesfingomielinas y ω-azidodihidroesfingomielinas aumentaron). Estos resultados evidenciaron que los compuestos **RBM2-31**, **RBM2-37**, **RBM2-40** y **RBM2-63** son apropiados para el estudio del metabolismo de SLs.

A continuación, se examinó la reacción "click" en disolución entre la ceramida **RBM2-37** (150 pmol) y una serie de cinco tags derivados de azadibenzociclooctino , ensayados a una concentración de 7.5 nmol y que difieren entre ellos en una unidad de metileno (Fig. 6.9).

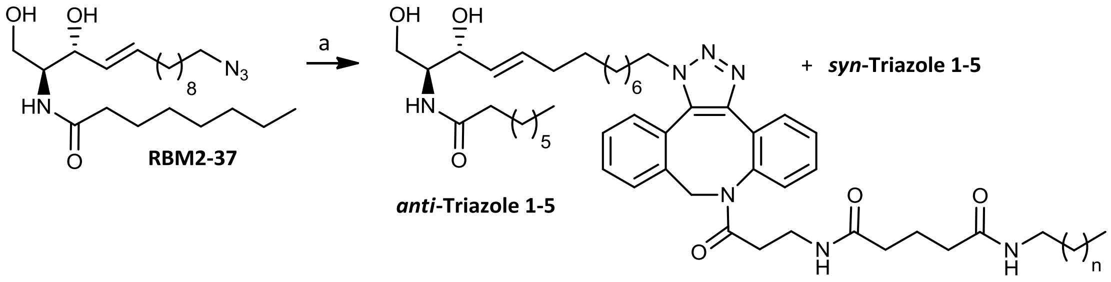

a) Tags **1**-**5**, MeOH, 37 °C, *overnight.*

**Figura 6.9** Reacción "click" entre la azida **RBM2-37** y los tags **1**-**5** en disolución y a baja concentración.

A pesar de la baja concentración de reacción (~0.2 μM para la azida), todos los aductos "click" fueron detectados por UPLC-TOF como picos únicos. No se detectó azida **RBM2-37**, evidenciando que la reacción "click" procedió cuantitativamente. Es destacable que los aductos "click" fueron detectados con una sensibilidad 8 veces mayor que la de la correspondiente azida, debido a la presencia de dos grupos amida adicionales que aumentan la sensibilidad de la molécula en este tipo de determinaciones analíticas.[38] Por otro lado, se optimizó la reacción "click" sobre extractos de células A549 que contenían metabolitos derivados del tratamiento previo con **RBM2-31**. Las condiciones de derivatización óptimas consistieron en la adición del tag sobre el extracto lipídico antes del proceso de extracción de SLs.

Finalmente, se llevó a cabo el marcaje de extractos de células A549 que contenían metabolitos, resultantes de la incubación con **RBM2-31** durante 6 h. Para que la reacción "click" procediera de manera cuantitativa y, por lo tanto, para que la desaparición de los metabolitos ω-azido fuera completa, fue necesaria la adición de 100 equiv de los tags **1-5**. Asimismo, se detectaron y diferenciaron una gran variedad de aductos "click"derivados de diferentes especies de SLs (ceramida, esfingomielina, etc.) con diferentes cadenas aciladas (C14-C24 y también C24:1) y diferentes unidades de triazol (dependiendo del tag). Sin embargo, exclusivamente con el tag **3** se obtuvo un perfil lipídico análogo al obtenido en la muestra control (no reacción "click"), con la presencia de esfingomielinas como metabolitos mayoritarios en ambos casos.

En el apartado 3.3.2 se presenta el desarrollo de un método para la conjugación intracelular y localización de ω-azido SLs mediante la reacción "click" con un nuevo marcador fluorescente.

En primer lugar, se sintetizó un nuevo marcador fluorescente (**D1**) derivado de un azadibenzociclooctino unido a una molécula de fluoresceína mediante un espaciador de 5 átomos de carbono. Por otro lado, la fluoresceína es un fluorocromo muy brillante ampliamente utilizado y, además, es hidrosoluble, generando moléculas permeables a las membranas celulares. El colorante **D1** resultó tener unas propiedades ópticas comparables con las de la fluoresceína, con un rendimiento cuántico de 0.20±0.04 en NaOH 0.1 M (en referencia a la fluoresceína en NaOH 0.1 M). En este apartado, se examinó la reactividad de **D1** con la azida **RBM2-87** en MeOH a temperatura ambiente y en medios de cultivo celular a 37 °C a diferentes tiempos de reacción (Fig. 6.10). En ambos casos, se alcanzaron conversiones próximas al 100% después de 60 min de reacción.

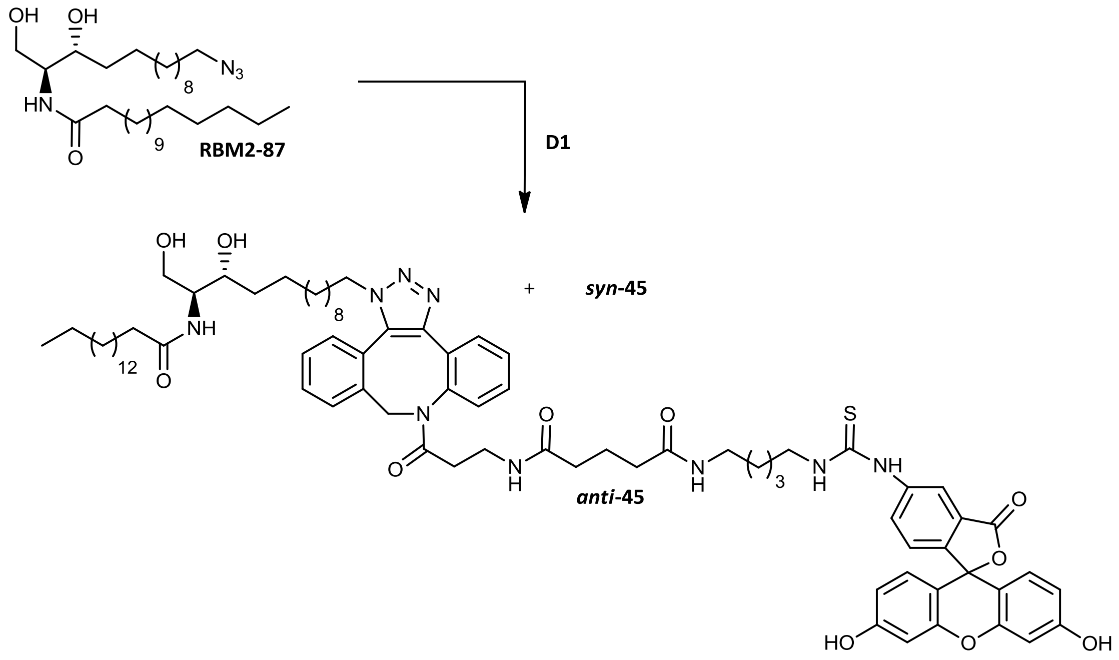

**Figura 6.10** Reacción "click" entre el marcador fluorescente **D1** y la azida **RBM2-87** en MeOH y medio de cultivo celular. Las concentraciones de ambos reactivos (1 mM) fueron equimolares.

A continuación, se llevaron a cabo estudios de internalización de **D1** en las líneas celulares cancerosas A549 y MCF-7. Mediante análisis por citometría de flujo se determinaron los máximos de fluorescencia para una concentración de 100 μM (concentración no citotóxica) a los 30 min de incubación. Así se determinaron las condiciones óptimas para una internalización máxima de **D1** en la célula. Por otro lado, el análisis por microscopía de epifluorescencia reveló una distribución citosólica extensa y uniforme de **D1**, sin mostrar difusión en el área nuclear. Para finalizar este apartado, se evaluó la conjugación y la visualización de ω-azido SLs mediante la reacción "click" con **D1** en células vivas. Con dicho propósito, se trataron células A549 y MCF-7 con la azida **RBM2-31** (10 μM) durante 16 h y, seguidamente, con el colorante **D1** (100 μM) durante diferentes tiempos de reacción (0.5, 1 y 2 h). El análisis mediante citometría de flujo reveló una fluorescencia entre 6 y 12 veces mayor en células A549 tratadas con **RBM2-31**, dependiendo del tiempo de incubación de **D1**. Así, a mayores tiempos de reacción la reacción "click" procedió con mayor eficacia y, por lo tanto, se detectaron niveles de fluorescencia más elevados. En el caso de las células MCF-7, cuando fueron pretratadas con **RBM2-31** mostraron una fluorescencia 22 veces más elevada después de 1 h de reacción, debido a la formación de los diferentes aductos "click". Asimismo, se visualizó la formación de aductos mediante microscopía confocal. Para células A549 pretratadas con **RBM2-31** durante 5 h y posteriormente con **D1**, se observó una fuerte fluorescencia localizada en el área perinuclear, posiblemente, asociada a membranas.

Debido a la importancia de los microdominios lipídicos y del uso de marcadores fluorescentes para su estudio, en el apartado 3.3.3 se describe una metodología para la visualización de ceramidas fluorescentes en membranas lipídicas. Esta nueva aproximación se basa en la generación *in situ* de estas ceramidas fluorescentes mediante CuAAC con un sistema alquino no fluorescente.[39] Para ello, las ceramidas **RBM2-77** y **RBM2-79** se incorporaron en vesículas multilamelares y, a continuación, se hicieron reaccionar, mediante una reacción de tipo "click" catalizada por Cu, con el alquino **46**, derivado de la naftalimida (Fig. 6.11). En estas condiciones se observó una fuerte señal fluorescente tras 1.5 h de reacción para ambas azidas ($\lambda_{exc}$=368 nm, $\lambda_{em}$=440) en comparación con el control. Asimismo, para visualizar la formación de las ceramidas fluorescentes mediante microscopía confocal, se incoporaron las sondas **RBM2-77** y **RBM2-79** en vesículas unilamelares gigantes. Después de la incubación con la naftalimida **46**, en presencia de Cu(I), se observó una intensa señal de fluorescencia intensa entre 450-500 nm. Sin embargo, en ausencia de Cu(I) no se observó ninguna señal fluorescente. Para confirmar la formación *in situ* de los aductos fluorescentes **47** y **48**, éstos fueron extraídos de las vesículas y posteriormente analizados por UPLC-TOF. De este modo, se pudieron detectar los picos correspondientes a las masas exactas de dichos aductos.

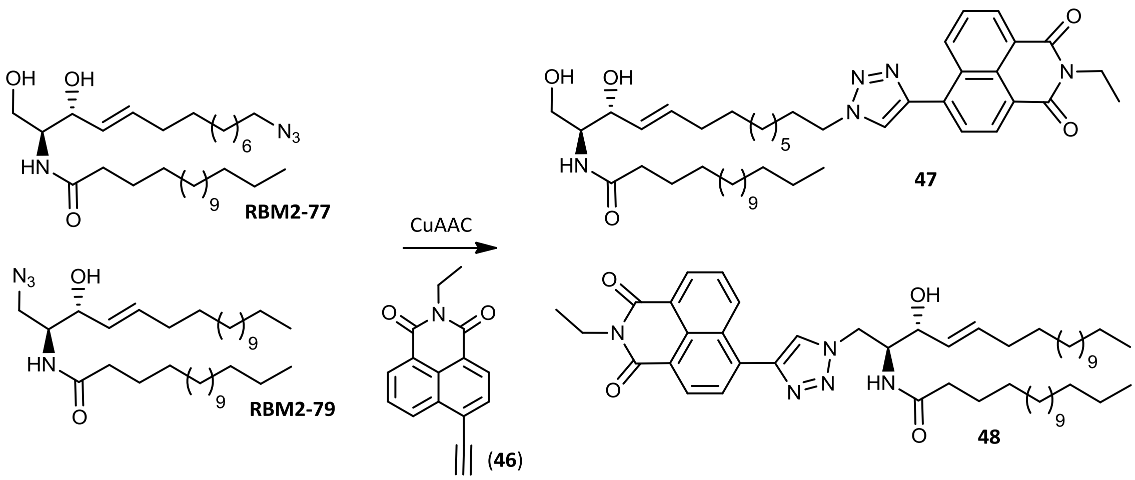

**Figura 6.11** CuAAC fluorogénica entre las azidas **RBM2-77** y **RBM2-79** y la naftalimida **46**. La reacción *click* requiere la presencia de ácido ascórbico y una mezcla 1:1 M de $CuSO_4$ y el ligando tris(triazolil)amino **49**.

En el último apartado de la discusión (3.4) se describen nuevas aproximaciones sintéticas para la obtención de las ceramidas no naturales $\Delta^6$ (**RBM2-85**) y $\Delta^{4,6}$ (**RBM2-76**). La preparación de estas ceramidas se requiere para la puesta a punto de un ensayo HTS para la determinación de la actividad del enzima Des1. Hasta el momento, los ensayos descritos en la literatura para la determinación de esta actividad enzimática no cumplen los requisitos adecuados para el desarrollo de un ensayo HTS. Por este motivo, se diseñó un ensayo basado en la desaturación de la ceramida **RBM2-85** y la posterior captura del dieno formado (**RBM2-76**) con un dienófilo fluorescente mediante una cicloadición de Diels Alder (DA). Para la adaptación de este ensayo a un protocolo de HTS, sería necesario atrapar el exceso de dienófilo fluorescente (Fig. 6.12).

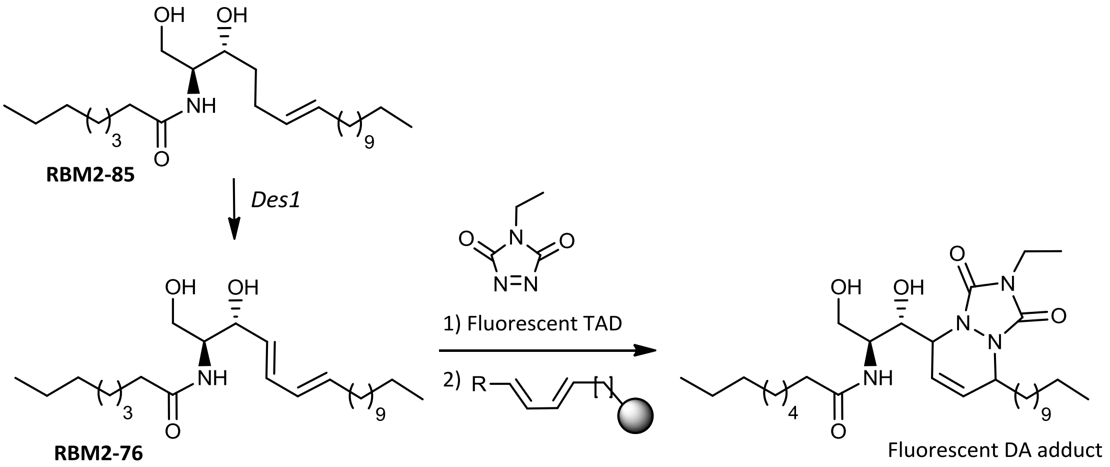

**Figura 6.12** Ensayo HTS diseñado para la determinación de la actividad Des1, utilizando la ceramida **RBM2-85** como sustrato de la enzima.

En la ruta sintética propuesta para la obtención de **RBM2-85** se utilizó nuevamente la reacción de metátesis cruzada como etapa clave. De este modo, la reacción de CM entre el intermedio **56** y el 1-trideceno dio lugar al compuesto **54** que, posteriormente, fue desprotegido en condiciones ácidas y *N*-acilado para generar la ceramida **RBM2-85**. Aunque esta ruta sintética ofrecía características interesantes, como las de ser más directa y sencilla, la formación de isómeros posicionales durante la reacción de CM ocasionó dificultades a la hora de aislar el producto deseado, a la vez que una disminución en el rendimiento global.

Para la síntesis de la ceramida **RBM2-76** se decició utilizar una reacción de Wittig como etapa clave para la formación del doble enlace *trans* entre C6-C7. Así, a partir de la reacción de Wittig entre el aldehído α,β-insaturado **62** y el iluro de fosfonio **66** y posterior *quenching* con MeOH a baja temperatura, se obtuvo una mezcla inseparable de dienoles (4*E*,6*E*)-**60** y (4*E*,6*Z*)-**63** en una relación 7:3. Los intentos de isomerización en presencia de yodo fueron infructuosos. La mezcla de dienoles fue desprotegida en medio ácido y posteriormente acilada para obtener los compuestos (4*E*,6*E*)-**RBM2-76** y (4*E*,6*Z*)-**RBM2-82** con un rendimiento bajo debido a la formación de productos secundarios durante la desprotección en medio ácido. La ceramida **RBM2-82** se identificó de forma inambigua mediante su síntesis independiente a partir el compuesto **63**, que se obtuvo de forma estereoselectiva mediante una reacción de Wittig convencional.

Por otro lado, a partir de una cicloadición de Diels Alder entre **RBM2-76** y el dienófilo PTAD se confirmó la formación del correspondiente aducto por FIA.

## Resumen y conclusiones

- Se ha utilizado una estrategia sintética basada en la reacción de metátesis cruzada para sintetizar varios derivados de esfingolípidos. Esta aproximación ha permitido la formación del doble enlace en C4-C5 con total selectividad *E*.
- El aldehído de Garner **4** se ha utilizado como precursor quiral para la construcción de la unidad 2-amino-1,3 diol con la estereoquímica requerida. Las adiciones diastereoselectivas de nucleófilos adecuados sobre este aldehído han proporcionado los intermedios sintéticos deseados con una alta selectividad *eritro* y con rendimientos elevados.
- Las ω-azidoceramidas se obtuvieron a partir de la ω-azidoesfingosina **RBM2-31,** sintetizada a partir de la reacción de CM de **7** con el alqueno terminal **11**. Los análogos saturados se obtuvieron a partir de la hidrogenación catalítica del intermedio **12** y su posterior desprotección y *N*-acilación.
- La ω-azido-3-cetoesfinganina **RBM2-63** se preparó a partir de la adición diastereoselectiva de un acetiluro de litio sobre el aldehído **4**. La subsiguiente funcionalización con un grupo azida y la oxidación selectiva del grupo hidroxilo secundario fueron las etapas cruciales de esta aproximación.

- Los derivados fosforilados **RBM2-35** y **RBM2-43** se obtuvieron a partir de la monofosforilación selectiva del grupo hidroxilo primario con dimetil clorofosfato en presencia de *N*-metilimidazol. La desprotección selectiva de los ésteres metílicos y *N*-Boc con TMSBr, seguida de metanolisis, proporcionó los fosfatos deseados.

- Se utilizó la aproximación *H*-fosfonato para la preparación de la ω-azidoceramida-1-fosfato **RBM2-47**. La posterior sililación de la especie *H*-fosfonato y la oxidación final resultaron las etapas cruciales para la obtención de este compuesto.

- La 1-azidoceramida **RBM2-79** se obtuvo también a partir de una ruta sintética basada en la reacción de CM.

- Se han llevado a cabo nuevas rutas sintéticas para la preparación de las ceramidas **RBM2-85** y **RBM2-76**. Cómo etapa clave para la obtención de **RBM2-85** se utilizó la reacción de CM entre el intermedio **53** y un alqueno terminal apropiado. La etapa clave en la síntesis de **RBM2-76** fue una reacción de Wittig *E*-selectiva entre el intermedio **59** y un iluro de fosfonio apropiado.

- Las azidas **RBM2-31**, **RBM2-37**, **RBM2-40** y **RBM2-63** se seleccionaron para estudiar su efecto sobre el esfingolipidoma de células cancerosas A549 y HGC-27. Estos compuestos resultaron ser inocuos y, además, presentaron variaciones insignificantes en los niveles de esfingolípidos endógenos en ambas líneas celulares. Asimismo, se detectaron diferentes metabolitos de estas azidas.

- Se evaluó la reacción “click” entre la azida **RBM2-37** y diferentes marcadores derivados de un sistema de azadibenzociclooctino (tags) a una concentración ~0.2 μM. Los aductos “click” se detectaron por UPLC-TOF con una elevada sensibilidad.

- Se optimizó la reacción “click” sobre los extractos celulares que contenían ω-azido SLs, mediante la adición de un exceso de tag **1** antes del proceso de extracción de SLs. Asimismo, se marcaron diferentes extractos celulares que contenían ω-azido SLs con los tags **1-5** mediante reacciones “click”. El análisis de los extractos por UPLC-TOF reveló la desaparición completa de los metabolitos de tipo ω-azido (marcaje cuantitativo), a la vez que la formación de los correspondientes triazoles.

- Se ha diseñado y sintetizado un nuevo marcador fluorescente **D1**, basado en una estructura de azadibenzociclooctino acoplada a fluoresceína. Se ha examinado la eficiencia de la reacción “click” de **D1** con la azida **RBM2-87**, tanto en disolución como en medios de cultivo celular, alcanzándose conversiones cercanas al 100% a los 60 min de reacción.

- Mediante estudios de sensibilidad en la señal de fluorescencia e internalización de **D1** en las líneas celulares A549 y MCF-7 se determinó la concentración y el tiempo de incubación de **D1** óptimos, siendo éstos 100 μM y 30 min, respectivamente.
- Se llevó a cabo la conjugación *in situ* de los metabolitos de **RBM2-31** mediante la reacción "click" con **D1** en células vivas. Las células A549 conjugadas mediante química "click" resultaron dar lugar a una fluorescencia 12 veces superior a las 2 h de reacción. Las células MCF-7 mostraron una fluorescencia media 17 veces superior cuando se conjugaron en las mismas condiciones. Asimismo, también se visualizó la formación intracelular de los aductos "click" mediante microscopía confocal.
- Las ceramidas **RBM2-77** y **RBM2-79** se incorporaron en vesículas unilamelares gigantes y, tras una reacción de tipo CuAAC fluorogénica, se visualizaron los correspondientes aductos "click" por microscopía confocal.

## Referencias

1. Kolb, H. C.; Finn, M. G.; Sharpless, K. B., Click chemistry: diverse chemical function from a few good reactions. *Angew. Chem., Int. Ed.* **2001,** 40, 2004-2021.

2. Saxon, E.; Bertozzi, C. R., Cell surface engineering by a modified Staudinger reaction. *Science (Washington, DC, U.S.)* **2000,** 287, 2007-2010.

3. Nilsson, B. L.; Kiessling, L. L.; Raines, R. T., Staudinger Ligation: A Peptide from a Thioester and Azide. *Org. Lett.* **2000,** 2, (13), 1939-1941.

4. Saxon, E.; Armstrong, J. I.; Bertozzi, C. R., A "Traceless" Staudinger Ligation for the Chemoselective Synthesis of Amide Bonds. *Org. Lett.* **2000,** 2, (14), 2141-2143.

5. Huisgen, R., 1,3-Dipolar Cycloadditions. Past and Future. *Angew. Chem., Int. Ed.* **1963,** 2, (10), 565-598.

6. Rostovtsev, V. V.; Green, L. G.; Fokin, V. V.; Sharpless, K. B., A Stepwise Huisgen Cycloaddition Process: Copper(I)-Catalyzed Regioselective "Ligation" of Azides and Terminal Alkynes. *Angew. Chem., Int. Ed.* **2002,** 41, (14), 2596-2599.

7. Tornoe, C. W.; Christensen, C.; Meldal, M., Peptidotriazoles on Solid Phase: [1,2,3]-Triazoles by Regiospecific Copper(I)-Catalyzed 1,3-Dipolar Cycloadditions of Terminal Alkynes to Azides. *J. Org. Chem.* **2002,** 67, 3057-3064.

8. Hong, V.; Presolski, S. I.; Ma, C.; Finn, M. G., Analysis and Optimization of Copper-Catalyzed Azide-Alkyne Cycloaddition for Bioconjugation. *Angew. Chem., Int. Ed.* **2009,** 48, 9879-9883.

9. Link, A. J.; Vink, M. K. S.; Tirrell, D. A., Presentation and Detection of Azide Functionality in Bacterial Cell Surface Proteins. *J. Am. Chem. Soc.* **2004,** 126, (34), 10598-10602.

10. Link, A. J.; Tirrell, D. A., Cell Surface Labeling of Escherichia coli via Copper(I)-Catalyzed [3+2] Cycloaddition. *J. Am. Chem. Soc.* **2003,** 125, (37), 11164-11165.

11. Seo, T. S.; Li, Z.; Ruparel, H.; Ju, J., Click Chemistry to Construct Fluorescent Oligonucleotides for DNA Sequencing. *J. Org. Chem.* **2002,** 68, (2), 609-612.

12. Seo, T. S.; Bai, X.; Ruparel, H.; Li, Z.; Turro, N. J.; Ju, J., Photocleavable fluorescent nucleotides for DNA sequencing on a chip constructed by site-specific coupling chemistry. *Proc. Natl. Acad. Sci. U.S.A.* **2004,** 101, (15), 5488-5493.

13. Beatty, K. E.; Liu, J. C.; Xie, F.; Dieterich, D. C.; Schuman, E. M.; Wang, Q.; Tirrell, D. A., Fluorescence Visualization of Newly Synthesized Proteins in Mammalian Cells. *Angew. Chem., Int. Ed.* **2006,** 45, (44), 7364-7367.

14. Beatty, K. E.; Xie, F.; Wang, Q.; Tirrell, D. A., Selective Dye-Labeling of Newly Synthesized Proteins in Bacterial Cells. *J. Am. Chem. Soc.* **2005,** 127, (41), 14150-14151.

15. Sawa, M.; Hsu, T.-L.; Itoh, T.; Sugiyama, M.; Hanson, S. R.; Vogt, P. K.; Wong, C.-H., Glycoproteomic probes for fluorescent imaging of fucosylated glycans in vivo. *Proc. Natl. Acad. Sci. U.S.A.* **2006,** 103, 12371-12376.

16. Hsu, T. L.; Hanson, S. R.; Kishikawa, K.; Wang, S. K.; Sawa, M.; Wong, C. H., Alkynyl sugar analogs for the labeling and visualization of glycoconjugates in cells. *Proc. Natl. Acad. Sci. U.S.A.* **2007,** 104, (8), 2614-9.

17. Gierlich, J.; Burley, G. A.; Gramlich, P. M. E.; Hammond, D. M.; Carell, T., Click Chemistry as a Reliable Method for the High-Density Postsynthetic Functionalization of Alkyne-Modified DNA. *Org. Lett.* **2006,** 8, (17), 3639-3642.

18. Meunier, S.; Strable, E.; Finn, M. G., Crosslinking of and Coupling to Viral Capsid Proteins by Tyrosine Oxidation. *Chem. Biol.* **2004,** 11, (3), 319-326.

19. Bruckman, M. A.; Kaur, G.; Lee, L. A.; Xie, F.; Sepulveda, J.; Breitenkamp, R.; Zhang, X.; Joralemon, M.; Russell, T. P.; Emrick, T.; Wang, Q., Surface Modification of Tobacco Mosaic Virus with “Click” Chemistry. *ChemBioChem* **2008,** 9, (4), 519-523.

20. Wittig, G.; Krebs, A., On the existence of low-membered cycloalkynes. I. *Chem. Ber.* **1961,** 94, 3260-75.

21. Agard, N. J.; Baskin, J. M.; Prescher, J. A.; Lo, A.; Bertozzi, C. R., A comparative study of bioorthogonal reactions with azides. *ACS Chem. Biol.* **2006,** 1, 644-648.

22. Baskin, J. M.; Prescher, J. A.; Laughlin, S. T.; Agard, N. J.; Chang, P. V.; Miller, I. A.; Lo, A.; Codelli, J. A.; Bertozzi, C. R., Copper-free click chemistry for dynamic in vivo imaging. *Proc. Natl. Acad. Sci. U.S.A.* **2007,** 104, 16793-16797.

23. Ning, X.; Guo, J.; Wolfert, M. A.; Boons, G.-J., Visualizing metabolically labeled glycoconjugates of living cells by copper-free and fast huisgen cycloadditions. *Angew. Chem., Int. Ed.* **2008,** 47, 2253-2255.

24. Laughlin, S. T.; Baskin, J. M.; Amacher, S. L.; Bertozzi, C. R., In Vivo Imaging of Membrane-Associated Glycans in Developing Zebrafish. *Science (Washington, DC, U.S.)* **2008,** 320, 664-667.

25. Link, A. J.; Vink, M. K. S.; Agard, N. J.; Prescher, J. A.; Bertozzi, C. R.; Tirrell, D. A., Discovery of aminoacyl-tRNA synthetase activity through cell-surface display of noncanonical amino acids. *Proc. Natl. Acad. Sci. U.S.A.* **2006,** 103, 10180-10185.

26. Beatty, K. E.; Fisk, J. D.; Smart, B. P.; Lu, Y. Y.; Szychowski, J.; Hangauer, M. J.; Baskin, J. M.; Bertozzi, C. R.; Tirrell, D. A., Live-cell imaging of cellular proteins by a strain-promoted azide-alkyne cycloaddition. *ChemBioChem* **2010,** 11, 2092-2095.

27. Marks, I. S.; Kang, J. S.; Jones, B. T.; Landmark, K. J.; Cleland, A. J.; Taton, T. A., Strain-Promoted "Click" Chemistry for Terminal Labeling of DNA. *Bioconjugate Chem.* **2011,** 22, 1259-1263.

28. Hannun, Y. A.; Obeid, L. M., Principles of bioactive lipid signalling: lessons from sphingolipids. *Nat. Rev. Mol. Cell Biol.* **2008,** 9, (2), 139-150.

29. Simons, K.; Toomre, D., Lipid rafts and signal transduction. *Nat. Rev. Mol. Cell Biol.* **2000,** 1, (1), 31-39.

30. Merrill, A. H., Jr., De novo sphingolipid biosynthesis: a necessary, but dangerous, pathway. *J. Biol. Chem.* **2002,** 277, 25843-25846.
31. Kolesnick, R., The therapeutic potential of modulating the ceramide/sphingomyelin pathway. *J. Clin. Invest.* **2002,** 110, (1), 3-8.

32. Wennekes, T.; van, d. B. R. J. B. H. N.; Boot, R. G.; van, d. M. G. A.; Overkleeft, H. S.; Aerts, J. M. F. G., Glycosphingolipids - Nature, function, and pharmacological modulation. *Angew. Chem., Int. Ed.* **2009,** 48, 8848-8869.

33. Langeveld, M.; Aerts, J. M., Glycosphingolipids and insulin resistance. *Prog. Lipid Res.* **2009,** 48, (3-4), 196-205.

34. Shapiro, D.; Segal, K., The synthesis of sphingosine. *J. Am. Chem. Soc.* **1954,** 76, 5894-5.

35. Garner, P., Stereocontrolled addition to a penaldic acid equivalent: an asymmetric synthesis of threo-β-hydroxy-L-glutamic acid. *Tetrahedron Lett.* **1984,** 25, 5855-8.

36. Yoshikawa, M.; Kato, T.; Takenishi, T., A novel method for phosphorylation of nucleosides to 5'-nucleotides. *Tetrahedron Lett.* **1967,** 50, 5065-8.

37. Oza, V. B.; Corcoran, R. C., A Mild Preparation of Protected Phosphate Esters From Alcohols. *J. Org. Chem.* **1995,** 60, 3680-4.

38. Nabetani, T.; Makino, A.; Hullin-Matsuda, F.; Hirakawa, T. A.; Takeoka, S.; Okino, N.; Ito, M.; Kobayashi, T.; Hirabayashi, Y., Multiplex analysis of sphingolipids using amine-reactive tags (iTRAQ). *J. Lipid Res.* **2011,** 52, (6), 1294-302.

39. Garrido, M.; Abad, J.; Alonso, A.; Goñi, F.; Delgado, A.; Montes, L. R., In situ synthesis of fluorescent membrane lipids (ceramides) using click chemistry. *J. Chem. Biol.* **2012,** 5, (3), 119-123.

# 7. Supporting Information

This Doctoral Thesis also contains supporting information in a CD format. The following material is included:

- PDF file of the Doctoral Thesis.
- NMR spectra of Section 3.1.
- NMR spectra of Section 3.2.
- NMR spectra of Section 3.3.
- NMR spectra of Section 3.4.